U.F.R. Sciences et Technologies
École Doctorale : Sciences et Ingénierie Ressources, Procédés, Produits et Environnement
Département de Formation Doctorale : Biologie Forestière

Thèse de Doctorat de l'Université Henri Poincaré, Nancy-Université
Spécialité : Biologie Végétale & Forestière

présentée par

Sacha Bohler

Les effets de l'ozone sur les processus foliaires du peuplier: Une approche protéomique.

Soutenu publiquement le 10 Novembre 2010 à Nancy devant la commission d'examen :

A. Cuypers	Pr., Univeristy of Hasselt, Belgique	Rapporteur
S. Lutts	Pr., Université de Louvain, Belgique	Rapporteur/Président du jury
E. Goulas	MC, Université de Lille	Examinateur
G. Müller-Starck	Pr., TU München, Allemagne	Examinateur
P. Dizengremel	Pr., Nancy Université	Examinateur/Directeur de thèse
J.-F. Hausman	Dr., CRP-Gabriel Lippmann	Examinateur/Codirecteur de thèse

Avec la présence des invités :

Y. Jolivet	MC, Nancy Université
J. Renaut	Dr., CRP-Gabriel Lippmann

Unité mixte de Recherche 1137, Ecologie et Ecophysiologie Forestières
Nancy-Université
Faculté des Sciences et Technologies, BP 239
F-54506 Vandoeuvre-lès-Nancy, France

INRA
Centre de Nancy
F-54280 Champenoux, France

Centre de Recherche Public - Gabriel Lippmann
Département Environnement et Biotechnologies
41, rue du Brill
L-4422 Belvaux, GD. Luxembourg

The present project was supported by the National Research Fund, Luxembourg


WHAT ARE YOU DOING, PIG?
BEING POPULAR.
WHAT MAKES YOU THINK YOU'RE POPULAR?
I'M SITTING IN THE POPULAR TREE.
IT'S CALLED A POPLAR TREE.
MIND HELPING ME DOWN SO I DON'T GET A BOO-BOO?


It's time to stop and ask for directions!

This is not a dedication

Four years. Four years is a very long time in which a lot can happen. And in the last years of my life a lot has happened, be it on a dark or on a light side. When I started my PhD I was told that it would be the worst four years of my life. It may have been true in so many more ways than professionally. As ***Terry Pratchett*** *wrote in his* ***Discworld*** *novel* ***Wyrd Sisters*** *'The duke had a mind that ticked like a clock and, like a clock, it regularly went cuckoo.' I felt like that a score of times in the last few years, and yet I got out of it (mostly) in one piece. Although the circumstances were not always the best, I thank each and every one of them for making me what I am today. And then I try to forget most of them.*

In his ***Discworld*** *novel* ***Hogfather****,* ***Terry Pratchett*** *wrote 'An education was a bit like a communicable sexual disease. It made you unsuitable for a lot of jobs and then you had the urge to pass it on'. I think there is nothing more to say to that.*

So why is this called 'This is not a dedication'? I think that a piece of work of over four years cannot be dedicated to one single outside person, and I can hardly dedicate it to myself. That is the reason why I specifically do not dedicate this work to anybody but to my past and all that led to today.

This page is in memory of my grandmother Suzanne Ceolotti-Schmuck who passed away during the time this work was done.

She was the wisest person I ever knew and I remember her lovingly.

Acknowledgements

The present project was supported by the National Research Fund, Luxembourg, AFR TR-PHD BFR06-044.

I would like to thank **Prof. Dr. Ann Cuypers** from the University of Hasselt, Belgium, and **Prof. Dr. Stanley Lutts** from the University of Louvain, Belgium, that they have kindly agreed to review this thesis and for the long hours of work this task takes. I would also like to thank **Dr. Estelle Goulas** and **Prof. Dr. Gerhard Müller-Starck** for having agreed to be members of the jury constituted for the defense of this work.

Many people have played major roles during this thesis and I would like to take the time to thank all of them.

I had a great number of supervisors during my four years as a PhD student, whom I am grateful to for their guidance and help, although it could become confusing at times, especially when corrections of reports and papers were involved.
I would like to thank **Prof. Dr. Pierre Dizengremel**, who welcomed me in his lab four years ago when I first proposed collaboration between the two labs. He believed in the project and let me manage the project with guidance but without pressure.
My first plant physiology teacher during my first year of Biology studies at the University of Luxembourg was **Dr. Jean-François Hausman**. He made plant physiology look easy. And interesting. Since that time he has played an important and much appreciated role in my career and I thank him for that.
When I first met **Dr Jenny Renaut**, she was still a PhD student. Now, she is the leader of the proteomics platform at CRPGL. Most of the things I know about proteomics I learned from her, and she has shown me how successful a scientific career can be. I thank her for that.
My thanks also go to **Dr Yves Jolivet**, whose input in experiments, analyses and paper-writing was always very valuable.

Furthermore I would like to thank **Prof. Dr Lucien Hoffmann**, the scientific Director of the EVA department of CRPGL, for allowing me to work in the department and for believing in my project when it was needed.

In four years I had the pleasure to work with many fine scientists.
I thank **Dr Kjell Sergeant** for his help with mass spectrometry, his input when it came to publications and reports and his overall help. Not to forget the very stimulating discussions we very often had.

But I still think that his skills in protein identification are a little bit scary and otherworldly.
Without **Dr Isabelle Lefèvre** and **Mouhssin Oufir** I would never have been able to produce the chromatography data that helped underline so many of the proteomic results and I am grateful for their help.

My thanks go to **Sébastien Planchon,** proteomic technical engineer, for his help in the proteomics lab, but also for talking me into starting martial arts, for having the same sense of humor than me and for his friendship.

During my first year biology studies I met **Pol Kieffer** who became a close friend. Later we became co-PhD students in CRPGL and the scientific discussions between us were always very fruitful. I would like to thank him for his friendship, the many games of *Magic: The Gathering* and for his eternal attempt to turn me into a better person.

Another co-PhD student from CRPGL was **Dr Thomas Durand**, who presented his PhD nearly exactly one year before me. He will forever stay in my memory as the guy who managed to hurt his own character in a *Dungeons & Dragons* game. Thanks go to him for cheering up the office and I sincerely hope that he can one day publish his fantasy novels.

Many thanks go to **Eva Lucic**, who was a dear friend during the PhD. Together we complained a lot about our work.

I am very grateful to **Dr Mathieu Bagard** for his help during the early stages of my PhD.

Thanks go to **Cosette Abdallah**, who I saw come into the office as a first year PhD student and who has immensely evolved since. To her I leave the important place of 'senior' PhD student in the office. I wish her good luck for the future.

I thank **Céline Leclercq**, our second technical engineer, whom I did not have the chance to work with that much, but who makes us laugh a lot.

My thanks also go to all those people with whom I have worked or shared an office over the last few years, students, trainees, technicians and scientists, and without whom I could not have done it or at least without whom it would have been at lot less fun.

I expressly want to thank **the trees** that died for the production of the paper on which this thesis is written. May they rest in peace.

Very personal thanks go to all the people in my private life without whom I would not stand where I stand today. They know who they are, and I owe them a lot of gratitude.

Abstract français

Depuis les révolutions industrielles des années 1700 et 1800, et pendant l'industrialisation des siècles les suivant, une accumulation de composés polluants a eu lieu dans l'atmosphère, principalement due à la combustion de matières fossiles comme le charbon et le pétrole. Outre les polluants directement émis comme les oxydes de souffre et d'azote, des polluants secondaires comme l'ozone se sont accumulés. Aujourd'hui, l'ozone est le troisième gaz responsable du réchauffement climatique, mais est également dangereux pour la santé humaine et responsable de dommages sur la végétation. Depuis les années cinquante, les effets de l'ozone sur les plantes et les réponses de ces dernières ont été étudiés de façon ciblée. Aujourd'hui, avec l'apparition de techniques permettant l'étude globale du transcriptome ou du protéome, il est possible d'aborder le problème d'une façon non biaisée, permettant des études plus complètes du stress.

Dans le cadre de ce travail, une étude protéomique des effets de l'ozone sur les processus foliaires du peuplier a été proposée. Cette technique, complétée par des approches biochimiques, physiologiques, et des observations morphologiques, a permis de confirmer certains résultats d'études ciblées, mais également d'émettre des nouvelles hypothèses sur les mécanismes d'action de l'ozone sur le métabolisme du peuplier. En parallèle, l'étude du stress a aussi permis d'éclaircir les changements du métabolisme lors de la croissance de feuilles en conditions de stress et en conditions normales. Dans les pages de ce document, les procédures, résultats et conclusions de ce travail seront présentés en détail.

English abstract

After the industrial revolution of the 1700s and 1800s, and the subsequent industrialization, many pollutants have accumulated in the atmosphere, mainly due to the use of coal and fossil fuels. Besides the primary pollutants such as nitrogen oxides and sulfur oxides, secondary oxides such as ozone started to accumulate. Nowadays, ozone is the third gas involved in global climate change, but is also a major health risk for humans, and induces considerable damage to vegetation. Starting in the 50s, ozone research was based on targeted studies. Nowadays, with the advent of global techniques such as transcriptomics and proteomics, new results can be produced in an unbiased way.

In the thesis presented here, a proteomic study of the effects of ozone on poplar leaf processes was carried out. With the help of this technique, complemented with biochemical and physiological approaches and with morphological observations, it was possible to confirm previous results, but also to elaborate new hypotheses concerning the effects of ozone on poplar leaf metabolism. In parallel, studying the stress also allowed to clarify some of the changes that occur in metabolism during leaf development, under stress conditions and under control conditions. In this document, the procedures, results and conclusions obtained during this study are presented in detail.

Mots Clés

Biochimie

Carbohydrates

Cycle de Calvin

DiGE

Fluorescence chlorophyllienne

Membrane

Métabolisme du carbone

Ozone

Peuplier

Photosynthèse

Pigments

Pollution atmosphérique

Protéomique

Stress végétal

Keywords

Atmospheric pollution

Biochemistry

Calvin cycle

Carbon metabolism

Carbohydrates

Chlorophyll fluorescence

DiGE

Membranes

Ozone

Photosynthesis

Pigments

Plant stress

Poplar

Proteomics

List of publications:

Proteomic study on poplar exposed to ozone and drought

S. Bohler, K. Sergeant, Y. Jolivet, L. Hoffmann, J.-F. Hausman, P. Dizengremel, J. Renaut.

Paper in preparation

Experimentation and writing

A DiGE study of thylakoids isolated from poplar leaves reveals a negative impact of ozone exposure on membrane proteins

S. Bohler, K. Sergeant, L. Hoffmann, P. Dizengremel, J.-F. Hausman, J. Renaut, Y. Jolivet

Submitted in Journal of Proteome Research (Impact Factor 2009: 5.132)

Experimentation and writing

Differential impact of chronic ozone exposure on expanding and fully expanded poplar leaves

S. Bohler, K. Sergeant, I. Lefèvre, Y. Jolivet, L. Hoffmann, J. Renaut, P. Dizengremel, J.-F. Hausman.

Tree Physiology 2010, 30, 1415-1432. (Impact factor 2009: 2.283)

Experimentation and writing

The impact of atmospheric composition on plants. A case study of ozone and poplar.

J. Renaut, **S. Bohler**, J.-F. Hausman, L. Hoffmann, K. Sergeant, A. Nagib, Y. Jolivet, P. Dizengremel.

Mass Spectrometry Reviews 2009, 28, 495– 516. (Impact Factor 2007: 10.896)

Participation in the writing

A DIGE analysis of developing poplar leaves subjected to ozone reveals major changes in carbon metabolism.

S. Bohler, M. Bagard, M. Oufir, S. Planchon, L. Hoffmann, Y. Jolivet, J.-F.Hausman, P. Dizengremel, J. Renaut.

Proteomics 2007, 7, 1584–1599. (Impact Factor 2007: 5.479)

Experimentation and writing

Courte introduction générale

Depuis les révolutions industrielles des années 1700 et 1800, et pendant l'industrialisation des siècles les suivant, une accumulation de composés polluants a eu lieu dans l'atmosphère, principalement due à la combustion de matières fossiles comme le charbon et le pétrole. Outre les polluants directement émis comme les oxydes de souffre et d'azote, des polluant secondaires comme l'ozone se sont accumulés. Aujourd'hui, l'ozone est le troisième gaz responsable du réchauffement climatique, mais est également dangereux pour la santé humaine et responsable de dommages importants sur la végétation. Depuis les années cinquante, les effets de l'ozone sur les plantes et les réponses de ces dernières ont été étudiés de façon ciblée. Bien que ces techniques aient produit des résultats importants, elles ont comme limite de nécessiter une hypothèse de départ. Aujourd'hui, avec l'apparition de techniques permettant des études globales telle que la transcriptomique ou la protéomique, il est possible d'aborder le problème de façon non ciblée, permettant des études plus complètes du stress.

La protéomique est l'étude de l'ensemble des protéines d'un organisme, d'un organe, d'un tissu ou d'une fraction d'un de ces éléments à un instant et dans des conditions données. Ce genre d'étude globale a comme avantage d'être non biaisée par des hypothèses de départ, et de pouvoir produire des résultats nouveaux et inattendus. Deux principales approches sont utilisées en protéomique, d'une part sur base de séparation des protéines par électrophorèse, et d'autre part sur base de séparation par chromatographie liquide. Dans l'étude présentée ici, la première technique a été choisie. Celle-ci est couplée a un marquage des protéines par des molécules fluorescentes, permettant la séparation en simultané sur un même gel de deux échantillons et d'un standard interne. Ceci permet la standardisation de tous les gels d'une même étude et une quantification à haut degré de fiabilité des différences d'abondance des protéines contenues dans les différents échantillons.

Dans le cadre de cette étude, le peuplier a été choisi comme modèle. Il s'agit d'un arbre facile à multiplier *in vitro*, à croissance rapide, et d'une grande importance écologique et économique. De plus, le génome du peuplier a récemment été séquencé, ce qui facilite grandement l'étude des protéines.

Les pages qui suivent sont subdivisées en trois expériences majeures, toutes basées sur une étude protéomique des effets de l'ozone sur le peuplier. Les études sont faites aussi bien sur le protéome soluble total des feuilles que sur le protéome de membranes de chloroplastes purifiées. Des analyses de pigments, de sucres, des mesures de croissance et de fluorescence chlorophyllienne

complémentent les études protéomiques. Les expériences sont basées sur une fumigation de peupliers par 120 ppb d'ozone sur des périodes de 1 mois à 35 jours pendant la phase lumineuse de la journée. Des cinétiques d'exposition ont été faites sur les feuilles jeunes en début du traitement, devenant adultes au cours des expériences. Des articles publiés à cette date tout comme des articles acceptés pour publication, ou encore en préparation, sont la base des chapitres présentés ci-après.

Courte conclusion générale

Les travaux présentés dans ce document ont permis de confirmer des éléments connus, de soutenir des hypothèses émises, mais aussi d'avancer de nouvelles hypothèses concernant les effets de l'ozone sur le peuplier et la réponse de ce dernier au stress. Il est connu depuis longtemps que l'exposition de plantes à l'ozone diminue la photosynthèse, au niveau biochimique (cycle du Calvin) et photochimique (chaîne de transport d'électrons du chloroplaste). L'hypothèse proposant que la partie biochimique soit atteinte avant la partie photochimique est supportée par nos résultats, compte tenu que les abondances des enzymes du cycle de Calvin sont atteintes avant celles des complexes membranaires du chloroplaste. Il a pu être confirmé que de nombreuses protéines du cycle de Calvin sont diminuées en abondance lors d'un traitement à l'ozone, dont en l'occurrence quatre enzymes régulées par un mécanisme d'oxido-réduction. Considérant que l'exposition à l'ozone mène à la formation de molécules réactives de l'oxygène dans les cellules, et donc à un changement de l'équilibre redox, c'est sans doute une désactivation de ces enzymes qui mène à la diminution du cycle de Calvin.

La chute accélérée des feuilles est un symptôme associé au stress ozone. Il a été longtemps proposé que l'ozone puisse relayer le signal au déclenchement de la sénescence dans les feuilles atteintes. En considérant les profils de variation d'abondance des protéines observées dans ce travail, l'ozone ne provoquerait pas une sénescence directement, mais par épuisement des ressources des feuilles lors d'une période de stress chronique prolongée.

En plus des observations réalisées sur les effets de l'ozone, le développement des feuilles du stade juvénile jusqu'au stade de maturité a également été étudié. Il a été démontré que les protéines responsables pour les principaux métabolismes foliaires augmentent en abondance pendant la phase de croissance, alors qu'elles restent relativement stables par après, illustrant ainsi la stabilité du métabolisme de feuilles non soumises à des conditions contraignantes. Il a également été démontré que les jeunes feuilles en croissance sont résistantes à l'ozone et présentent un développement très proche de celui de feuilles non traitées.

Dans l'avenir, les hypothèses émises ici devraient être confirmées, notamment par une étude du protéome soluble purifié de chloroplastes. Il serait également intéressant d'approfondir le sujet par l'étude de feuilles adultes dès l'apparition de la contrainte ozone, et de feuilles non encore initiées à ce moment.

D'une façon générale, le travail présenté ici a permis de répondre à certaines questions émises lors des dernières années, mais aussi de découvrir des voies pour des études futures.

Table of contents

Abbreviations

2DE	two dimensional electrophoresis
A	net CO_2 exchange
AA	ascorbate
ABA	abscisic acid
ADP	adenosyldiphosphatase
ANCOVA	analysis of covariance
ANOVA	analysis of variance
AOT40	accumulated exposure over a threshold concentration of 40 ppb
APX, AAperox	ascorbate peroxidase
ATP	adenosine triphosphate
ATPase	adenosine triphosphatase
CA1P	2-carboxyarabinitol-1-phosphate
CAM	crassulacean acid metabolism
CE	capillary electrophoresis
CH_4	methane
CO	carbon monoxide
CO_2	carbon dioxide
Cy dyes	cyanine dyes
cyt b6f	cytochrome b6f
DHAA	dehydroascorbate
DHAR	dehydroascorbate reductase
DHPC	1,2-diheptanoyl-sn-glycero-3-phosphocholine
DiGE	difference gel electrophoresis
DNA	deoxiribonucleic acid
DTT	dithiothreitol
EDA	extended data analysis
EST	expressed sequence tags
ET	ethylene
FACE	free-air carbon dioxide enrichment
fdx	ferredoxin
FeSOD	iron superoxide dismutase
FNR	ferredoxin-NADP+-oxidoreductase
Fv/Fm	maximum efficiency of photosystem II
GABA	γ-aminobutyric acid
GC	gas chromatography
GR	glutathione reductase
GS	glutamine synthetase
GSH	glutathione
GSSG	oxidized glutathione
H_2O_2	hydrogen peroxide
H_2S	hydrogen sulfide
H_2SO_3	sulfurous acid
H_2SO_4	sulfuric acid
HNO_3	nitric acid

HPAEC-PAD	high performance anion exchange chromatography coupled with pulsed amperometric detection
HPLC	high performance liquid chromatography
HSP70	heat shock protein 70
IEF	isoelectric focusing
IPG	immobilized pH gradient
IS	internal standard
JA	jasmonic acid
LHC	light harvesting complex
LSU	large subunit
Maldi-ToF	matrix-assisted laser desorption/ionization time-of-flight
MAPK	mitogen-activated protein kinase
MDH	malate dehydrogenase
MDHA	monodehydroascorbate
Mn-cluster	manganese cluster
mRNA	messenger ribonucleic acid
MS	mass spectrometry
MS-MS	tandem mass spectrometry
N_2O	nitrous oxide
N_2O_5	dinitrogen pentoxide
NAD(P)H	NADH and/or NADPH
NADH	nicotinamide adenine dinucleotide
NAD-ME	NAD dependant malic enzyme
NADPH	Nicotinamide adenine dinucleotide phosphate
NL	non-linear
NMR	nuclear magnetic resonance spectroscopy
NMVOC	non-methane volatile organic compounds
NO	nitrogen monoxide
NO_2	nitrogen dioxide
NO_3	nitrogen trioxide
NO_x	nitric oxides
NPQ	non-photochemical quenching
$O^{\bullet -}$	activated oxygen
O_2	molecular oxygen
O_3	ozone
OH	hydroxyl
ORP	O_3-responsive proteins
PC	plastocyanin
PC1	principal component 1
PC2	principal component 2
PCA	principal component analysis
PCD	programmed cell death
PEP	phosphoenol pyruvate
PEPc	phosphoenol pyruvate carboxylase
PhiPSII	quantum yield of photosystem II
PIN proteins	plant-specific pin-formed proteins

PMF	peptide mass fingerprint
ppb	parts per billion
PQ	plastoquinone
PSI	photosystem I
PSII	photosystem II
qP	photochemical quenching
QTL	quantitative trait loci
Q-ToF	quadrupole time-of-flight
ROS	reactive oxygen species
RP-HPLC-DAD	reverse phase high performance liquid chromatography with photodiode array detector
RuBisCO	ribulose-1,5-bisphosphate carboxylase/oxygenase
RuBisCO activase	ribulose-1,5-bisphosphate carboxylase/oxygenase activase
SA	salicylic acid
SAG	senescence-associated gene
SAM	shoot apical meristem
SDS-PAGE	sodium dodecyl sulfate polyacrylamide gel electrophoresis
SHMT	serine hydroxymethyltransferase
SO_2	sulfur dioxide
SO_3	sulfur trioxide
SSU	small subunit
TCA cycle	tricarboxylic acid cycle
TP	triose phosphate
UNECE	United Nations Economic Commission for Europe
UV	ultra violet
VOC	volatile organic compounds

Chapter 1

Introduction

1.1. Ozone pollution

Industrialization was an important step in recent human history to achieve today's society's economical and technological situation. History knows two industrial revolutions, one starting in the middle of the 1700s (called industrial revolution) and one in the middle of the 1800s (called technological revolution) (Ashton 1997; Hull 1999). They brought important advancements in mining, metallurgy, textile production and many other fields. One major breakthrough during the second industrial revolution was the development of petroleum based fossil fuels in addition to coal. Unfortunately, it also brought with it the beginning of a drastic increase in pollution, and in less than 150 years, mankind has among other things drastically changed the composition of the Earth's atmosphere. Two of the most prominent consequences of atmospheric perturbation in the past are probably acid rain and the depletion of the ozone layer.

The term acid rain was first used in the 1870s. It is a consequence of atmospheric sulfur and nitrogen pollution. Sulfur and nitrogen oxides are emitted when fossil fuels and coal are burnt. The water in the atmosphere washes out the oxides and acid is formed, which reaches the earth by precipitation (e.g. rain, snow, fog) (Singh and Agrawal 2008). Absorbed by the soil, acid precipitations affect the equilibrium of dissolution of important nutrients and minerals and acidify soils and surface water, presenting an extreme danger for vegetation and soil microorganisms (Breemen et al. 1984; Shortle and Bondietti 1992). An acidification of lakes and rivers is another consequence and presents a risk for aquatic ecosystems as well (Dillon et al. 1984).

Similarly to acid rain, the depletion of the stratospheric ozone layer is a consequence of atmospheric pollution. Already in the mid 70s, scientists predicted that chlorine compounds, then used as refrigerants and aerosol propellants, could destroy ozone (Molina and Rowland 1974). In the mid 80s, the first significant depletion in the ozone layer was measured over Antarctica (Solomon et al. 1986). Since then, the use of ozone depleting compounds has been forbidden or put under strict control, but even up to this day, it is not clear if the damage to the ozone layer can be completely or even only partially regenerated, since many new factors have appeared that might disturb the precarious equilibrium of the chemistry of the ozone layer (Weatherhead and Andersen 2006).

In more recent years, global changes in climatic factors have been measured. Climate change and global warming have become catchphrases for the media and have given birth to controversy between scientists, politics and different lobbying factions. Since the 1900s, the composition of the troposphere, the layer of air situated between the earth's surface and up to 10 km above, has factually changed in such a manner that the climate itself changed and may still change considerably

more. Industry, traffic and heating, mostly through the combustion of fossil fuels, have emitted important amounts of carbon dioxide (CO_2), carbon monoxide (CO), nitric oxides (NO_x), sulfurous compounds and methane and other volatile organic compounds (VOC) into the atmosphere. Even if these compounds are naturally present in the atmosphere, their levels strongly increased (Figure 1). The consequences are perturbations in the climate. The global average surface temperature increased by nearly 1°C in between the early 1900s and 2000, leading to a slow but steady melting of the polar icecaps and an increase in the global average sea level (Figure 2) (Bernstein et al. 2007).

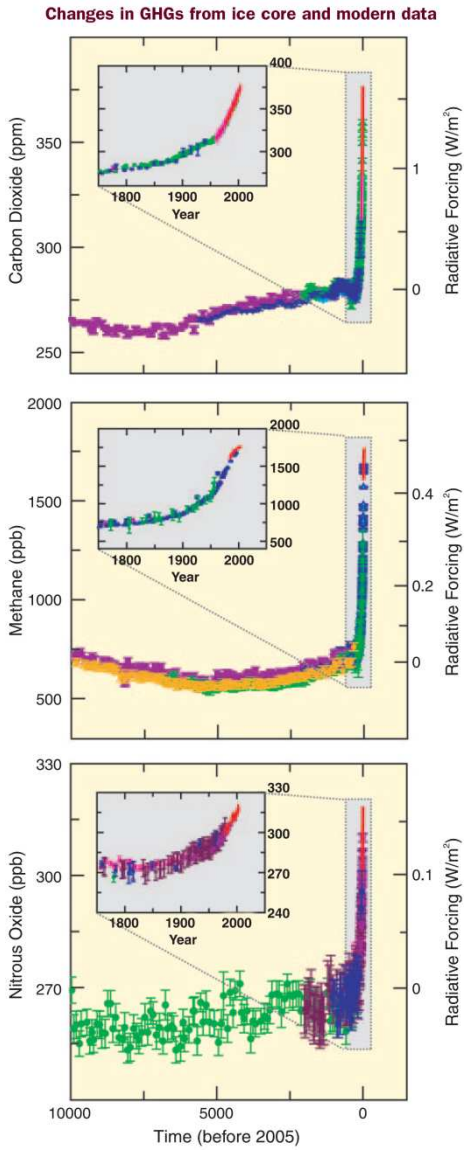

Figure 1: Atmospheric concentrations of CO_2, CH_4 and N_2O over the last 10,000 years (large panels) and since 1750 (inset panels). Measurements are shown from ice cores (symbols with different colors for different studies) and atmospheric samples (red lines). The corresponding radiative forcings relative to 1750 are shown on the right hand axes of the large panels. Source: (Bernstein et al. 2007)

Independently of climate change, many of the pollutants that accumulated during the last century induce health risks (D'Amato and Cecchi 2008; Dab et al. 1996; Luber and Prudent 2009). Respiratory diseases have become more frequent and more severe, especially in urban areas; asthmatic diseases and allergies for instance can be caused by air pollution. A particularly notable molecule in that

regard is ozone (O_3), specifically tropospheric ozone (Figure 3). In the stratosphere, ozone is the major component of the ozone layer, where it protects the earth surface from solar UV radiation, but its presence in the troposphere is less beneficial even at the very low concentrations that are present (at a scale of parts per billion (ppb)). Ozone is composed of three oxygen atoms and is derived from molecular oxygen (O_2) and NO_x. Under UV radiation, NO_x molecules are decomposed and generate activated oxygen atoms that can react with O_2 to form O_3. Other molecules like VOC and hydroxyl radicals are also involved in the regeneration and formation of ozone, and the reactions are detailed in paragraph 1.5.5. Atmospheric pollution (Renaut et al. 2009). The major part of tropospheric ozone is a consequence of human activity. It is considered a secondary pollutant since it is not emitted directly, but its formation is dependent on emitted pollutants like NO_x and VOC. The influence of stratospheric ozone on tropospheric ozone levels depends widely on the considered altitude. In the higher troposphere, 30 to 50% of the ozone may originate from the stratosphere, but in the lower troposphere this is no more than 10%. In recent years, lower-stratospheric ozone levels declined by up to 30%, which reduced the exchange of ozone between the two atmospheric layers even more (Fusco and Logan 2003). As detailed below, tropospheric ozone is a major ecological and health treat. It is the topic of the work presented in this document; any mention of ozone in the following pages refers exclusively to tropospheric ozone if not specified differently.

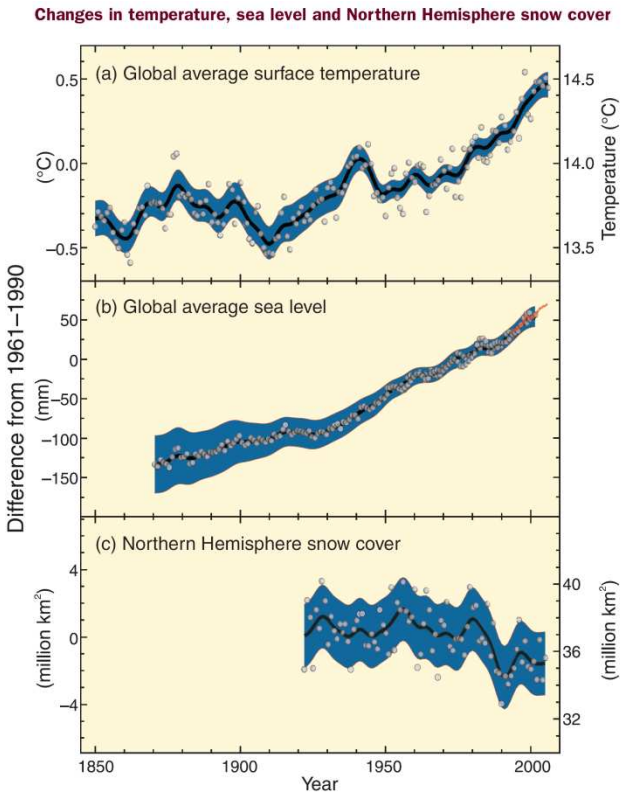

Figure 2: Observed changes in (a) global average surface temperature; (b) global average sea level from tide gauge (blue) and satellite (red) data; and (c) Northern Hemisphere snow cover for March-April. All differences are relative to corresponding averages for the period 1961-1990. Smoothed curves represent decadal averaged values while circles show yearly values. The shaded areas are the uncertainty intervals estimated from a comprehensive analysis of known uncertainties (a and b) and from the time series (c). Source: (Bernstein et al. 2007)

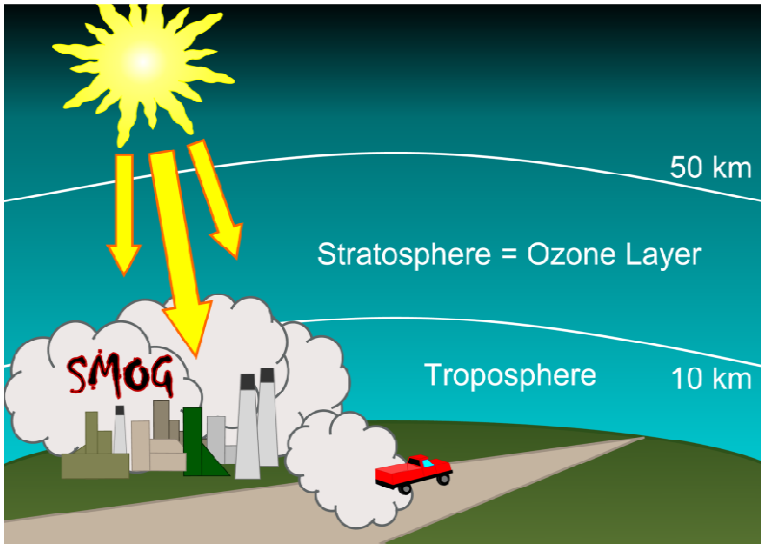

Figure 3: The secondary pollutant tropospheric ozone is produced by the interaction of primary pollutants, atmospheric constituents and UV radiation from the sun.

During the last century, background ozone concentrations have increased drastically. For instance measurements at mountain sites have shown that the levels have increased from 10 to 60 ppb, an increment of 500% (Marenco 1994).

Since the 1980s, steps were taken in Europe and North America to reduce the emission of pollutants that can result in ozone formation, decreasing NO_x and non-methane volatile organic compounds (NMVOC) by 30% in Europe and by 15-20% in North America (Table 1) (Jonson et al. 2006). In Asia however, emissions continue increasing (Streets et al. 2003).

Table 1: Anthropogenic emissions (Gg/year) for the EU25 and Germany, the Czech Republic and United Kingdom separately (Vestrengen et al. 2004), and from N. America (UNECE 2004). N. America includes Canada and USA. Source: (Jonson et al. 2006).

Region	1990		
	NO_x	NMVOC	CO
EU 25	15 991	16 869	61 213
Germany	2845	3591	11 212
Czech Republic	544	441	1257
United Kingdom	2771	2419	7417
N. America	25 775	21 264	97 651
	2002		
	NO_x	NMVOC	CO
EU 25	10 988	10 322	33 774
Germany	1499	1478	4311
Czech Republic	318	203	546
United Kingdom	1582	1186	3238
N. America	21 721	17 790	11 1562

Ozone pollution however does not entirely follow these trends. Although concentrations during local peak episodes seem to have slightly decreased, average annual levels have even increased, most notably in winter. Inconveniently, tropospheric ozone concentrations are very sensitive to meteorological and local conditions, and it is difficult to estimate whether the steps taken against ozone pollution can induce long term changes or not (Jonson et al. 2006).

When inhaled by mammals, ozone is an irritant molecule and it can induce respiratory diseases and even cancer when chronically inhaled (D'Amato and Cecchi 2008; Dab et al. 1996; Ebi and McGregor 2008; Luber and Prudent 2009). Furthermore, it does not only have a negative impact on human health, but also on plants. Common symptoms of ozone-exposed plants include necroses and chloroses, and the exposure to higher ozone concentrations can lead to a decrease in yield of crops and forests. It is estimated that 10% of European forest yield is lost due to ozone (Broadmeadow 1998).

1.2. Ozone and plant health

The effects of ozone on plants have been detected for the first time in California in the middle of the 20th century (Haagen-Smit et al. 1952) and since then a lot has been done to try and understand the processes that are involved in ozone sensitivity, resistance and response. Ozone is a relatively 'new' or unknown stressor for plants, considering that plants did not co-evolve with harmful concentrations of this pollutant. It is therefore not clear whether plants can have an ozone-specific response. On the other hand, on a cellular level, plants do not encounter ozone directly. Indeed it has been shown that once the molecule has penetrated the intercellular space through the stomata, it breaks down and forms reactive oxygen species (ROS) in the apoplast so quickly that the cells never actually encounter the ozone molecule (Figure 4) (Kanofsky and Sima 1995; Laisk et al. 1989). In this regard ozone stress is on one hand close to other stressors, and on the other hand very different. Most stress-inducing factors, be they biotic (e.g. viral, fungal) or abiotic (e.g. heavy metals, salt, drought) are directly sensed by the plant, which is not the case for ozone. However, most plant constraints induce an oxidative stress (Mittler 2002; Shao et al. 2008b), which is also true for ozone (Baier et al. 2005; Langebartels et al. 2002; Pell et al. 1997; Wohlgemuth et al. 2002). Therefore, although ozone exposure may be considered the typical inducer of an oxidative stress, it can also be considered atypical among stressors.

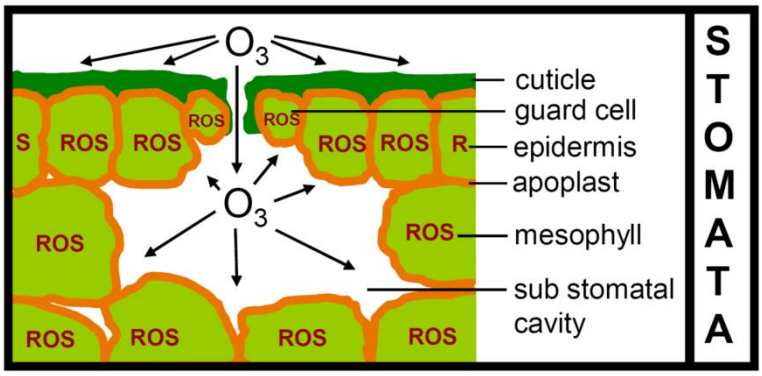

Figure 4: The path of ozone from the atmosphere to the cell. Ozone enters the leaves through the stomata and ruptures into ROS as soon as it touches the apoplast. ROS, reactive oxygen species.

Before continuing with reporting the known effects of ozone exposure on plants, it should be explained that studies on ozone come 'in different shapes and sizes', ozone exposure can be acute or chronic, with high or low concentrations, in chambers or in the field (Renaut et al. 2009). Very often, the experimental setups of ozone studies depend on the examined plant processes. Signaling and transcriptomic studies, which are very often (but not exclusively) carried out on quick growing model plants like *Arabidopsis thaliana* or tobacco, often use short-term high concentrations, for instance 200 to 500 ppb for a few hours only (Ludwikow et al. 2004; Rao et al. 2002; Schraudner et al. 1998). On the other hand, physiological or molecular studies often use long-term exposure systems, e.g. from 30 to 200 ppb for up to several months (Cabané et al. 2004; Leitao et al. 2007b; Miller et al. 1999; Ranieri et al. 2001). Basically, it is a choice between quickly provoking effects and mimicking reality. Although 300 ppb is never reached in nature yet, this concentration allows observing quick changes in signaling pathways or changes in transcript abundance which would possibly be too faint to be detected when lower concentrations are applied. Physiological studies often chose realistic conditions over speedy responses, which allow observing changes as they could happen in natural conditions. Chronic exposure is also very often the choice for studies on tree species, since trees are long lived plants and are more prone to suffer from chronic exposure that short lived species (Chen et al. 2009). Further realism can be achieved by the choice of chamber *versus* field trials. Chamber studies have the advantage that under controlled conditions, all observed effects should be due to the only variable factor. Furthermore, the use of chamber experiments allows for the maintenance of a reasonable reproducibility between experiments. In field trials, barely any parameters are controllable. Light, temperature, weather conditions, presence of pathogens and so on depend on seasons and years. These unpredictable factors can occur and mask the effects of the applied ozone concentration; furthermore field trials are nearly impossible to repeat in a reproducible way. Very

often ozone concentrations during field trials are not fixed, but follow the natural occurrence and multiplications thereof. Field trials can again be divided into two different procedure methods, on one hand open top chambers which enclose a group of trees (in pots or in the soil) and allow a relatively good control of semi natural conditions, and on the other hand fully open field conditions which in the end are the only way to study fully grown trees, but which render the control of environmental factors impossible or at least very difficult. Two large-scale experiments in the field have been done to this date. The first is the Aspen FACE (free-air carbon dioxide enrichment) near Rhinelander, WI, USA, consisting of twelve 30 m rings in which the concentrations of carbon dioxide and tropospheric ozone can be controlled (http://aspenface.mtu.edu). The second one is the Kranzberg forest site near Munich, Germany, with 60 year-old beech and spruce trees and a canopy high tubing system for controlled ozone exposure (Matyssek et al. 2010b). These studies showed that, in realistic conditions, the effects of ozone are not always as clear as in chamber experiments, and are relatively dependent on other climatic conditions. Nonetheless, many of the results from chamber studies were confirmed. Although it is clear that field experiments are the only way to study realistic conditions, chamber experiments remain the only way to do controlled and targeted studies. A further question in ozone research is whether studies on juvenile trees can be scaled up to mature trees, a subject that has been extensively reviewed (Kolb and Matyssek 2001; Samuelson and Kelly 2001). In many cases the effects on the metabolism and physiology on young and adult trees for the same effective ozone flux are similar, even if they can be stronger in younger trees. But for a given external ozone concentration the response can differ, since mature trees can have a different stomatal dynamic over one day, or have a different detoxification potential than their younger counterparts (Kolb and Matyssek 2001; Samuelson and Kelly 2001). It was proposed in a meta-analysis of ozone research that experiments are needed to study the effects of ozone from the juvenile tree to the adult plant, and that there is a strong species effect concerning the differences in sensitivity correlated to plant age (Wittig et al. 2007; Wittig et al. 2009). If there are differences in the response to ozone between juvenile and mature trees, it seems mainly to be a question of the effective ozone flux. Although it can therefore be dangerous to directly scale from seedlings to adult forest trees, it is not impossible, since the basic response remains similar. Furthermore, it remains very important to study the response of juvenile tress, since they are the mature trees of the future, and effects of ozone on the juvenile plants may have repercussions once they have grown to adult trees.

Plants can be differentially sensitive to ozone (Reich 1987). A first parameter that is often determinant for ozone sensitivity of a plant is its growth rate. Fast growing species like poplar are often relatively sensitive to ozone, while slow growing species like oak are relatively tolerant. This is

mostly due to the fact that quick growing species have a much higher gas exchange rate than slow growing ones (Bortier et al. 2000). The higher the stomatal conductance is, the more ozone enters the leaf and the higher the actual exposure of the plant is. The ability of a plant to control the level of stomatal opening is therefore a very important factor in ozone resistance. But it is not sufficient in itself to explain it, since trees with high stomatal opening can be relatively resistant or vice-versa. The second important factor is the ability of the plant to detoxify the ROS formed during ozone exposure. The primary defense mechanism against ozone is apoplastic ascorbate (Conklin and Barth 2004). Ascorbate peroxidases use ascorbate to reduce and detoxify hydrogen peroxide (H_2O_2) (formed directly or as the result of the transformation of other ROS) and dehydroascorbate reductase regenerates ascorbate using the cofactor nicotinamide adenine dinucleotide phosphate (NADPH). The level of ascorbate and the level of ascorbate regeneration play a major role in ozone resistance. If the apoplastic ascorbate barrier is overwhelmed and the ROS reach the cytosol, other detoxifying pathways like glutathione and superoxide dismutase also take part in ozone detoxification; nevertheless the ascorbate detoxification pathway remains the major protection against ROS. These two factors, stomatal control and detoxification capacity, are the main indicators for ozone sensitivity and resistance (Figure 5) (Castagna and Ranieri 2009; Di Baccio et al. 2008; Dizengremel et al. 2008).

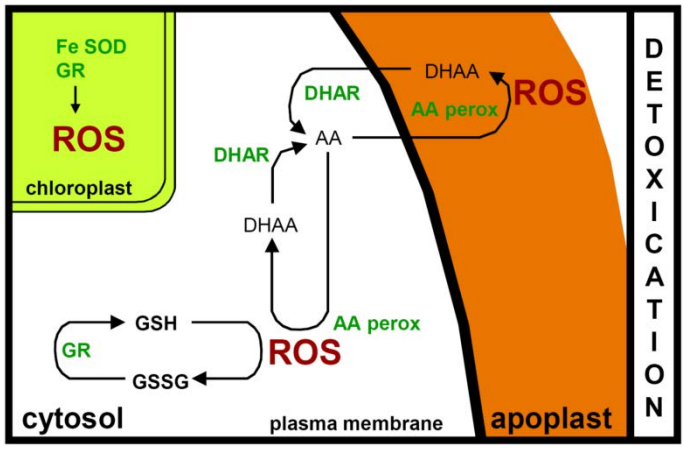

Figure 5: Detoxication processes in plant cells. AA, ascorbate; AAperox, ascorbate peroxidase; DHAA, dehydroascorbate; DHAR, dehydroascorbate reductase; GSH, glutathione; GR, glutathione reductase; FeSOD, iron superoxide dismutase; GSSG, oxidized glutathione.

The production of ROS in plant cells induces a number of signaling pathways, involving among others ethylene, jasmonate and salicylic acid (Figure 6) (Kangasjärvi et al. 2005). It is the interaction between these three growth regulators that will determine the outcome of the response. Ethylene and salicylic acid are activators of programmed cell death (PCD). Similar to a hypersensitive reaction in response to a pathogen attack, PCD induces the death of the cells directly affected by the exposure, and prevents the spreading of the stressor (Pasqualini et al. 2002). Although this is an interesting response for a pathogen attack, in which the site of infection is generally very localized and can be isolated from the rest of the tissue or organ by PCD, it is not as useful during ozone exposure. Ozone enters the leaves through the stomata which are spread over the whole leaf surface, and make nearly the entire leaf the 'infection' point. This leads to necroses on the whole surface of the leaves, a symptom relatively typical for ozone stressed trees. Jasmonate is an antagonist of ethylene and salicylic acid. Thereby it delays the onset of PCD, but cannot entirely stop it (Rao et al. 2000b).

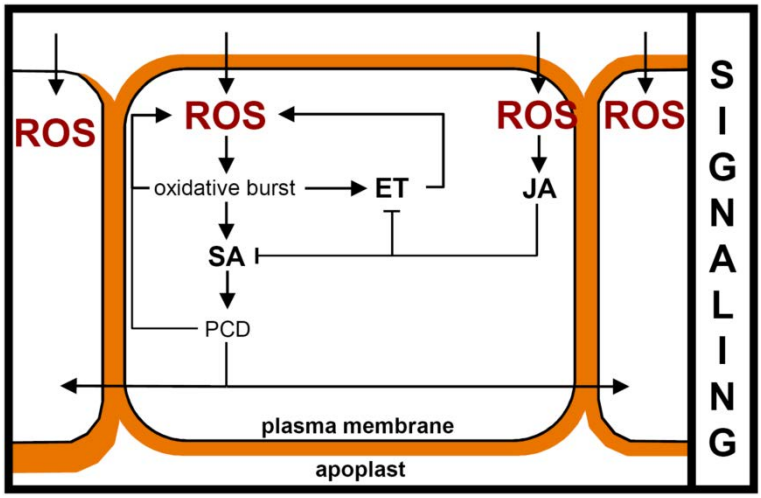

Figure 6: Signaling pathways during ozone stress involving ethylene (ET) salicylic acid (SA) and jasmonate (JA).

The effects of ozone on the metabolism of plants are reviewed in 1.5.7. Impact of ozone on plant cell metabolism (Renaut et al. 2009). Two interesting enzymes that respond strongly to ozone are ribulose-1,5-bisphosphate carboxylase/oxygenase (RuBisCO) and phosphoenolpyruvate carboxylase (PEPc) (Figure 7). RuBisCO is the primary carbon fixation enzyme in plants. It uses CO_2 originating from the atmosphere and fixes it to ribulose-1,5-bisphosphate (carrying 5 carbon atoms) to form 2 molecules of 3-phosphoglycerate (6 carbon atoms) (Bassham et al. 1950). PEPc on the other hand fixes CO_2 to phosphoenolpyruvate (3 carbon atoms) to form oxaloacetate (4 carbon atoms) (Mazelis and Vennesland 1957). It is the primary carbon fixation enzyme in plants with a C4 or crassulacean

acid metabolism (CAM), but not in plants with C3 metabolism. In C3 metabolism, it is involved in an anapleurotic pathway responsible for the replenishing of the tricarboxylic acid cycle (TCA cycle) with oxaloacetate and malate (Melzer and O'Leary 1987). Ozone exposure typically decreases the activity and abundance of RuBisCO in leaves (Bahi and Kahl 1995; Brendley and Pell 1998; Landry and Pell 1993; Pell et al. 1992; Pelloux et al. 2001) but increases the content of PEPc (Fontaine et al. 2003; Fontaine et al. 1999; Leitao et al. 2008). While the decrease in RuBisCO is probably a consequence of ROS induced damage to the protein structure, the increase in PEPc is clearly a regulatory factor, due to the need in energy for repair and detoxification pathways (Dizengremel 2001). Decreases in CO_2 fixation lead inevitably to reduced growth and biomass productivity as reviewed in two meta-analyses (Wittig et al. 2007; Wittig et al. 2009).

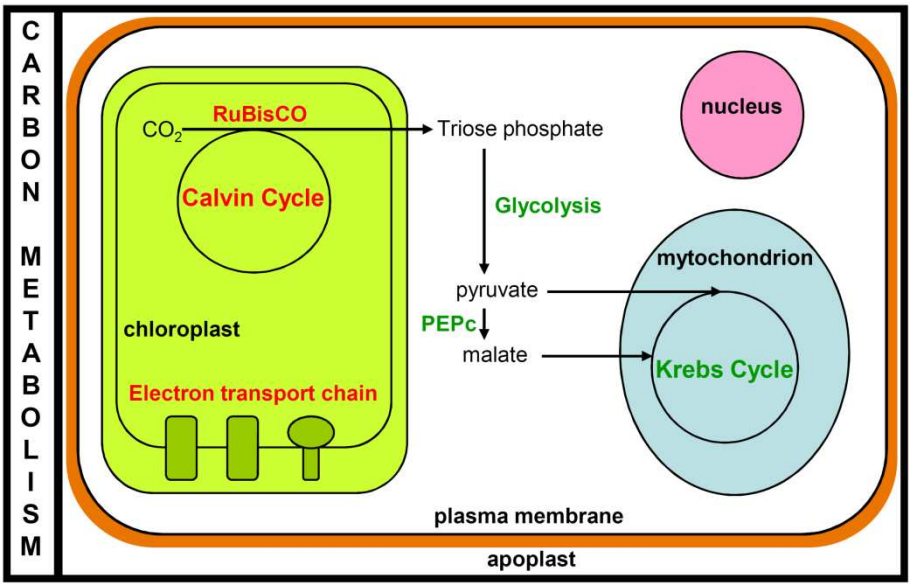

Figure 7 : Main variations in leaf carbon metabolism upon exposure to ozone. Red, decrease in protein abundance and activity; Green, increase in protein abundance and activity. RuBisCO, ribulose-1,5-bisphosphate carboxylase/oxygenase; PEPc, phosphoenol pyruvate carboxylase.

1.3. Poplar as a model tree

Studying abiotic stress like ozone exposure on woody plants is of interest for several reasons. Some herbaceous plants have developed a mechanism of avoidance in which they complete their life cycle before the stressor appears. Woody plants live over years and decades, and need to cope with stress situations year after year. As mentioned before ozone is a very recent stress factor, and there has been no co-evolution, making it a very dangerous factor. Contrarily to herbaceous plants that can die before completing their life cycle during prolonged ozone exposure, trees seem to be more resistant

and able to survive even strong ozone episodes, although with considerable damage, completing one year's life cycle to start over the following year.

Among forest trees, it is poplar that has been chosen as a model (Jansson and Douglas 2007). The genus *Populus* counts many species and hybrids. It belongs to the family of the *Salicaceae* and is present on nearly the entire northern hemisphere. Poplar is economically and ecologically relevant. This fast growing tree species is cultivated for its wood, for the production of paper and building wood. It is also a pioneer tree, important for the reforestation of deforested areas and for the stabilization of river banks. Besides economical and ecological relevance, poplar also presents advantages for research. For a tree species, poplar is relatively unproblematic to cultivate. It can be multiplied *in vitro* without the addition of growth factors and at a high success rate (Sellmer et al. 1989). Just as easily, it can be multiplied with cuttings that take root easily in soil or sand (Heilman et al. 1994). The quick growth of poplar is a further useful feature, since it allows studies on young trees in a relatively short time. Growth can for example reach over 1.5 m in only two to three months. Another advantage of poplar is its fully sequenced genome (Tuskan et al. 2006). Poplar (*P. trichocarpa*) was chosen as a tree for sequencing because of its relatively small genome size (480 Mb) and because of the advantages mentioned above. The complete EST database presents large advantages for functional genomics (i.e. transcriptomics, proteomics). Although the genome is not yet fully annotated, it is an important tool in molecular tree biology.

1.4. Proteomics and its advantages

The proteome can be described as the complete set of proteins of an organism (e.g. yeast), an organ (e.g. liver, leaf) or a tissue (e.g. epidermis, cambium) under specific circumstances and specific time points, or of a subset of these proteins (e.g. membrane proteome, proteome of the chloroplast lumen) (Wilkins et al. 1996). Proteomics is used in medical diagnostics as well as in fundamental research on human, animal, plant or microorganism models (Byrum et al. 2010; Kersten et al. 2009; Korolainen et al. 2010; Martyniuk and Denslow 2009; Quirino et al. 2010; Zhang et al. 2010). Proteomic approaches present certain advantages to other methodologies. In transcriptomics, the presence and abundance of transcripts is measured as a measure for gene activation, but the abundance of a transcript does not necessarily correspond to the abundance or activity of the protein. Post-transcriptional regulation can lead to a false estimation of the presence or abundance of the protein. Although in proteomics the abundance of a protein cannot be automatically correlated to the activity of its function, it is one step closer to reality than transcriptomics. Furthermore, some post-translational modifications like phosphorylation and acetylation can be detected by proteomic techniques (Farley et al. 2009), allowing at least partially to observe

regulation phenomena. Two main groups of techniques are used in proteomics, gel-based and gel-free approaches (Baggerman et al. 2005; Lambert et al. 2005; Lottspeich 2009; Poon and Mathura 2009).

Although a mix of proteins can be directly submitted to digestion and to analysis by mass spectrometry (MS) for protein identification, the mix is generally too complex for the MS techniques to yield sufficient and/or relevant information. This is why gel-based and gel-free approaches are used to fractionate the complex mixtures. In gel-free approaches, liquid chromatography is used to separate the proteins for example according to their hydrophobicity. This allows the collection of fractions that contain only a subset of the complexity of the initial extract. Several fractionations can follow each other to allow for better separation, either with different elution protocols or the use of different separation criteria (Gevaert et al. 2007). The advantage of gel-free approaches is that they allow the study of hydrophilic (soluble) proteins and hydrophobic (membrane) proteins in the same mix. These techniques are also more sensitive, and even low abundance proteins can easily be detected. Peptides can be labeled with different techniques (e.g. ICAT, iTRAQ) prior to fractionation, allowing a relative quantification of the peptides and thus the proteins (Patton 2002).

Gel-based approaches use polyacrylamide gel electrophoresis as a tool for protein separation. The most commonly used technique is a two dimensional electrophoresis (2DE), using in the first dimension a separation according to the protein's isoelectric point (isoelectric focusing, IEF), and in the second dimension a traditional sodium dodecyl sulfate polyacrylamide gel electrophoresis (SDS-PAGE) separation according to the molecular weight (Görg et al. 2000). In this technique protein charges must be conserved for the first dimension, since the isoelectric point of a protein depends on the charges of the residues of charged amino acids and the extremities of the peptidic chain. This also means that charged detergents cannot be used for protein extraction, making the extraction of membrane proteins a challenge. Another example of 2DE is Blue Native electrophoresis (Reisinger and Eichacker 2007; Wittig et al. 2006). For this technique membrane complexes, membrane proteins and/or soluble protein complexes are natively extracted from the membranes using low concentrations of detergents such as dodecylmaltoside, separated on a polyacrylamide gel in native conditions, and in a second dimension separated in denaturing conditions. Contrarily to classical 2DE where proteins are already denatured in the first dimension, Blue Native allows the visualization on the gel of protein complexes and of their subunits. The complexes are separated horizontally on the final gel, and the subunits of the different complexes follow vertical lines below the position of the complexes in the first dimension gel. These techniques are well established, but allow for variation in their use. For instance, membrane proteins can be solubilized using uncharged detergents. This way,

the proteins can be separated by IEF/SDS-PAGE (Babu et al. 2004). The disadvantages of gel-based techniques are the relative difficulty to study membrane proteins compared to gel-free approaches, and that low abundance proteins often remain undetected. The distinctive advantage though is the fact that the proteins are efficiently separated, and ideally only one protein is present in one spot on the gels. Furthermore, with the development of difference-gel electrophoresis (DiGE©, GE Healthcare) the quantification of proteins in a 2D gel and the reproducibility of 2DE have become reliable (Figure 8)(Patton 2002; Skynner et al. 2002). DiGE uses fluorescent dyes to label proteins. Up to three cyanine dyes (Cy2, Cy3 and Cy5) can be used in one single gel. In general, two of the dyes are used to labeling of the samples (Cy3 and Cy5) and one is used to label an internal standard (IS). The IS ideally is a mix of an equal amount of protein from each sample, and allows for standardization of all the gels of an experiment. More reliable than post-staining techniques such as Coomassie blue or silver staining, the DiGE technique has allowed a breakthrough in quantitative proteomics. Many analytical programs for DiGE gel images have been developed by different manufacturers (e.g. Decyder, GE Healthcare; Delta2D, Decodon; Same Spots, Nonlinear Dynamics). These software packages are the most important part of the DiGE system and allow that a huge amount of results is processed relatively quickly and reliably.

Protein identification is generally done by mass spectrometry (e.g. matrix-assisted laser desorption/ionization time-of-flight, Maldi-ToF, quadrupole time-of-flight, Q-ToF). Many different techniques exist, and all are based on the separation of charged peptides in an electromagnetic field. Proteins can be identified by peptide mass finger printing (PMF). Proteins are enzymatically digested before MS analysis, and the mixture of peptides from one gel spot analyzed by MS, resulting in a mass spectrum representing the signal intensity in relation to the mass/charge ratio (m/z) of the analytes. Comparing the experimental MS-spectrum with the theoretical spectrum of database entries allows the identification of the protein. However mainly due to the low specificity of PMF, resulting in both false positive and false negative identifications, this first and simple analysis method is currently questioned and often refused as sole method of protein identification (Song et al. 2010). Therefore, in the case a protein remains unidentified using PMF or to confirm identifications based on PMF, the specificity of the analysis can be increased by tandem mass spectrometry (MS/MS). Precursors (peptides) are selected and fragmented through collisions with inert gas molecules (generally N_2). A mass spectrum of the resulting fragments provides structural information (i.e. the sequence) of the selected precursor. Using specialized software, the resulting fragment mass spectrum can be matched to sequences present in databases (Hubbard 2010).

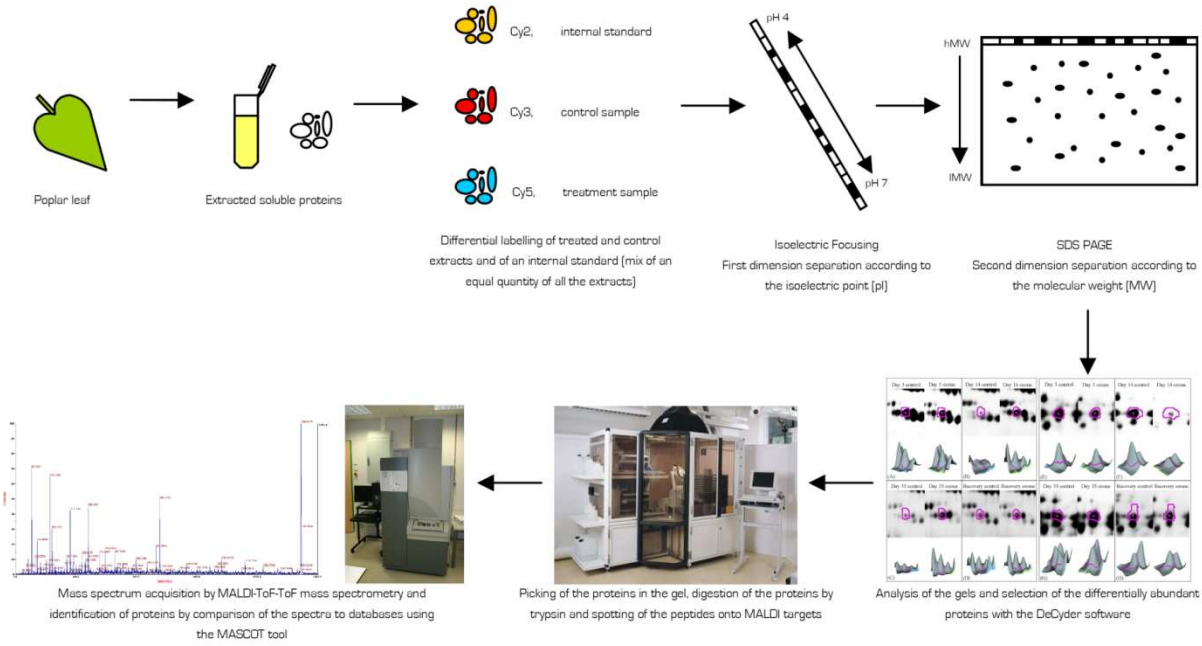

Figure 8: Workflow of a DiGE experiment, from the leaf to the protein identification.

The following section of Chapter 1 is an invited review paper in Mass Spectrometry Reviews that introduces the use of proteomic techniques in ozone research in plants. After the publication of the research paper in Chapter 2 (Bohler et al. 2007), we were invited by an editor of Mass Spectrometry Reviews to write this review. It contains complementary information to the introductory chapter presented above and is a snapshot of the situation of ozone studies at the time it was written.

1.5. Renaut et al. Mass Spectrometry Review 2009, 28:495-516

The impact of atmospheric composition on plants: A case study of ozone and poplar.

Renaut Jenny[1], Bohler Sacha[1,2], Hausman Jean-François[1], Hoffmann Lucien[1], Sergeant Kjell[1], Jolivet Yves[2], Dizengremel Pierre[2]

[1]CRP-Gabriel Lippmann, Department of Environment and Agrobiotechnologies (EVA), Luxembourg
[2]UMR 1137 Ecologie et Ecophysiologie Forestières INRA/UHP, IFR 110 "Génomique, Ecophysiologie et Ecologie Fonctionnelles", Nancy-Université, France

Keywords: High-throughput technologies, model plants, Ozone, poplar, tropospheric pollutants

1.5.1. Abstract

Tropospheric ozone is the main atmospheric pollutant causing damages to trees. The estimation of the threshold for ozone risk assessment depends on the evaluation of the means this pollutant impacts the plant and, especially, the foliar organs. The available results show that, before any visible symptom appears, carbon assimilation and the underlying metabolic processes are decreased under chronic ozone exposure. By contrast, the catabolic pathways are enhanced, participating to the supply of sufficient reducing power necessary to feed the detoxification processes. Reactive oxygen species delivered during ozone exposure serve both as toxic compounds and messengers for the signaling system. In this paper, we show that the contribution of genomic tools (transcriptomics, proteomics and metabolomics) for a better understanding of the mechanistic cellular responses to ozone largely relies on spectrometric measurements.

1.5.2. Introduction

The climate is composed of multiple elements such as solar radiation, temperature, precipitation, wind and so on. All these elements greatly influence the geographical distribution of vegetation, the cropping patterns and the types of vegetation (Viner et al. 2006). Since the beginning of the twentieth century, and especially in the late 50's during the expansion of the industrial era, climatologists hypothesized the impact of human activities on the elevation of greenhouse gases, and particularly CO_2 (Revelle and Suess 1957). The greenhouse effect, or surface warming due to the presence of atmospheric greenhouse gases (Keller 2003), is now considered as a fact and is affecting all ecosystems and living organisms' behavior. The gases involved in greenhouse effect are water vapor (+/- 60%), carbon dioxide (+/- 25%), and ozone (+/- 8%), the rest being traces of mainly methane and nitrous dioxide (Kiehl and Trenberth 1997). The anthropogenic perturbations are

resulting not only from emissions produced by energy use, but can also be a consequence of land use changes and urbanization (Karl and Trenberth 2003). The deforestation in the tropics is also responsible for the release of significant amounts of particulate matter and gases in the atmosphere (Fearnside 2000). There was, and still is, a large debate on the causes of global warming. Some argue that this temperature increase could indeed be due for example to a natural cycle of temperature changes that the Earth was experiencing for hundreds of millenniums or to higher solar activity (Keller 2007). Despite this continuing debate, the recording between 1995 and 2006 of 11 of the 12 years with highest global surface temperature since accurate numbers are available is a fact. In the 4th Assessment report of the Intergovernmental Panel on Climate Change, it is clearly stated that all continents and most oceans are affected by regional climate changes, and that anthropogenic warming influences both biological and physical systems (Parry et al. 2007). This is demonstrated by the melting of glaciers, ice caps or snow cover, the changes in precipitation rates, the sea-level rise, the phenological changes in flora and fauna, changes in community composition and so on.

In parallel to these climatic changes, the amount of pollutants in the atmosphere is also increasing. These anthropogenic molecules, pollutants and factors subject to global change (e.g. drought and CO_2) may interact and even exacerbate effects on plants. In this specific context, we intend to present in this review the impact of pollution and stress on plants via the example of the effect of tropospheric ozone on poplar.

1.5.3. Deleterious effects of stress in plants

Tropospheric ozone is the main component of photochemical air pollution and is recognized as being the cause for considerable damages in both natural and cultivated plants (Kley et al. 1999), including forest trees (Ashmore 2005). It can be surprising to appreciate how negative the impact of tropospheric ozone on human, animals, forest growth, crop yields, and species composition is (Ashmore 2005; Black et al. 2000; Bobbink 1998; Davison and Barnes 1998). However, realizing that ozone can be transported to another continent, and that it has an atmospheric lifetime of 1 to 2 weeks in summer and 1 to 2 months in winter (Akimoto 2003) helps to get a better picture of its putative effect worldwide. Currently, the concentrations of tropospheric ozone in developed and developing countries are above the levels considered as toxic for living organisms (Baldasano et al. 2003). But the question to be raised is: how does such an atmospheric pollutant interact with crop yield and thus disturb plant ecosystem equilibrium? This negative effect is usually referred to as plant stress. For most people, stress refers to the uncomfortable pressure or tension induced by our active and constricting so-called "modern" way-of-life. However, for plant scientists, stress also refers to a set of unfavorable conditions that alter the physiological status of plants. Indeed, farmers

or gardeners have for long known that their crops or their perennials are often able to adapt to different environmental changes but that this flexibility is also limited. Obviously, their adaptability, also known as phenotypic plasticity, is an essential mechanism in the plants' life cycle, since their anchoring to the soil does not allow them to escape adverse conditions. Whilst plant species are often limited to particular ecological niches, the competition pressure between species and between individuals within species forces plants to tolerate less advantageous up to extreme environmental conditions. These unfavorable conditions have been termed as stresses (Gaspar et al. 2002). However, it must be noted that the deviation of an environmental parameter from its optimum does not necessarily result in stress. According to Shulaev et al. (2008), environmental stress could then be defined in plants as changes in growth conditions, within the plant's natural habitat, that alter or disrupt its metabolic homeostasis. Such changes in growth conditions usually require an adjustment of metabolic pathways, aimed at achieving a new homeostasis, in a process usually referred to as acclimation (Mittler 2006). Stress factors, tending to restrict survival, development, geographical distribution and crop yield, may be classified in different ways, according to the authors: e.g. biotic or abiotic stresses and natural or anthropogenic stresses (Lichtenthaler 1996).

Abiotic stress factors cause extensive losses to agricultural plant production worldwide. Accordingly, individual or combined stress conditions have been studied elaborately by plant physiologists and molecular biologists. Because environmental factors such as salinity, drought and temperature are often the most important limitations to crop productivity, their effects on plants have been the topic of numerous scientific reports. However, the changes in the chemical climate of Europe and North America are nowadays an issue of growing concern. The climate, but also the chemical compositions of rainfall and the troposphere are being modified by anthropogenic emissions associated mainly with the combustion of fossil fuels. Consequently, beside the classical stress factors, mentioned above, emerging stressors (like tropospheric ozone), which were not previously met by plants during evolutionary times, start to cause injury to the ecosystems. Of course, plants are known to be acclimatizable to a quite large extent to non-optimal growth conditions, and in the field, plants are used to be routinely subjected to a combination of different abiotic stresses. In addition, tolerance to one or a combination of several different abiotic stresses is a well-known breeding target in crops, and successes are not exceptional. Nonetheless, little is known about the molecular mechanisms underlying the acclimation of plants at a long-term realistic exposure to specific stressors.

With the advent of the genomic era, it became obvious that a centralization of the research efforts was required. Consequently, and almost spontaneously, some model plant species imposed themselves to the plant scientists' community.

1.5.4. Poplar as a model for plant stress studies

Arabidopsis thaliana and rice (*Oryza sativa*) were the first plants whose genomes were completed (International Rice Genome Sequencing Project, 2005; The *Arabidopsis* Genome Initiative, 2001). These two plants have been considered as models for dicotyledons and monocotyledons, respectively. The completion of these two genomes opened new perspectives in molecular biology, particularly for large-scale analyses, such as genomics, transcriptomics and proteomics. Although an important number of physiological aspects can be approached by studying these two plants, the huge diversity of the plant kingdom cannot be covered by only two plants. In particular, woody (trees and shrubs) and herbaceous species are showing striking differences (Sterky et al. 2004). Woody plants are forming hard and long-lasting structures critical for their survival stature, competitive ability, and provision of habitat. These structures are very distinct from the soft stems or branches of herbaceous (especially annual) plants. Phenomena specific to trees can only be fully expressed after several years, such as wood formation, transition between juvenile and mature states, maturation or seasonality. Similarly, trees in temperate climates must also be able to withstand severe winter conditions and, to achieve this *sine qua non* condition allowing survival for many years, need to adapt their growth to the seasons. These specificities have raised the question of introducing the genome of a tree in the list of model species (Brunner et al. 2004). The choice of *Populus* was driven by its relatively small genome (550.10^6 bp), the rapid growth rate (some may reach up to 3 meters per year), a diploid inheritance, simplistic clonal propagation and because it can easily be transformed by *Agrobacterium tumefaciens* (Bradshaw et al. 2000). Furthermore, although being fundamentally different, *Arabidopsis thaliana* and poplars are phylogenetically relatively related, thereby allowing comparative biology for mechanisms conserved among angiosperms (Jansson and Douglas 2007).

Populus, from the *Salicaceae* family, is widely spread in the Northern hemisphere, on the European, the American and the Asian continents. The genus *Populus* represents more than 40 widely distributed species that cover many combinations of environmental aspects (e.g. from Arctic Circle down to North Africa). This also signifies that a broad spectrum of clones and hybrids is currently available to multiple purposes, both for scientific and applied purposes.

Besides being a model plant, *Populus* trees have also a quite important ecological and economical impact. They are used as shelterbelts and windbreaks, in bioenergy (biomass for wood and energy), in phytoremediation, against soil erosion (Isebrands and Karnosky 2001) but also as a high value wood for plywood applications. All these characteristics made *Populus* an ideal subject to become the model plant for woody species. In the 1990's already, *Populus* species were used for QTL

mapping (Bradshaw et al. 2000). Actually, in January 2008, more than 415000 *Populus* EST sequences are available in the NCBI database (http://www.ncbi.nlm.nih.gov/) for *Populus*. The completion of the genome sequencing of *Populus trichocarpa* was presented in 2006 (Tuskan et al. 2006).

1.5.5. Atmospheric pollution

The troposphere is the part of earth's atmosphere in which we live and where almost all human activities take place (Oke 1987). It ranges from the earth's surface to 10 to 15 km in height. The chemistry of the troposphere is very complicated and its equilibrium depends both on the processes of living organisms and ecosystems as well as on physical and chemical alterations of its properties. During the last century, industrialization and human activities (e.g. home heating or combustion engines) have influenced the tropospheric equilibrium, thereby leading to a variety of tropospheric compounds which, in high concentrations, must be considered as pollutants due to their often negative effects on animal and plant health (Lighty et al. 2000). The major elements of tropospheric compounds are nitrogen and sulfur, mainly as oxides, and carbon that is generally present in the form of hydrocarbons. Metals and halogen elements can play a role in the form of different salts or particles. In this chapter, we will give a brief overview of the most important tropospheric compounds and the reactions they are involved in.

Particulate matter in the troposphere can be solid or liquid. Ninety percent of tropospheric particles come from natural sources. They originate from volcanoes, forest fires, sea spray and wind action, but also include suspended bacteria and spores or pollen (Finlayson-Pitts and Pitts 2000). The anthropogenic part comes from combustion (coal, oil, waste, car exhaust) and from industrial processing (Viner et al. 2006). Particles are present in diameters ranging from 100 to less than 0.1 µm. Depending on the size, they remain suspended in the troposphere for longer or shorter time ranges, where the duration shortens with increasing size, and the migration distance of the particles changes accordingly. Particulate matter contains mostly carbon and silica, but can carry a vast range of metals, heavy metals and halogens.

Sulfur is present in the troposphere mainly as sulfur dioxide (SO_2) and hydrogen sulfide (H_2S), but also as sulfurous (H_2SO_3) and sulfuric acid (H_2SO_4) and sulfate salts in particulate matter (Oke 1987). Sixty-six percent of the tropospheric sulfur is emitted naturally and the major part is H_2S originating from bacteria. The combustion of sulfur binding fuels (e.g. coal, oil) by human activity counts for the second biggest participant of tropospheric sulfur, SO_2. In the troposphere, SO_2 is easily oxidized to sulfur trioxide (SO_3), which can react with water vapor to form H_2SO_4. Sulfuric acid is the major

component of acid rain, and together with settling sulfuric particles responsible for the acidification of soils around important sulfurous pollution sources.

Two carbon oxides can be found in the troposphere, carbon monoxide (CO) and carbon dioxide (CO_2) (Grace and Zhang 2006). Carbon monoxide is produced by incomplete combustion of carbon-based molecules, and the major source of CO is the combustion engine, thus road traffic. It is a very stable molecule but is absorbed effectively by oceans and soil microorganisms. Carbon dioxide is naturally produced by most living organisms through respiration, a production that is partially counterbalanced by the fixation of CO_2 either biologically (photosynthesis) or physically thus creating a natural equilibrium. An additional source of CO_2 is the complete combustion of carbon-rich molecules by human activity, thus increasing the CO_2 emissions and leading to an increase in CO_2 concentrations since the natural sinks can no longer cope with the quantity produced. Since ruminating animals release relatively high quantities of CO_2 and methane into the troposphere, intensive farming methods cannot be neglected as an additional source of atmospheric carbon dioxide.

Volatile organic compounds (VOC) originate mostly from natural sources, notably from the decomposition of vegetation. Only a small part is due to human activity, but a range of potentially toxic and very reactive molecules (e.g. acetaldehyde, formaldehyde, ethane) are added to the set of molecules present naturally (mainly methane). Once again the major source of anthropogenically formed VOCs is road traffic.

Nitric oxides are naturally formed by the decomposition of organic matter in soil and oceans. Through combustion of various compounds (e.g. coal, gas) and industrial activity (notably fertilizer factories) human activity produces nitrogen monoxide (NO). In itself a relatively harmless gas, it is easily oxidized to nitrogen dioxide (NO_2) in the troposphere, an irritant gas that is also involved in the formation of secondary pollutants like ozone (O_3).

In addition to these primary pollutants, a range of secondary pollutants, originating from the interaction of the aforementioned molecules, are present in the troposphere. One of the most important secondary pollutants is ozone (Oke 1987).

Ozone is formed by the interaction of NO_2 and the UV radiation of the sun. NO_2 absorbs UV radiation which results in the decomposition of the molecule into NO and an activated oxygen atom ($O^{\bullet -}$). On contact with molecular oxygen (O_2) O_3 is formed. The reaction is reversible when O_3 and NO react to form O_2 and NO_2, thus theoretically completing a cycle without net O_3 formation. But O_3-formation

only concludes a series of chemical reactions that transform NO to NO_2 before the cycle can be completed, thus consuming NO and replenishing the NO_2 pool (Figure 9). In the troposphere, hydroxyl radicals (OH) are always present. They act like a "detergent" for the troposphere by oxidizing and thus initializing the degradation of tropospheric molecules. Hydroxyl radicals themselves are formed mainly through photodissociation of O_3, resulting in the formation of activated oxygen atoms. Upon reaction of these activated oxygen species with water molecules, OH radicals are formed (Andreae and Crutzen 1997). This is the main source of OH radical formation, since O_3 and water vapor are relatively abundant in the troposphere, but some minor sources not presented here exist (Monks 2005).

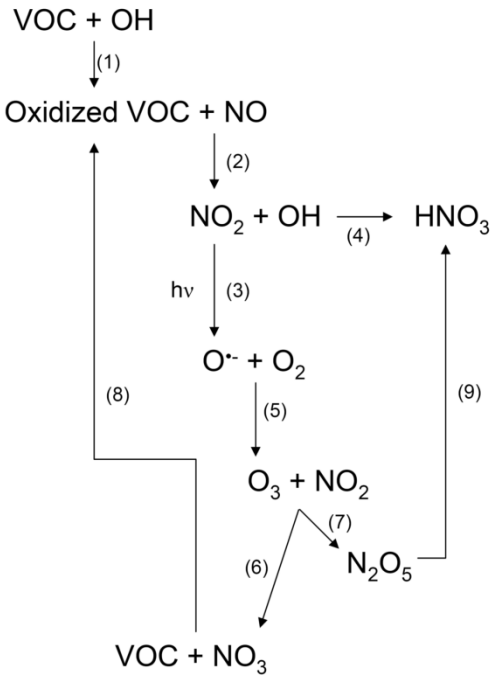

Figure 9: Tropospheric reactions of secondary pollutant formation. Starting with VOC oxidation and NO_2 formation, several reactions follow to form several compounds. (1) VOCs are oxidized by OH radicals. (2) Oxidized VOC can be reduced through NO to form NO_2, and the further pathway of the VOC often regenerates OH. (3) Under the influence of light, NO_2 fragments into NO + $O^{\bullet-}$. (4) NO_2 can also react with OH to form HNO_3. (5) $O^{\bullet-}$ + O_2 form O_3. (6) If enough O_3 and NO_2 are present, then they can react to form NO_3 (7) or N_2O_5. (8) NO_3 can oxidize VOC and thus "complete" a cycle. (9) N_2O_5 can form HNO_3 on contact with wet surfaces that included small atmospheric particles.

Hydroxyl radicals are very reactive and will oxidize many tropospheric components, notably VOC (n°1 on Figure 9). The subsequent decomposition can, under the right concentrations of both VOC

and NO, convert NO to NO_2 (2), thus fuelling the before mentioned reaction in which ozone is formed (3, 5). Hydroxyl radicals are very often regenerated after the complete oxidation of the VOC thus acting like a catalyst. But O_3 is not the only compound that can be formed from this point forward. Nitrogen dioxide can directly be oxidized by OH radicals to form nitric acid (HNO_3) (4). Furthermore NO_2 can react with O_3 to form NO_3 (6) or dinitrogen pentoxide (N_2O_5) (7) where the latter can lead to HNO_3 on contact with wet surfaces (9) (e.g. particulate matter) while NO_3 is capable of oxidizing VOC and thus refueling the cycle (8) (Finlayson-Pitts and Pitts 1997).

1.5.6. A special case among pollutants: tropospheric ozone

Different environmental factors are thought to affect plant growth and development by causing the excess accumulation of ROS (Wohlgemuth et al. 2002). Among these stressing agents are UV-B radiation and many air pollutants. Tropospheric ozone is the main component of photochemical air pollution and is recognized as being the cause for considerable damages in both natural and cultivated plants (Kley et al. 1999), including forest trees (Ashmore 2005).

Ozone concentrations in the troposphere increased four-fold during the last century and show peak values of 100-400 $nl.l^{-1}$ in urban and suburban areas worldwide (Kley et al. 1999; Marenco 1994). The definition of a unique threshold for risk assessment for natural stands and/or fields in Europe is made difficult due to the particularities of crops and trees, of the varying climatic conditions between northern and southern countries and the possible interaction with other constraints.

The concept of a critical level for ozone in Europe, introduced by UNECE (United Nations Economic Commission for Europe) was originally based on the accumulated exposure over a threshold concentration of 40 ppb (AOT40). A surplus of a threshold value for AOT40 of 10 ppm.h would indicate a risk of biomass loss of 10% (Vestrengen et al. 2004). More recently, a flux-based concept was developed in order to take into account the actual ozone flux in the leaf throughout the stomata (Ashmore et al. 2004; Emberson et al. 2000; Grünhage et al. 2004; Karlsson et al. 2004). Since, among the factors controlling the stomatal aperture, drought episodes and level of atmospheric CO_2 are predicted to increase in the future, the related decrease of stomatal conductance could protect plants (Tausz et al. 2007). This hypothesis, however, does not consider that the closure of stomata would have a negative impact on the net photosynthesis and consequently on crop yield. Ozone and factors linked to climate change (e.g. drought and CO_2) can however interact in more complicated ways (Matyssek et al. 2006) and this flux-based method presents limitation by ignoring the defense mechanisms of leaf cells (Matyssek et al. 2004). The concept of an “effective ozone flux”, which is

the balance between stomatal flux and intra-leaf detoxification capacity, has thus been proposed (Dizengremel et al. 2008; Musselman et al. 2006; Tausz et al. 2007; Wieser and Matyssek 2007).

In addition, especially in trees, interactive reactions were observed between ozone and VOC (isoprenoid compounds; (Loreto and Fares 2007; Loreto et al. 2004)). Ozone is able to increase the intracellular synthesis of these compounds which, once emitted, can contribute to the scavenging of ozone, thus modifying stomatal O_3 uptake (Fares et al. 2008; Loreto and Fares 2007).

1.5.7. Impact of ozone on plant cell metabolism

Two main approaches have been used to study ozone exposure consequences in plants. The first approach consists in exposing the plants for a short duration (from a couple of hours to maximum 2 days) to a peak value of ozone ranging from 300 ppb up to 1 ppm, also named 'acute ozone exposure'. This approach is valid when trying to describe visible symptoms in crops, but has been more and more replaced by a more realistic long-term (several weeks) weaker exposure of 100-300 ppb as summarized in Figure 10 (Samuelson and Kelly 2001).

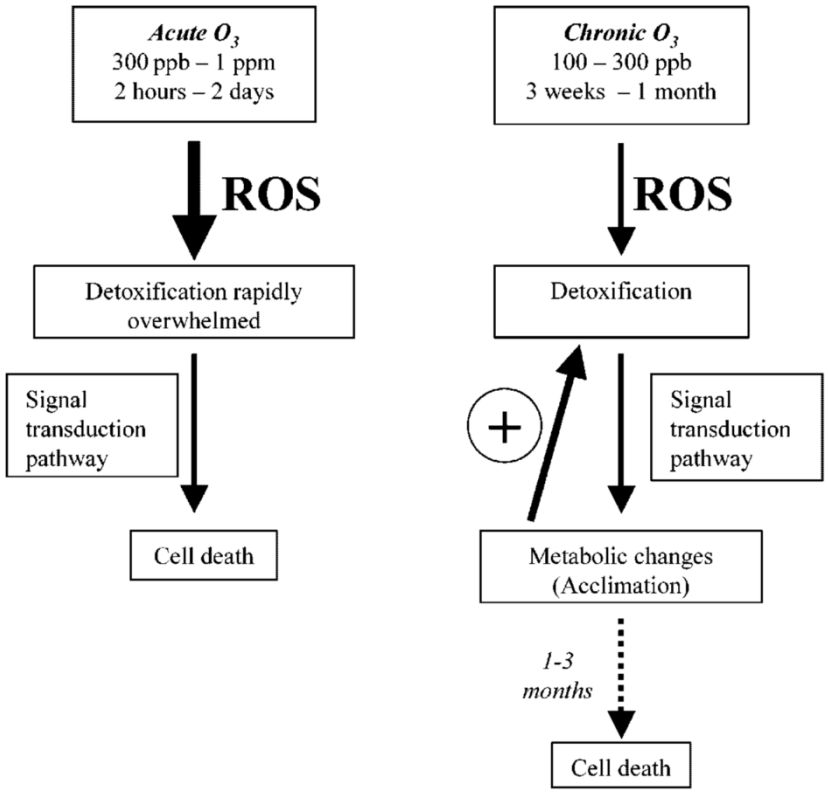

Figure 10: Schematic comparison of the different types of treatment commonly used in studies of plants exposed to ozone.

In optimal conditions, ROS are produced by reactions taking place at the level of the electron transport chains of chloroplasts and mitochondria and they are successfully removed by detoxification processes. An ozone attack however causes an increased production of ROS that are able to decrease the antioxidant capacity mainly present in the form of ascorbate, both in apoplast and inside the cell. The level of the perturbing ROS concentration partly depends on the external ozone concentration, but the degree of stomatal aperture heavily contributes to the flux regulation. An acute exposure (high concentration of ozone for a few hours or days) can rapidly lead to cell death whereas a chronic exposure, at least for the low doses, will allow the plants to acclimate. Acclimation is linked to a cellular mechanism including metabolic changes allowing an increase of detoxification processes as well as the occurrence of other defense systems (Foyer and Noctor 2003).

However, a prolonged exposure to realistic concentrations of ozone could lead to carbon disequilibrium, a progressive loss of chlorophylls and, ultimately to visible symptoms linked to cell death.

In this article, although the literature of the past 20 years has been examined for acute and chronic exposures and summarized in Table 2, we will focus on the effects of chronic ozone exposure, closer to realistic current conditions in the atmosphere

Table 2: This table is a non exhaustive synthesis of the last 20 years of research on ozone and plants. In this table we present articles divided in 2 main categories, acute and chronic stress, where acute studies use high ozone concentrations for short times (hours to days), and chronic studies use low to high concentrations for longer time periods (weeks, years, up to several growing seasons). Furthermore are presented detailed concentrations, plant type, the approach used in the study and the approximate age of the studied plants (y: young; a: adult; s: seedlings).

Treatment	Concentration (ppb)	Plant	Approach	Plant age	Reference
acute	300	Spinach	biochemical	s	(Luwe et al. 1993)
	300	Arabidopsis	biochemical	s	(Rao et al. 2002)
	300	Arabidopsis	biochemical	s	(Tuominen et al. 2004)
	300	Arabidopsis	biochemical	s	(Rao et al. 2000b)
	150-400	Tobacco	biochemical, molecular, morphological	s	(Schraudner et al. 1998)
	250	Arabidopsis	molecular	s	(Conklin and Last 1995)
	350	Arabidopsis	transcriptomic	s	(Ludwikow et al. 2004)
	200	Arabidopsis	transcriptomic	s	(Matsuyama et al. 2002)
	200	Rice	proteomic, morphological	s	(Agrawal et al. 2002)
	200	Bean Maize	proteomic, morphological, molecular	s	(Torres et al. 2007)
	200	Rice	integrative	s	(Cho et al. 2008)

	150	Poplar	physiological	y	(Guidi et al. 1998)
	180	Poplar	physiological, biochemical	y	(Gupta et al. 1991)
	100-300	Poplar	physiological, biochemical, morphological	y	(Strohm et al. 1999)
	300	Poplar	physiological, molecular, morphological	y	(Koch et al. 1998)
	150	Poplar	physiological, biochemical, molecular	y	(Ranieri et al. 2000)
	200	Birch	biochemical, morphological	y	(Vahala et al. 2003)
	300	Poplar	biochemical, molecular	y	(Koch et al. 2000)
	150	Poplar	biochemical, molecular, morphological	y	(Diara et al. 2005)
chronic	77	Soybean	biochemical	s	(Cheng et al. 2007)
	40-80	Bean	biochemical	s	(Leitao et al. 2007b)
	70	Plantago	biochemical	s	(Lyons et al. 1999)
	150, 300	Arabidopsis	molecular	s	(Sharma and Davis 1994)
	150	Arabidopsis	molecular	s	(Miller et al. 1999)
	150	Arabidopsis	transcriptomic	s	(D'Haese et al. 2006)
	40-120	Rice	proteomic, molecular, morphological	s	(Feng et al. 2008)
	50-130	Birch	morphological	y	(Pääkkönen et al. 1995)
	elevated	Poplar	morphological, physiological	y	(Yun and Laurence 1999)
	elevated	Poplar	morphological, physiological	y	(Bortier et al. 2000)
	elevated	Beech	physiological	a	(Löw et al. 2007)
	40, 90	Birch	physiological, biochemical	y	(Einig et al. 1997)
	elevated	Beech	physiological, biochemical	a	(Blumenröther et al. 2007)
	200	Maple	biochemical, physiological	y	(Gaucher et al. 2003)
	50-300	Maple	biochemical, morphological	y	(Gaucher et al. 2006)
	90	Birch	biochemical	y	(Landolt et al. 1997)
	elevated	Beech	biochemical	a	(Haberer et al. 2007)
	200	Spruce	biochemical	y	(Sehmer et al. 1998)
	ambient	Spruce Beech	biochemical	y	(Lux et al. 1997)
	200	Pine	biochemical	y	(Fontaine et al. 1999)
	200	Pine	biochemical, molecular	y	(Fontaine et al. 2003)
	60	Poplar	biochemical, molecular	y	(Ranieri et al. 2001)
	60, 120	Poplar	biochemical, molecular	y	(Cabané et al. 2004)
	60	Poplar	biochemical	y	(Degl'Innocenti et al. 2002)
	120	Poplar	proteomic, biochemical, morphological	y	(Bohler et al. 2007)
	elevated	Birch	metabolomic, biochemical, morphological	y	(Kontunen-Soppela et al. 2007)

1.5.7.1. Ozone, ROS and signaling

In the apoplast of plants ozone rapidly reacts with water and cellular constituents leading to the generation of reactive oxygen species in an oxidative burst, resembling that induced by avirulent pathogens (Overmyer et al. 2003; Overmyer et al. 2000; Wohlgemuth et al. 2002). This biphasic oxidative burst is generated and maintained, after perception of the presence of ozone, by the action of superoxide-generating NADPH-oxidase and other cell wall oxidases (Joo et al. 2005). Because of this similarity it is not surprising that an overlap exists between the downstream signaling pathways of plant hypersensitive response and ozone. The knowledge on ozone-induced signal transduction was reviewed by (Rao and Davis 2001), and their hypothetical model illustrates the

complexity of the signal transduction. Several plant hormones were shown to have an antagonistic impact on ozone-induced cell death. While ethylene and salicylic acid initiate and propagate the spread of lesions, jasmonic acid appears to be a major determinant in containment (Overmyer et al. 2000; Rao et al. 2000b; Vahala et al. 2003), partially by direct suppression of ethylene signal transduction (Tuominen et al. 2004). However, the regulation of the balance between these components is more complex, involving a rapid increase in ethylene and a slower rise in jasmonic acid. This observation suggests that ethylene functions early and it has been shown before that the early accumulation of ROS responsible for the spreading of cell death is indeed ethylene dependent (Moeder et al. 2002). Nonetheless, ethylene is also thought to counteract the spread of lesions. Through ethylene-induced expression of ethylene receptors some of the increased number of receptors is no longer occupied resulting in desensitization of ethylene signaling (Moeder et al. 2002; Wang et al. 2002). This mechanism could partially explain the antagonistic effects of jasmonic acid and ethylene (Schenk et al. 2000). What becomes apparent is a complex picture, with the plant growth regulators salicylic acid, jasmonic acid, abscisic acid and ethylene interacting with the levels of ROS to fine-tune the response (Kangasjärvi et al. 2005; Rao et al. 2002). Despite the different studies, spurred by the higher impact of ozone on agriculture in a changing environment, several key-questions concerning ozone detection and signal transduction are unanswered and contradicting results have been obtained in different studies. Furthermore, signal transduction seems to be highly dependent on the species used but also on the developmental status of the plant and on the microenvironment where the samples are taken. A striking example of this difference is the expression of salicylic acid induced (mitogen-activated protein kinase) MAPK. Although this gene is rapidly induced after exposure of tobacco (Samuel et al. 2000), no changes in expression of this gene were recorded in ozone-treated mature beech (Jehnes et al. 2007).

1.5.7.2. Effects on metabolic pathways

The effects of a chronic exposure to ozone (100-300 ppb) on plants are based on the succession of a series of events (Figure 11): uptake of the pollutant, production of ROS, attack of cell membranes resulting in the decrease of the anti-oxidative detoxification capacity, changes in metabolic pathways up to a possible disequilibrium in carbon budget. These biochemical events are known as “hidden injury” and precede changes in growth and appearance of visible symptoms (chlorosis, necrosis).

During the daylight, when photosynthesis is active, and when there is no strong drought the leaf stomata are generally widely open to allow the uptake of CO_2 and the release of O_2. Concomitantly, ozone molecules enter the plant leaves through the stomata, which could be considered as the main obstacle to the ozone flux (Kollist et al. 2000). However, different studies showed that the stomatal

and internal resistances to ozone are very low, depending on the calculation mode (van Hove et al. 1999). On contact with the apoplast, the molecule fragments into ROS (Kanofsky and Sima 1991; Kanofsky and Sima 1995; Laisk et al. 1989). Several studies pointed out that stomatal conductance of plants exposed to ozone decreases (stomatal closure) (Bortier et al. 2000; Guidi et al. 2001; Moraes et al. 2006), but other showed no effect (Fontaine et al. 1999; Guidi et al. 2001; Reichenauer et al. 1997) or even a rise in stomatal conductance (Padu et al. 2006). Usually, ozone tolerant plants close their stomata in response to the pollutant, which is described as an avoidance mechanism, in contrast with sensitive ones. Although the stomata are the most efficient entrance point of ozone into plant leaves, direct attack of the surface of the leaves, more precisely the cuticle and leaf resins by ozone is documented (Mankovská et al. 2005). Thereby the leaf surface is damaged and this very important defense line that protects the leaves against water loss, pathogen intrusion and mechanical wounding is stripped off.

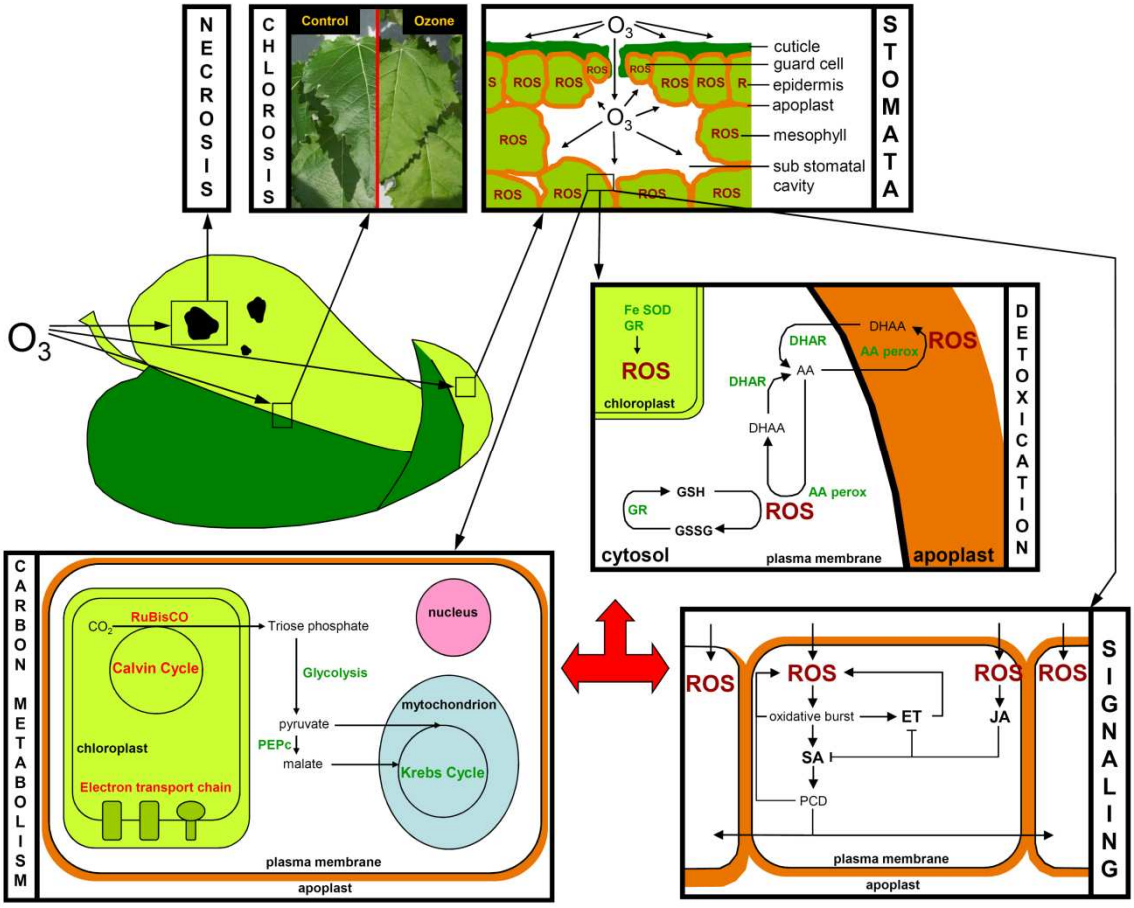

Figure 11: This figure illustrates the most important aspects of the effects of ozone on plant leaves: Visual symptoms: the development of necrosis and chlorosis on the leaves can be observed upon ozone exposure; Stomata: the diffusion of ozone into the leaves via the stomata to the primary sites of contact; Detoxification: the

most important detoxification pathway for ozone is ascorbate, other pathways that involve SOD and glutathione are also induced; Signaling: ozone activates ethylene/salicylic acid and jasmonate signaling pathways that lead to different responses, the jasmonic acid pathway can inhibit the routes of ethylene and salicylic acid; Carbon metabolism: photosynthesis is generally reduced during exposure at the photochemical and the biochemical levels, whereas respiration is increased, including the anaplerotic pathway that involves PEPc. AA: ascorbic acid, AAperox: ascorbic acid peroxidase, DHAA: dehydroascorbic acid, ET: ethylene, GR: glutathione reductase, GSH: reduced glutathione, GSSG: oxidized glutathione, JA: jasmonic acid, PCD: programmed cell death, PEPc: phosphoenolpyruvate carboxylase, ROS: reactive oxygen species, RuBisCO: ribulose-1,5-bisphosphate carboxylase/oxygenase, SA: salicylic acid, SOD: superoxide dismutase.

ROS, issued from ozone, trigger an antioxidant response (Baier et al. 2005). They first impact the cell wall and can be detoxified by ascorbate (Plöchl et al. 2000). However, the ascorbate pool is quickly exhausted (Iglesias et al. 2006) and if the regeneration and transport to the apoplast are not efficient enough (Luwe et al. 1993), ROS accumulate inside cells causing damage and producing yet more reactive molecules. This increase in the oxidative load of the cells creates an oxidative stress, to which the cell mechanisms have to adapt to avoid further damage. Several studies have looked into the importance of detoxification mechanisms, which could be considered as constitutive and inductive, during ozone stress (Musselman et al. 2006). A first constitutive detoxifying barrier represents the total antioxidant system (apoplast + symplast) at the time of ozone attack. This first barrier is tightly related to the level of ascorbate, mostly apoplastic one, which was primarily proposed as a good indicator for ozone tolerance (Tausz et al. 2007; Turcsányil et al. 2000). However, high apoplastic ascorbate levels do not correctly explain ozone tolerance (D'Haese et al. 2005; Eller and Sparks 2006) and the antioxidative capacity of the apoplastic space can be overwhelmed (Foyer and Noctor 2005). An inductive response has thus to take place, allowing exchanges of antioxidants between the symplastic detoxification system and the apoplast (Dizengremel et al. 2008; Noctor 2006). The symplastic system for regenerating antioxidants is more sophisticated, implying metabolites as glutathione and NAD(P)H, the latter appearing as a key compound for supplying the needed reducing power (Dizengremel et al. 2008; Noctor 2006).

Genetically modified plants over-expressing dehydroascorbate reductase present an increased resistance to ozone stress, while plants inhibited for this enzyme become more sensitive (Sanmartin et al. 2003). Other authors demonstrated that ascorbate peroxidase activity and mRNA increased during ozone stress (Sehmer et al. 1998; Wiese and Pell 1997). A study on wheat and tobacco plants

over-expressing dehydroascorbate reductase (DHAR) highlighted the central role of this enzyme for ascorbate production and stomatal movement. It was shown that the rise of ascorbate level through DHAR provides better protection against oxidative stress as compared to a reduced stomatal conductance (Chen and Gallie 2005).

The capacity to maintain and regenerate the detoxifying potential of leaves, linked to the amount of available NAD(P)H, ultimately depends on the changes in carbon metabolism (Dizengremel 2001). In general it can be stated that photosynthesis is repressed during ROS-challenge, while the respiration pathways are enhanced (Dizengremel and Petrini 1994). Many studies on different organisms and with different fumigation kinetics and concentrations showed that carbon fixation rates or net photosynthesis drop under ozone stress (Guidi et al. 2001; Guidi et al. 1998; Reichenauer et al. 1997; Zheng et al. 2002). It must be noted that juvenile trees are more sensitive than mature trees (Wittig et al. 2007). Ribulose-1,5-bisphosphate carboxylase/oxygenase (RuBisCO), the primary carbon fixation enzyme in C3 plants, presents a decreased activity (Degl'Innocenti et al. 2002; Dizengremel et al. 1994; Fontaine et al. 1999; Pell et al. 1992; Pelloux et al. 2001). A reduced abundance of large and small RuBisCO subunit mRNA (Bahi and Kahl 1995; Pelloux et al. 2001) as well as reduced protein abundance (Bohler et al. 2007; Fontaine et al. 1999; Gaucher et al. 2003; Landry and Pell 1993; Pelloux et al. 2001; Wiese and Pell 1997) have been demonstrated. Changes in RuBisCO structure are also possible, leading to aggregation and increased destruction of existing molecules of this enzyme (Junqua et al. 2000; Landry and Pell 1993). Reduction of RuBisCO activase mRNA and protein content have also been observed (Degl'Innocenti et al. 2002; Pelloux et al. 2001), underlining the effects on the biochemical part of photosynthesis. Further abundances of enzymes of the Calvin cycle decreasing after ozone stress are triose-phosphate isomerase, aldolase, sedoheptulose-1,7-bisphosphatase, ribulose-5-phosphate-3-epimerase and phosphoribulokinase (Bohler et al. 2007). Effects on the photochemistry are also visible, in studies showing a higher turnover of the Photosystem II (PSII) D1 protein (Goode and Buchhold 1992; Ranieri et al. 2001) or a reduced abundance of oxygen evolving complex proteins (Ranieri et al. 2001). A similar conclusion could be drawn from the observation of diminished chlorophyll and carotenoid contents (Bortier et al. 2000; Iglesias et al. 2006; Ranieri et al. 2001) as well as of the induction of the xanthophyll pathway (Ranieri et al. 2001). Still, the quantum efficiency and quantum yield seem to remain stable in resistant ecotypes while it decreases in sensitive ones (Guidi et al. 2001), showing the capability of some plants or ecotypes to adapt the photosynthetic mechanisms to the stress at hand.

During chronic ozone treatment in C3 plants, the progressive decrease in RuBisCO activity and quantity is interestingly accompanied by a strong increase in phosphoenol pyruvate carboxylase

(PEPc) activity (Degl'Innocenti et al. 2002; Fontaine et al. 2003; Fontaine et al. 1999; Gaucher et al. 2003; Gaucher et al. 2006; Leitao et al. 2008; Sehmer et al. 1998), mRNA (Fontaine et al. 2003) and protein abundance (Fontaine et al. 2003; Fontaine et al. 1999) (Figure 12). This stimulation of PEPc activity, linked to the anaplerotic pathway, is also related to more intense activities of several enzymes of glycolysis and pentose phosphate pathway (Dizengremel et al. 2008; Dizengremel and Petrini 1994; Dizengremel et al. 1994; Sehmer et al. 1998) providing a higher amount of reducing power for repair and detoxification mechanisms. By contrast, in C4 plants, where PEPc is the primary carbon fixing enzyme, there is a strong decrease of PEPc and a weaker diminution of RuBisCO, the stomatal resistance giving the impression to be the principal factor of resistance to ozone (Leitao et al. 2007a).

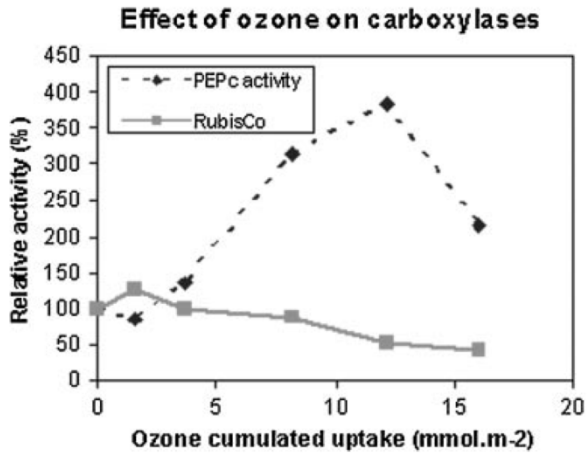

Figure 12: Changes in RuBisCO and PEPc activities of poplar mature leaves fumigated during 1 month with 100 ppb ozone.

In C_3 plants, an important unsolved question concerns the unavoidable competition for PEP between the anaplerotic pathway and the isoprenoid synthesis pathway (Loreto et al. 2007). A third competing pathway is the phenylpropanoid pathway linked to the increased synthesis of phenolic compounds and lignins (Cabané et al. 2004).

1.5.8. High-throughput technologies bring new insights on effects of ozone in poplars

Nowadays, taking largely advantage of the availability of fully sequenced genomes of *Arabidopsis*, rice or *Populus*, large-scale/high-throughput tools are available to approach relevant biological issues and unravel the interaction and the regulation of complex molecular networks. The primary goal of "omics" strategies is the non-targeted identification of all gene products present in a determined

biological sample (Weckwerth 2003). By their nature, these technologies reveal unexpected properties of biological systems. Among these tools of the functional genomics era, transcriptomics, metabolomics and proteomics (Figure 13) are the most commonly used quantitative techniques. Transcriptomics allows the analysis of expression of thousands of mRNAs via microarray studies; metabolomics is used for profiling of the metabolite composition and proteomics, the complement of proteins present in a cell, a tissue or an organism at one time point. Contrary to the genome, entities such as the transcriptome, proteome and metabolome are highly dynamic and their composition greatly depends on the interaction between the genome of the target of the study (representing the potential) and its environment.

Taken together, the development of these different approaches resulted in a paradigm shift in the way scientists are running experiments. Instead of using hypothesis-driven analyses, data are collected in a non-biased and broader way (Holtorf et al. 2002). However, this could also bring some new questions as a lot of genes or proteins cannot be assigned to a certain function.

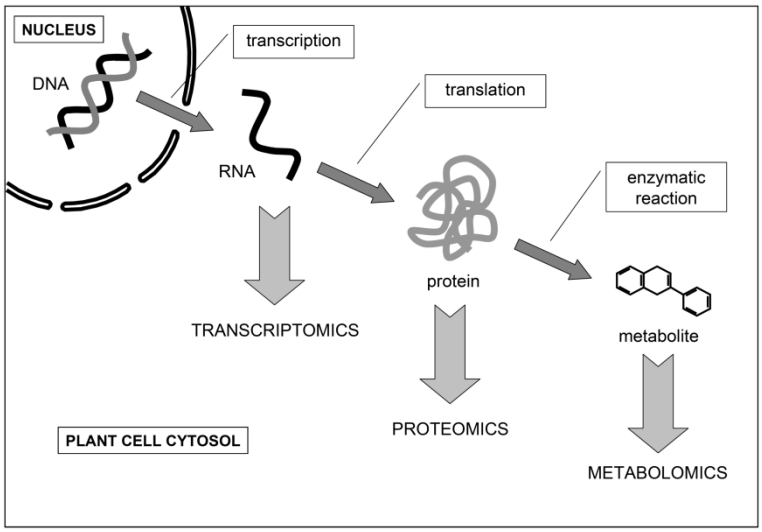

Figure 13: From DNA to metabolites. This scheme illustrates the different steps from transcription over translation to the enzymatic reaction that lead from a gene to a metabolite. After each step, the pool or part of the pool of RNAs, proteins, or metabolites can be studied with the so-called relevant 'omics' techniques, transcriptomics, proteomics, and metabolomics, respectively.

Although it is really tempting to compare the results obtained via the different techniques, discrepancies usually appear between the data. This can be due to technical limitations and/or different statistical treatments, as well as the fact that variations observed at one level cannot

always be traced back to another level due to post-translational modifications, but also turnover rates of metabolites, or changes in biochemical properties of the enzymatic pathways.

1.5.8.1. Transcriptomics

Changes in mRNA levels are mostly due to variations in the transcriptional rate of genes. They indicate changes in the environment or the developmental program or a response to external stimuli (Holtorf et al. 2002).

A large part of the works on transcriptome patterns in plants treated with ozone relates to acute ozone exposure. This latter condition leads to the occurrence of a rapid ROS burst which, by itself or by the intermediary of other signaling molecules, could trigger multiple signaling pathways able to modify gene expression (Desikan et al. 2001; Grant et al. 2000; Mahalingam et al. 2006). With an ozone-sensitive ecotype, genes with hydrolase activity are rapidly up-regulated, suggesting the occurrence of an oxidative cell death pathway (Mahalingam et al. 2006). By contrast, genes with associated functions in carbon assimilation and energy are down-regulated as well as genes with signal transduction function which could be involved in stress/defense signaling. Ethylene, which was often associated with ozone sensitivity, appears to be involved in the regulation of some of these genes. However, ethylene signaling may also dominate in the early regulation of genes for the ozone tolerant *Arabidopsis* ecotype (Col-0) submitted to acute ozone exposure (Tamaoki et al. 2003). In this ecotype, numbers of significantly up-regulated genes are categorized in the rescue/defense genes. In fact, at an early stage of ozone fumigation, ethylene signaling does not operate alone but jasmonic acid signaling takes also place while salicylic acid tends to act as an antagonist. An opposite behavior occurs at a later stage (48h) with the down-regulation of ethylene and jasmonic acid synthesis simultaneously to the salicylic acid synthesis (D'Haese et al. 2006). At this later stage, genes involved in programmed cell death and senescence are up-regulated. Thus, a complex network of interaction between hormones takes place to regulate gene expression in response to an acute ozone dose and to confer ozone tolerance or sensitivity (Kangasjärvi et al. 2005).

Relative to a longer duration of acute ozone exposure (48h), an important set of genes associated with the secondary metabolism (anthocyan synthesis) and defense responses could be induced (D'Haese et al. 2006). At this stage of ozone stress, the anthocyans appeared to play an important role as antioxidants. The up-regulation of genes involved in lignin biosynthesis, callose deposition, cellulose synthesis and pectin esterification would connect to the cell wall stiffening. Genes responsible for the production of antimicrobial compounds are also up-regulated, as opposed to genes involved in cell elongation that are down-regulated.

With chronic long-term ozone exposure, the gene number with a modulated expression is generally lower. An explanation for this reduced rate of changes in gene expression could be that these experiments were conducted in open-air conditions where control plants are already submitted to a combination of stress factors (Miyazaki et al. 2004). Nevertheless, using moderately ozone-tolerant *Populus*, Gupta et al. (2005) showed that 1.5 times higher ambient ozone concentrations lead to a higher expression of many signaling and defense-related genes. Senescence-associated genes (SAGs) and genes involved in the flavonoid pathway are also up-regulated while several photosynthesis and energy-related genes are down-regulated. Thus, genes with similar functions appear to be regulated in both conditions of acute and longer ozone exposure. Compared to the effect of enrichment in CO_2, O_3 is more efficient in up- or down-regulating gene expression (Gupta et al. 2005). Considering that expression profiles for a stress condition are dependent on the intensity and the duration of the stress, the comparison between different environmental conditions is certainly not obvious (Tamaoki et al. 2004). However, when the expression profiles of plants exposed to different stresses were compared, it seemed that ozone and UV-B share the highest level of common changes in gene expression (Matsuyama et al. 2002; Tamaoki et al. 2004).

1.5.8.2. Proteomics

In previous studies, the effect of ozone on the protein content of tissues was analyzed in different herbaceous plants and trees. However, these studies only focused on the analysis of certain classes of expected proteins, involved in photosynthesis, carbohydrate metabolism or response to pathogens. Upon exposure to ozone, activation of different pathogenesis-related proteins is observed. In tobacco, for example the activity of ß-1,3-glucanase and chitinase and their mRNA levels increase in leaves exposed to ozone (Schraudner et al. 1992). Variations of other PR-proteins, but also peroxidase, superoxide dismutase, phenylalanine ammonia-lyase, 4-coumaroyl-COA ligase, hydroxyproline-rich glycoprotein precursor 1, RuBisCO, RuBisCO activase, PEPc are similarly observed upon ozone exposure (Brendley and Pell 1998; Pääkkönen et al. 1998b; Pelloux et al. 2001; Sehmer et al. 1998; Sharma and Davis 1994; Tang et al. 1999). The most popular approach used in proteomics relies on the separation of proteins from complex mixtures on 2D gels, followed by the excision of the spots of interest (e.g. differentially expressed proteins) and identification by mass spectrometry after enzymatic digestion (Gevaert and Vandekerckhove 2000; Pandey and Mann 2000). Tang et al. (1999) carried out a comparative analysis of leaf clover proteins exposed to ozone by 2D electrophoresis and observed the appearance of several groups of small polypeptides (ORP, O_3-responsive proteins), but these proteins could not be identified.

Agrawal et al. (2002) analyzed the response to a short exposure to ozone (up to 72 hours) in rice seedlings by 2D electrophoresis and detected 56 proteins that were differentially expressed. In short, an increase in abundance was observed for PR-proteins, SOD, ascorbate peroxidase, RuBisCO LSU, proteases, calreticulin and calcium-binding proteins, while a decrease was observed for proteins involved in photosynthesis and carbohydrate metabolism.

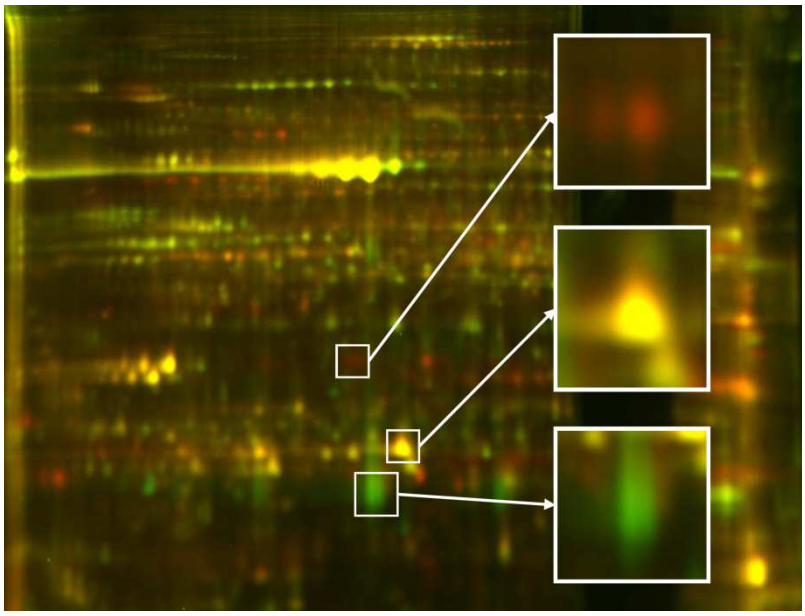

Figure 14: A DiGE gel that contained one control (Cy5, green) and one ozone-treated (Cy3, red) sample. The details show one protein at increased abundance after ozone exposure (red) one protein present in equal abundance in both samples (yellow), and one protein at lower abundance after ozone exposure (green).

More recently, in 2007, two articles have been published on 2D electrophoresis. The first article is based on the effect of ozone on two crops, bean and maize, and presents proteins whose abundance is up- or down-regulated (Torres et al. 2007). 25 and 12 spots have been selected from bean and maize, respectively, on 2D gels of pH range 4 to 7, and 26 spots have been identified by MALDI-TOF or Q-TOF. In a second article, Bohler et al. (2007) investigated the response of poplar to ozone with 2D electrophoresis coupled with a DiGE experiment. On a pH range of 4 to 7, 144 spots have been picked from the gels and almost 50% were identified, mostly proteins involved in carbon metabolism. Currently, a complementary experiment is carried out, still on leaf proteins, on a broader pH range (pH 3-10 NL) with the DiGE technique, to supplement the proteomic approach in poplar (example of gel in Figure 14). The current analysis will allow checking the expression of proteins in leaves during 27 days of exposure to ozone stress.

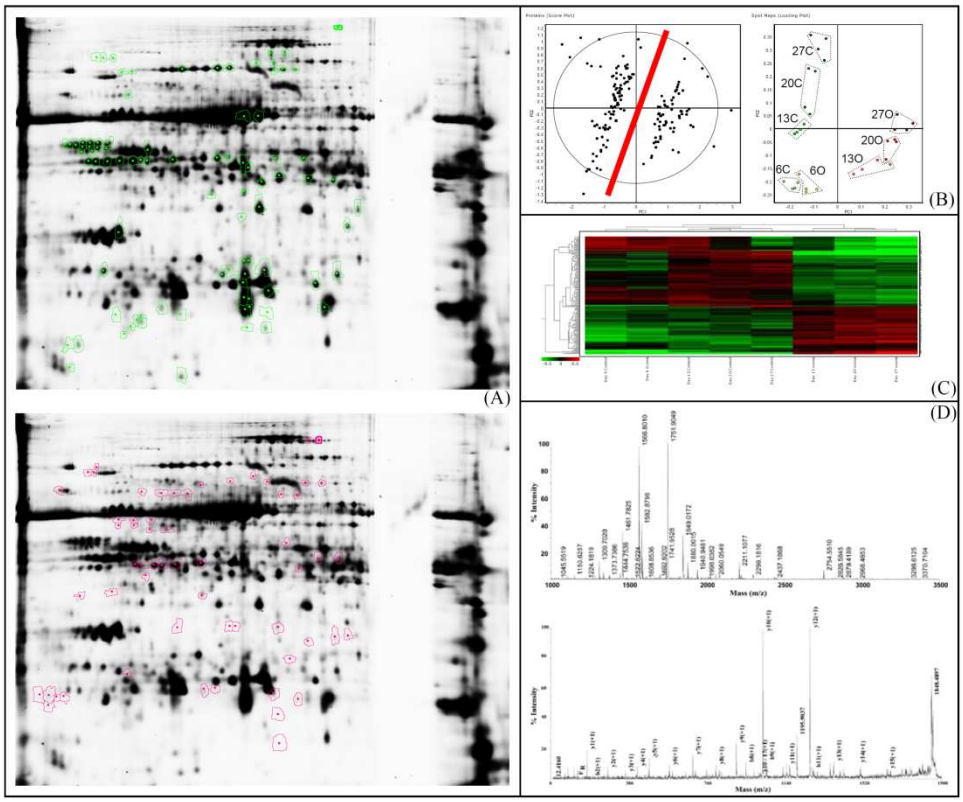

Figure 15: Analysis workflow of DiGE gels. (A) Scanned gels were analyzed with Decyder™ v6.14 Software, and spots of interest were selected by ANOVA statistical analysis: $p < 0.05$ and an absolute ratio of at least 1.5 fold. Green spots are less abundant after ozone exposure whereas red spots are more abundant. (B) A principal component analysis of the proteins of interest resulted in a score plot that contained the proteins, and a loading-plot containing the Experimental groups. C, control; O, ozone; 6, 13, 20, and 27 days of treatment. (C) The pattern analysis shows how the different experimental groups can be regrouped statistically. 6C and 6O are close because the effects of the treatment are minor to this point. Days 13, 20, and 27 are collected in two groups, C and O, the variations between treated and control become higher than the differences between time-points. (D) The proteins of interest are analyzed with MALDI-ToF-ToF mass spectrometry. MS spectra (top) and MSMS spectra (bottom) identify the proteins.

With the 2D-DiGE technique or two-dimensional difference gel electrophoresis (as reviewed in Renaut et al. (2006) proteins are extracted from different samples and labeled with three fluorescent dyes (Cy2, Cy3 and Cy5). Labeled samples can then be combined and separated using bidimensional electrophoresis on a single gel. Differentially expressed proteins can rapidly be detected and quantified. Thus, DiGE reduces gel-to-gel variability, has a wide dynamic range that allows for the detection of low abundance proteins and is designed to directly accommodate subsequent MS analysis. In the current analysis, DiGE allows rigorous statistical analyses of changes in protein abundance that reflect biochemical changes in poplar exposed to ozone (Figure 15).

A principle component analysis (PCA) was used to analyze the gels. In the score plot there is a clear separation of proteins being more (right side) or less (left side) abundant after ozone exposure (Figure 15B). In the loading plot the spot maps are separated along two axes, PC1 explaining 62% of the variation (ozone) and PC2 explaining 12 % of the variation (time).

Pigment-protein complexes were studied by 2D gels in 2 clones of poplar submitted to ozone fumigation (Ranieri et al. 2001). Extracted with a gentle detergent, non-denatured complexes are separated in the first dimension according to their masses on a Deriphat gel before being separated on a SDS-PAGE. Unfortunately, the results only show a decrease in the Coomassie staining intensity between non-treated and fumigated plants. Currently, a similar method, the 2D Blue-Native-PAGE is also used in our laboratories, coupled with the DiGE method, to unravel small biological variations in poplar exposed to ozone during 4 weeks.

1.5.8.3. Metabolomics

Nowadays, the non-targeted profiling of metabolites is gaining more and more interest for plant biologists (Bovy et al. 2007; Guy et al. 2008; Shulaev et al. 2008). Due to the enormous diversity of metabolites present in all plants (estimated to exceed more than 200,000 (Weckwerth 2003)), the full catalogue of metabolites (or metabolome) is so far impossible to be covered by a single technique. Indeed, the different classes of metabolites require the use of gas chromatography coupled with mass spectrometry (GC/MS), high performance liquid chromatography and MS (HPLC/MS), capillary electrophoresis (CE/MS) or even nuclear magnetic resonance spectroscopy (NMR) (Dettmer et al. 2007; Weckwerth 2003).

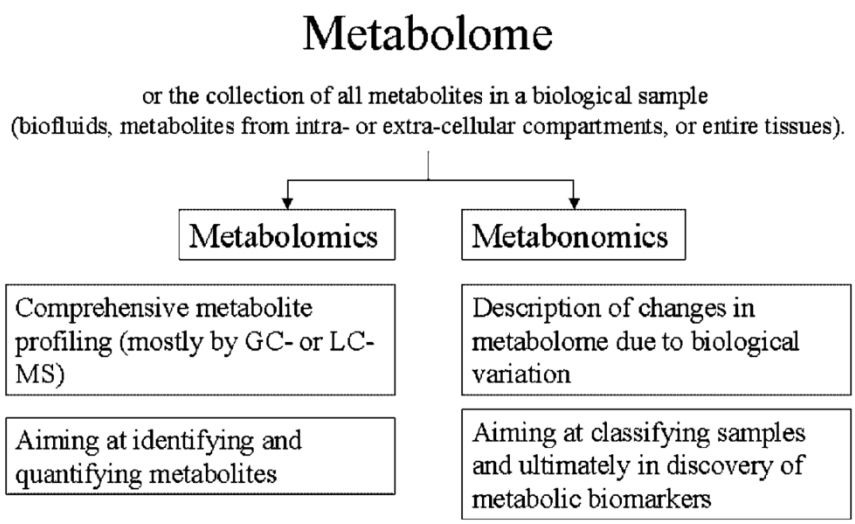

Figure 16: Goals for metabolome investigations. Strategies to tackle metabolome depend on the goal of the investigator: quantitative analyses are called the metabolomic approach, whereas classification of samples and biomarker discovery are referred to as metabolomic studies.

So far, only two references of metabolomic studies applied to ozone stress exist in literature. In these two studies, HPLC and GC/MS are used to analyze the samples. Silver birch trees are exposed for a long-term experiment (7 years) to 1.5-fold the ambient ozone concentration. In the first experiment, 339 metabolites are recorded and quantified in the leaves (Kontunen-Soppela et al. 2007), and in the second one, 283 compounds are quantified (Ossipov et al. 2008). All the compounds are not exactly identified, but it appears that phenolic compounds accumulate in the leaves of birch exposed to ozone, and that this accumulation was even more important in leaves of the trees sensitive to O_3 than in a tolerant genotype (Ossipov et al. 2008). Carbohydrate and lipid contents are also modified upon ozone exposure (Kontunen-Soppela et al. 2007). Although these studies are promising in trying to catalogue important metabolites accumulated or degraded in stress conditions, more investigations are needed to unravel the role of the different compounds insensitivity or tolerance to tropospheric ozone.

1.5.8.4. Integration of 'Omics' Results

Systems biology involves that a biological system is analyzed, not only by studying a single phenomenon, but by considering a broader view which includes all elements of this biological system. Although omics-approaches offer a holistic view on the molecular changes in the organism after exposure to a changing environment, the quantitative analysis of the global transcriptome and more pronounced of the proteome and metabolome is currently lagging behind the mere identification of mRNAs, proteins and metabolites. Despite the development of ever more sensitive

instrumentation and the description and application of a wide range of techniques for absolute and relative quantification, the first complete quantitative description of a proteome or metabolome is far from reached. A major problem in this is the dynamic range in which metabolites and proteins are present in living systems (Baginsky and Gruissem 2004; Bino et al. 2004; Rose et al. 2004; Sumner et al. 2003). Current state-of-the-art techniques in both scientific domains try to avoid this hurdle by selecting a subset of compounds of interest out of the bulk, and a targeted analysis of the obtained fractions. This does not only offer the benefit of revealing low abundant compounds but furthermore keeps the generated data manageable. The impact of ozone pollution on the complexes of the light-driven reactions in chloroplasts is studied after subcellular fractionation and a focused analysis of the chloroplastic proteome (Sacha Bohler, submitted paper 3.2. Bohler et al. submitted in Journal of Proteomics). In a recent article Cho et al. (2008) describe the integration of transcriptomics, proteomics and metabolomics of ozone-exposed rice seedlings. Although the total metabolome profile was obtained, only the quantitative changes in the amino acids and some derivatives (γ-aminobutyric acid (GABA) and glutathione) were calculated. Nevertheless, even the complete analysis of the proteome and metabolome only gives a static view on the cellular physiology. Current approaches to both are based on snapshots, a sample is taken, the analysis performed and information about molecular changes is obtained by comparing the snapshots from different samples. The possibility to use this static approach for a full mechanistic description is recently questioned and dynamic approaches, following the flux of metabolites through pathways (fluxomics) or the synthesis and degradation of proteins (protein turnover) (Doherty and Beynon 2006; Kruger and Ratcliffe 2007; Pratt et al. 2002; Schwender et al. 2004), are currently being developed.

1.5.9. Direct oxidation of amino acids and proteins by ozone

The chemistry of ozone, the study of which was honored in 1995 by granting the Noble Prize in chemistry to Molina, Crutzen and Sherwood Rowland (http://nobelprize.org/nobel_prizes/chemistry/laureates/1995), is complex and involves cycles of formation and decomposition (view headings 1.5.5 and 1.5.6). Common to both the formation and decomposition of ozone, itself being a strong oxidant, is the involvement of reactive oxygen species. Therefore, apart from the indirect, metabolism-mediated impact of ozone on global plant cell metabolism (see main text heading 1.5.7) exposure to ozone can also directly oxidize amino acids, peptides and proteins (Uppu and Pryor 1994).

Although bubbling a gas mixture containing 2.6% ozone through a solution of amino acids is an overstatement of natural conditions, the complete oxidation of Met and Trp in 5 minutes illustrates

the impact ozone may have on amino acids (Kotiaho et al. 2000). Based on this and other studies a reactivity order was derived and Met, Trp, Tyr, His and Cys are found to be most prone to ozone oxidation although with variations, probably due to the method used for detection (Mudd et al. 1969; Pryor et al. 1984). For Met and Cys the oxidation products are known, respectively methionine sulfoxide and cysteic acid. For Trp, His and Tyr mixtures of products are observed and the dominant product formed depends on the conditions used and the method of analysis (Pryor and Uppu 1993; van de Weert et al. 1998).

Contrary to studies on free amino acids and small peptides relatively little is known on the *in vitro* treatment of proteins with ozone. The oxidation rates of amino acids in proteins vary widely, suggesting that the susceptibility to ozone oxidation depends on the size and amino acid composition of the proteins and on their secondary and tertiary structure. This finding was confirmed by comparing the oxidation rates of two proteins with a similar monomeric size but different quaternary structures (Berlett et al. 1996). However, for lysozyme conflicting results were obtained (Kuroda et al. 1975; Pryor and Uppu 1993), leaving the topic open for further research.

The functional effects of *in vitro* ozone oxidation depend on the position and function of the oxidized amino acid. Nonetheless, the observation that ozone-induced oxidation can result in the formation of dityrosine (Verweij et al. 1982) cross-linking proteins (Heinecke et al. 1993), illustrates that ozone exposure can seriously impair the function of proteins. Similarly the ozone-caused inactivation of glyceraldehyde-3-phosphate dehydrogenase is linked to the oxidation of a -SH group located at the active site (Knight and Mudd 1984). Although a protocol for chemical oxidation was used, the oxidative inactivation of bovine surfactant protein B was recently linked to the presence of oxidized forms of Met and Trp (Manzanares et al. 2007). Using chromatography and mass spectrometry, the oxidation products were identified as methionine sulfoxide and kynurenine/N-formylkynurenine, identical to the derivatives formed after ozone exposure (Figure 17).

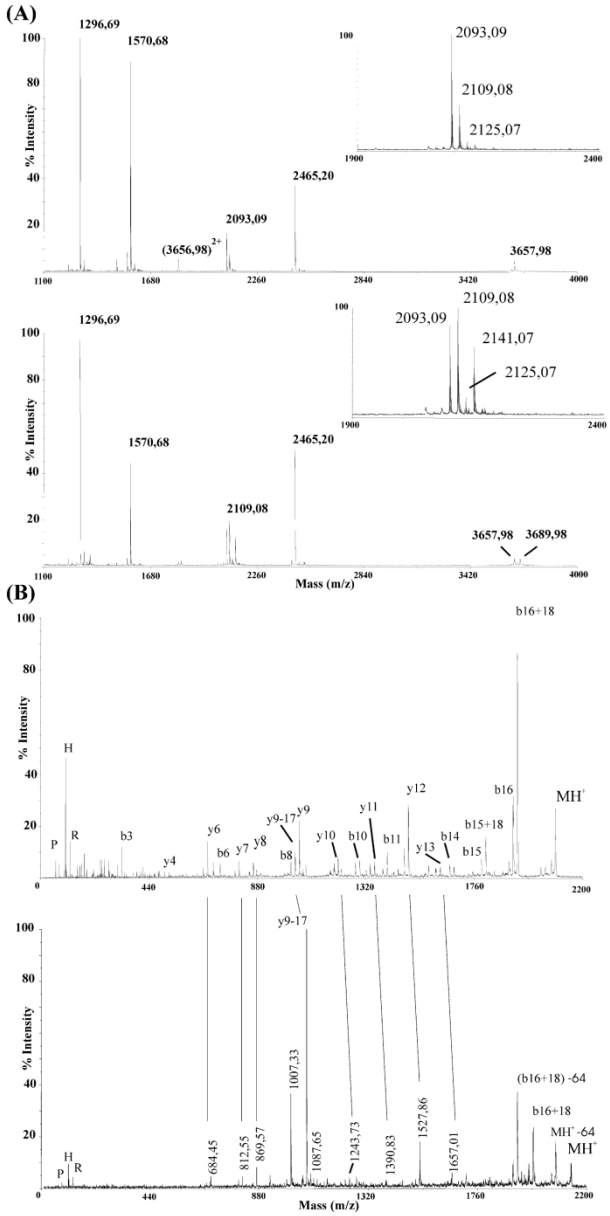

Figure 17: Illustration of the impact atmospheric pollution can have on biomolecules. (A) A 4700 calibration mixture of six peptides (Applied Biosystems, foster City, CA) was dried, re-dissolved, and either shielded (upper spectrum) or exposed to a polluted atmosphere (lower spectrum). Two of the six peptides contain either Trp alone or Trp and Met for, respectively, *m/z* 3657 and *m/z* 2093. The impact of the exposure can be seen in the insets; *m/z* 2093.09 corresponded to unoxidized, 2109.08 to singly oxidized, 2125.07 to doubly and 2141.07 to triply oxidized peptide. Similarly, the signal at *m/z* 3657.98 in the shielded sample is split after exposure to pollution. (B) Product-ion spectra of the peptides that correspond to *m/z* 2093.09 (upper spectrum) and 2141.07 (lower spectrum) in the exposed sample. The peptide is human ACTH 1-17 (SYSMEHFRWGKPVGKKR). In the upper spectrum, the most intense peaks are labeled; y- and b-ions are indicated according to the standard nomenclature, whereas immonium ions are labeled with a capital. The MS/MS spectrum was submitted to a database search that resulted in peptide identification. The neutral loss of 64 Da observed in the lower MS/MS spectrum indicates the presence of an oxidized methionine. The remaining two oxygen atoms are due to oxidation of tryptophan, as indicated by the shift between the y8 ion (GKPVGKKR) and higher mass y-ions. This double oxidation is known to be caused by reactive oxygen species (See part IX) and results in the conversion of tryptophan to N-formylkynurenine. (KS, unpublished results)

1.5.10. Conclusion

The amazing amount of data produced by proteomic approaches, but also transcriptomics, metabolomics or even phenomics, allows the plant scientists to combine and integrate complementary approaches to get insight on gene function and plants' ability to cope with multiple

stress factors. Although the techniques are evolving very rapidly, the global molecular changes that will be observed will always remain part of the total scheme. The next challenging step towards the full understanding of plant stress response will then depend on our ability to link and interpret the amount of data that will come out of research projects such as the exposure of poplars to tropospheric ozone. At the end, it should never be forgotten that the final aim of these researchers on ozone is to understand how the plant cell reacts to the stressing agent in order to elaborate appropriate remedies to the problem.

Chapter 2

A global proteomic approach to ozone exposure of poplar

2.1. General introduction

In 2007, the use of global approaches to study ozone-stressed plants was still relatively rare. When the research paper in this chapter was published (2.2. Bohler et al., Proteomics 2007, 7:1584-1599 (Bohler et al. 2007)), only one proteomic (Agrawal et al. 2002) and a few transcriptomic studies existed (D'Haese et al. 2006; Gupta et al. 2005; Lee and Yun 2006; Li et al. 2006; Ludwikow et al. 2004; Matsuyama et al. 2002; Miyazaki et al. 2004; Olbrich et al. 2005; Tamaoki et al. 2004; Tamaoki et al. 2003; Tosti et al. 2006) (Table 3). As represented in Table 3, only two of the transcriptomic studies had a tree species as a plant model, and the proteomic study used rice. As indicated in Chapter 1, existing studies at that time remained mostly targeted on prominent enzymes like RuBisCO or PEPc, on plant growth regulators, and on comparisons to resembling constraints like pathogen attacks. That is the reason why a proteomic study of the leaf processes influenced by ozone exposure was carried out to bring new insights in ozone research in an unbiased and global way.

Table 3: Overview of publications using global approaches for the study of ozone on plants.

Publication	Plant model	Ozone concentration	Exposure duration
Proteomics			
Agrawal et al. 2002	*Oryza sativa*	200 ppb	3 days
Transcriptomics			
Tosti et al. 2006	*Arabidopsis thaliana*	300 ppb	3 hours
Li et al. 2006	*Arabidopsis thaliana* and *Thellungiella halophila*	20 – 25% above ambient ozone concentrations	12 days
Lee et al. 2006	*Capsicum annum*	150 ppb	3 days
D'Haese et al. 2006	*Arabidopsis thaliana*	150 ppb	2 days
Olbrich et al. 2005	*Fagus sylvatica*	300 ppb	30 days
Gupta et al. 2005	*Populus tremuloides* clone 216	1.5 times ambient	5 years
Tamaoki et al. 2004	*Arabidopsis thaliana*	200 ppb	7 days
Miyazaki et al. 2004	*Arabidopsis thaliana*	21 % above ambient	days
Ludwikow et al. 2004	*Arabidopsis thaliana*	350 ppb	3 and 6 days
Tamaoki et al. 2003	*Arabidopsis thaliana*	200 ppb	12 hours
Matsuyama et al 2002	*Arabidopsis thaliana*	200 ppb	24 hours

The fumigation experiment took place in 8 walk-in fumigation chambers (1.2 x 1.2 x 2 m; lxdxh). Four chambers were randomly selected for the ozone-enriched treatment and four for control conditions. Environmental factors (light, temperature, relative humidity) were set as described in the following research paper. Ten poplar saplings were used per chamber and watered to field capacity daily. The

experimental setup is illustrated in Figure 18. The study was elaborated to give a maximum coverage of the fumigation period. The first sampling of leaves was done after 3 days of treatment, to observe early effects on leaf protein variation, the second harvest was at day 14, for medium term changes, and the third sampling point was after 35 days of treatment, marking the end of the fumigation period. A fourth sampling was done after 45 days, i.e. after 10 additional days of recovery in an ozone free atmosphere. Morphological parameters (stem height and diameter, leaf loss and formation) were registered and observations of visible symptoms (i.e. chloroses, necroses) were inventoried regularly. The sampled leaves were used for the proteomic experiment and samples of days 14 and 35 were also submitted to pigment quantification by HPLC. All the experiments conducted during this thesis are based on the experimental setup presented here. Information about the originality of the different experiments is presented in the respective chapters.

The research paper in this chapter is an overview of poplar leaf protein responses to ozone. The DiGE technique allows for an unbiased approach independently of known facts. This allows on one hand to confirm previously known results from a new angle, but also to detect prior unknown changes ozone may cause in poplar leaves.

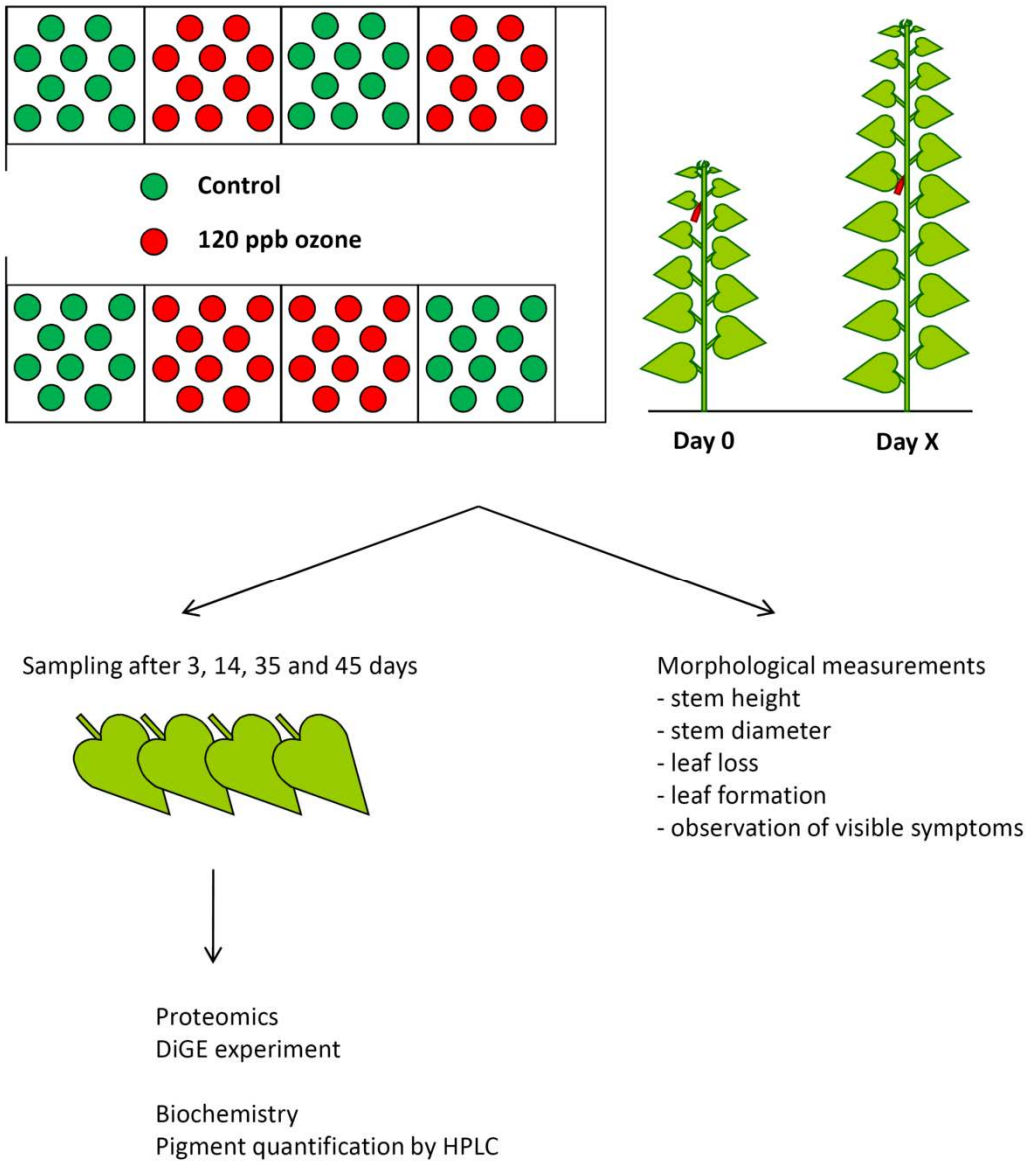

Figure 18: Experimental setup of the first experiment.

2.2. Bohler et al., Proteomics 2007, 7:1584-1599

A DiGE analysis of developing poplar leaves subjected to ozone reveals major changes in carbon metabolism

Bohler Sacha[1,2], Bagard Matthieu[2], Oufir Mouhssin[1], Planchon Sébastien[1], Hoffmann Lucien[1], Jolivet Yves[2], Hausman Jean-François[1], Dizengremel Pierre[2], Renaut Jenny[1]

[1]Centre de Recherche Public - Gabriel Lippmann, Département Environnement et Agrobiotechnologies, 41, rue du Brill, L-4422 Belvaux, Luxembourg.

[2]Unité Mixte de Recherche 1137 “Ecologie et Ecophysiologie Forestière”, Institut National de la Recherche Agronomique (INRA) - Université Henri Poincaré - Nancy I, IFR 110 "Genomique, Ecophysiologie et Ecologie Fonctionnelles", Nancy-Université, Boite Postale 239, F-54506 Vandoeuvre-les-Nancy CEDEX, France

Keywords: plant stress, chloroplast, electron transport, pollutant, photosynthesis, Populus.

2.2.1. Abstract

Tropospheric ozone pollution is described as having major negative effects on plants, compromising plant survival. Carbon metabolism is especially affected. In the present work, the effects of chronic ozone exposure were evaluated at the proteomic level in young poplar leaves, exposed to 120 ppb of ozone for 35 days. Soluble proteins (excluding intrinsic membrane proteins) were extracted from leaves after 3, 14 and 35 days of ozone exposure, as well as 10 days after a recovery period. Proteins (pI 4 to 7) were analyzed in a 2D DiGE experiment, followed by MALDI-ToF-ToF identification. Additional observations were obtained on growth, lesion formation and leaf pigments analysis. Although treated plants showed large necrotic spots and chlorosis in mature leaves, growth decreased only slightly and plant height was not affected. The number of abscised leaves was higher in treated plants, but new leaf formation was not affected. A decrease in chlorophylls and lutein contents was recorded. A large number of proteins involved in carbon metabolism were identified. In particular, proteins associated with the Calvin cycle and electron transport in the chloroplast were repressed. In contrast, proteins associated with glucose catabolism increased in response to ozone exposure. Other identified enzymes are associated with protein folding, nitrogen metabolism and oxidoreductase activity.

2.2.2. Introduction

Over the past several decades, ozone has become one of the major atmospheric pollutants. Even though stratospheric ozone protects life on earth from harmful solar UV radiation, tropospheric ozone is toxic for most organisms. Increases in this anthropogenic pollutant are associated with increasing industrialization. Tropospheric ozone is a secondary pollutant, meaning that it is not emitted directly and is a consequence of the emission of primary pollutants like NOx and VOC, mainly by industry and car exhausts. Another necessary factor for ozone formation is UV radiation, explaining why ozone pollution is the highest during summer. Under the influence of UV radiation, molecules like NOx are fragmented, producing activated oxygen atoms. These highly energetic particles tend to react very quickly with atmospheric oxygen to form ozone. In the 1970s and 1980s, tropospheric ozone concentrations greatly increased in the northern hemisphere. Although the ozone level seems to have leveled out or even decreased in some regions, average daily concentrations of over 50 ppb remain frequent, and in some locations summer concentrations of 120 ppb are not uncommon (Derwent et al. 2003; Oltmans et al. 2006).

Tropospheric ozone is detrimental to plants. It is estimated that ozone is responsible for a 10% reduction in the yield of European forest (Broadmeadow 1998). Both the extent of damage to a plant and the degree of its response are strongly correlated with ozone concentration and duration of exposure, and also with plant species or variety within a species. Depending on these factors, ozone can cause a decrease in growth, in the number of newly formed leaves, and in overall biomass production (Bortier et al. 2000; Landolt et al. 2000; Le Thiec and Manninen 2002). This effect on biomass is accompanied by necrotic lesion formation, chlorosis and accelerated senescence of leaves (Bortier et al. 2000; Strohm et al. 1999). At the cellular level, carbon fixation in plants exposed to ozone significantly decreases (Guidi et al. 2001; Guidi et al. 1998; Soldatini et al. 1998) with leaves exhibiting lower RubisCO activity (Fontaine et al. 1999; Pelloux et al. 2001), the primary carbon fixation enzyme in C3 plants. At the molecular level, lower levels of transcripts and proteins have been shown for RuBisCO and RuBisCO activase (Miller et al. 1999; Pelloux et al. 2001). In addition, the photochemical part of photosynthesis decreased due to a loss or inactivation of some photosystem II associated proteins (Ranieri et al. 2001). Similarly, chlorophyll fluorescence measurements indicate that the efficiency of the photochemical reaction decreases (Guidi et al. 2001). A partial explanation for the decrease in efficiency is an accumulation of ATP and reducing power from the electron transport chain, induced by the above mentioned decrease in the activity of the Calvin cycle. Collectively, these events result in damage or down-regulation of photosystems. In contrast to RuBisCO, activity, transcript levels and protein abundances of PEPc are strongly increased in response to ozone stress. This enzyme activates the anaplerotic pathway and coupled

with the decrease in carbohydrate content of leaves (Iglesias et al. 2006), suggests that reducing power and carbon skeletons released from these carbohydrates are reallocated for possible detoxication of oxidative molecules and repair of damage caused by oxidative stress.

Ozone enters the leaves through stomata and is rapidly degraded in the apoplast, resulting in the production of ROS. These reactive molecules attack cell walls and membranes. A primary detoxication of ROS takes place in the apoplast through ascorbate oxidation, inducing a release of reduced ascorbate from the cells to the apoplast (Landry and Pell 1993; Luwe et al. 1993). Furthermore, an increase in molecules and enzymes with antioxidative properties has been reported in response to ozone exposure (Conklin and Last 1995; Gupta et al. 1991; Sharma and Davis 1994).

Although many studies on ozone stress in plants have been conducted over the last two decades, many open questions remain, and the exact mechanism of ozone stress is not yet precisely known. Global studies, based on transcriptomics and proteomics, can provide important information on the processes involved in stress responses. This type of studies provides a more global picture of how the whole metabolism of an organism is responding rather than just a limited subset of the organism. Proteomic studies are complementary to transcriptomics. Although it is difficult to observe the whole set of proteins of an organism (in the present study for example only the soluble proteins of a pI between 4 and 7 were analyzed), proteomics is situated one step up the transcriptional/translational chain. While proteomics has been used to study other abiotic stresses, such as low temperature (Renaut et al. 2004), global studies of ozone response in plants are few. One proteomic study has been carried out on rice (Agrawal et al. 2002), but none have been conducted on trees. In the present work, the effects of ozone are evaluated in young poplar trees, submitted to 120 ppb of ozone for 35 days. Soluble proteins in a pI range from 4 to 7 were analyzed using 2D DiGE technology, thus covering a major part of enzymatic proteins. In addition, information on growth, lesion formations and leaf pigments analysis were collected and analyzed.

2.2.3. Material and methods

2.2.3.1. Plant material

Poplar clones (*Populus tremula* L. x *P. alba* L. (*Populus* x *canescens* (Aiton) Smith) - clone INRA 717-1-B4) were multiplied *in vitro*, rooted and transferred to a mix of peat/perlite (1/1 [v/v]) and were acclimated in phytotronic chambers at 75%/85% relative humidity (day/night) with a 14 h light period (Sun T Agro, Philips, Eindhoven, The Netherlands; intensity: 250–300 $\mu mol.m^{-2}.s^{-1}$) and 22°C/18°C ± 2°C (day/night) prior to the beginning of the experiment. After 2 weeks trees were transplanted into 5 L pots containing peat (Gramoflor SP1 Universel) fertilized with 15 g of slow-

release nutritive granules (Nutricote T-100, N/P/K/MgO 13/13/13/2, Fertil, Boulogne-Billancourt, France). Drainage was improved by a 2 cm thick layer of clay beads at the bottom of the pots. When 10 leaves were fully expanded, plants were transferred to 8 fumigation chambers. In the fumigation chambers, 4 lots of 10 plants each were used per treatment. Plants were acclimated to fumigation chambers for one week at 75%/85% relative humidity (day/night) with a 14 h light period at a photon flux density at plant height of 350 $\mu mol.m^{-2}.s^{-1}$ provided by incandescent sodium lamps (Sun T Agro, Philips, Eindhoven, The Netherlands) and 22°C/18°C ± 2°C (day/night) temperatures.

2.2.3.2. Ozone treatment

Ozone treatments were performed in the fumigation chamber over 35 days using the conditions previously described. Over this period of time, a chronic stress can be established and have full impact on the plants. Four groups of 10 plants each were exposed to charcoal filtered air supplemented with 120 ppb of ozone for 13 h per day for 35 days during the light period. Exposure during the light period more closely simulates natural ozone exposure that mostly occurs throughout the light period of the day. Another 4 groups of 10 plants, used as controls, were exposed to charcoal-filtered air. Ozone was generated from pure O_2 with two ozone generators (OZ500 Fischer, Bonn, Germany, and CMG3-3 Innovatec II, Rheinbach, Germany) and continuously monitored by an ozone analyzer ($O_3$41M, Environment S.A., Paris, France). Leaf n° 4, numbered from the last leaf emerged at the apex, was tagged at the beginning of the treatment. These leaves were harvested for analysis after 3, 14 or 35 days of treatment. In order to monitor recovery, a fourth sampling was carried out 10 days after the treatment of the plants with ozone has ceased (i.e. 45 days after the initiation of the experiment). These samples are referred to as “recovery” samples.

2.2.3.3. Morphological measurements

Stem elongation, diameter increase and observations of visible symptoms on leaves were recorded during the whole experiment. Growth measurements (height and diameter) were carried out after 0, 14, 25 and 35 days of exposure. Height measurement was based on the length of the stems from the collar to the apex and the diameter expansion was estimated via measurements of the stem 1.5 cm above the collar with a caliper. The number of newly formed leaves, as well as the number of abscised leaves, was recorded daily. Concomitantly, visible symptoms of ozone treatment (chlorosis and necrosis) were also recorded.

2.2.3.4. Soluble protein extraction

In this study, the proteomics are based on young poplar leaves (4^{th} fully expanded leaf, at the beginning of the treatment). Five hundred milligrams of fresh leaf material, corresponding to nearly a whole leaf at day 3 and to merely a quarter of a leaf at day 35, were ground in liquid nitrogen. The

obtained powder was re-suspended in solubilization buffer (50 mM Tris-HCl, 25 mM EDTA, 500 mM thiourea, 0.5% w/v DTT (Koistinen et al. 2002)) and centrifuged at 15,000 x g (4°C, 15 min). Supernatant was then mixed with the extraction buffer (20% TCA and 0.1% w/v DTT in ice-cold acetone) up to 25 mL and kept overnight at –20°C. The material was centrifuged for 45 min at 35,000 x g and 4°C. The pellets were washed with ice-cold acetone containing 0.1% w/v DTT and centrifuged again at 4°C. This washing step was repeated three times. The pellets were finally freeze-dried. Dried samples were re-suspended in labeling buffer (7 M urea, 2 M thiourea, 4% w/v CHAPS, 30 mM Tris) and incubated for 1 h at room temperature. Prior to quantification, the pH of the lysate was adjusted to 8.5. The protein concentration was determined using a quantification kit (2D Quant Kit, GE Healthcare, Little Chalfont, UK) using bovine serum albumin (2 $mg.mL^{-1}$) as the standard. After extraction, proteins were used for a multiplexed analysis by fluorescence difference gel electrophoresis (DiGE) (Skynner et al. 2002).

2.2.3.5. Protein labeling.

Protein extracts and the pooled internal standard were labeled prior to electrophoresis with the CyDyes™ (GE Healthcare). A pooled "internal standard", for gel normalization, was prepared containing an equal protein quantity of each of the 24 samples. Twelve gels were run simultaneously, 3 per sampling date containing one control and one treated sample each, plus the internal standard. Each protein extract was labeled at the ratio 240 pmol Cy2 (internal standard), Cy3 (controls) or Cy5 (treated) protein minimal labeling dye for 30 µg of protein, vortexed, and incubated on ice for 30 min (Skynner et al. 2002). The reactions were quenched by addition of 1.2 µL of 10 mM lysine, vortexed, and incubated on ice for 10 min in the dark. An equal volume of '2X lysis' buffer (7 M urea, 2 M thiourea, 4% w/v CHAPS, 2% w/v DTT, and 2% v/v pH 4–7 IPG buffer) was added. The samples were vortexed and incubated on ice for a further 15 min in the dark. Then the pooled Cy2-labeled internal standard was combined with the Cy3-labeled and Cy5-labeled extracts of each batch. Ninety micrograms of proteins (30 µg of each sample) were loaded on each gel and separated by 2D electrophoresis. An additional 220 µg were added on gels meant for later protein identification.

2.2.3.6. Bidimensional electrophoresis.

Immobiline DryStrips (GE Healthcare, pH 4-7, 24 cm) were rehydrated overnight with rehydration buffer (7 M urea, 2 M thiourea, 1% w/v CHAPS, 0.4% w/v DTT, 0.5% v/v IPG buffers, 0.002% v/v bromophenol blue). Proteins were cup-loaded and isoelectric focusing (IEF) was carried out on an Ettan IPGphor Manifold (GE Healthcare) with the following settings: gradient steps of 150 V for 3 h, 2,000 V for 3 h, 4,000 V for 3 h, 8,000 V for 3 h and a constant step at 8,000 V for 7 h at 20°C with a

maximum current setting of 50 µA/strip in an IPGphor IEF unit (GE Healthcare). After the IEF, the IPG strips were equilibrated for 15 min in equilibration buffer (50 mM Tris (pH 8.8), 6 M urea, 30% v/v glycerol, 2% w/v SDS) supplemented with 1% w/v DTT. A second equilibration step of 15 min with the same equilibration buffer, containing now 2.5% w/v iodoacetamide, was carried out afterwards. The IPG strips were then sealed with 0.5% agarose in SDS running buffer on top of gradient gels (280 x 210 x 1 mm) cast in the 2DE optimizer (Nextgen, Huntingdon, UK) from 8 to 14% w/v acrylamide and 0.1% N,N'-methylenebisacrylamide. The gels were poured between low fluorescent glass plates, of which one plate was bind-silane treated. The SDS-PAGE step was performed at 15°C in Ettan Dalt II tanks (GE Healthcare) at 2.5 W per gel for 18 h.

2.2.3.7. Image capture and analysis.

Cy2, Cy3 and Cy5 labeled protein images were produced by excitation of gels at 488, 532 and 633 nm respectively and emission at 520, 590 and 680 nm respectively using Typhoon Variable Mode Imager 9400 (GE Healthcare) at a resolution of 100 µm. Images were analyzed using the Decyder v6.05.11 software (GE Healthcare) (Figure 19). The gel chosen for picking was fixed (40% ethanol, 10% acetic acid) for 1 h, then stained by overnight immersion in Sypro Ruby (BIO-RAD), destained (40% ethanol, 10% acetic acid) for 1 h and rinsed in water. The gel was scanned at 470 nm excitation wavelength and 618 nm emission. Selected spots of interest were located (absolute abundance variation of at least 1.5-fold, $p<0.05$) and a picking list was generated. Spots of interest were excised from gels using the Ettan Spot Picker from the Ettan Spot Handling Workstation (GE Healthcare). After washing and desalting in 50 mM ammonium bicarbonate / 50% (v/v) methanol, followed by 75% (v/v) acetonitrile, spots were then digested with Trypsin Gold (mass spectrometry grade, Promega, Madison, WI, USA, 10 $\mu g.mL^{-1}$ in 20 mM ammonium bicarbonate) using the Ettan Digester robot (GE Healthcare) from the same workstation. Automated spotting of the samples was carried out with the spotter of the Ettan Spot Handling Workstation (GE Healthcare). Peptides dissolved in a 50% acetonitrile containing 0.5% TFA (0.7 µL) were spotted on MALDI-TOF disposable target plates (4800, Applied Biosystems, Foster City, CA, USA) prior to the deposit of 0.7 µL of α-cyano-4-hydroxycinnamic acid (7 mg/mL, 50% (v/v) acetonitrile, 0.1% (v/v) TFA, Sigma Aldrich, St. Louis, MO, USA). Peptide mass determinations were carried out using the Applied Biosystems 4800 Proteomics Analyzer (Applied Biosystems). Both peptide mass fingerprinting (PMF) and tandem mass spectrometry (MS/MS) in reflectron mode analyses were carried out with the samples. Calibration was carried out with the peptide mass calibration kit for 4700 (Applied Biosystems). Proteins were identified by searching against the SWISS-PROT, TREMBL and NCBI databases using MASCOT (Matrix Science, www.matrixscience.com, London, UK). All searches were carried out using a mass window of 50 ppm and with "Viridiplantae" as taxonomy. The search parameters allowed for

carboxyamidomethylation of cysteine and oxidation of methionine. Homology identification was retained with a probability set at 95%. Estimation for false positives was made by searching a randomized NCBI database, generated using emboss:shuffleseq, with the same search criteria.

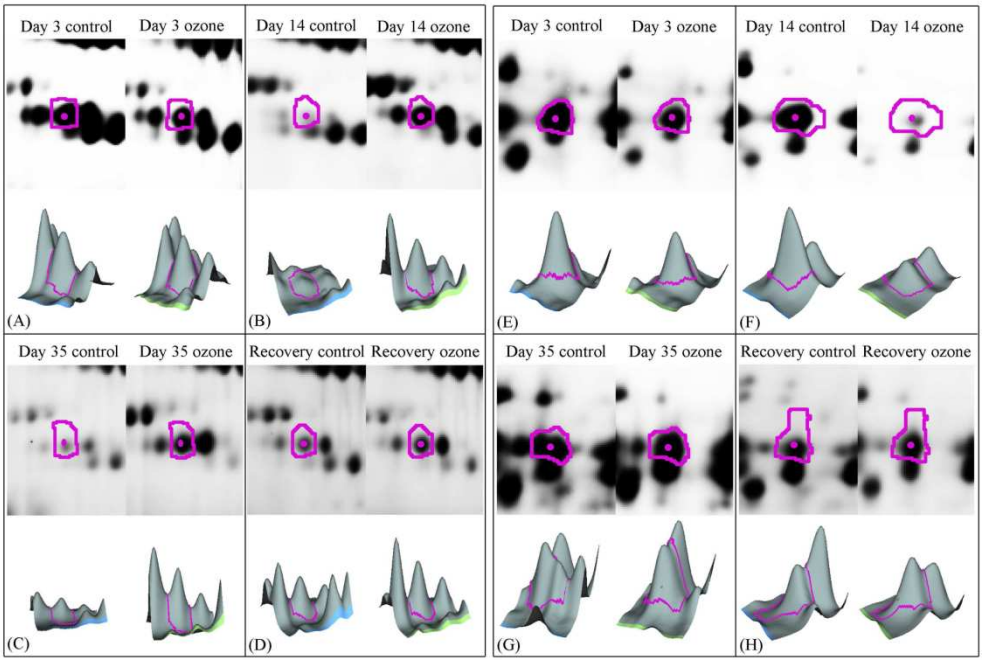

Figure 19: Examples of one protein present in higher abundance (A–D) (protein disulfide-isomerase) and one protein present in lower abundance (E–H) (RuBisCO activase) during ozone stress, as presented in Decyder v6.05.11 software (GE Healthcare). Gel views and 3-D views give a visual appreciation of the variations in protein abundance.

2.2.3.8. Pigment extraction

All steps were performed in the dark at 4°C. Pigments were extracted, using an Eppendorf Thermomixer at 1400 rpm and at 4°C, in 1 mL of a 100% acetone solution for 1 h, from leaf samples (± 100 mg FW, avoiding areas of necrosis) previously ground in liquid nitrogen and kept frozen. After centrifugation (10,000 x g, 10 min), the pellet was discarded and the supernatant was filtered through a 0.22 µm GHP membrane filter.

2.2.3.9. Analysis of pigments using reverse phase high performance liquid chromatography with photodiode array detector (RP-HPLC-DAD)

Pigment analyses were carried out using a Dionex HPLC ICS2500-BioLC (Sunnyvale, CA, USA), with an AS50 autosampler, a GS50 gradient pump and a PAD-100 photodiode array detector. The separation was performed with a Zorbax (Agilent Technologies, Santa Clara, CA, USA) Bonus-RP C14 (250 x 4.6 mm i.d.; 5 µm particle size) column operated at a temperature of 40°C. The mobile phase consisted

of water (eluent A), of acetonitrile (eluent B), of 0.5 M ammonium acetate in methanol (20/80, v/v; eluent C), pH 4.6 and of ethyl acetate (eluent D). The gradient program was as follows: 100% C to 90% B (2 min), 90% B to 81% B and 10% D (0.6 min), 81% B and 10% D to 76% B and 14% D (7.4 min), 76% B and 14% D to 70% B and 20% D (1 min), 70% B and 20% D to 58.5% B and 35% D (6.6 min), 58.5% B and 35% D to 27.9% B and 69% D (2.4 min), 27.9% B and 69% D to 90% B (2 min), 90% B to 100% C (3 min) and column equilibration at 100% C during 5 min. Total run time was 30 min. The injection volume for all samples was 20 µL. Simultaneous monitoring was set at 447 nm (lutein), 431 nm (Chlorophyll a) and 458 nm (Chlorophyll b), at a flow-rate of 1.0 $mL.min^{-1}$. Spectra were recorded from 190-800 nm. Pigments were identified by HPLC by their retention time and spectral data was compared to standards and quantified using six-points calibration curves with custom-made external standard solutions (DHI Water and Environment, Danemark and Carotenature, Switzerland) ranging from 1 µg/mL to 10 µg/mL and every 10 injections, a check standard solution was used to confirm the calibration of the system.

2.2.3.10. Statistical analysis

Statistical analysis was carried out with 3 biological replicates for proteomics, 3 biological and 2 technical replicates for pigment analysis and 24 biological repetitions for growth, for each condition on each sampling date. When analyzing protein abundance, only statistically significant results were considered (Two-Way ANOVA, $p<0.05$, with control/treated and sampling dates as factors) and differentially expressed proteins with an absolute ratio of at least 1.5-fold were selected. A PCA was run on the 529 proteins matched on every gel and on the different spot maps for qualitative appreciation of the proteomic results. Two-Way ANOVA and PCA were performed on Decyder Extended Data Analysis (v.1.0.11.4). For morphological measurements and pigments, significance was calculated via a One-Way ANOVA, with control/treated as factors and growth and pigment concentration respectively as the response. Hypothetical increases in significance beyond the observed treatment were estimated by an ANCOVA test, with sampling dates as a cofactor. These analyses were performed on MINITAB Statistical Software v.13.20.

2.2.4. Results

2.2.4.1. Morphological Data

After 6 days of ozone fumigation, necrotic lesions appeared on the surface of mature leaves (Figure 20A). After 35 days of treatment, necrosis had spread to approximately 20% of the leaf surface, especially on adult leaves that were young at the beginning of the treatment. The extent of necrotic areas varied from plant to plant but all stressed trees were affected. Lesions appeared exclusively on

mature leaves. Furthermore, mature leaves of ozone treated plants exhibited a chlorotic appearance (Figure 20B).

The leaves chosen for analysis were considered young sink leaves at the beginning of the treatment. Around day 14, their expansion phase had ended (4.2. Bohler et al. Tree Physiology in press) and their physiological role changed from sink to source leaves. From this point forward the leaves could be referred to as adult leaves. At this point, these leaves started developing necrotic patches, which expanded until the end of the treatment. Necrotic patches were avoided when collecting tissues for protein extraction.

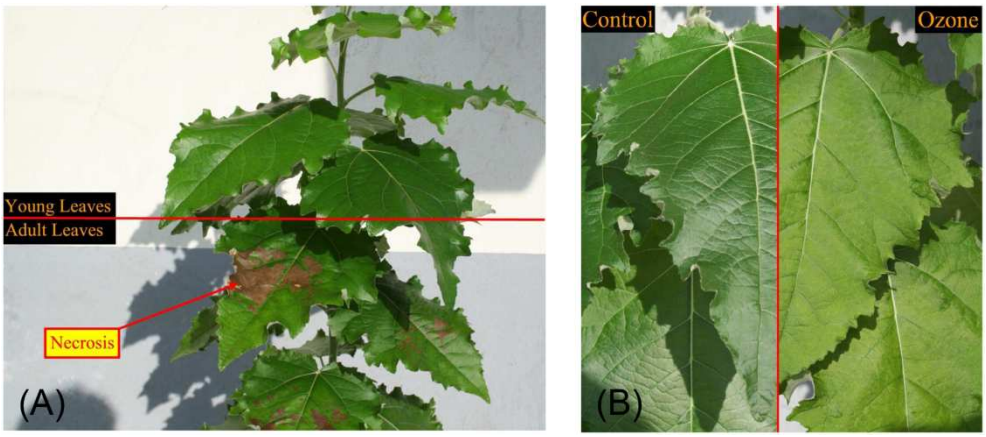

Figure 20: (A) Necrotic lesions and (B) chlorosis on adult poplar leaves exposed for 35 days to ozone. Necroses were most extended on adult leaves that were still young at the beginning of the treatment.

Ozone treated plants did not show any difference in height compared to control plants (Figure 21A). Differences in secondary growth (diameter) were evident however, and diameter was significantly decreased only on day 25 (Figure 21B), with a significant trend for developing further differences. Increased leaf abscission was observed in ozone-treated plants after 27 days of treatment and continued to increase until the end (Figure 21C). The formation of new leaves was not perturbed by the ozone treatment (Figure 21D). Although primary growth and leaf formation did not vary during the 35 days of fumigation, the statistical tendency test ANCOVA gave a significant probability that differences would appear after an extended fumigation period. In Table 4, we present the proteins with a significant variation for the ozone factor. For these proteins, the table also shows the significance level for both factors and the interaction between them.

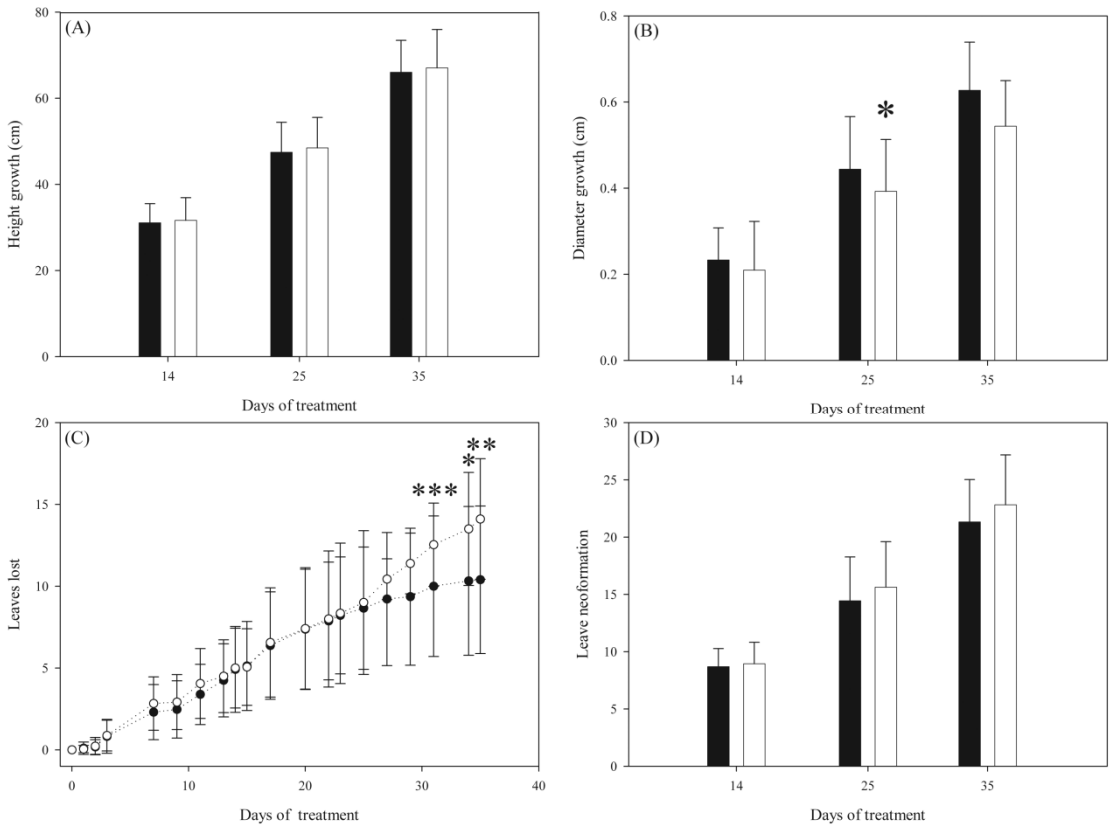

Figure 21: Effects of ozone on (A) growth in height, (B) growth in diameter, (C) leaf abscission and (D) new leaf formation. All these parameters were determined relative to the beginning of the treatment (day 0). The p-value was calculated by One-Way ANOVA (* $p<0.05$; ** $p<0.01$; *** $p<0.001$; ozone *vs*. control). Open bars and symbols represent ozone treatment, closed bars and symbols represent control plants.

2.2.4.2. Pigment analysis

HPLC pigment analysis showed a reduction in chlorophyll a content in ozone-treated leaves at 14 and 35 days of treatment (Figure 22A) and of chlorophyll b content at 35 days (Figure 22B). The ratio between chlorophyll a and b dropped significantly only on day 14 (Figure 22C). Lutein also decreased significantly in ozone-exposed leaves after 14 and 35 days (Figure 22D).

2.2.4.1. Proteomics

Per gel, an average 1900 protein spots were detected. Of these 1900 spots, 529 could be matched in all the gels. This number reflects a technical problem. As one of the gels was of lower quality only these spots could be matched with sufficient confidence on all the gels. A total of 147 proteins were determined to be significantly different at $p<0.05$ (Two-Way ANOVA) and at an absolute variation of at least 1.5-fold by comparing the control to the treatment. Only 144 proteins were picked in Sypro

Ruby (BIO-RAD) stained gels loaded with 310 µg of proteins (Figure 23). Finally, 71 proteins were identified with sufficient confidence (Table 4). After grouping spots identified as the same protein, approximately the same number of proteins was shown to increase or decrease in abundance. Twenty-five isoforms of enzymes from the carbon metabolism were found to decrease in abundance during ozone exposure while 4 isoforms increased. Three isoforms of proteins involved in electron transport increased. In the chloroplast electron transport chain, 17 protein isoforms were found to decrease in abundance. Two enzymes associated with nitrogen metabolism were found to increase in abundance, whereas one was found to decrease. Two enzymes with oxidoreductase activity were found to increase in abundance. Only one protein associated with secondary metabolism could be found to decrease in abundance. Five isoforms of proteins involved in protein folding increased in quantity while two were reduced. Nine proteins were ranked as 'Miscellaneous' and of these, two and seven of them showed a decrease or an increase in abundance, respectively. Detailed variations and functions of the identified proteins are presented in the Discussion.

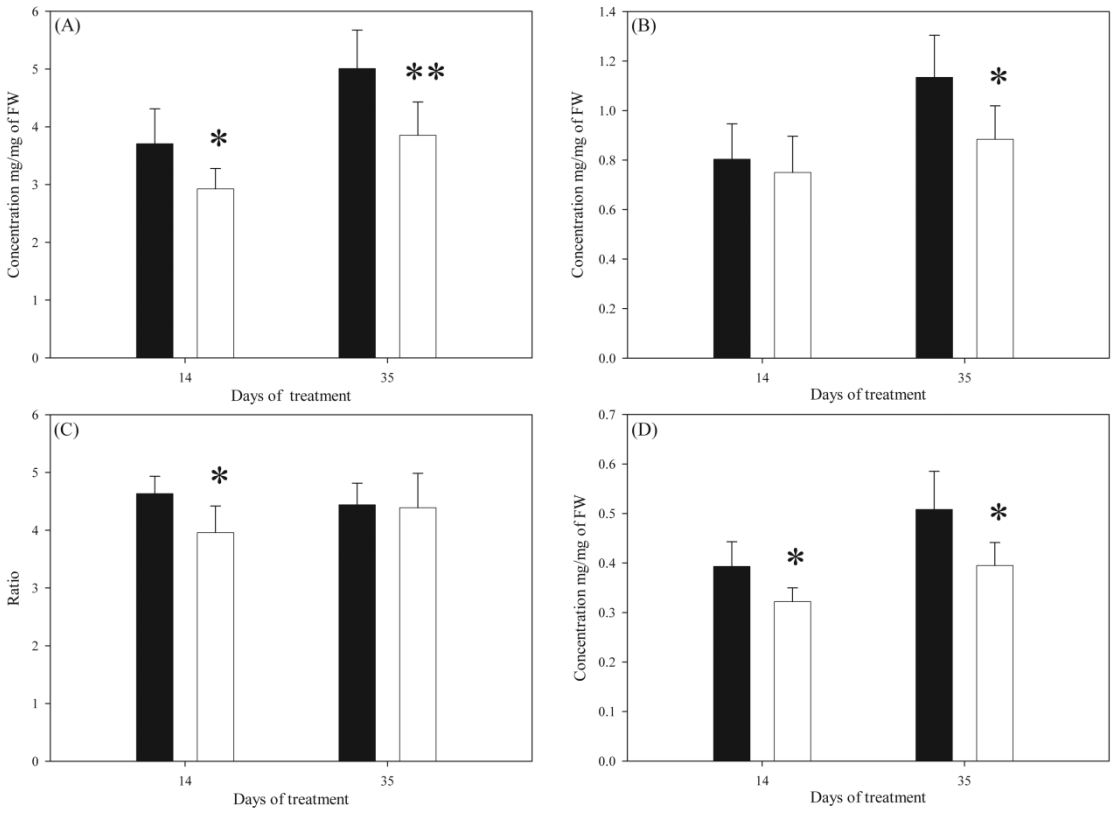

Figure 22: Effects of ozone on (A) chlorophyll a content, (B) chlorophyll b content, (C) chlorophyll a/b ratio, (D) lutein content. Results are shown in mg.mg–1 (FW). The p-values were calculated by One-Way ANOVA (* $p<0.05$; ** $p<0.01$; ozone *vs*. control). Open bars represent ozone treatment, closed bars represent control plants.

The search in the randomized NCBI database revealed 3 possible false positives (296, 459 and 1777), although the hits did not show any peptide recognition by MS/MS, leaving the risk for false positives insignificant, since all the proteins discussed here were identified by MS/MS.

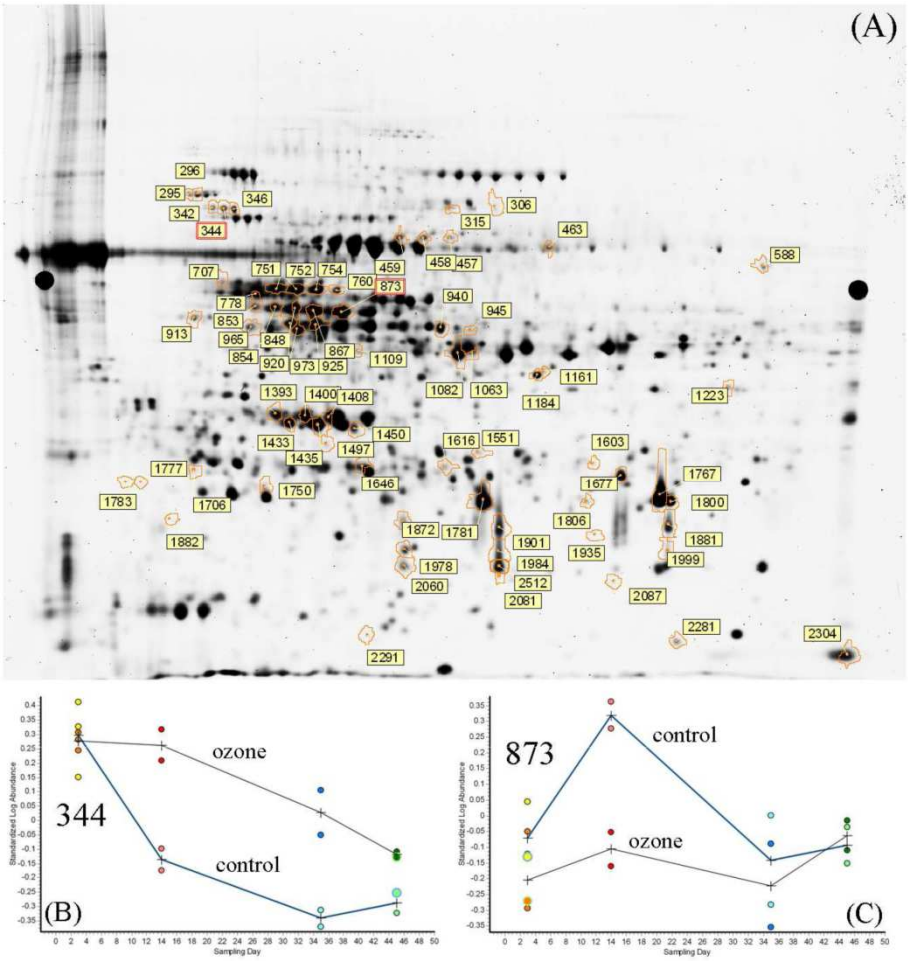

Figure 23: (A) SYPRO Ruby-stained gel with the positions of all identified proteins. The assigned spot numbers are shown. Examples of one protein present in higher abundance (B) (protein disulfide-isomerase, spot number 344) and one protein present in lower abundance (C) (ribulose bisphosphate carboxylase activase, spot number 873) during ozone exposure.

2.2.1. Discussion

Poplar, besides the common characteristics of woody plants (e.g. ecological and economic importance, long term perennial life cycle), is also easily propagated *in vitro* and can be readily transformed. Poplar is considered a fast growing tree, which would allow the effects of the ozone to be manifested in a reasonable period of time. Poplar is considered to be sensitive to ozone partially because of its rapid growth and high gas exchange rate (Gerosa et al. 2003). Additionally, the recently sequenced genome of *Populus trichocarpa* (Tuskan et al. 2006) will facilitate gene and

protein identification in the future, strengthening the position of poplar as a model for forest trees studies. The clone used in this study (*Populus tremula* L. x *P. alba* L. (*Populus* x *canescens* (Aiton) Smith) - clone INRA 717-1-B4) is especially amenable to *in vitro* multiplication. It is moderately sensitive to ozone, and thus exhibits a physiological response without completely dying in response to the ozone treatment.

Tropospheric ozone can reach concentrations of 120 ppb on summer days. The choice of 120 ppb for this study is realistic. Furthermore, previous studies have shown that for this selection of poplar, a chronic exposure to 120 ppb is sufficient to induce measurable physiological changes, without risking complete mortality (Cabané et al. 2004).

Throughout the discussion, proteins are referred to by their function and not necessarily by the entire name given in Table 4. The corresponding spot numbers, which can also be found in Table 4 and Figure 23A will thus be given in brackets as a reference to their specific identity.

The PCA analysis of the 529 matched proteins showed that some proteins lie outside of the 95% confidence interval. In the loading plot (Figure 24A), proteins positioned around the PC2 axis are highly significant when considering the ANOVA p-value for the ozone factor, while most of the proteins running along the PC1 axis are highly significant for the time factor. Concomitantly, in the score plot (Figure 24B) axis 1 separates the experimental groups according to the sampling time while the axis 2 is responsible of the groups' separation according to the treatment. 38% of the variation on the gels is due to the sampling date (PC1), and 24% is due to the treatment (PC2). The groups 'ozone' and 'control' at day 3 are very close to each other while the next sampling dates clearly separate, showing that a variation gradually appears over time. Moreover, the 2 groups corresponding to the recovery period remained clearly separated, leading to the conclusion that a 10 days period of recovery was not sufficient to compensate the effect of the ozone treatment from a proteomic point of view.

Table 4: List of proteins identified by mass spectrometry. a: Function of the protein obtained via the MASCOT software (www.matrixscience. com) from the NCBInr database; b: accession number form the NCBInr database; c: Spot number represents the number on the master gel; d: MOWSE score probability (Protein score) for the entire protein and for ions, complemented by the percentage of the confidence index (C.I.); e: theoretical molecular weight; f: theoretical isoelectric point; g: average ratio of the protein abundance (ozone/control) on different days (3, 14, 35, and after recovery). Positive values of ratio are given as such, while negative values are given according to the following formula: given value = -1/average ratio; h: p-value of the Two-Ways ANOVA for the ozone factor, the time factor and the interaction between both (*: p<0.05; **: p<0.01).

Protein Name[a]	Accession Number[b]	Spot Number[c]	MASCOT Scores[d]				Protein MW[e] (kDA)	Protein pI[f]	Average Ratio[g]				ANOVA significance[h]		
			Protein Score	Protein Score C.I. %	Total Ion Score	Total Ion Score C.I. %			Day 3	Day 14	Day 35	Recovery	ozone	time	interaction
Carbon metabolism															
carbonate dehydratase (EC 4.2.1.1) 1b - Populus tremula x Populus tremuloides	gi|7436820	1603	123	100.00	28	40.53	35518	6.99	-1.03	1.68	2.00	1.00	*	**	
putative phosphoglycerate mutase [Oryza sativa (japonica cultivar-group)]	gi|56785335	306	114	100.00	77	100.00	61172	5.42	-1.07	2.23	1.80	1.64	**	*	
		315	205	100.00	168	100.00	61172	5.42	-1.11	2.00	1.84	1.47	**	**	
nodule-enhanced malate dehydrogenase [Glycine max]	gi|3273828	1161	149	100.00	85	100.00	43961	6.91	1.11	1.09	2.01	1.52	**	**	
rubisco small subunit [Coffea arabica]	gi|24940140	2304	68	96.97	57	99.92	20816	8.49	1.11	-1.56	-1.83	-2.56	**	**	
ribulose-1,5-bisphosphate carboxylase/oxygenase activase 1 [Gossypium hirsutum]	gi|12620881	707	162	100.00	100	100.00	48490	5.54	1.04	-2.52	-1.62	-1.09	**	**	**
		853	268	100.00	186	100.00	48490	5.54	1.03	-2.68	1.07	-1.08	*	*	*
ribulose-1,5-bisphosphate carboxylase/oxygenase activase [Malus x domestica]	gi|415852	754	331	100.00	289	100.00	48489	8.2	-1.51	-3.35	-1.31	1.28	**		*
		760	323	100.00	261	100.00	48489	8.2	-1.12	-2.01	-1.75	-1.17	**		
rubisco activase [Chenopodium quinoa]	gi|21950712	751	334	100.00	241	100.00	48197	6.56	-1.26	-3.65	-1.19	1.06	**	**	*
		752	241	100.00	169	100.00	48197	6.56	-1.51	-3.50	-1.58	1.16	**	**	**
		848	423	100.00	321	100.00	48197		-1.19	-2.77	-1.03	-1.12	**	**	*
		867	413	100.00	320	100.00	48197	6.56	-1.31	-2.90	-1.04	-1.13	**	**	*
rubisco activase [Zantedeschia aethiopica]	gi|13430334	1706	116	100.00	68	99.99	37462	6.7	1.02	-1.12	-1.18	-4.25	*	**	*
ribulose bisphosphate carboxylase activase [Nicotiana tabacum]	gi|19990	873	301	100.00	259	100.00	48765	8.14	-1.34	-2.66	-1.21	1.07	*	*	
ribulose bisphosphate carboxylase activase B [Triticum aestivum]	gi|7960277	854	406	100.00	318	100.00	48316	6.92	-1.06	-3.06	1.11	-1.02	*	*	*
Rubisco activase beta form precursor [Larrea tridentata]	gi|32481067	778	121	100.00	74	100.00	48539	6.78	-1.38	-2.31	-1.31	1.28	*	*	*
RuBisCO activase small isoform precursor [Oryza sativa]	gi|8918361	2087	160	100.00	117	100.00	48416	5.85	-1.15	-2.11	1.13	-2.51	**	**	
RuBisCO subunit binding-protein alpha subunit, chloroplast precursor (60 kDa chaperonin alpha subunit)	gi|1351030	1497	148	100.00	130	100.00	57858	4.84	-1.12	-1.44	-2.01	-2.46	**		
Chain C, D-Ribulose-5-Phosphate 3-Epimerase From Solanum tuberosum Chloroplasts	gi|4930132	1677	158	100.00	124	100.00	24820	5.75	-1.06	-1.62	-1.42	-1.01	**		
phosphoribulokinase [Pisum sativum]	gi|1885326	925	284	100.00	228	100.00	39326	5.41	-1.08	-1.33	-1.97	-1.85	*		
sedoheptulose-bisphosphatase precursor [Arabidopsis thaliana]	gi|22136118	965	119	100.00	94	100.00	42943	6.47	-1.04	-1.28	-1.22	-1.57	*	**	
OSJNBa0042F21.13 [Oryza sativa (japonica cultivar-group)] homolog of sedoheptulose-1,7-bisphosphatase precursor [Oryza sativa (indica cultivar-group)]	gi|38347311	973	173	100.00	124	100.00	42875	5.64	-1.23	-1.55	-1.17	-1.54	**		
triosephosphate isomerase [Fragaria x ananassa]	gi|7650502	1646	83	99.89	65	99.98	33765	7.64	1.22	-1.38	-2.91	-4.03	**	*	**
chloroplast latex aldolase-like protein [Manihot esculenta]	gi|56122688	945	178	100.00	145	100.00	34112	6.22	-1.05	-1.63	1.22	-1.95	*	**	
		1063	277	100.00	234	100.00	34112	6.22	-1.24	-1.68	-1.28	-2.86	**		
plastidic aldolase [Nicotiana paniculata]	gi|4827253	1082	366	100.00	329	100.00	43186	6.38	-1.11	-1.34	-1.02	-1.65	*	**	

chloroplast phosphoglycerate kinase [Populus nigra]	gi|3738261	1109	217	100.00	187	100.00	50493	8.54	-1.13	-1.61	1.45	-2.75	*	*	**
putative beta-hydroxyacyl-ACP dehydratase [Oryza sativa (japonica cultivar-group)]	gi|50931539	1935	76	99.55	55	99.84	23729	8.98	-1.16	-1.89	-2.99	-4.64	**	**	**
Electron transport															
Chain B, Wild-Type Pea Fnr	gi|4930124	1223	135	100.00	88	100.00	35236	6.54	-1.05	7.18	-1.11	2.17	*	**	*
putative quinone-oxidoreductase QR2 [Oryza sativa (japonica cultivar-group)]	gi|50940963	1800	158	100.00	141	100.00	21720	6.08	-1.04	2.49	3.58	2.29	**	**	**
		1806	150	100.00	123	100.00	21720	6.08	1.04	6.34	12.12	4.82	**	**	**
photosystem II oxygen-evolving complex protein 1 - rice (strain Nihonbare)	gi|482311	1393	396	100.00	332	100.00	26651	5.13	1.31	-1.62	-1.33	-1.74	*		
		1400	355	100.00	290	100.00	26651	5.13	-1.02	-1.86	-1.05	-1.67	*		
		1408	402	100.00	327	100.00	26651	5.13	-1.10	-1.88	-1.16	1.07	*	**	
33 kDa polypeptide of oxygen-evolving complex [Arabidopsis thaliana]	gi|15451006	1433	225	100.00	173	100.00	35500	5.55	-1.05	-1.56	-1.41	-1.77	*	**	
oxygen evolving enhancer protein 1 precursor [Bruguiera gymnorrhiza]	gi|9229957	1435	277	100.00	255	100.00	35388	6.48	-1.16	-1.39	-1.96	-1.78	*		
unnamed protein product [Pisum sativum] homologue of Oxygen-evolving enhancer protein 1, chloroplast precursor (OEE1) (33 kDa subunit of oxygen evolving system of photosystem II) (OEC 33 kDa subunit) (33 kDa thylakoid membrane protein).	gi|20621	1616	179	100.00	171	100.00	35148	6.25	1.25	-1.94	-5.76	-10.80	**	**	**
		1750	233	100.00	203	100.00	35148	6.25	1.11	1.11	-3.20	-4.69	**	**	*
23 kDa polypeptide of oxygen-evolving complex (OEC) [Arabidopsis thaliana]	gi|21592906	1767	112	100.00	87	100.00	28281	6.9	-1.03	-1.90	-1.64	-1.40	**	**	
		1781	93	99.99	68	99.99	28281	6.9	-1.19	-1.96	-1.17	-1.53	**	**	
unnamed protein product [Pisum sativum] homologue of Oxygen-evolving enhancer protein 2, chloroplast precursor (OEE2) (23 kDa subunit of oxygen evolving system of photosystem II) (OEC 23 kDa subunit) (23 kDa thylakoid membrane protein).	gi|20617	1901	124	100.00	84	100.00	28217	8.29	-1.01	-2.40	-2.41	-1.90	**	**	*
		1872	98	100.00	58	99.91	28217	8.29	1.14	-1.72	-1.87	-1.86	**	**	*
		1984	150	100.00	98	100.00	28217	8.29	-1.10	-2.45	-2.63	-2.35	**	**	**
		1999	113	100.00	82	100.00	28217	8.29	-1.14	-2.79	-2.18	-1.80	**	**	
		2060	170	100.00	120	100.00	28217	8.29	-1.01	-2.10	-1.45	-1.74	**	**	*
		2081	82	99.86	32	65.09	28217	8.29	-1.04	-2.37	-1.75	-1.57	**	**	**
		2512	103	100.00	53	99.71	28217	8.29	-1.04	-2.22	-2.27	-1.80	**	**	**
		1881	111	100.00	71	100.00	28217	8.29	1.02	-2.94	-2.33	-2.10	**	**	**
Nitrogen/Protein metabolism															
cytosolic glutamine synthetase GSbeta1 [Glycine max]	gi|10946357	940	337	100.00	288	100.00	39234	5.48	-1.13	3.92	2.37	1.88	*	**	
cytosol aminopeptidase; leucine aminopeptidase [Petroselinum crispum]	gi|1483563	463	74	99.18	55	99.83	31317	5.33	-1.31	1.03	2.29	1.38	*	**	**
putative alanine aminotransferase [Oryza sativa (indica cultivar-group)]	gi|29569153	588	372	100.00	276	100.00	54203	8.01	-1.75	-2.55	-1.58	-2.25	**		
Oxidoreductase activity															
cytosolic ascorbate peroxidase 2 [Glycine max]	gi|37196687	1551	97	100.00	77	100.00	27214	5.65	1.04	1.92	1.57	1.70	**	*	*
putative NAD(P)H oxidoreductase, isoflavone reductase [Arabidopsis thaliana]	gi|23297378	1184	221	100.00	190	100.00	34270	6.33	1.30	2.80	3.37	2.21	**		*
Secondary metabolism															
(-)-camphene synthase [Abies grandis]	gi|2411485	1978	73	99.11			71661	6.16	1.39	-1.14	-2.70	-2.65	**	**	**
Protein folding															
putative heat shock protein 70 [Arabidopsis thaliana]	gi|24030296	295	694	100.00	565	100.00	77208	5.17	1.24	1.17	3.16	-1.22	*	**	**
		296	650	100.00	516	100.00	77208	5.17	1.19	1.31	3.05	-1.41	*	**	**
protein disulfide-isomerase (EC 5.3.4.1) - castor bean	gi|2146797	342	87	99.96	59	99.95	55891	4.95	-1.05	1.87	2.47	1.36	**	**	**
		344	86	99.95	66	99.99	55891	4.95	-1.08	2.52	2.37	1.47	**	**	**
		346	96	100.00	61	99.96	55891	4.95	1.01	2.37	1.87	1.54	**	**	
glycine-rich RNA-binding protein [Euphorbia esula]	gi|2645699	2291	128	100.00	93	100.00	16903	6.29	1.07	-1.86	-1.47	-4.01	**	**	**
thylakoid lumen rotamase [Spinacia oleracea]	gi|2864602	913	137	100.00	125	100.00	50229	5.29	1.28	-1.10	-2.60	-1.47	*	**	
EF-Tu [Glycine max]	gi|18776	920	311	100.00	261	100.00	52417	6.21	-1.02	-1.40	-1.02	-1.81	**	**	
Miscellaneous															
nucleoside diphosphate kinase [Arabidopsis thaliana]	gi|16398	2281	191	100.00	163	100.00	16387	7.88	1.21	1.53	2.00	1.50	**	**	
myo-inositol 1-phosphate synthase [Sesamum indicum]	gi|9858816	457	189	100.00	151	100.00	56626	5.59	1.32	2.77	3.84	1.63	**	*	
		458	443	100.00	379	100.00	56626	5.59	1.01	3.23	1.68	1.09	*	**	
		459	192	100.00	128	100.00	56626	5.59	-1.12	2.94	2.21	-1.15	*	**	*
translationally controlled tumor protein [Hevea brasiliensis]	gi|4193388	1882	91	99.99	59	99.93	19132	4.5	1.86	2.60	1.29	1.11	*		
Translationally controlled tumor protein homolog (TCTP) (HTP)	gi|20140865	1777	153	100.00	95	100.00	18961	4.53	1.93	1.88	1.01	-1.05	*		
		1783	71	98.41	36	85.88	18961	4.53	1.44	1.90	1.81	1.26	**		
harpin binding protein 1 [Vitis sp. NL-2003]	gi|38679337	1450	350	100.00	302	100.00	31582	7.82	-1.05	-1.03	-2.34	-1.78	**	**	**

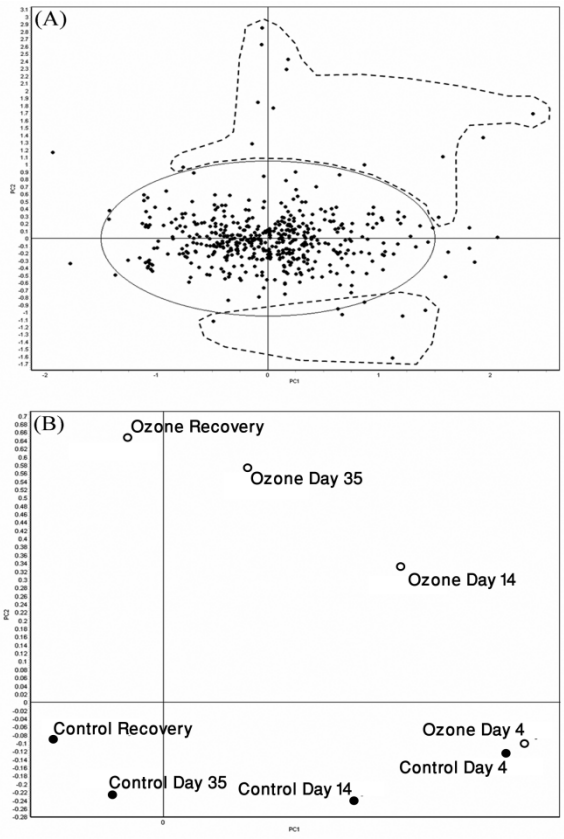

Figure 24: Principal component analysis of the different experimental groups. (A) Loading plot of the 529 proteins matched on all the gels. The spots encircled by dotted lines are significant for the ANOVA *p*-value concerning the treatment factor. (B) Score plot of the different experimental groups, showing a separation along both axes. PC1 is separating the data according to sampling dates and PC2 according to the treatment.

2.2.1.1. Carbon metabolism (Figure 25)

In plants, ozone is known to have specific negative effects on carbon metabolism (Dizengremel 2001). In Figure 25, interactions established from the results of our proteomic study and information from the literature are presented to illustrate different effects of ozone on carbon metabolism. In plants exposed to high concentrations of ozone, RuBisCO activity drops, in parallel with decreases in RuBisCO large and small subunits mRNA and protein content (Miller et al. 1999; Pelloux et al. 2001). Reductions in RuBisCO activase transcript and protein abundance have also been reported (Pelloux et al. 2001). In the present study we demonstrated a permanent depletion in RuBisCO activase content as early as 3 days after ozone treatment (754, 752) which persisted until the end of the treatment (707, 760, 752). However, for one isoform, a large decrease occurred only after the recovery period (1706). These observations are in agreement with the decrease in RuBisCO activity very early during ozone stress previously reported (Fontaine et al. 1999; Pelloux et al. 2001). In the period between day 14 and the recovery (day 45), up to 24 isoforms of enzymes of the Calvin cycle decreased quantitatively. Most of these are involved in the regeneration of ribulose-1,5-bisphosphate (i.e. triose-phosphate isomerase (1646), aldolase (945, 1063), sedoheptulose-1,7-bisphosphatase (965, 973), ribulose-5-phosphate-3-epimerase (754, 760), phosphoribulokinase (925)), one is an isoform of RuBisCO small subunit (2304), and one is a RuBisCO subunit binding protein (1497). This indicates that the initial drop of RuBisCO activity may have repercussions on the

complete Calvin cycle. Indeed, since RuBisCO activity drops, CO_2 fixation is reduced. Consequently fewer molecules of triose-phosphate enter the regeneration pathway and a lower amount of enzymes are needed for ribulose-1,5-bisphosphate regeneration, leading to a down-regulation of enzymes associated with Calvin cycle. In addition, less triose-phosphate is transported out of the chloroplast, thus leading to a decreased availability of substrates for energy production and tissue synthesis through glucose catabolism. After 35 days of treatment, some of the RuBisCO activase isoforms were back to normal (853, 754, 751, 848, 867, 873, 854, 778, 2087), and after the recovery period, most of them returned to their initial level (707, 760, 752), indicating that mechanisms may be induced to neutralize the effect of the pollutant. But at day 35, the ribulose-1,5-bisphosphate regeneration enzymes are at their most repressed status, suggesting that the adaptation to the ozone stress happens gradually, and that the complete Calvin cycle may be back to normal only after a longer recovery period.

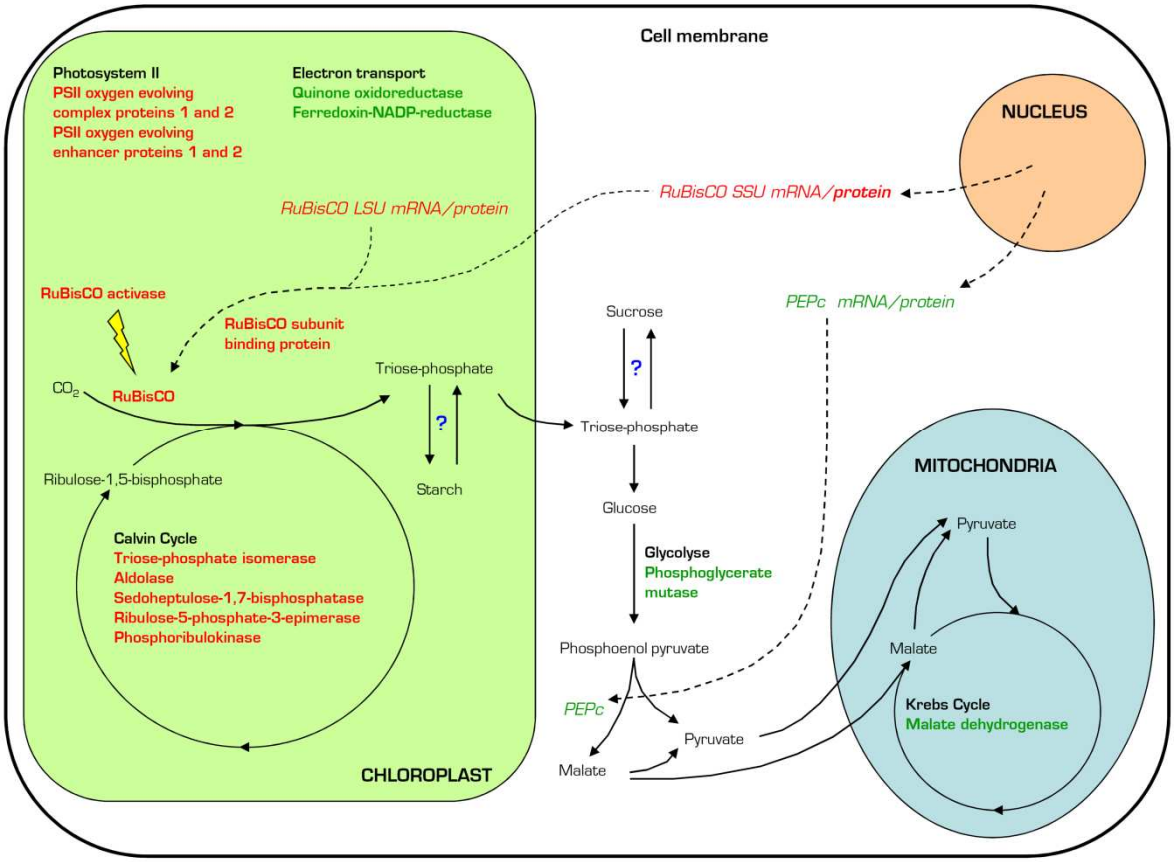

Figure 25: Carbon metabolism in ozone-treated leaves. Information in *italics* is drawn from literature, whereas information presented in **bold** has been collected during the present proteomic study. Proteins and transcripts presented in red decrease in abundance, whereas those presented in green increase.

Similarly, a number of PSII proteins significantly decreased, starting at day 14 (i.e. PSII oxygen evolving complex protein 1 (1393, 1400, 1408, 1767, 1781) and 2 (1433) and oxygen evolving enhancer protein 1 (1435, 1616, 1750) and 2 (1901, 1872, 1984, 1999, 2060, 2081, 2512, 1881). Most of the isoforms that were low in the ozone-treated plants remained low even after the recovery period. Interestingly, the decrease in abundance for the photosystem proteins was similar to the observed results for the ribulose-1,5-bisphosphate regenerating enzymes. Since the Calvin cycle is the major sink for ATP and NADPH in the chloroplast, the down-regulation of the cycle would lead to an accumulation of ATP and NADPH in the organelle. To avoid photooxidative damage, a down-regulation of the electron transport chain through the PSII may also be necessary (Ranieri et al. 2001). This hypothesis is supported in our results by the reduced quantity of PSII proteins as well as by the decrease in chlorophyll content (Figure 22). Since electrons can no longer be transported, the light harvesting complexes containing the chlorophylls and lutein will probably be decoupled to avoid uncontrolled electron leakage. The fact that both chlorophyll a and b decrease over the treatment may indicate that mainly PSII is affected, since PSII and light harvesting complex II contain the majority of chlorophyll b (Green and Durnford 1996). Whether or not the decrease in lutein is due to the dismantling of photosystems or to its role in detoxication as a carotenoid cannot be stated at this point. Similar to the Calvin cycle enzymes, PSII associated proteins had not returned back to control levels after the recovery period, possibly due to a slower regulation process. Furthermore, two proteins from the electron transport chain not belonging to PSII were identified, quinone oxidoreductase (1800, 1806), responsible for reducing quinone, and ferredoxin-NADP-reductase (FNR) (1223), an electron acceptor after photosystem I (PSI). Both these proteins increased in abundance, contrary to PSII proteins, possibly to avoid electron leakage.
In contrast to the Calvin cycle, glucose catabolism is thought to increase in response to ozone stress. The activity of PEPc was shown to increase in spruce (Sehmer et al. 1998), Aleppo pine (Fontaine et al. 1999) and sugar maple (Gaucher et al. 2006). Moreover, this increase in activity was concomitant with an increase in PEPc transcripts and protein abundance (Fontaine et al. 2003). Other enzymes, linked to glycolysis (phosphofructokinase) and the pentose phosphate pathway (glucose-6-phosphate dehydrogenase) also increased under ozone treatment (Sehmer et al. 1998). In the present study, we were able to identify two enzymes associated to the glucose catabolism that increased during the ozone treatment: phosphoglycerate mutase (306, 315), involved in glycolysis, and malate dehydrogenase (1161), homologous to the mitochondrial form, involved in the Krebs cycle. Two isoforms of phosphoglycerate mutase were also identified, one which increased significantly from day 14 through the recovery period (306) and one that increased from day 14 through day 35 (315) while the enhanced malate dehydrogenase content became significant after 35

days and remained so after the recovery period. The pattern of abundance of these two enzymes indicates that glucose catabolism might be up-regulated as has been previously suggested (Dizengremel 2001). Since ozone exposure in plants is known to induce an oxidative stress response (Conklin and Last 1995; Ludwikow et al. 2004), the up-regulation of glucose catabolism could partly be due to a need for energy and reducing power for detoxication and repair of damages caused by oxidative molecules. Indeed, an increase in detoxication enzymes, e.g. ascorbate peroxidase (APX), superoxide dismutase, glutathione reductase in response to ozone exposure has been previously reported (Sehmer et al. 1998). The low impact on the reduction in diameter growth (Figure 21B) could either be a consequence of a redistribution of energy for detoxication and repair, or due to a general shortage in energy due to the declining supply of carbon from photosynthesis.

2.2.1.2. Other functions

In leaves, nitrogen assimilation mainly happens through plastid glutamine synthetase (GS2). In senescent leaves however, it shifts towards the cytosol, and the cytosolic isoform (GS1) is induced (Brugière et al. 2000). This shift was also shown to happen during water stress (El Khatib et al. 2004). On the other hand, GS2 is responsible for recycling ammonia released during photorespiration but may be replaced by GS1 in stress situations. More information about this point will be provided by a study in progress in our team. In the present study, we were able to identify a cytosolic GS (940) that increased in quantity at 14 and 35 days, and was still elevated after the recovery period. This could be held in parallel to the accelerated senescence occurring as a response to ozone treatment (Figure 20B and Figure 21C). This hypothesis may also be supported by the up-regulation of a cytosolic aminopeptidase (463), which may be responsible for protein degradation.

The identification of a statistically significant increase in ascorbate peroxidase (1551) is in agreement with increased APX mRNA levels and activity reported in the literature (Conklin and Last 1995; Gaucher et al. 2006). It plays a role in peroxide reduction by facilitating the oxidation of ascorbate. The isoflavone reductase (1184) present in higher abundance in the ozone-treated leaves could be responsible for reducing oxidized isoflavones, but is also highly homologous with an enzyme that is thought to be involved in glutathione redox state control (Petrucco et al. 1996).

Several proteins involved in protein folding were identified. Two isoforms of heat shock protein 70 (HSP70, 295, 296) and 3 isoforms of disulfide isomerase (87, 86, 96) are over-expressed during ozone stress. Since these proteins are responsible for correct protein folding during post-translational modification, protein transit and when proteins lose their structural integrity, the results suggest that some direct damage to the proteins may occur during ozone stress. Very little can be said about the three additional proteins ranked under “protein folding” (i.e. glycine-rich RNA-binding protein

(2291), thylakoid lumen rotamase (913) and elongation factor Tu (920)). All three decreased in response to ozone, but no precise role can be attributed to them.

Some of the proteins listed in Table 4 are not discussed above. They are mainly proteins for which the exact role during ozone stress cannot be clearly stated. Their function may either not be clear, or the available information is insufficient to suggest any sustainable hypothesis.

When the abundance of proteins after the recovery period is taken into account, it is apparent that many proteins still varied significantly compared to the controls and that for several of them the differences were greater. This could either mean that some effects of ozone exposure are irreversible, or that a ten day period is too short for a full recovery.

Statistically speaking, most of the proteins that were significantly different due to the ozone treatment also showed length of exposure to ozone (time) as a significant variable. Of the identified proteins, many are known to vary during senescence, and by the end of the ozone treatment, many of the leaves were extensively damaged and near death. This explains why these proteins are significantly different for the time factor. The fact that approximately the same proteins are significant for the ozone factor suggests that ozone is inducing an accelerated senescence in the leaves. This would also explain why ozone treated plant have a higher rate of leaf abscission (Figure 21C).

Taking into account all the results collected during this study, the effects of ozone on young poplar leaves could be summarized as follows. A deleterious effect of ozone exposure on photosynthesis was readily apparent since several enzymes of the Calvin cycle and electron transport chain were shown to decrease in abundance. The observed variations could be associated to a decrease in substrates for glucose catabolism and energy production. A shortage of energy is also suggested by increase of some enzymes in ozone-treated leaves that are involved in glucose catabolism. Although no direct evidence was found, there could be a remobilization of carbon from starch and sucrose to feed carbon catabolism, or even a remobilization of carbon from source organs. A detailed analysis of leaf carbohydrate content could give further information about the use of stored carbon. Seeing how metabolic pathways associated with the chloroplast are strongly affected, future studies may focus specifically on a thorough proteomic examination of the chloroplast by native proteomics and by western blot verification.

Additionally, a proteomic study of a wider array of leaves at different levels of maturity should be considered. It is known that leaves that were mature and fully developed at the beginning of ozone treatment behave differently than young ones for some enzyme activities (personal communication

from Matthieu Bagard). A comparison between this study and one on adult leaves would thus be of interest.

In conclusion, our initial proteomic approach of the response of young poplar leaves to ozone complements physiological and morphological observations and clearly emphasizes the complexity of the response to high concentrations of ozone.

2.2.2. Acknowledgements.

We acknowledge Dr Henry-Michel Cauchie from the Centre de Recherche Public - Gabriel Lippmann for his expertise help with statistics, Dr Michael Wisniewski from the Appalachian Fruit Research Station, Kearneysville, West Virginia , USA, for his corrections of the used English language and Dr Kris Laukens from University of Antwerp, Center for Proteome Analysis and Mass Spectrometry, for the generation of the decoy database.

This study was supported by the Luxembourg Ministry of Culture, Higher Education and Scientific Research (S.B.'s PhD fellowship BFR06/044).

2.2.3. Supplemental Data

Supplemental Figures 1: Abundance profiles for all discussed proteins are presented in charts. On the x axis are the days of treatment and on the y axis the standard abundance exported from the Decyder software. Multiple lines of the same color represent spots containing the same protein function. Green circles represent control and red triangles treatment conditions

Chapter 3

The poplar chloroplast membrane proteome under ozone exposure

3.1. General introduction

From the previous chapter it is clear that the effect of ozone on the chloroplast metabolism is crucial, even more so considering the importance of that metabolism in plant life. The chloroplast is the site of CO_2 fixation and photosynthesis. Those reactions were originally the cause of the oxygenation of the earth's atmosphere and subsequently of the formation of the ozone layer and the development of life on land. Chloroplasts are only found in eukaryotes (algae and higher plants), but the ancestor of this organelle was a prokaryotic cyanobacterium (Deschamps et al. 2008; Deusch et al. 2008). The theory of endosymbiosis that states that a prokaryotic cell ingested a photosynthetic prokaryote, but that this cell was not digested and ultimately co-evolved into a chloroplast is now generally accepted (Cavalier-Smith 2000; Margulis 1971; Mereschkowsky 1905). Although it would seem that this is the origin of the higher plant chloroplast, the situation seems a little more complicated for algae. Several instances of phagocytosis probably took place during evolution and led to the formation of more complex chloroplasts having three or more membranes (Archibald 2009; Vesteg et al. 2009). The higher plant chloroplast is bound by a double membrane called the envelope and the internal structure is formed of an intensive system of membranes called thylakoids that can either be stacked (grana) or free (lamellae). The cytosol of the chloroplast is called stroma, and the internal space of the thylakoids is called lumen (Kutík 1998; Taiz and Zeiger 2002) (Figure 26). Although chloroplast contains its own multiploid DNA, it codes for less than 80 proteins and most of the chloroplastic proteins are coded in the nucleus (Sugiura 1992). They are synthesized in the cytosol to be imported into the chloroplast thanks to an N-terminal targeting peptide (Soll and Schleiff 2004).

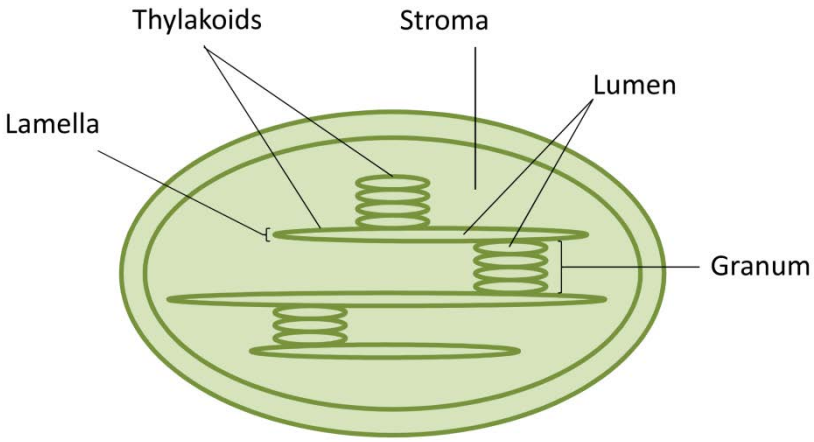

Figure 26: Higher plant chloroplast structure

As already mentioned, one of the most important cellular functions in plants, photosynthesis, takes place in the chloroplast. Although photosynthesis is a complex process, it can be summarized into the production of reduced sugars from light energy. It can be roughly divided into two parts: the photochemical part, harvesting sunlight to produce reducing potential (NADPH) and energy (ATP); the biochemical part, using the energy and the reducing power from the photochemical part to fix atmospheric CO_2 and produce reduced sugars, also called Calvin-Benson cycle or Calvin cycle (Bassham et al. 1950). Although these are among the most important chloroplastic processes, many other pathways exist in this organelle, like photorespiration, fixing O_2 instead of CO_2 (Bauwe 2010; Rajinikanth et al. 2007), or chlororespiration, an electron transport chain similar to the one of the mitochondrion (Casano et al. 2000; Peltier and Cournac 2002).

The processes of photosynthesis involve a large number of proteins, the suborganellar location of which highly depends on the function they accomplish. The enzymes of the biochemical part, which mostly catalyze reactions involving soluble substances like carbohydrates and carbonic acids are mostly soluble and located in the stroma, although some can be membrane-bound (e.g. fructose bisphosphate aldolase). The enzymes of the photochemical part on the other hand are grouped into four major membrane complexes, photosystem I, photosystem II, cytochrome b6f (cyt b6f) and ATPase (Figure 27). Some subunits of the complexes are membrane bound; others are associated to the membrane on the luminal or stromal side of the membrane (Nelson and Yocum 2006). The role of the photochemical part is the transport of electrons through three of the four membrane complexes. The process involves the activation of electrons from a special pair of modified chlorophyll molecules composing the reaction center of PSII (P680). This activation occurs with the help of light energy collected by light harvesting complexes composed of proteins, chlorophyll and other pigments. The electrons are then transported through PSII and transferred to cyt b6f by plastoquinone, where their energy allows the transfer of protons from the stroma to the lumen. The electrons are then transferred to plastocyanin and then to PSI, where they are activated in another reaction center (P700). The reactivated electrons are then transported through PSI and transferred to ferredoxin, a soluble protein, which is finally used as an electron donor by ferredoxin-$NADP^+$-oxidoreductase to transform $NADP^+$ into NADPH. In PSII, H_2O is split into O_2 and H^+ to collect electrons that regenerate P680, also called oxygen evolution. In summary, this process allows the formation of NADPH, a molecule with high reducing potential, and the formation of an H^+ gradient between lumen and stroma by (i) the splitting of water (ii) the transfer of H^+ from stroma to lumen and (iii) the use of H^+ during NADPH production. The ATPase complex then uses the H^+ gradient to generate the energy needed to transform ADP into ATP. NADPH and ATP produced during this process are mainly used in the Calvin cycle.

As could be observed in Chapter 2, many of the Calvin cycle enzymes presented detectable changes during the proteomic study. But only a few membrane complex proteins could be seen. Due to their association with the membrane, these proteins are hydrophobic. The protocol generally used for protein solubilization in 2DE is efficient for hydrophilic, soluble proteins, but not for hydrophobic membrane proteins. It is therefore necessary to use a modified solubilization tool to study membrane proteins. This is done by adding a detergent to the solubilization buffer, but there are certain limits to this. Detergents have a hydrophobic region, allowing their interaction with hydrophobic molecules, and generally a charged region to permit their solubilization in water. As already stated in 1.4. Proteomics and its advantages, charged detergents cannot be used in IEF. Charged detergents would cover the proteins, uniformly charging them and masking the proteins own charge and prevent pI based fractionation. This is why a non-charged detergent has to be used to solubilize membrane proteins for IEF.

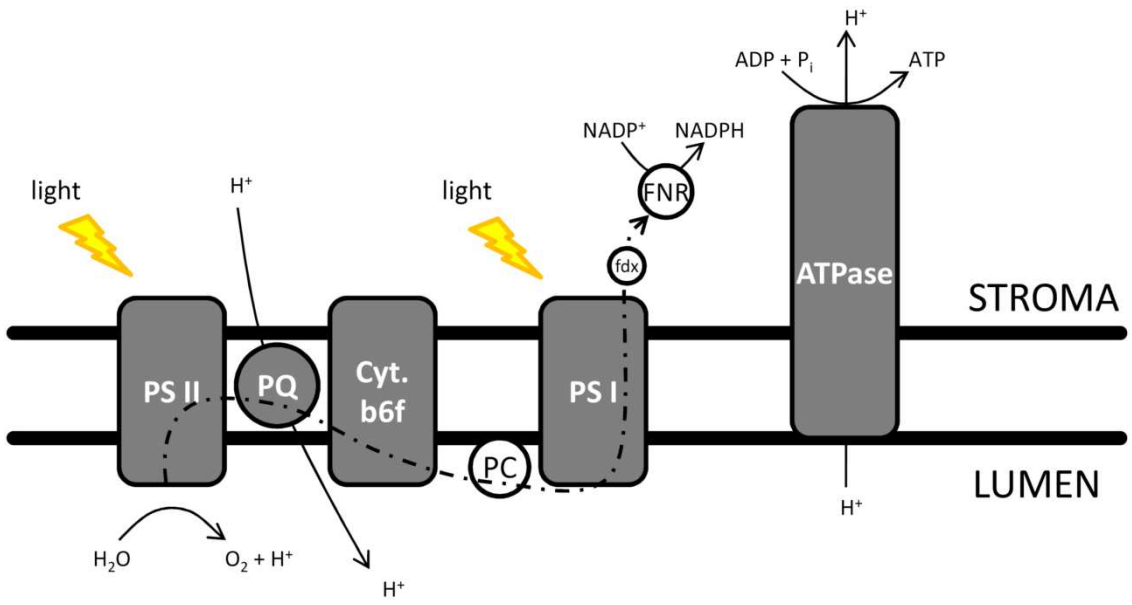

Figure 27: Chloroplast electron transport chain. ATPase, adenosine triphosphatase; Cyt. b6f, cytochrome b6f; fdx, ferredoxin; FNR, ferredoxin-$NADP^+$-oxidoreductase, PC, plastocyanin; PQ, plastoquinone; PSI, photosystem I; PSII, photosystem II,

In the research paper of the current chapter, the chloroplast membrane proteome was specifically targeted to complement the information of the research paper in Chapter 2. The experimental setup basically resembles the one of Chapter 2 with a slightly changed time line (Figure 28). Chloroplasts were isolated after 7, 14, 21 and 28 days of ozone treatment and membrane proteins were extracted for use in a DiGE experiment. Detailed information is presented in 3.2.3. Material and

methods. The data in this research paper is the first part of a larger experiment, the second part of which will be presented in Chapter 4.

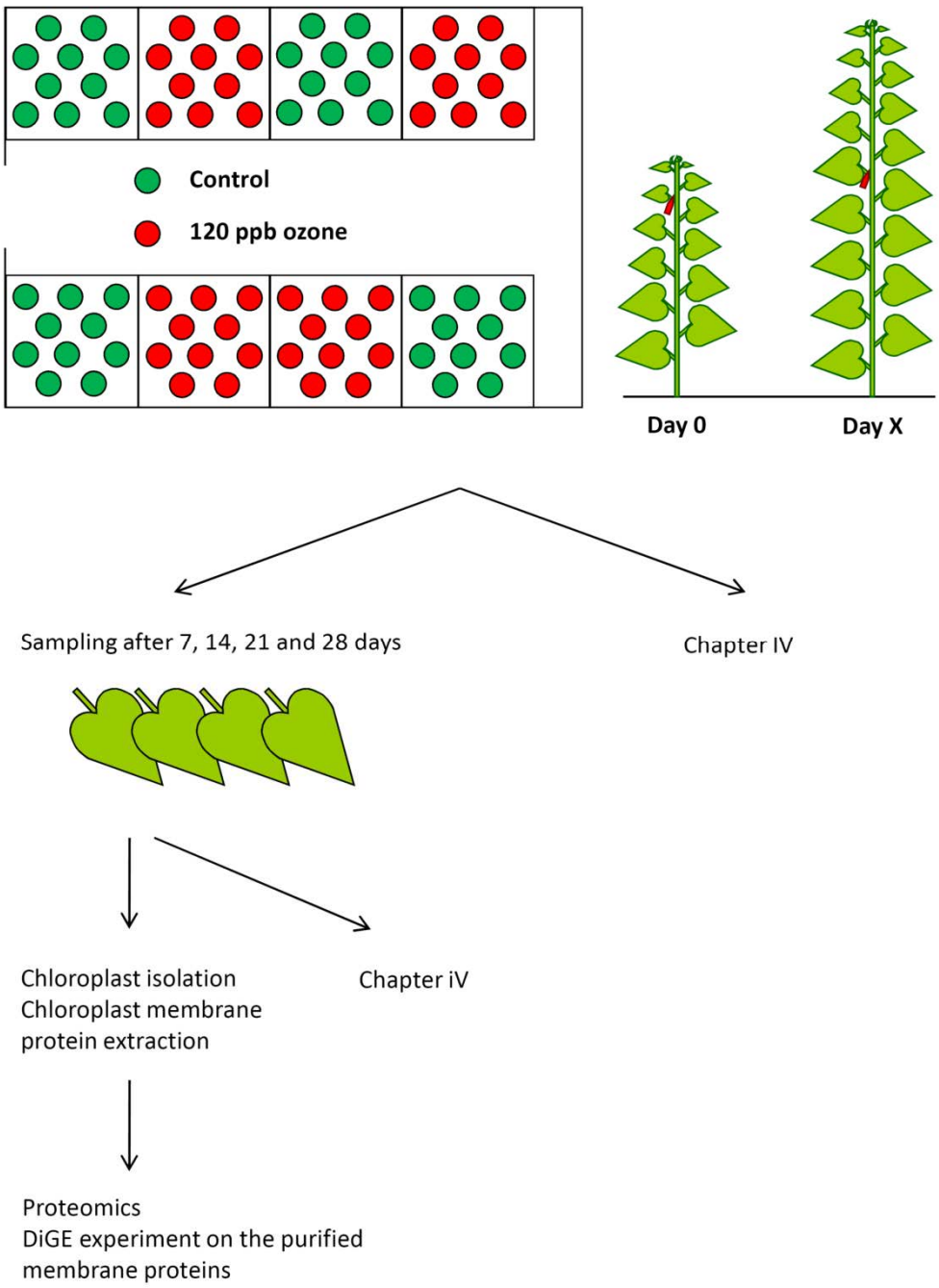

Figure 28: Experimental setup of the second experiment, part 1, chloroplast membrane proteome.

3.2. Bohler et al. submitted in Journal of Proteomics

A DiGE study on thylakoids isolated from poplar leaves reveals a negative impact of ozone exposure on membrane proteins.

Bohler Sacha[a,b,c], Sergeant Kjell[a], Hoffmann Lucien[a], Dizengremel Pierre[b,c], Hausman Jean-Francois[a], Renaut Jenny[a], Jolivet Yves[b,c].

[a]CRP-Gabriel Lippmann, 41 rue du Brill, L-4422 Belvaux, GD. Luxembourg, Department Environment and Agro-biotechnologies

[b]Nancy-Université, UMR 1137 Ecologie et Ecophysiologie Forestières, F-54506 Vandoeuvre-lès-Nancy, France.

[c]INRA, UMR 1137 Ecologie et Ecophysiologie Forestières, Centre Nancy, F-54280 Champenoux, France.

Keywords: Air pollution, chloroplast, membrane, photosynthesis, primary carbon metabolism, proteomics.

3.2.1. Abstract

Populus tremula L. x *P. alba* L. (*Populus* x *canescens* (Aiton) Smith) - clone INRA 717-1-B4 saplings were submitted to a chronic 120 ppb ozone exposure for 28 days. Chloroplasts were isolated and the membrane proteins, solubilized using the detergent DHPC, were analyzed in a DiGE experiment comparing control versus exposed plants. An important number of extrinsic photosystem proteins and ATPase subunits were detected to vary in abundance. The general trend was a decrease in abundance, except for ferredoxin-$NADP^+$-oxidoreductase (FNR) that increased during the first 7 days of exposure. The up-regulation of FNR would increase NAPDH production for reducing power and detoxification inside and outside of the chloroplast. Later on, FNR and a number of PS and ATPase subunits decrease in abundance. This could at the same time be a consequence of an oxidation of the proteins and a protective measure against photooxidation induced by the known decrease in Calvin cycle activity.

3.2.2. Introduction

Since the industrialization age, human activity has led to the accumulation of many types of pollutants, among which tropospheric ozone is today one of the most prominent. This secondary

pollutant is the consequence of the interaction between primary pollutants (e.g. nitrous oxides, volatile organic compounds) and sunlight, and has negative impacts on animal and plant life (Ebi and McGregor 2008; Sandermann 1996).

Many studies have shown the effects of ozone on plants (for reviews see (Dizengremel and Petrini 1994; Heath 2008; Kangasjärvi et al. 2005; Matyssek et al. 2010a; Renaut et al. 2009; Sandermann 1996)) and many of these studies showed that chloroplast localized processes are strongly affected. Perhaps the most easily observed impacts of ozone on the chloroplast concern the shape and the structure of the organelle. It has been repeatedly shown that chloroplasts become smaller, the stroma electron denser under electron microscopy, and the thylakoids distorted under ozone exposure (Günthardt-Goerg et al. 2000; Kivimäenpää et al. 2004; Oksanen et al. 2001; Pääkkonen et al. 1996; Prozherina et al. 2003). Other studies report changes in chlorophyll fluorescence, mainly decreases in Fv/Fm, a parameter that is used in plant physiology to estimate the maximum efficiency of PSII (Anderson et al. 2003; Bagard et al. 2008; Lorenzini et al. 1999; Wittmann et al. 2007) and variations in pigment content (Bagard et al. 2008; Bohler et al. 2007; Lütz et al. 2000; Ranieri et al. 2000) indicating a serious impact on photosynthesis. Furthermore, an effect of ozone on soluble Calvin cycle proteins is known and it is clear that ozone leads to decreased CO_2 fixation by negatively influencing the abundance of RuBisCO (Bagard et al. 2008; Bohler et al. 2007; Brendley and Pell 1998; Lütz et al. 2000; Pääkkonen et al. 1996; Pelloux et al. 2001). On the other hand, relatively little is known about the effects of ozone on the subunits of the photosynthetic complexes, photosystems I and II. A few studies reported decreases in the abundance of the reaction center proteins (e.g. D1, D2, PSI core complex) or light harvesting complexes (LHC I, LHCII) (Ranieri et al. 2001; Ranieri et al. 2000) but information about the many extrinsic subunits of both photosystems is rare.

Both PSI and PSII are multi-protein membrane complexes composed of membrane intrinsic proteins, constituting the reaction centers, and extrinsic proteins with different roles. In PSII, the extrinsic proteins assemble and stabilize the oxygen evolving manganese cluster (Mn-cluster) that is responsible for the splitting of water into oxygen and hydrogen resulting in the transfer of electrons to the PSII reaction center (Hankamer et al. 1997; Ohta et al. 2003). In PSI the extrinsic proteins are mostly responsible for the stabilization and cross linking of PSI with plastocyanin on the electron acceptor side, and with ferredoxin on the donor side (Fromme et al. 2001). Although both photosystems seem to be able to function at least partially *in vitro* without part or all of the extrinsic subunits, they play an important role *in vivo* to stabilize, regulate and increase the efficiency of the electron transport chain.

In previous studies, we observed that ozone negatively impacted photosystem proteins, but only a small fraction of the subunits were ever detected (Bohler et al. 2007) (4.2. Bohler et al. Tree Physiology in press). In the present study, the chloroplast membrane proteome of ozone-treated poplar leaves was studied. With this targeted proteome study we tried to elucidate the effects of ozone on the electron transport chain of chloroplasts, thereby adding useful information that was unavailable from our previous studies (Bohler et al. 2007; Renaut et al. 2009) (4.2. Bohler et al. Tree Physiology in press).

3.2.3. Material and methods

3.2.3.1. Plant material and ozone treatment

Poplar clones (*Populus tremula* L. x *P. alba* L. (*Populus* x *canescens* (Aiton) Smith) - clone INRA 717-1-B4) were multiplied *in vitro*, transferred to a mix of peat/perlite (Gramoflor SP1 Universel), transplanted into 5 L pots containing peat/perlite fertilized with 15 g of slow-release nutritive granules (Nutricote T-100, N/P/K/MgO 13/13/13/2, Fertil, Boulogne-Billancourt, France) after 2 weeks and grown at 75%/85% relative humidity (day/night) with a 14 h light period (Sun T Agro, Philips, Eindhoven, The Netherlands; intensity: 250–300 $\mu mol.m^{-2}.s^{-1}$) and 22°C/18°C ± 2°C (day/night) over a period of 5 weeks.

For the ozone treatment, plants were transferred into 8 fumigation chambers with 10 plants per chamber and acclimated for 3 weeks prior to the treatment start. Four randomly selected chambers were used for control treatment and the other 4 for ozone treatment. Control plants were grown in charcoal filtered air while treated plants were exposed to charcoal filtered air supplemented with 120 ppb of ozone for 13 h per day during the light period. Environmental conditions (light, temperature, relative humidity) were as described above. Leaf n° 5 (approximately 8 x 5 cm), counted from the last leaf emerged at the apex, was tagged at the beginning of the treatment on each plant. Those leaves were harvested after 7, 14, 21 and 28 days of exposure. For day 7, four leaves per chamber were harvested and pooled, whereas they were two for days 14 to 28 (between 8 and 12 g fresh weight per chamber and per sampling date). Leaves were put on ice and immediately used to isolate the chloroplasts. Four biological replicates were made per condition per sampling date, each replicate corresponding to one chamber.

3.2.3.2. Chloroplast isolation

Chloroplasts isolation (Eichacker et al. 1996) was done at 4°C. Leaves were roughly cut and put into a pre-cooled isolation buffer (400 mM sorbitol, 50 mM HEPES KOH pH 8.0, 2 mM EDTA Na_2 NaOH pH 7.5). Leaves were homogenized in a blender with three quick pulses and the solution was filtered

through gaze. The homogenized leaves were re-suspended in isolation buffer, homogenized and filtered a second time. The recovered chloroplast suspensions were pooled and filtered through a nylon membrane (20 µm mesh). The suspension was centrifuged for 4 min at 400 x g to remove the cell fragments. The supernatant was then centrifuged for 10 min at 8,000 x g to pellet the plastids. After discarding the supernatant the pellet was re-suspended in 2.5 mL isolation buffer. A continuous Percoll gradient was created by centrifuging 60% Percoll (v/v in isolation buffer) at 30,000 x g for 15 min. The chloroplast suspension was slowly pipetted on top of the Percoll gradient and centrifuged for 45 minutes at 8,000 x g. The green band corresponding to the chloroplasts was collected and washed twice by adding washing buffer (400 mM sorbitol, 400 mM HEPES KOH pH 8.0, 1 mM EDTA Na_2 NaOH pH 7.5) and centrifuged for 5 min at 8,000 x g. Finally, the pellet containing the chloroplasts was solubilized in 2 mL washing buffer and immediately frozen in liquid nitrogen.

3.2.3.3. Solubilization of chloroplast membrane proteins

Chloroplast membranes were disrupted twice using a French press cell disrupter (Thermo Electron Corporation, Waltham, Massachusetts, U.S.) at 20,000 Psi and subsequently pelleted using an optima L-90K ultracentrifuge (Beckman Coulter, Brea, California, U.S.) for 1 hour at 200,000 x g as previously described (Goulas et al. 2006). The pellet was re-suspended in 2 mL suspension buffer (10mM Tris, 1mM EDTA, 250 mM sucrose, pH 7.5). The membrane fraction was cleaned using the ReadyPrep 2-D Cleanup Kit (Biorad, Hercules, California, U.S.) according to the instructions of the manufacturer and the proteins were finally solubilized in labeling buffer (7 M urea, 2 M thiourea, 0.5% Triton 100x, 30 mM Tris, 1.5 mM 1,2-Diheptanoyl-sn-Glycero-3-Phosphocholine (DHPC) (Avanti Polar Lipids, Alabaster, Alabama, U.S.)) as previously described (Babu et al. 2004). After adjusting the pH to 8.5 the protein concentration was determined using the 2D Quant Kit (GE Healthcare, Little Chalfont, UK). The proteins were used for a multiplexed analysis by fluorescence difference gel electrophoresis (DiGE) (Skynner et al. 2002). Protein extracts and a pooled internal standard were labeled with CyDyes™ (GE Healthcare) prior to electrophoresis (Kieffer et al. 2009). Ninety micrograms of proteins (two samples of 30 µg each and 30 µg of internal standard) were loaded on each gel and separated by 2D electrophoresis.

3.2.3.4. Bidimensional electrophoresis.

The volume of each sample mix consisting of two samples and the internal standard was adjusted to 450 µL with labeling buffer. To this 2.7 µL of Destreak Reagent (GE Healthcare), 9 µL of IPG buffer 3-10 NL (GE Healthcare) and 5 µL of a saturated bromophenol blue solution were added. Sample loading on ReadyStrip IPG strips pH 3-10 NL, 24 cm (Biorad) was done overnight by passive rehydration. Isoelectric focusing was carried out on an Ettan IPGphor Manifold (GE Healthcare) in an

IPGphor IEF unit (GE Healthcare). The following protocol was used: 150 V for 4 h, gradient to 500 V for 3 h, 500 V for 3 h, gradient to 1,000 V for 3 h, 1,000 V for 3 h, gradient to 10,000 V for 3 h, 10,000 for 6 h until approximately 83,000 Vhrs were reached, at 20°C with a maximum current setting of 75 µA per strip. The second dimension was run on precast 12.5% polyacrylamide gels using the Ettan DALT 12 Buffer Kit according to the instructions of the manufacturer (The Gel Company, Tübingen, Germany). An Ettan DALT 12 Electrophoresis system (GE Healthcare) was used for the second dimension run.

3.2.3.5. Image capture and analysis

The gel images of the different samples were acquired using a Typhoon Variable Mode Imager 9400 (GE Healthcare) at a resolution of 100 µm according to the instructions provided for each dye. Images were analyzed using the Decyder v6.5.14.1 software (GE Healthcare). Selected spots of interest (absolute abundance variation of at least 1.5-fold, ANOVA $p<0.01$) were located and a picking list was generated. Spots of interest were excised and digested as previously described (Bohler et al. 2007). MS and MS/MS spectra were acquired using an Applied Biosystems 4800 Proteomics Analyzer (Applied Biosystems, Sunnyvale, CA, USA), calibrated using the 4700 peptide mass calibration kit (Applied Biosystems). Proteins were identified by searching against the NCBI poplar protein databases (downloaded 2009.06.11, 99,629 sequences) and poplar EST (downloaded 2009.06.11, 419,944 sequences) using MASCOT (Matrix Science, www.matrixscience.com, London, UK). All searches were carried out allowing for a mass window of 150 ppm for the precursor mass and 0.75 Da for fragment ion masses. The search parameters allowed for carboxyamidomethylation of cysteine as fixed modification and oxidation of methionine and of tryptophan (single oxidation, double oxidation and kynurenin formation) and for pyrrolidone carboxylic acid (N-terminal glutamine and glutamic acid) as variable modifications. Homology identification was retained with a probability set at 95%.

3.2.3.6. Statistics

The statistical analysis was done with the Extended Data Analysis package (EDA) of the Decyder software (GE Healthcare). Four biological replicates per sampling date were used, where each replicate represents one fumigation chamber. Normalization and standardization were done, by logarithmic transformation and standardization against the internal standard respectively, as described by the manufacturer. A Two-Way ANOVA was used for the differential protein abundance determination, using the treatment condition as factor 1, and the sampling time as factor 2. A p value < 0.01 for condition 1 and an absolute abundance variation of at least 1.5-fold between control

and treatment were considered significant. A principal component analysis was performed with the EDA module.

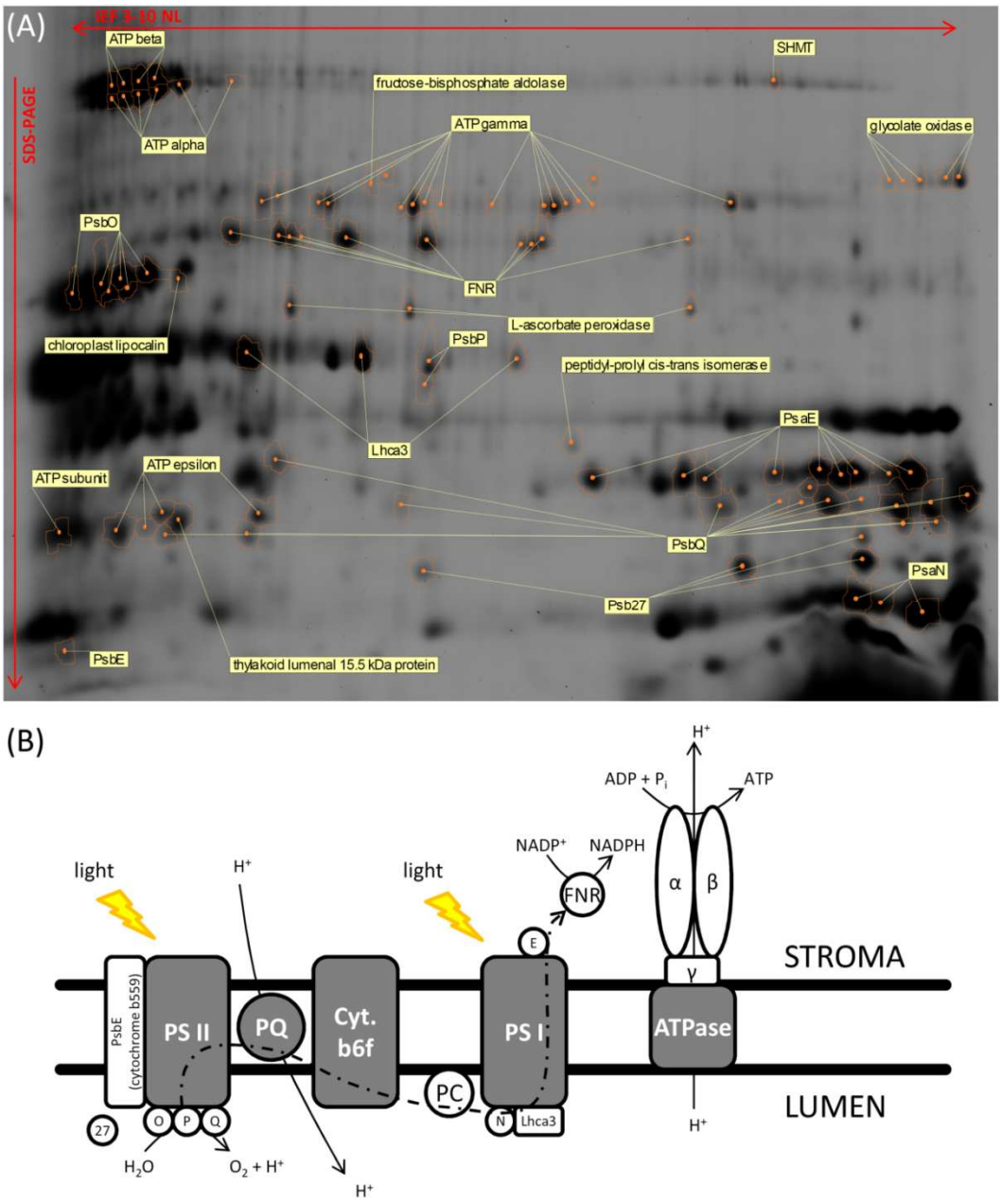

Figure 29: (A) Cy2 gel view with identified protein spots in orange. Horizontal separation was done by IEF 3-10 NL, vertical separation by SDS-PAGE as described in 3.2.3. Material and methods. (B) Representation of the chloroplast electron transport chain and the positions of the subunits that vary due to ozone exposure. White elements represent all the identified subunits that vary due to ozone, gray elements regroup the remaining subunits of the electron transport chain. Abbreviations: 27, O, P, Q = Psb27, PsbO, PsbP, PsbQ; N and E = PsaN, PsaE; PQ = plastoquinone, PC = plastocyanin, Cyt. B6f = cytochrome b6f, FNR = ferredoxin-$NADP^+$ oxidoreductase. Dashed line: electron transport path.

3.2.4. Results and Discussion

A total of 587 protein spots could be matched on at least 93% (15 out of 16) of the 2D gels. The statistical analysis of those 587 proteins provided a list of 174 spots that were significantly different in abundance at a threshold of p-value<0.01 and applying the false discovery rate detection. Finally 98 spots could be significantly identified by Maldi-ToF MS/MS (Table 5, Figure 29A, Supplemental Table 1).

The score plot of a principal component analysis allowed separating the experimental groups along two axes, explaining 81.5% of the variation (Figure 30A). The axis PC1 separates the experimental groups according to the sampling time, and explains 55.2% of the variation, the axis PC2 separates them according to the treatment conditions and explains 26.3% of the variation. This indicates that there is a developmental effect that is more important than the ozone effect. As already described previously (4.2. Bohler et al. Tree Physiology in press) proteins largely follow the same pattern of variation under control and treatment conditions, accounting for the high significance of time. Nevertheless ozone induces small but significant changes in those patterns, accounting for the second most important source of variation. The loading plot shows two groups of differentially abundant proteins, one positioned on the top half of the graph that represents the spots decreasing in abundance during ozone treatment, and one on the lower half that represents the spots increased in abundance (Figure 30B). It is clear from the representation in Figure 30B that the applied ozone treatment repressed the abundance of more proteins than it increased.

The isolation of chloroplast membrane proteins allowed us to get more precise information about the influence of ozone exposure on the chloroplast membrane proteome complementing our previous work (Bohler et al. 2007) (4.2. Bohler et al. Tree Physiology in press). Using DHPC as a detergent for membrane proteins, as previously described (Babu et al. 2004), is efficient for membrane associated proteins and proteins with few transmembrane domains, but remains insufficient for proteins with multiple transmembrane helices.

Although the purity of the chloroplast isolation seems good, absolute purity is rarely attained (Yuan et al. 2010). Two of the identified proteins are known to originate from other organelles, namely glycolate oxidase, which only exists in peroxisomes, and serine hydroxymethyltransferase (SHMT), which, with the glycine decarboxylase complex, makes up for 50% of the soluble mitochondrial matrix proteins (Rajinikanth et al. 2007). SHMT exists in the chloroplast, but our data indicates that the form identified here is located in the mitochondria. However, an argument against mitochondrial contamination is that no protein of the mitochondrial electron transport chain or of the mitochondrial ATPase could be detected, although they are abundant and should be expected if

there was a contamination by mitochondrial membranes. The presumed contamination by peroxisomes and mitochondria could result from the fact that the chloroplasts had to be isolated during the day when the plants were actually exposed to ozone. The accumulation of starch during the day increases the density of the chloroplasts in an irregular way, and the starch granules can disrupt the chloroplast membranes during isolation (Neuhaus and Schulte 1996). For that reason the chloroplast band on the Percoll gradient was more diffuse than when the isolation is done in the early morning, when the starch content of chloroplasts is minimal and the chloroplast density more homogeneous.

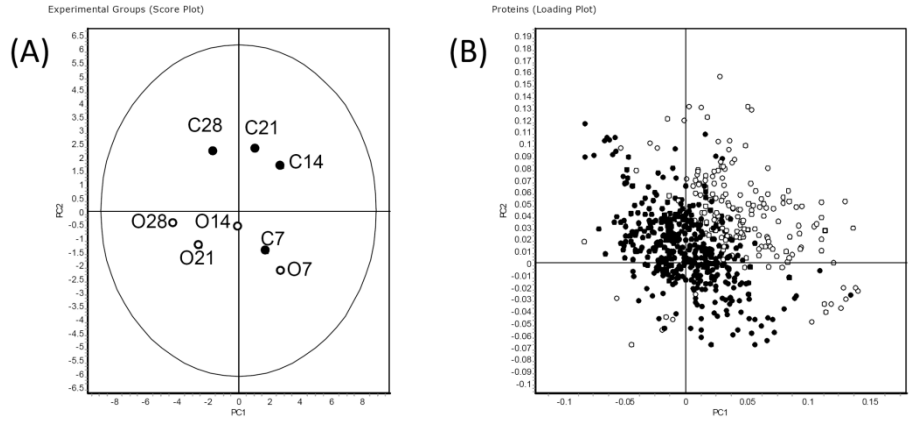

Figure 30: Principal component analysis. (A) Score plot of the experimental groups (PC1 55.2% and PC2 26.3% of the variation), closed dots represent controls (C) while open dots represent treatment (O) groups. (B) Loading plot of protein spots present in at least 15 out of 16 gel images. Open dots represent significantly different proteins at ANOVA $p<0.01$ for condition 1 (controls vs. ozone-treated).

Within the results presented here, four extrinsic protein subunits of PSII and one of its intrinsic subunits were detected to be differentially abundant after ozone treatment. These are PsbO, PsbP, PsbQ and Psb27 for the extrinsic ones and PsbE for the intrinsic one (Figure 29B). The extrinsic proteins of PSII are responsible for the assembly, maintenance and protection of the Mn-cluster (Ohta et al. 2003). Although oxygen evolution is still active *in vitro* without these proteins, it is supposed that they stabilize and enhance oxygen evolution *in vivo* (Ohta et al. 2003). In addition to the stabilization of the Mn-cluster, mostly by modulating Ca^{2+} and Cl^- requirements, PsbO and PsbP are thought to interact and stabilize the intrinsic D1 and D2 proteins respectively. In mutants lacking PsbO and/or PsbP a strong decrease in D1 and/or D2 content has previously been shown (Yi et al. 2008). PsbQ adds to the general stability of the PSII complex. Although mutants of this subunit seem to grow normally in standard light conditions, they quickly die in low light. It was hypothesized that they can only grow in normal light conditions due to constant repairs, which become insufficient in

low light conditions (Yi et al. 2006). Contrarily to the 3 subunits presented above, Psb27 is not present in the functioning PSII complex. It is involved in the reassembly of the manganese cluster of PSII after disassembly of the complex. It binds to the D1 protein and allows the correct assembly of the Mn-cluster by preventing the other extrinsic subunits (e.g. PsbO, PsbU, PsbQ) to bind to the complex (Roose and Pakrasi 2008). The only intrinsic protein identified in this study, PsbE, or cytochrome b559 alpha subunit, is not involved in the direct linear electron transport. It belongs to an alternative circular transport chain allowing it to be reduced by Qb, and able to indirectly reduce the reaction center $P680^+$, which normally is done by the Mn-cluster. PsbE is thought to have a photoprotective role (Stewart and Brudvig 1998).

The decrease in abundance of the subunits of nearly the complete donor side of PSII observed here would lead to a decreased reducing potential of the reaction center P680. The reaction centers would thus remain oxidized, and the electron transport chain interrupted. P680 in its oxidized state is very reactive and can induce damage to the reaction center (Anderson and Chow 2002). Although not detected here, it was previously shown that the D1, D2 and Cp 47 proteins, components of the intrinsic part of the PSII complex, also decrease in abundance in ozone-treated plants (Ranieri et al. 2001). If that is the case, and considering the results of the present study, this would mean that PSII is negatively impacted by ozone in a general manner.

For PSI, 3 proteins were identified. The luminal subunits PsaN and Lhca3 and the stromal subunit PsaE (Figure 29B). Similarly to PsbQ of PSII, mutants lacking a functional PsaN subunit were previously shown to grow normally in optimum conditions, but to show strong deficiencies in stress conditions (Haldrup et al. 1999). The same study showed a reduction of 50% of the transfer of electrons from plastocyanin to the PSI reaction center P700, indicating an involvement of PsaN in this transfer. The subunit PsaE seems to play a role in fdx cross linking, and therefore may play a role in the transfer of electrons from PSI to fdx (Fromme et al. 2001; Sétif 2001). Similarly to PSII, all the identified proteins of PSI decreased in abundance during ozone stress.

Ferredoxin-$NADP^+$-oxidoreductase, which marks the end of the electron transport chain by transforming $NADP^+$ into NADPH is also differentially abundant (Figure 29B). Although all the previously mentioned proteins were reduced in abundance, ferredoxin-$NADP^+$-oxidoreductase increased in abundance at day 7, before decreasing at the later time points (Table 5).

Finally, three of the four extrinsic subunits of ATPase were detected to decrease in abundance, these are the subunits alpha, beta and gamma (Figure 29B). The subunit delta was also detected but a second protein was present in the same spot, rendering the quantification unreliable.

A major question in ozone research remains whether the photochemical or the biochemical part of photosynthesis are first impaired during exposure. We have previously found that, according to proteomic results of whole leaf soluble protein extracts, the biochemical part is the first to respond, and this is now more and more accepted in literature (Bagard et al. 2008; Dizengremel 2001; Dizengremel et al. 2009; Heath 2008). We reported that RuBisCO activase, RuBisCO large subunit and a number of other Calvin Cycle proteins decreased in abundance before changes in the abundance of photosystem proteins can be detected (Bohler et al. 2007) (4.2. Bohler et al. Tree Physiology in press). The precise targeting of membrane and membrane-associated proteins of the present study allowed detecting changes due to ozone exposure in photosystem proteins as early as 7 days, although the major part of the identified proteins significantly changed in abundance only from day 14 on. Fourteen days chronologically coincides with the first changes in Calvin cycle proteins previously reported but also with first significant decreases in the chlorophyll fluorescence factors Fv/Fm and non-photochemical quenching, which indicated damage occurring to the electron transport chain (Bohler et al. 2007). It could be the higher sensitivity in the present study (chloroplast membrane proteome instead of soluble leaf proteome) that allowed us to detect these earlier changes. The sensitivity of many techniques can be directly related to the complexity of the analyzed sample (Lopez 2000). Therefore, it is likely that changes in the abundance of Calvin cycle enzymes could be detected earlier as well if the purified soluble chloroplast proteome was targeted.

One of the earliest observations in the present study is the increase in abundance of ferredoxin-$NADP^+$-oxidoreductase after 7 days of ozone exposure. Considering that this enzyme is responsible for the reduction of $NADP^+$ to NADPH, it could be concluded that there is a call for reducing power at this point. The cofactor NADPH can among other things be used for the regeneration of oxidized ascorbate. Ascorbate is used for the detoxification of ROS produced by ozone exposure, and in the 'water-water' cycle, to scavenge H_2O_2 produced during excess photon dissipation during photosynthesis (Asada 1999). The present results also show a drop in abundance of L-ascorbate peroxidase starting at day 14, but no variation at day 7. In the chloroplast two forms of ascorbate peroxidase are present, one soluble and one attached to the thylakoid membrane. Double mutants of these 2 enzymes have been shown to be more sensitive to high light conditions and to accumulate ROS (Maruta et al. 2010). The same report has shown that chloroplastic ascorbate peroxidases are very quickly inactivated when ascorbate levels drop below a certain concentration. Similarly, it has been previously reported that increased ascorbate regeneration, which uses NADPH as a source of electrons, can be very important as a defense against ozone (Eltayeb et al. 2007). It can therefore be postulated that during the first days of exposure, an increased production of NADPH by ferredoxin-$NADP^+$-oxidoreductase is used for the regeneration of ascorbate, for the detoxification of ROS

originating from ozone or from oncoming photooxidative damage. Furthermore, reducing power can be exported from the chloroplast using the malate valve (Scheibe 2004). Malate is produced by chloroplastic NADP-malate dehydrogenase, using oxaloacetate and NADPH, and can be exported into the cytosol, where it can be used to produce NAD(P)H, imported into the mitochondria and used in the TCA cycle or other pathways.

In summary, the following hypothesis can be established (Figure 31). After 7 days of ozone exposure (Figure 31A) an oxidative stress has arisen. At this point, ferredoxin-$NADP^+$-oxidoreductase is increased in abundance. The NADPH accumulated from the decrease in Calvin cycle activity and the newly formed NADPH could be used among other things to reduce oxidized ascorbate, used in detoxification processes. At this point the first photosystem subunits decrease in abundance, indicating the possible onset of photooxidative damage. At day 14 (Figure 31B), ascorbate peroxidase starts decreasing, as does ferredoxin-$NAPD^+$-oxidoreductase. This could indicate that recycling of ascorbate can no longer be insured. If electrons cannot be used to reduce $NADP^+$ they can react with O_2 and this would result in the formation of ROS. Added to the ROS produced due to ozone exposure, this is perceived as a signal that leads to a decreased replacement of damaged D1 protein by inhibiting its translation (Takahashi and Murata 2008). Possibly as a consequence of this mechanism and of oxidative and photooxidative damage to the chloroplast membrane complexes, more and more subunits of the photosystems decrease in abundance as do the subunits of ATPase.

Outside of the differentially abundant proteins, a random picking of the major spots allowed to identify a couple of photosystem proteins that did not vary in abundance. This indicates that it is not a general degradation of the photosystems, but a controlled and targeted effect on select subunits that might have a regulatory function. Unfortunately, little is currently known about the regulation of photosystems.

Besides those discussed above, a number of other proteins were differentially abundant. The most prominent amongst those proteins is a homologue to patatin like protein 3, since it is the only identifiable protein that increases in abundance. Patatin-like proteins have a phospholipase activity and have been detected to be induced during pathogen attack (Dhondt et al. 2000). It is likely that it is involved in membrane phospholipid metabolism and could be responsible for repairing damage in the chloroplast membrane that occurred due to the oxidative nature of ozone stress (Pell et al. 1997).

Table 5: Identified differentially expressed proteins. All spots containing the same protein function are represented as the number of them decreasing / remaining stable / increasing in abundance (- / o / +). Detailed information about abundance variation and statistical analysis are given in Supplemental Table 1.

Protein name	Number or protein spots			
	Day 7 (- / o / +)	Day 14 (- / o / +)	Day 21 (- / o / +)	Day 28 (- / o / +)
Oxygen evolving complex 33 kDa photosystem II protein [*Nicotiana tabacum*] (PsbO)	1 / 4 / 1	5 / 1 / 0	6 / 0 / 0	5 / 1 / 0
Oxygen-evolving enhancer protein 2, chloroplast precursor, putative [*Ricinus communis*] (PsbP)	0 / 1 / 0	2 / 0 / 0	2 / 0 / 0	2 / 0 / 0
Oxygen-evolving enhancer protein 3, chloroplast precursor, putative [*Ricinus communis*] (PsbQ)	5 / 6 / 0	10 / 1 / 0	10 / 0 / 0	7 / 4 / 0
Oxygen-evolving enhancer protein 3-1, chloroplast precursor, putative [*Ricinus communis*] (PsbQ)	0 / 1 / 0	0 / 1 / 0	1 / 0 / 0	0 / 1 / 0
Putative oxygen evolving enhancer protein 3, identical [*Solanum demissum*] (PsbQ)	0 / 2 / 0	0 / 2 / 0	2 / 0 / 0	2 / 0 / 0
Photosystem II 11 kDa protein precursor, putative [*Ricinus communis*] (Psb27)	1 / 3 / 0	1 / 3 / 0	4 / 0 / 0	3 / 1 / 0
PSII cytochrome b559 8kDa subunit [*Nicotiana sylvestris*] (PsbE)	0 / 1 / 0	0 / 1 / 0	1 / 0 / 0	0 / 1 / 0
Light-harvesting complex I protein Lhca3 [*Populus trichocarpa*]	0 / 3 / 0	3 / 0 / 0	3 / 0 / 0	3 / 0 / 0
Photosystem I reaction center subunit N, chloroplast precursor, putative [*Ricinus communis*] (PsaN)	0 / 3 / 0	0 / 3 / 0	2 / 1 / 0	1 / 2 / 0
Putative photosystem I reaction centre subunit IV [*Populus x canadensis]* (PsaE)	4 / 5 / 0	4 / 5 / 0	7 / 2 / 0	2 / 7 / 0
Chloroplast ferredoxin-NADP+ oxidoreductase precursor [*Capsicum annuum*]	0 / 5 / 4	7 / 2 / 0	9 / 0 / 0	8 / 1 / 0
Predicted protein [*Populus trichocarpa*] homologous to chloroplast ferredoxin-NADP+ oxidoreductase precursor [*Capsicum annuum*]	0 / 0 / 1	1 / 0 / 0	1 / 0 / 0	1 / 0 / 0
ATP synthase beta subunit [*Populus alba*]	0 / 2 / 0	2 / 0 / 0	2 / 0 / 0	2 / 0 / 0
ATPase beta subunit [*Populus tomentosa*]	0 / 2 / 0	0 / 2 / 0	2 / 0 / 0	2 / 0 / 0
ATP synthase CF1 alpha subunit [*Populus trichocarpa*]	1 / 5 / 0	3 / 3 / 0	5 / 1 / 0	5 / 1 / 0
ATP synthase CF1 epsilon subunit [*Populus alba*]	0 / 4 / 0	3 / 1 / 0	4 / 0 / 0	4 / 0 / 0
ATP synthase family [*Arabidopsis thaliana*].	0 / 1 / 0	1 / 0 / 0	1 / 0 / 0	1 / 0 / 0
ATP synthase gamma chain 2, chloroplast, putative [*Ricinus communis*]	1 / 12 / 0	11 / 2 / 0	12 / 0 / 0	11 / 2 / 0
ATP synthase gamma chain, chloroplastic	0 / 2 / 0	1 / 1 / 0	1 / 1 / 0	2 / 0 / 0
Fructose-bisphosphate aldolase [*Zea mays*]	0 / 1 / 0	1 / 0 / 0	1 / 0 / 0	1 / 0 / 0
Glycolate oxidase [*Mesembryanthemum crystallinum*]	0 / 5 / 0	4 / 1 / 0	5 / 0 / 0	3 / 2 / 0
L-ascorbate peroxidase, putative [*Ricinus communis*]	0 / 3 / 0	2 / 1 / 0	3 / 0 / 0	3 / 0 / 0
Precursor of transferase serine hydroxymethyltransferase 2 [*Populus trichocarpa*]	0 / 1 / 0	1 / 0 / 0	1 / 0 / 0	1 / 0 / 0
Peptidyl-prolyl cis-trans isomerase, putative [*Ricinus communis*]	0 / 1 / 0	1 / 0 / 0	1 / 0 / 0	1 / 0 / 0
Predicted protein [*Populus trichocarpa*] homologous to patatin-like protein 3 [*Nicotiana tabacum*]	0 / 1 / 1	0 / 0 / 2	0 / 1 / 1	0 / 2 / 0
Chloroplast lipocalin [*Ipomoea nil*]	0 / 1 / 0	0 / 1 / 0	1 / 0 / 0	1 / 0 / 0
Predicted protein [*Populus trichocarpa*]	0 / 1 / 0	1 / 0 / 0	1 / 0 / 0	0 / 1 / 0

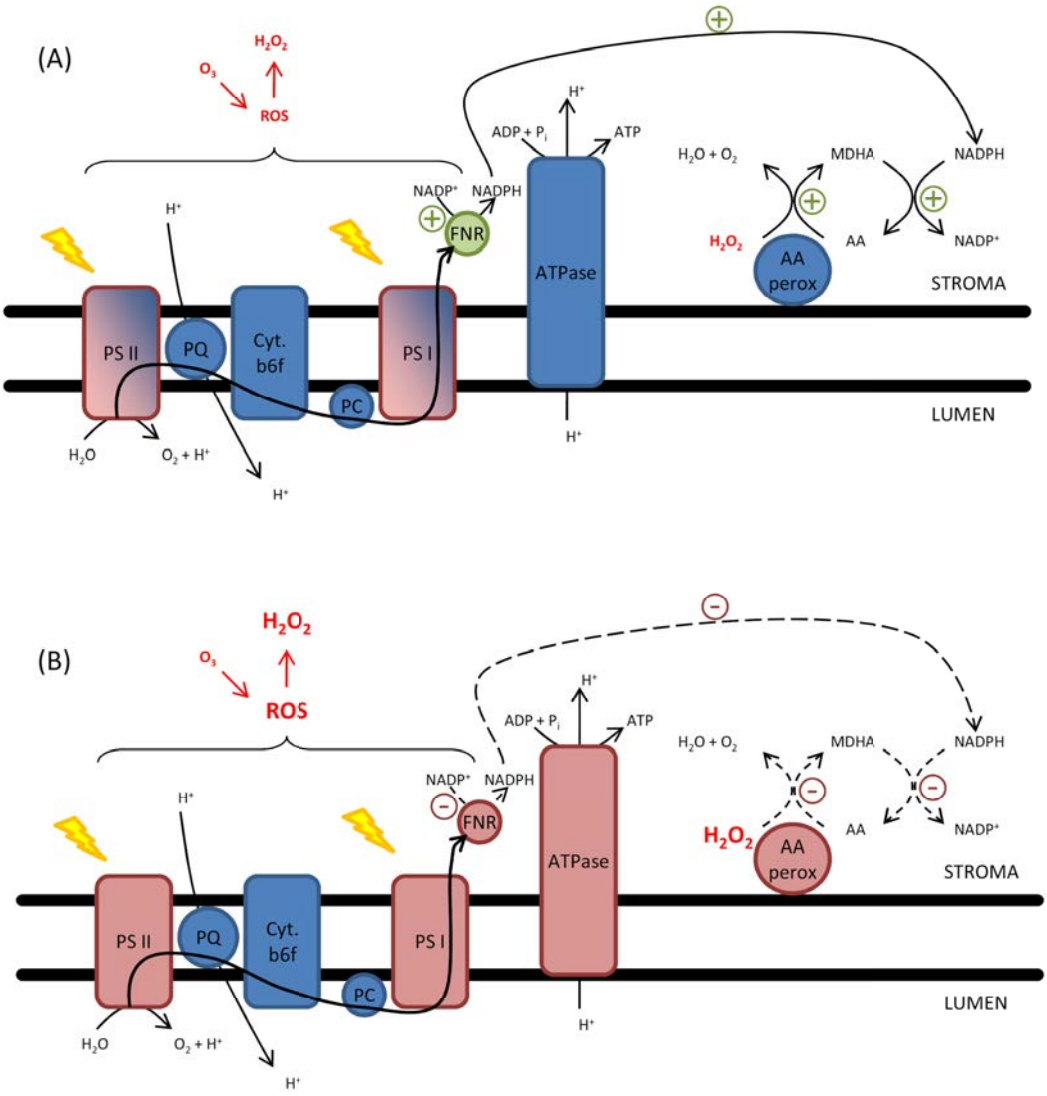

Figure 31: Progression in the changes observed in the chloroplast electron transport chain from (A) day 7 to (B) days 14 to 28. Red elements represent a decrease in abundance, green element an increase. Half red/blue elements represent elements that are only partially decreased in abundance at that time. Abbreviations are similar to Figure 29B; AAperox = ascorbate peroxidase, MDHA = monodehydroascorbate, AA= ascorbate.

3.2.5. Conclusion

After 7 days of exposure, the reducing power in the chloroplasts could be increased by FNR producing more NADPH that can be used inside or outside of the chloroplast for the detoxification of ROS generated directly or indirectly by ozone exposure. After 14 days, photosystem and ATPase subunits and ascorbate peroxidase decrease in abundance, indicating that rescue attempts that were still active after 7 days failed and that the chloroplast response processes can no longer counteract the prolonged ozone exposure. Decrease of photosystem subunits can be a measure

against photooxidative stress and/or a consequence of ROS-induced damage. The results of this study indicate that when a chronic ozone exposure lasts for too long, protective measures can become overwhelmed by the oxidative nature of the stress, leading to a decrease in abundance of photosystem subunits and other proteins of the chloroplast membranes. Unfortunately, it is not clear whether this is due to a regulatory phenomenon or caused by accumulated damage to the protein complexes.

3.2.6. Supplemental Material

Supplemental Table 1: Full description of the statistical results obtained during the analysis of the effect of ozone treatment compared to control values at each time point. Average ratios are expressed and p-values of Two-Way ANOVA are represented with (i) ozone treatment (cond1); (ii) time course (cond2) and (iii) interaction between these 2 factors (interact). **Spot**: number of the spot on the Master gel; **NCBI**: accession returned by the search in database; **Blast**: the accession of the protein obtained after blasting the accession obtained in NCBI database if not providing a full name for the protein's function (e.g. 'predicted or hypothetical protein'); **Protein name**: Name of the protein as returned either by the search in the database or after blasting the accession obtained in the NCBI database.

Available on request: Full data of protein identification. **Spot** : number of the spot on the Master gel; **Protein** : the accession of the protein obtained after blasting the accession obtained in NCBI database if not providing a full name for the protein's function (e.g. 'predicted or hypothetical protein'); **NCBI** : accession returned by the search in database; **Observed** : Experimental m/z value (Da/z); **Mr** (**expt**); Calculated mass of the unprotonated precursor (Da); **Mr** (**calc**): Molecular mass calculated from the matched peptide sequence (Da); **Delta**: Difference (error) between Mr (expt) and Mr (calc); **Start- End**: Position of the sequence in the database entry; **Miss**: Number of missed cleavage sites; **Ions**: Individual ions' score; **Peptide**: Sequence of the peptide in 1-letter code. The residues that bracket the peptide sequence in the protein are also shown, delimited by periods. If the peptide forms the protein terminus, then a dash is shown instead. Modified amino acids are indicated by (ox) for oxidized a.a., W(dox) for double oxidized tryptophan, W(kyn) for kynurenine, E(pyro-glu) for a pyrrolidone carboxylic acid.

In this table, the name of the protein and the species in which this protein was characterized as well as the MASCOT score (protein score as given by the GPS software (Applied Biosystems)) and the expected value as given in the GPS software (Applied Biosystems) are represented as ' **Score'** and ' **expect'.**

Data added during manual validation of the identifications are added in red.

3.2.7. Funding

This study was supported by the Fonds National de la Recherche Luxembourg (FNR) (S.B.'s PhD scholarship AFR TR-PHD BFR06-044).

3.2.8. Acknowledgements

Our thanks go to Dr. Estelle Goulas and Dr Lutz Eichacker for their expertise in chloroplast isolation, to Sébastien Planchon and Céline Leclercq for their technical assistance during the proteomic analyses and to Jacques Banvoy for his help with the fumigation chambers.

Chapter 4

Leaf development and ozone exposure, a natural phenomenon and a stress induced response.

4.1. General Introduction

The life cycle of higher plants can be roughly divided into two phases: vegetative and reproductive development. For annual plants, this cycle corresponds to a single season and the plant dies after completion of its reproductive development. For non-annual plants, the reproductive development is delayed, to the second year for biennials and up to decades for perennials, and the vegetative development is resumed every year, as is the reproductive development in perennial. The vegetative development involves leaf, stem and root formation, bud development and, in woody plants, radial growth. The reproductive development involves flowering and seed formation, a process that is well described in numerous plant species.

The formation of leaves, the site of photosynthesis and thus the source from which the plant draws the energy for its life cycle, is an important event. Leaf formation can be divided into three phases: leaf initiation at the site of the shoot apical meristem (SAM) and possibly dormancy at the bud level, bud development to the state of an adult fully expanded leaf, and finally senescence and abscission. Among these three phases, leaf initiation and senescence are well studied in model plants like *Arabidopsis* (initiation and senescence) (Benkova et al. 2003; Buchanan-Wollaston et al. 2005; Grbic and Bleecker 1995; Reinhardt et al. 2003; Saiga et al. 2008; Schoof et al. 2000) and poplar (mainly senescence) (Andersson et al. 2004; Keech et al. 2007; Keskitalo et al. 2005).

The process of leaf initiation is tightly controlled in plants (Fleming 2005), as is illustrated by the different modes of leaf organization along the stem (phyllotaxis). Leaf formation is initiated at the SAM, the site at the stem tips where cells constantly divide, and is controlled by multiple genes (Saiga et al. 2008; Schoof et al. 2000). New leaf primordia always appear at the site of the SAM the furthest away from the previous primordium, in an auxin-controlled process. A steady flux of auxin is at all times directed from the apex to the base by PIN proteins (auxin efflux transporters) (Reinhardt et al. 2003) and the existing leaf primordia act as sinks for auxin (Benkova et al. 2003). Thus, the highest concentration of auxin on the meristem surface will always be at the point furthest away from existing primordia, and leaf initiation will happen here. After leaf initiation, the leaf acquires its polarity (adaxial/abaxial side) (Eshed et al. 2001; McConnell et al. 2001) and will grow to its full size.

At the end of a leaf's life lies senescence. Senescence can be induced by a number of external factors like photoperiod (autumn senescence), a stress factor or leaf age; moreover the process of senescence changes according to the nature of the initiating factor. Senescence initiation is correlated with ethylene signaling but does not depend on it (Grbic and Bleecker 1995); likewise

salicylic acid and jasmonic acid signaling seems to be involved (Buchanan-Wollaston et al. 2005). Although it is a destructive process that leads to the leaf's death, senescence is generally beneficial for the whole plant and is highly regulated and initiated long before visual symptoms can be seen (Hopkins et al. 2007). During the process of senescence, cell components are catabolized to recycle carbon and nitrogen (Andersson et al. 2004). Although the mitochondrial catabolism is not increased, it remains stable and active until very late in the senescence process (Keskitalo et al. 2005). Glutamine synthetase and proteases, enzymes typically involved in nitrogen remobilization, are up-regulated (Andersson et al. 2004). The remobilized carbon, nitrogen and other elements are transported out of the leaf to other regions of the plant, for example to leaves higher on the stem or to roots, depending on the trigger that initiated senescence. The photosynthetic machinery is dismantled during senescence (Andersson et al. 2004) and chlorophyll synthesis is halted (Keskitalo et al. 2005). The degradation of present chlorophylls leads to the typical yellow to red color of senescent leaves that is due to the carotenoids and flavonoids that remain in the leaves. At the end, the cells in the leaf die and the leaf is finally abscised.

Even if these two phases are well-studied, information about the physiological state of a leaf between initiation and senescence is only poorly represented in literature. Some reports exist about the control underlying leaf shape development (Eshed et al. 2001; Maayan et al. 2008). Nonetheless only very few describe the metabolic changes in leaf expansion and during leaf life. For that reason, the following research paper does not only focus on the effects of ozone on a developing leaf, but will also try to give an overview of some physiological and molecular aspects involved in leaf development. In Chapter 2, it was shown that visible symptoms like necroses and chloroses only appear on adult leaves, but not on expanding leaves, therefore the expansion phase seems to be of particular interest. Although there are comparisons between the effects of ozone on young leaves and on mature leaves, relatively few observe the changes that occur while the leaf is growing. It was previously reported that older leaves accumulate more H_2O_2 when exposed to ozone, which is probably why they develop visible symptoms but young leaves do not (Oksanen et al. 2004). A reason for this increased resistance to ozone in young leaves could be differences in leaf anatomy between mature and young leaves that would decrease the amount of ozone entering the leaves (Bagard et al. 2008). Other studies report that younger leaves have a better detoxification capacity than older leaves (Nogués et al. 2008; Ranieri et al. 1996).

Furthermore, the ozone response presents aspects similar to leaf senescence like decreased photosynthesis and increased catabolism (Bohler et al. 2007; Mikkelsen and Heide-Jørgensen 1996; Miller et al. 1999; Pell et al. 1999). This and the higher leaf shedding observed in ozone trees have

established the hypothesis that ozone can induce a signal for an accelerated senescence. A precise comparison of the leaf proteome during the entire lifespan of ozone treated and ozone free leaves was therefore attempted to observe changes in the different steps of leaf development. This is the second part of the experiment described in Chapter 3. Chlorophyll fluorescence measurements were made during the fumigation period to estimate photosynthetic parameters that cannot be observed at a molecular level. The total soluble leaf proteome was extracted and submitted to a DiGE experiment (Figure 32). Detailed information is available in the material and methods section of the research paper that follows.

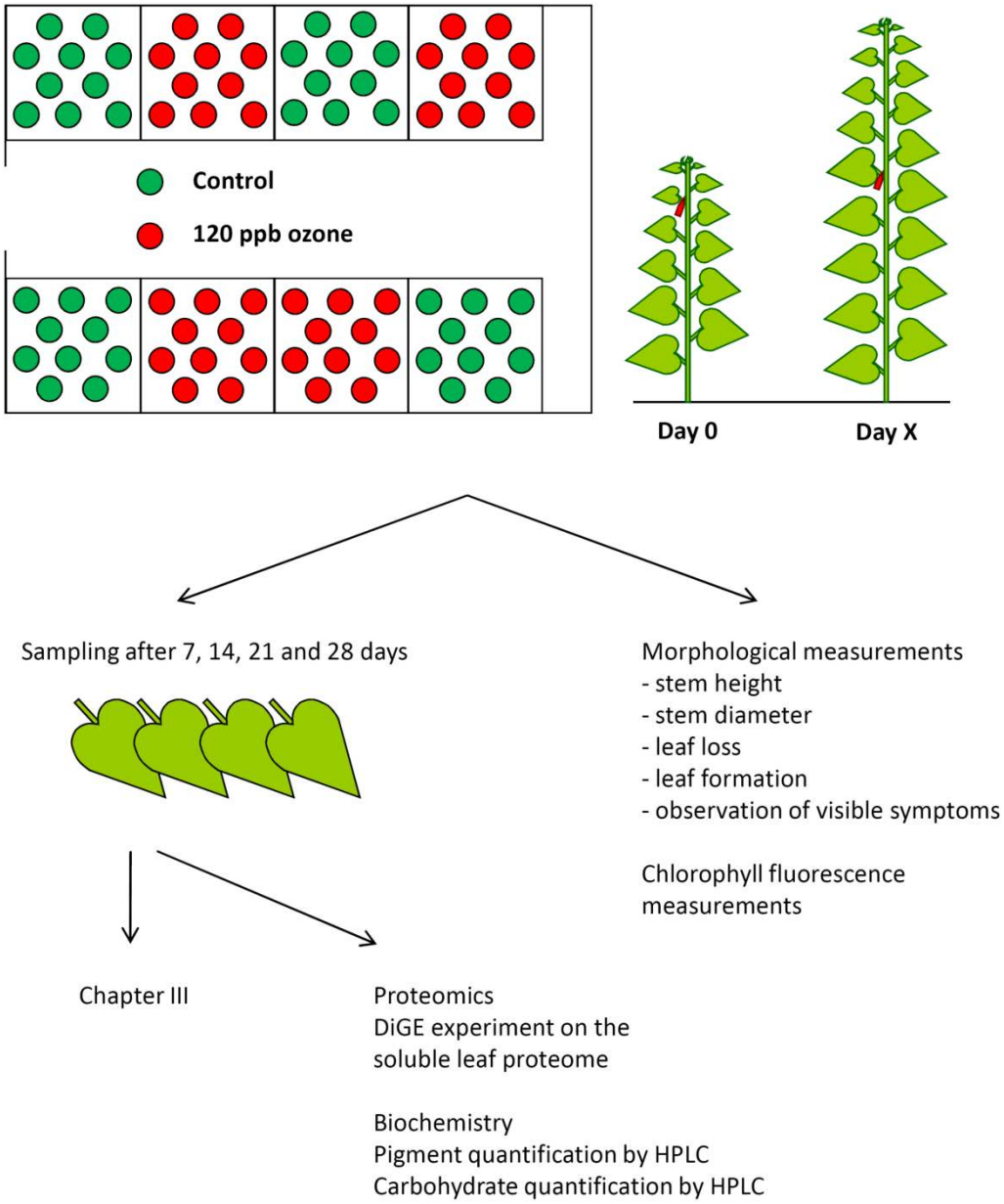

Figure 32: Experimental setup of the second experiment, part 2, soluble leaf proteome, leaf development and chlorophyll fluorescence.

4.2. Bohler et al. Tree Physiology in press

Differential impact of chronic ozone exposure on expanding and fully expanded poplar leaves

Bohler Sacha[a,b], Sergeant Kjell[a], Lefèvre Isabelle[a], Jolivet Yves[b], Hoffmann Lucien[a], Renaut Jenny[a], Dizengremel Pierre[b], Hausman Jean-Francois[a].

[a]CRP-Gabriel Lippmann, 41 rue du Brill, L-4422 Belvaux, GD. Luxembourg, Department Environment and Agro-biotechnologies

[b]Nancy-Université, UMR 1137 Ecologie et Ecophysiologie Forestières, F-54506 Vandoeuvre-lès-Nancy, France.

Keywords: Air pollution, biochemistry, different in gel electrophoresis DiGE, photosynthesis, primary carbon metabolism, proteomics.

4.2.1. Abstract

Populus tremula L. x *P. alba* L. (*Populus* x *canescens* (Aiton) Smith) - clone INRA 717-1-B4 saplings (50 cm apex to base and carrying 19 leaves on average) were followed for 28 days. Half of the trees were grown in charcoal filtered air while the other half was exposed to 120 ppb of ozone for 11 hours a day during the light period. The expanding leaf number 4 was tagged at the beginning of the experiment and finished expansion between 7 and 14 days. These leaves were harvested weekly for biochemical and proteome analysis using quantitative bidimensional electrophoresis (DiGE). Independent of the ozone treatment, all the analyses allowed distinguishing expanding from adult leaves. The results indicate that during the expansion phase (day 0 to 7) the enzymatic machinery of the leaves is set up, and remains dynamically stable in the adult leaves (days 14 to 28). Although ozone had no apparent effect on expanding leaves, the metabolic stability in fully expanded leaves observed in ozone free plants was disturbed after two weeks of exposure and a stress induced response became apparent.

4.2.2. Introduction

The formation of leaves, the site of photosynthesis and thus the source from which the plant draws the energy for its life cycle, is an important event in plant development. Leaf formation can be divided into three phases: (1) leaf initiation at i.e. the site of the shoot apical meristem which can be followed by bud dormancy, (2) development to the state of a fully expanded adult leaf and finally (3) senescence and abscission. Among these three phases, leaf initiation and senescence are

well studied in model plants like *Arabidopsis* (initiation and senescence) (Buchanan-Wollaston et al. 2005; Grbic and Bleecker 1995) and poplar (mainly senescence) (Keskitalo et al. 2005); however, less studies focus on leaf expansion.

The process of leaf initiation is tightly controlled (Fleming 2005) by multiple genes (Saiga et al. 2008; Schoof et al. 2000) and auxin fluxes (Benkova et al. 2003; Reinhardt et al. 2003). In the process of senescence initiation, several growth regulators (e.g. ethylene, salicylic acid and jasmonic acid) can be involved (Buchanan-Wollaston et al. 2005; Grbic and Bleecker 1995; Reinbothe et al. 2009). As leaf initiation, senescence is tightly regulated (Hopkins et al. 2007) allowing the plant to recycle carbon and nitrogen (Andersson et al. 2004) before leaf abscission.

Information about the physiological and biochemical variation of a leaf between initiation and senescence is only poorly represented in literature. It was shown that the photosynthetic rate increases in expanding leaves, that chlorophyll accumulates, and that respiration is highest during the expansion phase (Kennedy and Johnson 1981; Reich 1983). Some reports exist about the control underlying leaf shape development (Eshed et al. 2001), but only very few describe the metabolic changes in leaves during expansion and adult leaf life (Maayan et al. 2008).

Tropospheric ozone is a secondary pollutant formed by the decomposition of nitric oxides under solar UV radiation, a decomposition catalyzed by a number of other atmospheric components such as volatile organic compounds and hydroxy radicals (Oke 1987). During the industrialization age, background concentrations and the number and intensity of peak episodes of ozone have increased. As recently reviewed, ozone has a negative effect on plants (Fuhrer 2009; Renaut et al. 2009; Tkacz et al. 2008). Ozone enters the leaves through the stomata and upon contact with the apoplast the molecule degrades into reactive oxygen species (Rao et al. 2000a). These highly reactive ROS attack cell components like lipids and proteins, and induce a series of signaling pathways involving several plant growth regulators (Castagna and Ranieri 2009; Kangasjärvi et al. 2005). Reduction in biomass yield, symptoms like chloroses and necroses on leaves and alterations of metabolism are typical plant responses to ozone exposure (Degl'Innocenti et al. 2002; Guidi et al. 2001). It is well known that the impact ozone may have on plants depends on the effective ozone flux, which is a balance between the degree of stomatal opening and the level of antioxidant defense (Dizengremel et al. 2008; Wieser and Matyssek 2007).

In a previous study we have shown that exposure of poplar to 120 ppb of ozone during one month leads to the formation of necroses in adult leaves, but not in expanding ones (Bohler et al. 2007). Variations in carbon metabolism and other cellular functions were clearly visible after 14 days of

treatment, but nearly absent after only a few days, except for RuBisCO activase that decreased as early as after 3 days (Bohler et al. 2007). It was confirmed that physiological parameters of photosynthesis and photorespiration do not change in leaves under expansion under ozone stress, and that variations only appear after full expansion of the leaves (Bagard et al. 2008).

The present study attempts to give an overview of the proteome changes observed during the development of leaves upon ozone exposure. These results will be compared with the observed changes during normal leaf development. The discussion of the results of this proteomic study will be supported by morphological measurements and biochemical analyses of pigments and carbohydrates.

4.2.3. Material and methods

4.2.3.1. Plant material and ozone treatment

Plant material was obtained and treated as previously described (Bohler et al. 2007). Briefly, poplar clones (*Populus tremula* L. x *P. alba* L. (*Populus* x *canescens* (Aiton) Smith) - clone INRA 717-1-B4) were multiplied in vitro, transferred to a mix of peat/perlite (Gramoflor SP1 Universel), transplanted into 5 L pots containing peat/perlite fertilized with 15 g of slow-release nutritive granules (Nutricote T-100, N/P/K/MgO 13/13/13/2, Fertil, Boulogne-Billancourt, France) and grown at 75%/85% relative humidity (day/night) with a 14 h light period (Sun T Agro, Philips, Eindhoven, The Netherlands; intensity: 250–300 µmol.m^{-2}.s^{-1}) and 22°C/18°C ± 2°C (day/night) over a period of 5 weeks.

For the ozone treatment, plants were transposed into 8 fumigation chambers with 10 plants per chamber. Four chambers were randomly used as controls and 4 for ozone treatment. Control plants were grown in charcoal filtered air while treated plants were exposed to charcoal filtered air supplemented with 120 ppb of ozone for 13 h per day during the light period or to charcoal-filtered air for controls. All other conditions (humidity, light and temperature) were as described above. Leaf n° 4, counted from the last leaf emerged at the apex, was tagged at the beginning of the treatment on each plant. They are referred to as leaves of interest. Two leaves from each chamber were harvested for analysis and immediately frozen in liquid nitrogen after 0, 7, 14, 21 and 28 days of treatment.

4.2.3.2. Morphological measurements

Growth (height and diameter) as well as the number of newly formed leaves was determined for each plant after 0, 7, 14, 21 and 28 days of exposure. Height measurement was based on the length of the stems from the collar to the apex and the diameter expansion was estimated via

measurements of the stem 1.5 cm above the collar with a caliper. The number of abscised leaves was recorded daily. Concomitantly, visible symptoms of ozone treatment (chlorosis and necrosis) were recorded.

The lobe length (petiole excluded) and width of the leaves of interest were measured on each sampling date between 0 and 21 days of treatment. Leaf area was calculated using a formula developed specifically for this poplar clone (Bagard et al. 2008).

4.2.3.3. Chlorophyll fluorescence

Chlorophyll fluorescence measurements were performed on the leaf just below the leaf of interest (leaf number 5) with a Fluorescence Monitoring System FMS 1 (Hansatech, Norfolk, England). Leaf clips were attached to target leaves 20 min prior to measurements for dark acclimation. The following program was created on the Fluorescence Monitoring Software 3.11 based on the default program from the manufacturer: Gain setting 50, modulating light intensity setting 1, script logging on. Fv/Fm was measured for 2.5 sec at an intensity of 90 units with a light pulse of 0.8 sec. After 10 sec actinic light was switched on to 30 units and after an additional 300 sec, PhiPS2 was measured for 2.5 sec at an intensity of 90 units with a light pulse of 0.8 sec. Actinic light was then switched off and after 10 sec F_o' was measured for 2 sec. Three plants per chamber were measured at each sampling date, amounting to 12 measurements per treatment per sampling date.

4.2.3.4. Soluble protein extraction and labeling

Proteins were extracted from 1 leaf per chamber per sampling date, i.e. 4 leaves per treatment and per date, amounting to 4 biological replicates. Soluble protein extraction was carried out as described previously (Kieffer et al. 2009), with small modifications. Briefly, 300 mg of fresh leaf material were ground in liquid nitrogen and proteins were suspended in precipitation buffer (20% TCA and 0.1% w/v DTT in ice-cold acetone) and washed three times with ice-cold acetone containing 0.1% w/v DTT. Precipitated protein pellets were freeze-dried. Dried samples were re-solubilized in labeling buffer (7 M urea, 2 M thiourea, 4% w/v CHAPS, 30 mM Tris) and the pH of the supernatant was adjusted to 8.5. The protein concentration was determined using the 2D Quant Kit (GE Healthcare, Little Chalfont, UK) according to the manufacturer's instructions. After extraction, proteins were used for a multiplexed analysis by fluorescence difference gel electrophoresis (DiGE) (Skynner et al. 2002).

Protein extracts and a pooled internal standard were labeled with CyDyes™ (GE Healthcare) prior to electrophoresis as previously described (Kieffer et al. 2009). Ninety micrograms of proteins (two

samples of 30 µg each and 30 µg of internal standard) were loaded on each gel and separated by 2D electrophoresis.

4.2.3.5. Bidimensional electrophoresis.

To each sample mix consisting of two samples and the internal standard and completed up to 450 µL with lysis buffer (labeling buffer without Tris), 2.7 µL of Destreak Reagent (GE Healthcare), 9 µL of IPG buffer 3-10 NL (GE Healthcare) and 5 µL of a saturated bromophenol blue solution were added. Sample loading on ReadyStrip IPG strips pH 3-10 NL, 24 cm (Biorad, Hercules, California, U.S.) was done overnight by passive rehydration. Isoelectric focusing was carried out on an Ettan IPGphor Manifold (GE Healthcare) in an IPGphor IEF unit (GE Healthcare). The following protocol was used: 150 V for 2 h, 300 V for 2 hours, gradient to 1,000 V over 6 h, 1,000 V for 1 h, gradient to 8000 V over 4 h, 8,000 V until approximately 70,000 Vhrs were reached at 20°C with a maximum current setting of 50 µA per strip. The second dimension was run as previously described (Kieffer et al. 2009).

Additional preparative gels were run as described above with 300 µg of an unlabeled protein sample. Glass plates were pre-treated with bind silane (GE Healthcare) to guaranty adherence of the gels to the glass plates during gel picking. These gels were post-stained with Lava Purple (Fluorotechnics, Sydney, Australia) according to the manufacturer's instructions.

4.2.3.6. Image capture and analysis.

The gel images of the different samples were acquired using a Typhoon Variable Mode Imager 9400 (GE Healthcare) at a resolution of 100 µm according to the instructions provided for each dye. Images were analyzed using the Decyder v6.5.14.1 software (GE Healthcare). Selected spots of interest (absolute abundance variation of at least 1.5-fold, ANOVA $p<0.01$) were located and a picking list was generated. Spots of interest were excised and digested as previously described (Bohler et al. 2007). MS and MS/MS spectra were acquired using an Applied Biosystems 4800 Proteomics Analyzer (Applied Biosystems, Sunnyvale, CA, USA). Calibration was carried out with the peptide mass calibration kit for 4700 (Applied Biosystems). Proteins were identified by searching against the NCBI poplar protein databases (downloaded 2009.06.11, 99,629 sequences) and poplar EST (downloaded 2009.06.11, 419,944 sequences) using MASCOT (Matrix Science, www.matrixscience.com, London, UK). All searches were carried out allowing for a mass window of 150 ppm for the precursor and 0.75 Da for. The search parameters allowed for carboxyamidomethylation of cysteine as fixed modification and oxidation of methionine, oxidation of tryptophan (single oxidation, double oxidation and kynurenin) and for pyrrolidone carboxylic

acid (N-terminal glutamine and glutamic acid) as variable modifications. Homology identification was retained with a probability set at 95%.

The sub-cellular localization of the proteins was estimated with the following tools: ChloroP 1.1 Server (http://www.cbs.dtu.dk/services/ChloroP/), MITOPROT (http://ihg2.helmholtz-muenchen.de/ihg/mitoprot.html), and PTS1 predictor (http://mendel.imp.ac.at/mendeljsp/sat/pts1/PTS1predictor.jsp).

4.2.3.7. Chlorophyll and carotenoid analysis

Pigments were extracted from 1 leaf per chamber per sampling date, i.e. 4 leaves per treatment and per date, amounting to 4 biological replicates. Two extracts were made per sample, amounting to 2 technical replicates. Pigment extraction was carried out as previously described (Bohler et al. 2007). In order to assess the recovery of the method, β-apo-8'-carotenal was added as internal standard to the extraction mixture to reach a final concentration of 20 $\mu g.mL^{-1}$. Identification and quantification of chlorophylls and carotenoids were carried out as previously described (Andre et al. 2007), with some modifications. A gradient system was used involving four mobile phases. Eluent A was 100% water; eluent B 100% acetonitrile, eluent C 80% methanol v/v with 0.5 M ammonium acetate at pH 7.2, and eluent D 100% ethyl acetate. The flow rate was 1 $mL.min^{-1}$ and the column temperature was 26°C. The gradient elution profile was as previously described (Kieffer et al. 2009).

4.2.3.8. Carbohydrate analysis

Carbohydrates were extracted from 1 leaf per chamber per sampling date, i.e. 4 leaves per treatment and per date, amounting to 4 biological replicates. Carbohydrate extraction was carried out as previously described (Kieffer et al. 2009). Carbohydrates were separated by high performance anion exchange chromatography coupled with pulsed amperometric detection (HPAEC-PAD) as previously described (Oufir et al. 2008).

4.2.3.9. Starch analysis

Extraction was done as previously described (Gaucher et al. 2003) with some modifications. Approximately 100 mg of fresh weight poplar leaves were ground in liquid nitrogen, mixed thoroughly with 750 µL of 70% v/v methanol and centrifuged for 10 minutes at 17,000 g at 4°C. The pellet was re-suspended in 750 µL of 70 % v/v methanol and centrifuged once more. The pellet containing the starch was then dried for 1 hour at 30°C. Starch was subsequently degraded to glucose by adding 500 µL of 2% v/v HCl to the dried pellet and incubated at 99°C for 2 hours. After a centrifugation of 10 minutes at 17,000 g and 4°C the supernatant was collected.

Starch was quantified by a spectrophotometric method using the anthrone reagent. A glucose solution of 1 $mg.mL^{-1}$ was used as a standard. Five µL of lysate were mixed with 45 µL water, 50 µL 2% v/v HCl and 1.5 mL anthrone reagent (0.15% [w/v] anthrone, 71% v/v sulfuric acid), incubated at 99°C for 20 min and cooled on ice. The absorbance was read at 620 nm.

4.2.3.10. Statistical analysis

Statistical analysis was carried out with the following number of replicates: 4 biological replicates for proteomics, carbohydrates and starch, 4 biological and 2 technical replicates for pigment analysis, 12 biological replicates for fluorescence and 40 biological repetitions for growth, for each condition at each sampling date. The proteomic effects of leaf development were tested with a One-Way ANOVA on control samples only. The average ratio was calculated for each time point versus day 0. Effects of ozone were tested with a Two-Way ANOVA, with treatment as factor one and time as factor two. The average ratio was calculated for each time point versus its control counterpart. Differentially abundant proteins with an absolute ratio of at least 1.5-fold for minimum one time point and a p-value<0.01 were selected. A Principle Component Analysis was run for qualitative appreciation of the proteomic results. ANOVA and PCA were performed on Decyder Extended Data Analysis (v.1.0.14.1). For morphological measurements, carbohydrates, starch and pigments, significance was calculated via a One-Way ANOVA, with control/treated as factors and growth and concentrations respectively as the response. These analyses were performed on MINITAB Statistical Software v.15.1.1.0.

4.2.4. Results

4.2.4.1. Morphological measurements

Stem height growth of ozone treated and untreated plants (Table 6) was strongest between the first seven days of the experiment but continued until the end of the experiment. There were no significant effects of ozone. Similarly, stem diameter (Table 6) increased all through the fumigation period in both growth conditions. Significantly lower diameter growth was observed for treated plants between days 7 and 21. Exposed and control plants shed their lower leaves during the experiment. For treated plants, leaf loss became significantly higher starting at day 24 (Figure 33A). The rate of new leaf formation in fumigated plants also increased significantly starting at day 14 (Figure 33B).

The leaves of interest (leaf number 4 counted from the top and tagged at the beginning of the treatment) had a strong growth between days 0 and 7 that continued briefly between days 7 and 14. Leaf length significantly increased between days 0 and 7, leaf width between days 0 and 14

(Figure 34A) (8 x 5 to 20 x 15 cm). A statistically significant difference in leaf area between control and ozone conditions was detected only at day 14 (Figure 34B). Leaves probably reached maximum expansion shortly after 7 days into the experiment.

Table 6: Percent increment of stem height and stem diameter compared to day 0 ± standard deviation, in control and treated plants. Statistical significance was tested by One-Way ANOVA between controls and treated. Significance is shown by bold numbers at p<0.001, n = 40.

		7 days	14 days	21 days	28 days
Height	Control	34.60% ± 3.65	68.88% ± 7.88	98.77% ± 12.84	126.68% ± 20.13
(cm)	Ozone	34.31% ± 8.03	71.00% ± 10.34	102.45% ± 13.91	133.71% ± 18.58
Diameter	Control	22.98% ± 6.65	**44.39% ± 9.52**	**60.58% ± 11.40**	**74.32% ± 14.93**
(cm)	Ozone	19.96% ± 7.62	**34.61% ± 7.09**	**37.83% ± 6.52**	**45.15% ± 6.54**

Pinpoint sized necroses started appearing on ozone exposed plants after approximately 14 days. They first developed on mature leaves, and started to show up only very rarely on young leaves later in the experiment. Leaves of interest developed necroses when they were mature. The necroses spread over mature leaves and were clearly visible at the end of the treatment on all exposed plants. The young and mature leaves of exposed plants also showed a marked chlorosis starting around day 21, with a loss of glossiness of the cuticle.

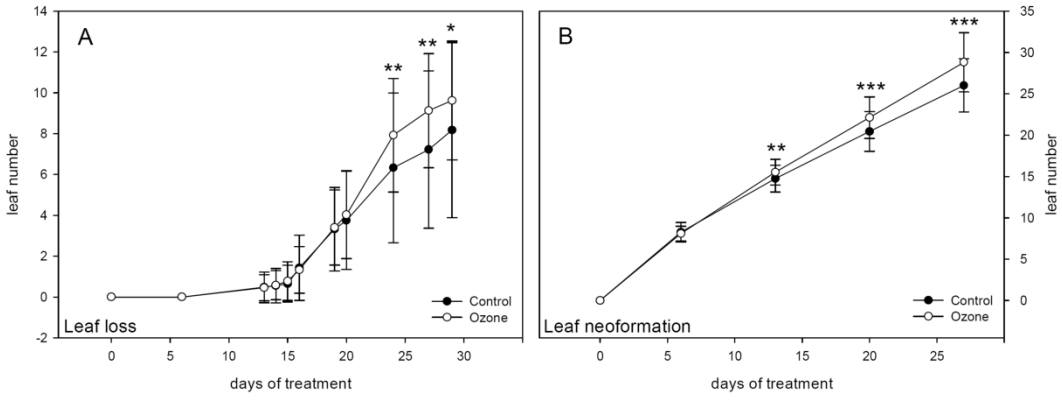

Figure 33: (A) Leaf loss count since day 0 and (B) new leaf formation since day 0. Statistical significance was tested by One-Way ANOVA between control and treated and is represented as follows: * p<0.05; ** p<0.01; *** p<0.001. n = 40. Error bars represent standard deviation.

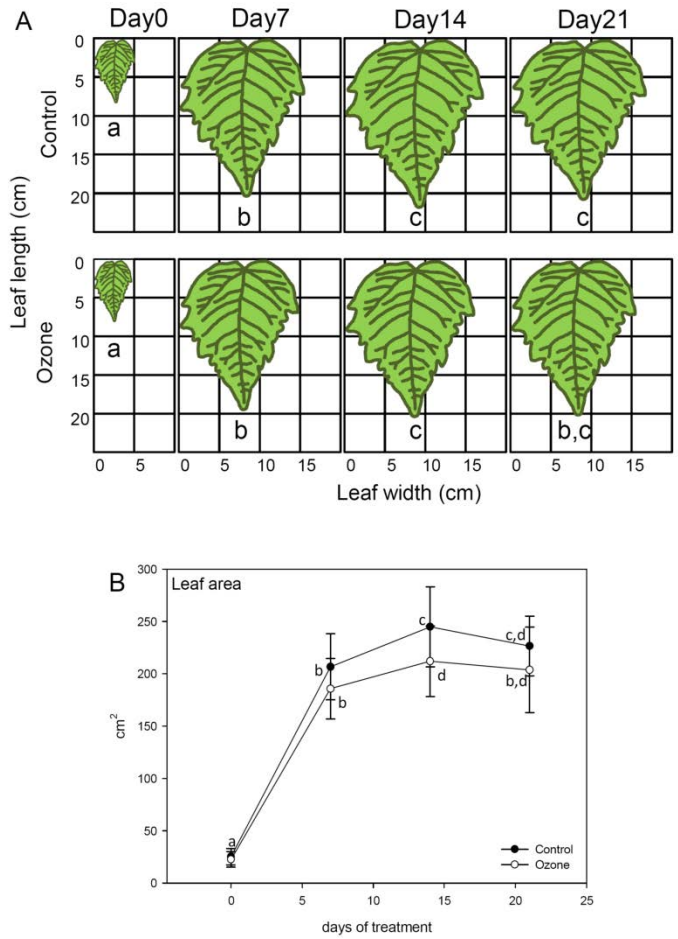

Figure 34: (A) Representation of leaf size from measured lobe length and width (B) Calculated leaf area. Statistical significance in (A) is for the values of leaf width only. Statistical significance was tested by One-Way ANOVA between control and treated (B) and between each time point of one condition against day 0 of the same condition (A and B). Letters represent statistical significance for $p<0.05$, n = 16 for days 0 and 7, n = 12 for day 14 and n = 8 for day 21. Error bars represent standard deviation.

4.2.4.2. Chlorophyll fluorescence

Only two chlorophyll fluorescence parameters changed during ozone treatment, maximum quantum yield of photosystem II (Fv/Fm) and non-photochemical quenching (NPQ) (Figure 35). Fv/Fm increased until day 14 in ozone free leaves and then remained stable until the end of the experiment, while in treated leaves it rose only until day 7 and dropped again from day 14 on. From day 14 to the end of the treatment Fv/Fm was distinctly lower in treated leaves (Figure 35A). NPQ decreased gradually over the time course of the experiment in both growth conditions, but from day 14 on remained significantly higher in ozone treated leaves (Figure 35B). The quantum yield of photosystem II (PhiPSII) and photochemical quenching (qP) decreased gradually over the time course of the experiment in treatment and control conditions and showed no significant variation due to ozone exposure (data not shown).

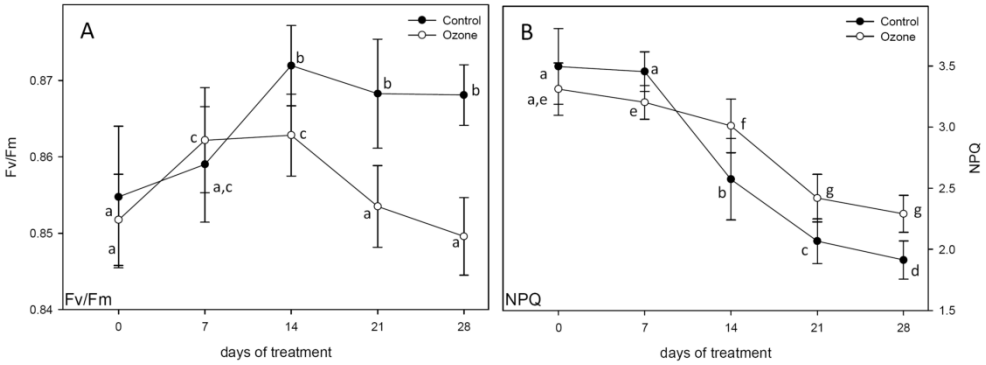

Figure 35: (A) Fv/Fm, maximum quantum yield of photosystem II and (B) non photochemical quenching (NPQ), calculated from chlorophyll fluorescence. Statistical significance was tested by One-Way ANOVA between control and treated and between each time point of one condition against day 0 of the same condition. Letters represent statistical significance for ANOVA $p<0.05$. n = 12. Error bars represent standard deviation.

4.2.4.3. Pigments

Contents of chlorophyll a and b (Figure 36A), lutein and neoxanthin (Figure 36B), increased in control leaves until day 21, then remained at the same level until day 28. In ozone exposed plants the highest concentration for these pigments was already reached at 14 days, except for neoxanthin where it was reached at 21 days. For each of these pigments, the content was significantly lower in ozone treated plants from day 14 on. Violaxanthin and zeaxanthin are represented as a ratio of their content to that of chlorophyll a as previously described (Niyogi et al. 1997) (Figure 36C and D). Both ratios clearly decreased over time in both growth conditions, but remained higher in exposed plants at the later time points, starting at days 14 (violaxanthin) and 21 (zeaxanthin). The ratio violaxanthin/zeaxanthin was higher in treated plants, although significantly only on day 14 (Figure 36E). Beta-carotene (Figure 36F) behaved similarly in the two conditions, increasing until day 21.

4.2.4.1. Carbohydrates

Measured carbohydrate levels were stable (glucose, sucrose and starch) or slightly increasing (fructose) during the first 7 days in control plants, then their content decreased more or less strongly at day 14 (Figure 37A, B, C and D). Sucrose content then immediately increased again until day 21 to remain stable until day 28, while glucose and fructose remained at a low level at day 21 and rose again at day 28. Starch levels rose slowly in control leaves from day 14 to day 28. Carbohydrate content in ozone exposed plants roughly followed the pattern of control leaves, with some significant changes. Fructose levels were significantly higher in treated plants at days 14 and

21, glucose and sucrose only at day 14. Starch on the other hand was higher in treated plants at days 21 and 28.

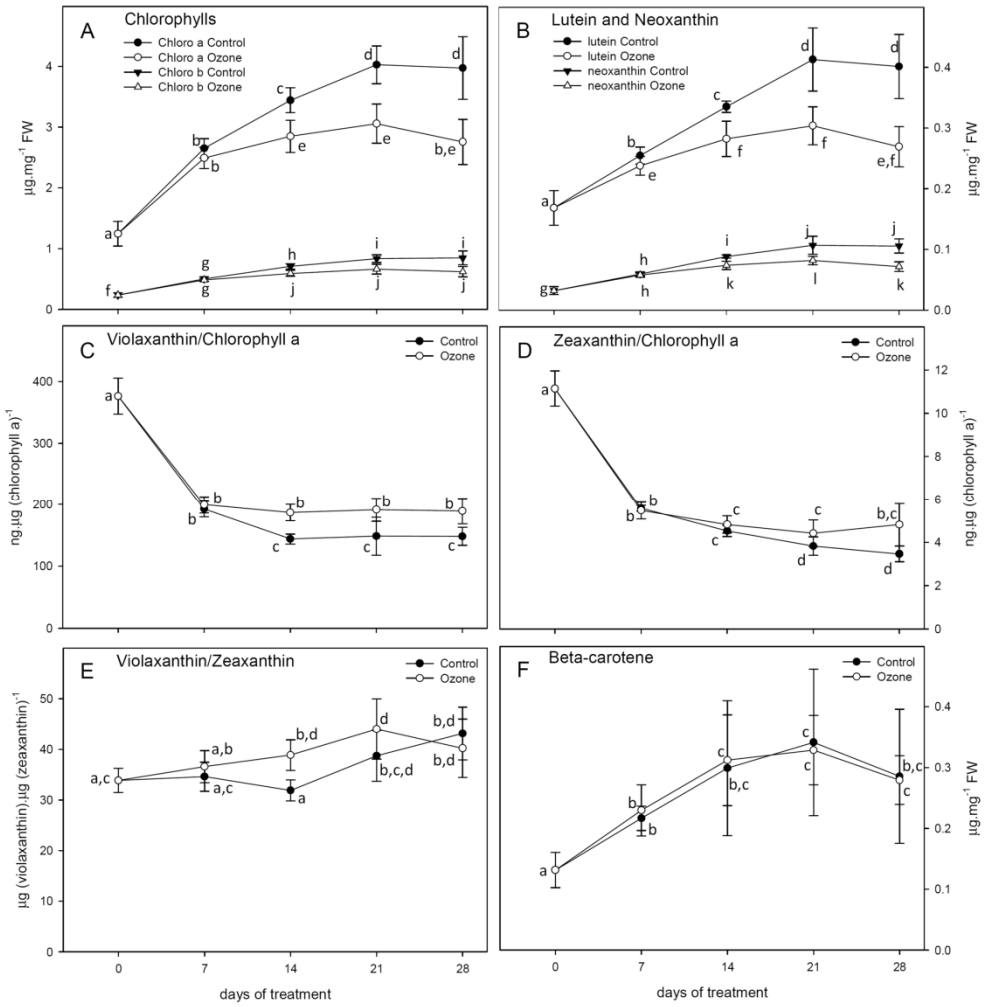

Figure 36: Quantification of the pigments (A) chlorophyll a and chlorophyll b, (B) lutein and neoxanthin, (C) violaxanthin and (D) zeaxanthin, expressed as their ratio to chlorophyll a, (E) the ratio between violaxanthin and zeaxanthin; (F) beta-carotene. Statistical significance was tested by One-Way ANOVA between control and treated and between each time point of one condition against day 0 of the same condition. Letters represent statistical significance for ANOVA $p<0.05$. n = 8. Error bars represent standard deviation.

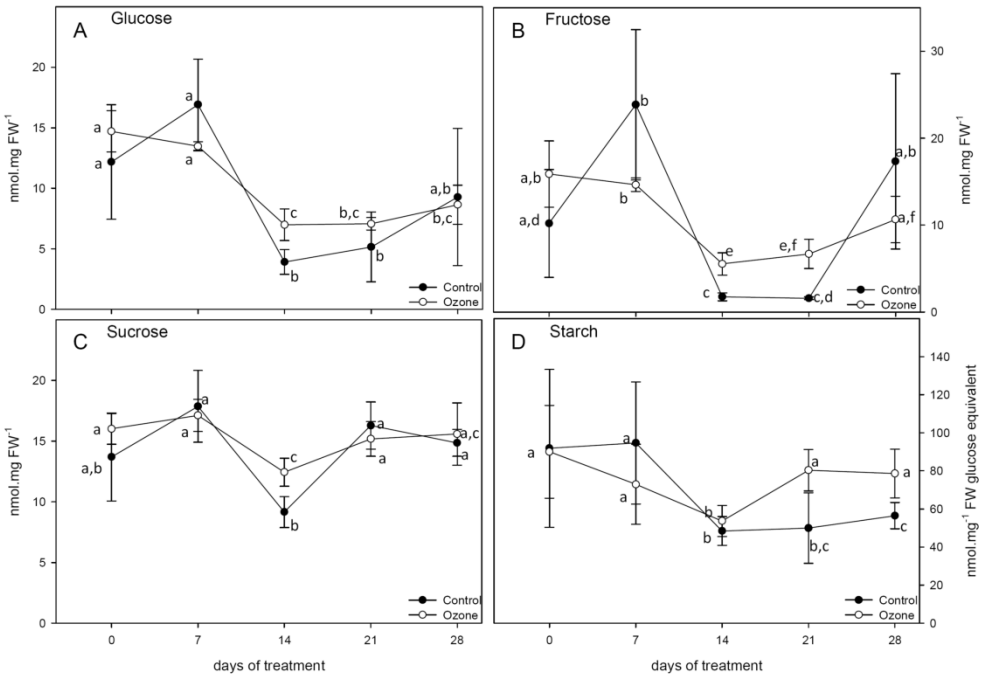

Figure 37: Quantification of (A) glucose, (B) fructose and (C) sucrose and (D) starch. Statistical significance was tested by One-Way ANOVA between control and treated and between each time point of one condition against day 0 of the same condition. Letters represent statistical significance for ANOVA $p<0.05$. n = 4. Error bars represent standard deviation.

4.2.4.2. Proteomics

The proteomic effects of normal leaf development were tested with a One-Way ANOVA on control spot maps only. The average ratio was calculated for each time point versus day 0. Effects of ozone were tested with a Two-Way ANOVA, with treatment as factor one and time as factor two. The average ratio was also calculated for each ozone treatment time point versus its control counterpart. Differentially abundant proteins with an absolute ratio of at least 1.5-fold for minimum one time point and a p-value<0.01 were selected. When considering leaf development and ozone treatment, the intensity of a total of 470 protein spots was significantly different. Of these, 404 proteins could be matched and picked on preparative gels. Finally, 216 proteins could be significantly identified. The proteins discussed below are presented in the summarizing Table 7. A detailed table is available in

Supplemental Table 2. This made a final total of 162 identified spots for leaf development, 123 for ozone exposure, of which 69 were common to both conditions (Figure 38A). The distribution of the spot maps on the PCA plots shows that the most important differences were between the samples of day 0, corresponding to small immature leaves, and the other samples corresponding to mature

leaves (Figure 38B), indifferent of the growth conditions. When the day 0 gels are removed from the PCA to focus on the effects ozone has during leaf development, it becomes visible that the organization along the axes separates the spot maps according to time and condition (Figure 38C). It also illustrates that the results of the different biological repetitions for each time point and condition are grouped together, even though not perfectly. In the cluster analysis, the day 0 gels cluster together, as do the day 7 gels, independently of the treatment (Figure 38D). The effects of ozone treatment become visible with day 14 when the experimental points become clustered according to the treatment. The variations in abundance of 6 prominent proteins for ozone-free and ozone treated samples are illustrated in (Figure 39), and the abundance profiles for all proteins discussed below can be found in Supplemental Figures 2.

Table 7: Summary of identified proteins in carbon metabolism, protein metabolism, protein folding, protein synthesis, detoxification and pathogenesis-related. In the table can be found: protein name, number of spots containing the protein increasing and decreasing in abundance in both conditions and the number of significant varying proteins that are common to both conditions, and the sub-cellular localization of the proteins as determined by the tools described in the material and methods section. The variations up (increased abundance) and down (decreased abundance) represent the most prominent trend of the protein abundance observed. A table with detailed information is available in Supplemental Table 2.

	Number of spots identified					
	Ageing		Ozone		In common	
Protein name	**up**	**down**	**up**	**down**		**subcel. loc.**
Carbon metabolism						
carbonic anhydrase	**1**	0	0	**1**	**1**	chl
rubisco subunit binding-protein alpha subunit	**1**	0	0	0	0	chl
rubisco subunit binding-protein beta subunit	0	**1**	0	0	0	chl
ribulose-1,5-bisphosphate carboxylase/oxygenase large subunit	**8**	0	0	**10**	**2**	chl
ribulose bisphosphate carboxylase/oxygenase activase 1	**5**	**6**	0	**9**	**9**	chl
ribulose-1,5-bisphosphate carboxylase/oxygenase activase 2	**1**	**1**	0	**2**	**2**	chl
transketolase 1 (chloroplastic)	**4**	0	0	**7**	**3**	chl
transketolase 1 (cytosolic)	**1**	0	0	**3**	**1**	cyt
glyceraldehyde 3-phosphate dehydrogenase, (chloroplastic)	**3**	0	0	0	0	chl
glyceraldehyde 3-phosphate dehydrogenase, (cytosolic)	**3**	**1**	0	0	0	cyt
phosphoglycerate kinase, putative	0	**1**	0	**7**	**1**	chl
triosephosphate isomerase (cytosolic)	**1**	**3**	0	**3**	**2**	cyt
fructose 1,6-bisphosphatase	0	0	0	**1**	0	cyt
fructose-bisphosphate aldolase (chloroplastic)	0	**2**	0	0	0	chl
fructose-bisphosphate aldolase (cytosolic)	0	**1**	0	**1**	0	cyt
sedoheptulose-1,7-bisphosphatase	**3**	**1**	0	0	0	chl

NADP-dependent malic protein	**3**	**2**	**2**	0	**2**	cyt
NAD-dependent malate dehydrogenase	0	**1**	0	0	0	cyt
malate dehydrogenase	0	**2**	0	**1**	0	mit
glycolate oxidase	0	0	0	**1**	0	per
enoyl-ACP reductase	0	**1**	0	0	0	n.a.
quinone oxidoreductase-like protein	**1**	**1**	0	**1**	**1**	cyt
mitochondrial lipoamide dehydrogenase	**2**	0	0	**1**	0	mit
lactoylglutathione lyase	**1**	0	0	0	0	cyt
ATP synthase beta subunit	**1**	0	0	0	0	chl
light-harvesting complex I protein Lhca1	**2**	0	0	**2**	**2**	chl
light-harvesting complex I protein Lhca3	**3**	0	0	**2**	**2**	chl
light-harvesting complex II protein Lhcb1	**2**	0	0	0	0	chl
oxygen evolving enhancer protein 1	**7**	**2**	0	**2**	**2**	chl
oxygen-evolving enhancer protein 2	**2**	0	0	**1**	**1**	chl
chloroplast oxygen-evolving enhancer protein	**1**	0	0	**1**	**1**	chl
photosystem I reaction center subunit II	**1**	0	0	0	0	chl
chloroplast photosystem I protein	**1**	0	0	0	0	chl
PSI reaction center subunit III	**1**	0	0	0	0	chl
ferredoxin-NADP oxidoreductase	**4**	**1**	0	**3**	**2**	chl
polyphenol oxidase	0	0	**3**	0	0	chl
Protein metabolism						
glutamine synthetase	**1**	0	**1**	0	**1**	cyt
vitamin-b12 independent methionine synthase, 5-methyltetrahydropteroyltriglutamate-homocysteine	0	**3**	0	**1**	**1**	cyt
s-adenosylmethionine synthetase 4	0	**3**	0	0	0	cyt
alanine aminotransferase 2	0	**2**	0	**3**	**2**	per
serine carboxypeptidase (carboxypeptidase D)	0	0	**1**	0	0	per
glycyl-tRNA synthetase / glycine--tRNA ligase	**1**	0	0	0	0	cyt
mitochondrial serine hydroxymethyltransferase	0	**1**	0	0	0	mit
Protein folding						
heat shock protein	0	**1**	0	0	0	chl
chloroplast HSP70	**1**	**1**	0	0	0	chl
heat shock protein 90	0	0	**1**	0	0	cyto
heat shock protein 70	0	**2**	**2**	0	0	cyto
heat shock protein, putative	**2**	**3**	**2**	0	**2**	cyto
protein disulfide isomerase, putative	**1**	**1**	**2**	0	**2**	cyto
isomerase peptidyl-prolyl cis-trans isomerase	0	**1**	0	0	0	chl
protein grpE, putative	0	**1**	0	0	0	chl
Protein synthesis						
60S acidic ribosomal protein P0	**1**	**2**	0	0	0	cyt
ribonucleoprotein	0	**1**	0	**1**	**1**	chl
ribosome recycling factor	**1**	0	0	**1**	**1**	n.a.
chloroplast translational elongation factor Tu	0	**2**	0	**2**	**2**	chl
eukaryotic translation initiation factor 5A isoform I	0	**1**	0	**1**	**1**	cyt
translation elongation factor G	**1**	0	0	**1**	**1**	cyt
Detoxification						

monodehydroascorbate reductase	0	**1**	0	0	0	cyt
cytosolic ascorbate peroxidase	**1**	**2**	0	0	0	cyt
glutathione-s-transferase theta	**1**	0	0	**3**	**1**	cyt
glutathione peroxidase	**1**	0	0	0	0	n.a.
catalase	**2**	**1**	0	**5**	**3**	per
peroxidase	**1**	**1**	**4**	0	0	cyt
Pathogenesis-related						
class I chitinase	**1**	0	**2**	0	**1**	cyt
class IV chitinase	0	0	**1**	0	0	cyt
acidic endochitinase SE2	0	0	**2**	0	0	cyt
beta-1,3 glucanase	**1**	0	**4**	0	**1**	cyt
kunitz trypsin inhibitor TI3	0	0	**1**	0	0	cyt

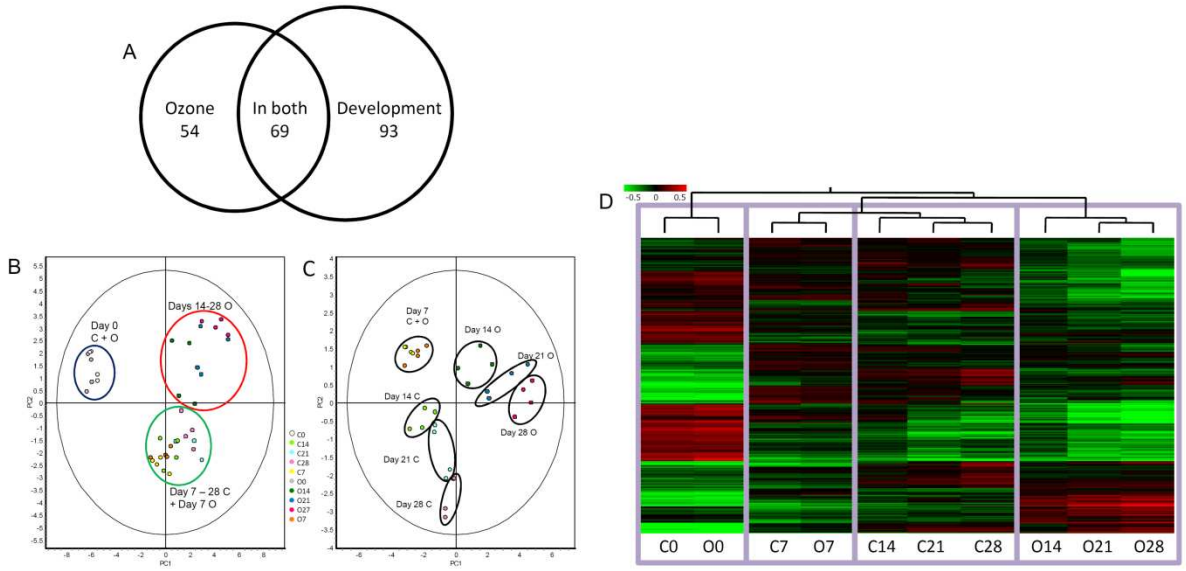

Figure 38: (A) Venn diagram of the number of identified proteins for each treatment and the overlap, (B) PCA of all gel images, (C) PCA analysis of all gel images excluding day 0, (D) cluster analysis of all experimental groups. C = control, O = ozone, numbers 0 to 28 indicate days of treatment.

4.2.5. Discussion

4.2.5.1. Leaf development in control plants

In plants, leaves are the site of photosynthesis, and hence the major site of carbon metabolism. They are morphologically and physiologically specialized on light-energy absorption, CO_2 uptake and assimilation and energy production. Only little information can be found about expanding leaves, but it is considered that photosynthesis and chlorophyll content increase during leaf expansion (Kennedy and Johnson 1981; Nogués et al. 2008). In the present study, important

proteomic changes in primary carbon metabolism were observed during leaf expansion. The changes in carbon metabolism during leaf development between days 0 and 7 are summarized in Figure 40. An important number of the identified proteins involved in carbon metabolism belong to the Calvin cycle, and are present as more than one isoform (Table 7). Most of these increased in relative abundance during the seven first days of development, in parallel to the leaf expansion phase (Figure 34). One of the proteins that increased in abundance is RuBisCO LSU. This increase in RuBisCO LSU is one of the few observations concerning leaf development that has previously been reported (Maayan et al. 2008). In parallel with the accumulation of Calvin cycle proteins during the first seven days (i.e. chloroplastic glyceraldehydes-3-phosphate dehydrogenase, transketolase, sedohoheptulose-1,7-bisphosphatase) was the increase in abundance of photosystem proteins, as was already observed previously (Maayan et al. 2008), and associated pigments (Figure 36). Both phenomena seem logic for expanding leaves, where chloroplasts are slowly developing and photosynthesis is activated, as is illustrated by the chlorophyll fluorescence parameter Fv/Fm (Figure 35). During the first seven days of leaf expansion, a drop in abundance of some glycolytic proteins was observed (i.e. cytosolic fructose bisphosphate aldolase, triose phosphate isomerase). These enzymes are involved in the first half of glycolysis where glucose is transformed into triose phosphate. It is known that glycolysis and mitochondrial respiration are inhibited by light in adult leaves (Tcherkez et al. 2005), but are probably very active in expanding leaves (Reich 1983). Since photosynthesis is only increasing slowly during leaf expansion, it is most probable that carbohydrates for the catabolism are imported into the young leaves in a source/sink relationship with older leaves (Dickson 1989). This is also illustrated by the high concentration of glucose and fructose at the early time points (Figure 37). As the chloroplastic metabolism is built up, more triose phosphate is produced by the Calvin cycle and the leaf starts sustaining itself. Although most of these molecules are diverted into storage carbon molecules during the day, a part of it starts fueling glycolysis. After seven days, most carbon metabolism proteins observed seemed to have reached a more or less stable level, and it is probably between 7 and 14 days of expansion that the leaf became mature and switched its role from sink to source leaf. It is also during this time that glucose and fructose levels were lowest as carbohydrates were exported to younger leaves in a now inverted source/sink relationship. Mitochondrial malate dehydrogenase levels dropped during the first 7 days of the experiment, indicating a switch in the substrate for the Krebs cycle from pyruvate to malate.

Between 7 and 28 days of the experiment, Calvin cycle and glycolysis enzymes remained at relatively stable levels. Chloroplast electron transport chain proteins on the other hand continued to increase in abundance. As the plants grew, younger leaves shaded the older ones. To keep a

sufficient level of photosynthesis, it is likely that the machinery was adapted to a more efficient use of the available light (Ishida et al. 1999).

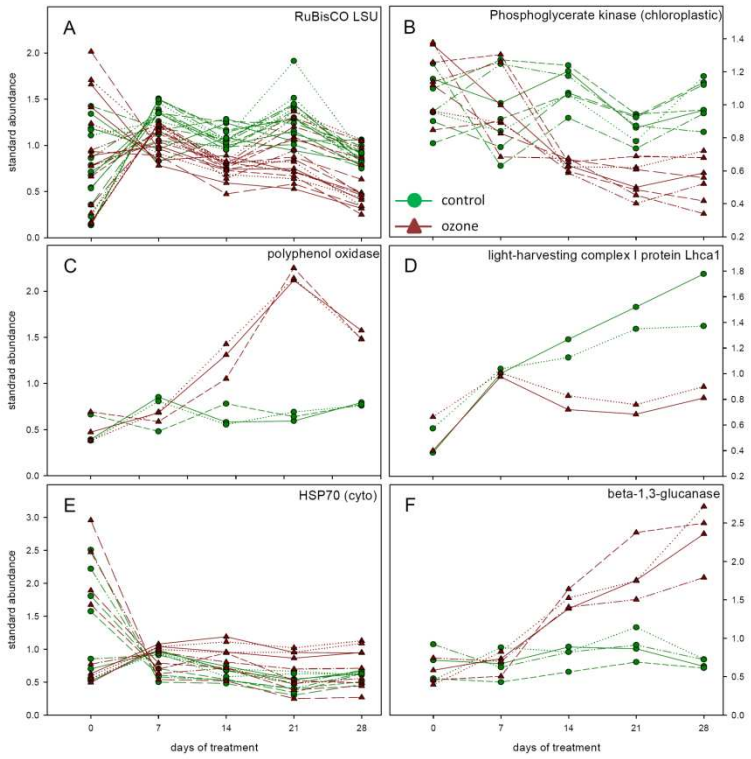

Figure 39: Examples of variation in protein abundance of a selection of prominent proteins. Values are calculated from the exported normal abundance from Decyder software. Multiple lines of the same color and symbol represent separate protein spots containing the same protein function. Similar figures for all the discussed protein spots can be found in Supplemental Figures 2.

Cytosolic glutamine synthetase increased gradually over the experiment. This enzyme is responsible for ammonium fixation from primary nitrogen uptake, but also from protein recycling and photorespiration (Bernard and Habash 2009). Since primary nitrogen assimilation mostly happens in roots, it can be assumed that the increase in GS observed in leaf development was due to an increase in ammonium recycling from proteins, possibly simply due to their turnover, and the increase in ammonium production in photorespiration. Methionine synthase and S-adenosylmethionine synthase were observed to decrease over the entire time course of the experiment, the strongest decrease clearly being during the first seven days. S-adenosylmethionine is the precursor for several pathways, like biotin, polyamines, ethylene, and acts as a general donor for methyl groups (Amir et al. 2002). A similar behavior could be observed for alanine aminotransferase, which catalyses the transfer of amino groups to different substrates (Orzechowski et al. 1999). Translational elongation factors and ribosomal proteins decreased in abundance in different patterns over the time of the experiment. This shows that protein synthesis was lower in a mature leaf. This is logical, since during the development the leaf is 'built' with and by proteins. Only elongation factor G increased in abundance between days 0 and 7, and a ribosome recycling factor and elongation factor G are increased at day 28. They are both involved

in the disassembly of ribosomal subunits and RNA at the end of protein translation (Fujiwara et al. 2004). Chaperones like HSP70 and disulfide isomerase, responsible for correct protein folding, also show a downward trend, confirming the reduced protein synthesis in mature leaves. Some isoforms of HSP are at relatively low levels from the beginning, showing that specific isoforms may be specifically needed during the developmental phase, while others are needed to maintain basic metabolism. All of these changes indicate that the general metabolic activity in the adult leaves is lower than in the developing leaves.

Up- and down-variations among the isoforms of the identified detoxification proteins are not always consistent, which could have been due to different isoforms for each identified spot, or to unidentified post translational modifications. Catalase showed an upward trend in abundance at the beginning of the experiment, and a downward one to the end. Catalase is one of the major enzymes of peroxisomes (Reumann and Weber 2006). They are among other things responsible for the detoxification of H_2O_2 from photorespiration. The increase in abundance of catalase would therefore be linked to the increase of RuBisCO which is responsible for O_2 fixation in photorespiration. The levels of some peroxidase isoforms were stable throughout the 28 days, while some were higher at day 0 and reached the level of the others at day 7. It has been shown before that peroxidase activity in leaves can be associated with leaf expansion and is highest shortly before the end of leaf growth (Macadam et al. 1992). A large part of peroxidase activity can be associated to the cell wall (Bacon et al. 1997), but in this study it is not possible to distinguish between cell wall or alternate localization of the identified enzymes. It is possible that peroxidase activity protects the cells from the ROS formed during leaf expansion and cell wall development, while catalase was responsible for those formed during photorespiration.

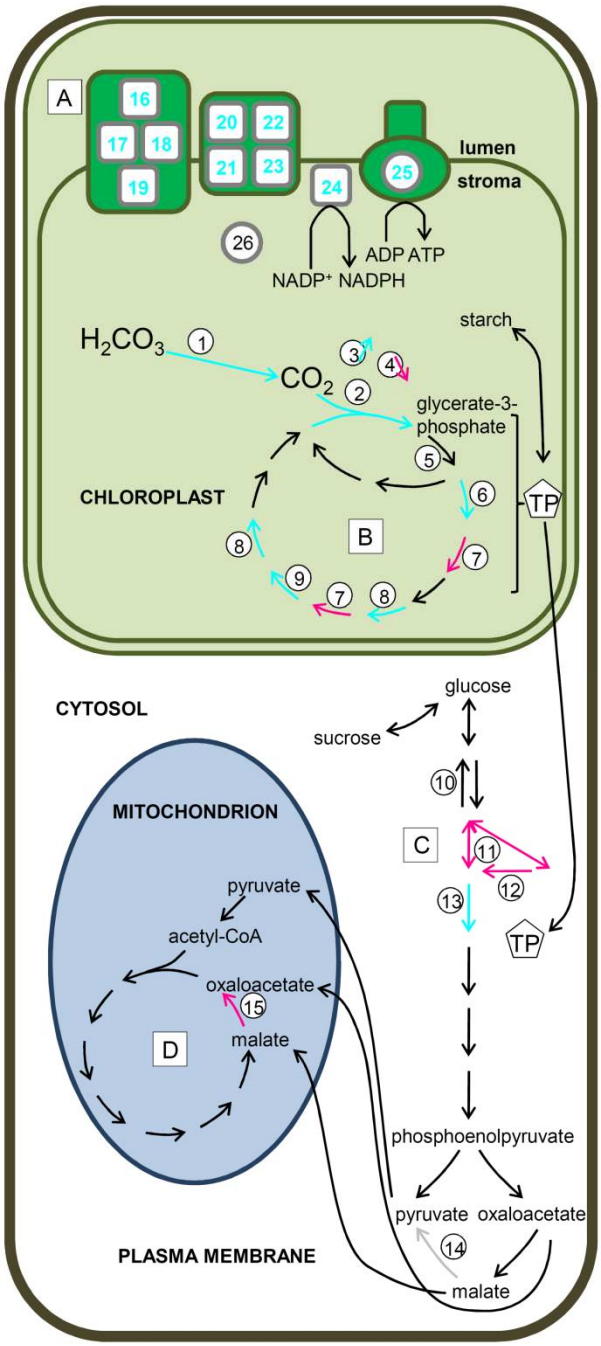

Figure 40: Representation of the changes in protein abundance of the primary carbon metabolism in a developing leaf at day 7 compared to day 0 in ozone-free and in ozone treated conditions alike. Magenta arrows indicate a reduced abundance while cyan arrows or numbers indicate an increased abundance of the protein. A grey arrow indicates a protein presenting a downward and upward variation in different spots. (A) chloroplast electron transport chain, (B) Calvin cycle, (C) glycolysis, (D) Krebs cycle. TP, triose phosphate. 1, carbonic anhydrase; 2, RuBisCO; 3, RuBisCO activase; 4, RuBisCO subunit binding; 5, phosphoglycerate kinase; 6, glyceraldehyde-3-phosphate dehydrogenase; 7, fructose-1,6-bisphosphate aldolase; 8, transketolase; 9, sedoheptulose-1,7-bisphosphatase; 10, fructose-1,6-bisphosphatase; 11, fructose-1,6-bisphosphate aldolase; 12, triose phosphate isomerase; 13, glyceraldehyde-3-phosphate dehydrogenase; 14, NADP malic enzyme; 15, NADP malate dehydrogenase; 16, oxygen evolving enhancer protein; 17, oxygen evolving enhancer protein 1; 18, oxygen evolving enhancer protein 2; 19, light harvesting complex II protein Lhcb1; 20, PS1 reaction center subunit II; 21, PS1 reaction center subunit III; 22, Light harvesting complex I protein Lhca1; 23, Light harvesting complex I protein Lhca3; 24, ferredoxin-$NADP^+$-reductase; 25, ATPase beta; 26, polyphenol oxidase.

4.2.5.2. Changes due to ozone treatment

It was shown in a previous publication from our group that there were barely any changes in the proteome profiles of poplar leaves after 3 days of ozone treatment, but that changes appeared after 14 days and 35 days (Bohler et al. 2007). In the present study the time points were adjusted to those results, to get a better understanding of the variations on a smaller time-scale (28 days *vs*

35 days) but with more observation points (every 7 days). The observations tend to confirm the previous results.

No effects at all could be observed in the current experiment before 14 days of treatment at a proteomic or biochemical level, probably due to small experimental or technical differences between the two experiments (e.g. size of the plants at the beginning of the treatment, small differences in conditions due to technical fluctuations, variation of precise fumigation concentrations due to non-automated ozone adjustment). From day 14 on, effects were visible on the proteomic (Table 7 and (Figure 41) biochemical (Figure 36 and Figure 37) physiological (Figure 35) and morphological levels (Table 6 and Figure 33).

For carbon metabolism, 4 enzymes of different functions presented a decreased abundance in the Calvin cycle due to ozone, including RuBisCO, which was previously shown clearly to be reduced by ozone exposure (Brendley and Pell 1998; Miller et al. 1999; Pell et al. 1992; Pelloux et al. 2001). Similarly, carbonic anhydrase, RuBisCO subunit binding protein and RuBisCO activase, all involved in the optimal functioning of RuBisCO, were present at lower levels than in controls. This undoubtedly resulted in reduced carbon fixation and triose phosphate production. Since part of the triose phosphate is exported to the cytosol as a substrate for sucrose synthesis or glycolysis, this would have had an impact on these pathways. The analyses showed that 3 proteins of glycolysis upstream of triose phosphate were reduced by the treatment, but no changes could be detected for enzymes of the lower part of glycolysis, which could be expected to respond to the variations of the Calvin cycle. It was notable that starch levels were higher in treated leaves. Starch accumulates during the day in chloroplasts, to be used during the night by the carbon catabolism to produce energy and sustain growth (Smith and Stitt 2007). Possibly, the lower levels of carbon that still were produced during the day were preferentially stored in the chloroplast as starch, which could then have been used in the night for respiration and repair. It should also be noted that an import of carbon molecules could come from senescing leaves, which were more abundant in ozone treated trees (Figure 33). Furthermore, phloem translocation could be impaired by ozone.

The cytosolic NADP dependent malic enzyme downstream of glycolysis was higher in abundance in treated plants. This enzyme catalyses the conversion of malate to pyruvate. Mitochondrial malate dehydrogenase (MDH) on the other hand decreased in abundance. It has been shown that under ozone exposure, PEPc is typically induced (Fontaine et al. 2003). The high molecular weight of this enzyme made it impossible to observe it in this proteomic study. PEPc leads to malate production through the anapleurotic pathway. This malate can then be imported into the mitochondrion and converted to pyruvate by the NAD dependent malic enzyme (NAD-ME) that has been shown to be

induced by ozone (Dizengremel et al. 1994). The NADH produced by this conversion could then be used in the respiratory chain (Dizengremel 2001). Although no variation of NAD-ME could be observed in the present study, the decreased MDH could shift the balance to the conversion of malate to pyruvate rather than oxaloacetate. The cytosolic NADP-ME was observed to increase in abundance, which would also point to a preferential use of pyruvate as a precursor for the mitochondrion, instead of malate. The reaction also leads to the production of NADPH in the cytosol, needed for the regeneration of for instance ascorbate (Dizengremel et al. 2009). Although there is no evidence for this here, it has been previously shown that the second half of glycolysis is induced under ozone exposure, as is the Krebs cycle. An increased activity of phosphofructokinase and fumarase was previously revealed (Dizengremel et al. 1994; Sehmer et al. 1998).

During ozone exposure, we also observed changes in two enzymes involved in photorespiration, the mitochondrial dihydrolipoamide dehydrogenase and the peroxisomal glycolate oxidase, which both showed a late downward trend. Although these are only two proteins of the pathway, these results are in agreement with previously published observations (Bagard et al. 2008). It is probable that a decrease in photorespiration is directly linked to the decrease in RuBisCO abundance, hence CO_2 and O_2 fixation.

The effects on the primary carbon metabolism discussed above mostly became visible at day 14. Changes in the abundance of chloroplast electron transport chain proteins on the other hand mostly appeared at 21 days of exposure. The effects on the biochemical part of photosynthesis seemed to appear before the effects on the photochemistry, as already suggested (Dizengremel 2001; Dizengremel et al. 2009; Heath 2008). If the biochemistry was affected first, and the Calvin cycle was inhibited, ATP and NADPH could accumulate in the chloroplast, and act on the regulation of the electron transport chain. Pigment concentrations dropped already after 14 days of treatment (Figure 36). Fluorescence parameters also varied already significantly after 14 days of treatment. The strong decrease in Fv/Fm (Figure 35A) showed that there was a loss in the maximum efficiency of photosystem II. The relative increase in NPQ when compared to control illustrates that the electron flow was too high for the photochemical processes and had to be quenched at least partially by the xanthophyll cycle, as already shown (Castagna et al. 2001). Indeed the levels of violaxanthin and zeaxanthin relative to chlorophyll a are higher in treated leaves. Altogether this shows that there is an effect on photochemistry before variations in protein abundance can be detected. Polyphenol oxidase, a protein that is thought to play a protective role in the chloroplast electron transport chain (Sherman et al. 1991), was higher in abundance in

treated leaves starting at day 14, showing that an oxidative attack occurs on this level as early as 14 days.

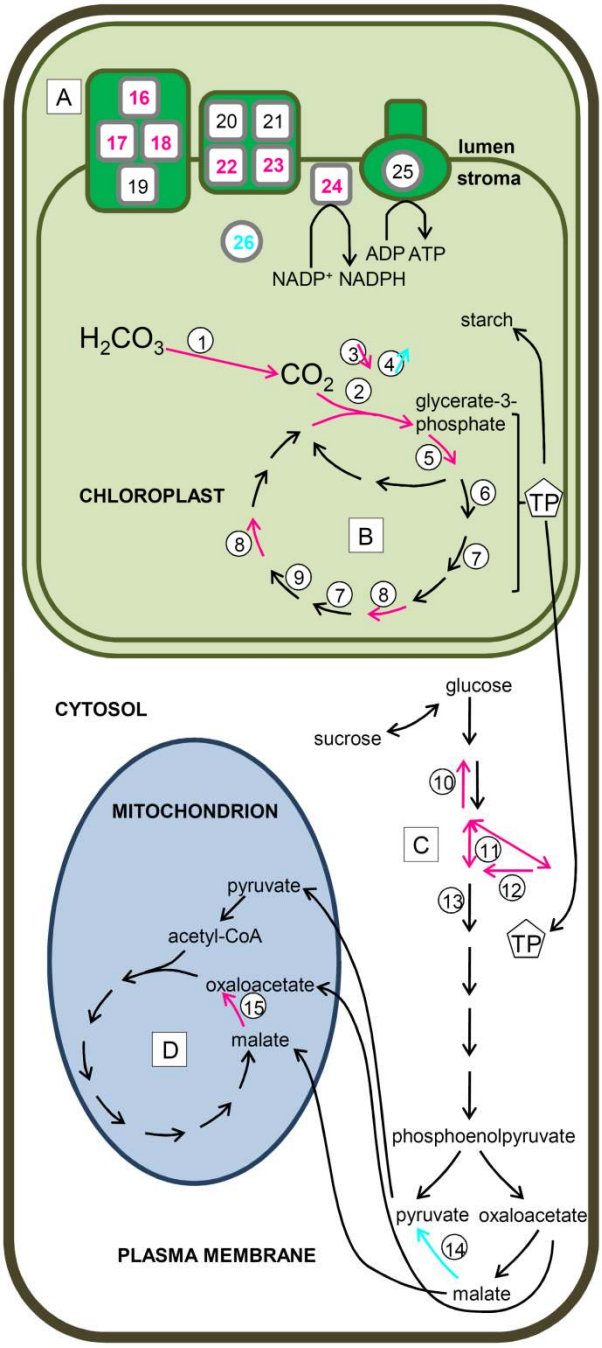

Figure 41: Representation of the changes in protein abundance of the primary carbon metabolism of an ozone treated leaf compared to a control leaf on day 28. Magenta arrows or numbers indicate a reduced abundance while cyan arrows or numbers indicate an increased abundance of the protein. Numbered items correspond to the ones presented in the legend of Figure 40.

Since ozone clearly leads to an oxidative stress and to the formation of ROS like H_2O_2 (Diara et al. 2005), it would be expected that detoxifying proteins would increase, most notably ascorbate related detoxification (Luwe et al. 1993). In the present study, the abundance of the observed ascorbate peroxidase did not vary under ozone exposure, although it has been shown to increase in activity (Sehmer et al. 1998). Other peroxidases increased in abundance. They could be responsible

for some of the ozone induced ROS detoxification, since they are often associated to cell wall detoxification (Bacon et al. 1997), where ozone-induced ROS first appear. Catalases on the other hand were present at lower abundance in ozone treated leaves. Since catalases are involved in photorespiration-induced H_2O_2 detoxification (Reumann and Weber 2006), the reduction in RuBisCO abundance could explain the decrease of this enzyme. A reduced fixation of O_2 would decrease the rate of photorespiration.

Pathogenesis related proteins are proteins that were initially found to be involved in pathogen attack (van Loon 1997), but recently also associated with different types of abiotic stress (Renaut et al. 2004; Sandermann et al. 1998). Here, we observed an increase in abundance of multiple isoforms of chitinase. It is known that chitinases are induced by many stress conditions, ethylene, salicylic acid and jasmonic acid, which all play a role in ozone stress signaling (Kangasjärvi et al. 2005). It was also shown that acidic class III chitinases can be secreted into the apoplast, which is the primary location of ozone attack (Arie et al. 2000). Similar to chitinase, the abundance of several beta-1,3-glucanases increased. The upward variation of these two pathogenesis related proteins was probably due to the ozone-induced oxidative burst (Wohlgemuth et al. 2002) that is also typical for a pathogen attack.

4.2.6. Ozone and leaf expansion

If little is known about leaf expansion in general, even less is known about it in combination with ozone exposure. It was shown in previous observations that necroses only appear once leaves are fully expanded (Bagard et al. 2008; Bohler et al. 2007). In the present study it was shown that leaves expanding during the treatment grow to a slightly smaller area than normally expanding leaves but with barely any statistical significance. As discussed above, leaf expansion is complete after a little more than 7 days, which is also visible on the proteomic level. The proteomic variations could clearly be divided into changes between 0 and 7 days and changes between 7 and 28 days (Figure 42). In the first phase, ozone had strictly no effect on the protein level. Ascorbate peroxidase and peroxidase levels were highest at the beginning of leaf expansion than in the mature leaf, which could have conferred a certain resistance to ROS to the young leaves. Under ozone exposure, peroxidases were induced only on later time points, which supports this hypothesis. Similarly, the higher levels of chaperones in young leaves could protect them from ozone induced damage. These considerations could explain why younger leaves are more resistant to ozone, simply because cellular processes are very active and the inherent antioxidant potential is stronger (Nogués et al. 2008). Protective measures that are already in place because they are required for the expansion process can handle the ozone treatment and the effective ozone flux is

not sufficient to induce a response. It has also been shown that the parenchyma of developing leaves is denser than in mature leaves (Paoletti et al. 2009). In denser tissue, less ozone reaches the inner leaf tissues that remain protected from a direct ozone exposure.

Furthermore, 162 identified protein spots varied during leaf development, 123 for ozone exposure, and only 69 of these changed under both conditions. This does not mean the proteins different in the two conditions have different functions. Some proteins, like those related to pathogenesis, were indeed mostly stable during leaf development and only varied under ozone treatment. But in general shifts between different isoforms of the same protein function were observed. For instance, 7 isoforms of phosphoglycerate kinase varied under ozone exposure, and only one during leaf expansion. On the other hand, more different isoforms of photosystem related proteins varied in leaf development than under ozone stress. This illustrates the specificity of both processes. Unfortunately the data could not clarify if the different protein spots that were identified as having the same general function were true isoforms or rather identical polypeptides separated during electrophoresis due to post-translational modifications.

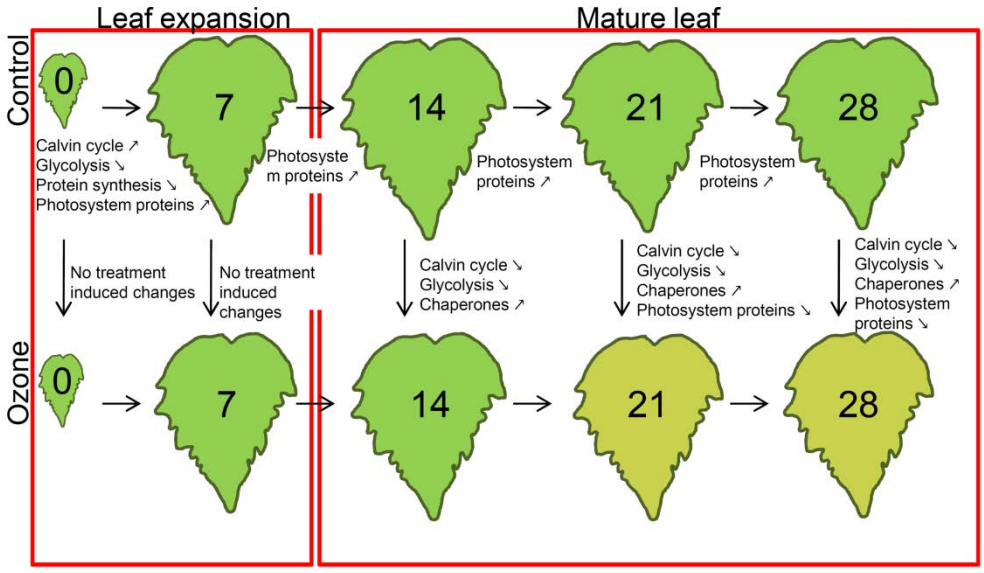

Figure 42: Summary of the proteomic variations in developing leaves and in ozone treated leaves. The clear distinction between the expansion phase and the fully expanded leaf is underlined. Effects of ozone only appear in the adult leaf.

4.2.7. Conclusion

In the present study, we clearly showed that there is a difference between expanding and mature leaves (Figure 42). Once the primary metabolism is setup, carbon sources change. Similarly, protein synthesis and protection mechanisms change over that time. In ozone treated plants, effects due to

the exposure only appear once leaves are mature, and involve primary metabolism, detoxification, protein metabolism and other functions. Expanding leaves on the other hand show no variation whatsoever in response to ozone, and this could be due to the fact that the very active cell processes in expanding leaves are sufficient to cope with the ozone threat. Furthermore, it was shown that specific isoforms of the same proteins vary in one or the other condition, showing the specificity of the natural process of leaf expansion and of the stress induced ozone response.

4.2.8. Supplemental Material

Supplemental Table 2: Full description of the statistical results obtained during (i) the analysis to the effect of ozone treatment compared to control values at each time point AND (ii) the ageing of the leaves upon control conditions compared towards the value at day 0. Average ratios are expressed and p-value of Two-Ways ANOVA are represented for the ozone experiment with (i) ozone treatment (cond1); (ii) time course (cond2) and (iii) interaction between these 2 factors (interact), while only the p-value of One-way ANOVA is represented for the comparison of the different time points in the development of the leaf under control conditions.

Supplemental Figures 2**: A**bundance profiles for all discussed proteins are presented in charts similar to Figure 39. On the x axis are the days of treatment and on the y axis the standard abundance exported from the Decyder software. Multiple lines of the same color represent spots containing the same protein function. Green circles represent control and red triangles treatment conditions.

Available on request: Full data of protein identification are provided. **Spot**: number of the spot on the Master gel; **Protein**: the accession of the protein obtained after blasting the accession obtained in NCBI database if not providing a full name for the protein's function (e.g. 'predicted or hypothetical protein'); **NCBI**: accession returned by the search in database; **Observed**: Experimental m/z value (Da/z); **Mr** (**expt**): Calculated mass of the unprotonated precursor (Da); **Mr** (**calc**): Molecular mass calculated from the matched peptide sequence (Da); **Delta**: Difference (error) between the Mr (exp) and Mr (calc); **Start – End**: position of the sequence in the database entry; **Miss**: Number of missed cleavage sites; **Ions**: Individual ions' score; **Peptide**: Sequence of the peptide in 1-letter code. The residues that bracket the peptide sequence in the protein are also shown, delimited by periods. If the peptide forms the protein terminus, then a dash is shown instead. Modified amino acids are indicated by (ox) for oxidized a.a., W(dox) for double oxidized tryptophan, W(kyn) for kynurenine, E(pyro-glu) for a pyrrolidone carboxylic acid.

In this table, the name of the protein and the species in which this protein was characterized as well as the MASCOT score (protein score as given by the GPS software (Applied Biosystems)) and the expected value as given in the GPS software (Applied Biosystems) are represented as ' **Score'** and ' **expect'.**

Data added during manual validation of the identifications are added in red.

4.2.9. Funding

This study was supported by the Fonds National de la Recherche Luxembourg (FNR) (S.B.'s PhD scholarship AFR TR-PHD BFR06-044).

4.2.10. Acknowledgements

Our thanks go to Mouhssin Oufir for his help with the carbohydrate quantification, to Dr Henry-Michel Cauchie and Dr Thomas Udelhoven for their help with statistics, to Sébastien Planchon for his technical assistance during the proteomic analyses and to Jacques Banvoy for his help with the fumigation chambers.

Chapter 5

Proteomic study on poplar exposed to ozone and drought

5.1. Introduction

Drought is one of the most widespread abiotic stress factors on Earth. Not only arid regions are subjected to drought but more and more drought periods are reported in temperate regions such as Western and Central Europe and are furthermore expected to become more and more severe and longer due to climate change (Bernstein et al. 2007; Ciais et al. 2005; Kreuzwieser and Gessler 2010). Drought can have a strong negative effect on plant growth (Shao et al. 2008a). It was shown that many morphological parameters such as stem length and diameter, biomass or leaf area can be reduced by drought; the extent of this reduction depends on the species and the severity of the constraint (Anyia and Herzog 2004; Leuschner et al. 2001; Ogaya et al. 2003; van Hees 1997). Root growth and number of radicles can be stimulated by mild drought but are reduced by strong water deficit (Leuschner et al. 2001; Sharp et al. 2004; Sponchiado et al. 1989). One of the primary effects of drought on plants is the closure of leaf stomata (Bota et al. 2004; Flexas et al. 2004). The physiological process is controlled by abscisic acid (ABA), a plant growth regulator mainly produced in the roots and transported to the shoots and leaves (Seki et al. 2007). Its drought-induced accumulation in leaves is caused by a decrease in ABA catabolism and leads to stomatal closure and consequently a drop in stomatal conductance. This lessening in gas exchange leads to a reduced CO_2 content in the leaf cells and thus has repercussions on photosynthesis (Bota et al. 2004). Net CO_2 exchange is quickly reduced by water deficit, but decreases in RubisCO activity and protein abundance are often observed only at later stages during chronic drought (Bota et al. 2004; Parry et al. 2002; Pelloux et al. 2001). Photochemistry is relatively resistant to drought, and only decreases in ATP production were observed (Flexas and Medrano 2002; Tezara et al. 1999). Photooxidative damage and photoinhibition were only detected in very severe cases of drought when structural changes in the photochemical machinery can be observed (Giardi et al. 1996; Ögren and Öquist 1985). Due to the shrinkage in internal CO_2 and the subsequent relative accumulation in O_2, photorespiration tends to increase under drought (Brestic et al. 1995; Noctor et al. 2002). Mitochondrial respiration on the other hand tends to decrease, during day and night (Atkin and Macherel 2009). One of the typical responses to drought is the accumulation of solutes like sucrose, fructose and other sugars and polyols, but also proline and free amino-acids in the plant tissues (Peuke et al. 2002; Rennenberg et al. 2006). This leads to an increase in osmotic pressure and a better water retention.

The occurrence of simultaneous ozone and drought episodes is relatively common considering that they are at least partially caused by the same meteorological phenomena. Periods of long days with strong solar irradiation and little cloud cover are prone to induce the accumulation of ozone and

drought. It was suggested that mild drought could protect plants against ozone-induced damage by causing the closure of stomata and thus preventing the entry of ozone into the leaves. But relatively little is known about the physiological and molecular interaction of the responses to the two constraints. The interaction of ozone and drought is highly dependent on the severity and the length of occurrence of both stressors (Matyssek et al. 2006), but generally the combined stress was shown to be more deleterious than their single components (Inclán et al. 1998; Pääkkönen et al. 1998a). Drought in combination with ozone can indeed significantly reduce stomatal conductance, even in cases where ozone stimulates stomatal conductance (Le Thiec and Manninen 2002; Pearson and Mansfield 1993). On the other hand growth and leaf area can be decreased by a combined treatment, which is not astonishing since it can be a consequence of both ozone and drought alone (Le Thiec and Manninen 2002; Pääkkönen et al. 1998c). Declines in RuBisCO, RuBisCO activase and increases in PEPc activity and protein abundance were reported to be similar in double stressed *Pinus halepensis* and in ozone treated ones (Fontaine et al. 2003; Pelloux et al. 2001), but no data is available for deciduous trees to date.

As illustrated by these results, knowledge about the effect of combined ozone and drought stress is limited. Mild drought can to some extent protect plants against ozone, but to have this effect drought stress should appear before ozone exposure. The present experiment aimed at analyzing the effect of the application of a gradual drought stress on plants during an existing ozone treatment. The basic setup described in Chapter 2, Chapter 3 and Chapter 4 was maintained for this experiment, except that each chamber contained 4 well-watered and 4 drought-treated saplings (Figure 43). Soil water content was adjusted twice a day and kept at approximately 35% for drought stressed plants. Gas exchange parameters were measured three times a week. Stem growth and leaf size were checked at the same dates as leaf samplings at 7, 14, 21 and 28 days. Soluble leaf proteins were extracted and used in a DiGE-based proteomics experiment. This should allow the observation of physiological and molecular responses of plants facing a situation expected to become increasingly recurrent in the prospect of climate change. The proteomic study should allow an unbiased overview of the changes in the leaf soluble proteome and shed new light on the effects of a combined ozone/drought treatment on poplar leaves.

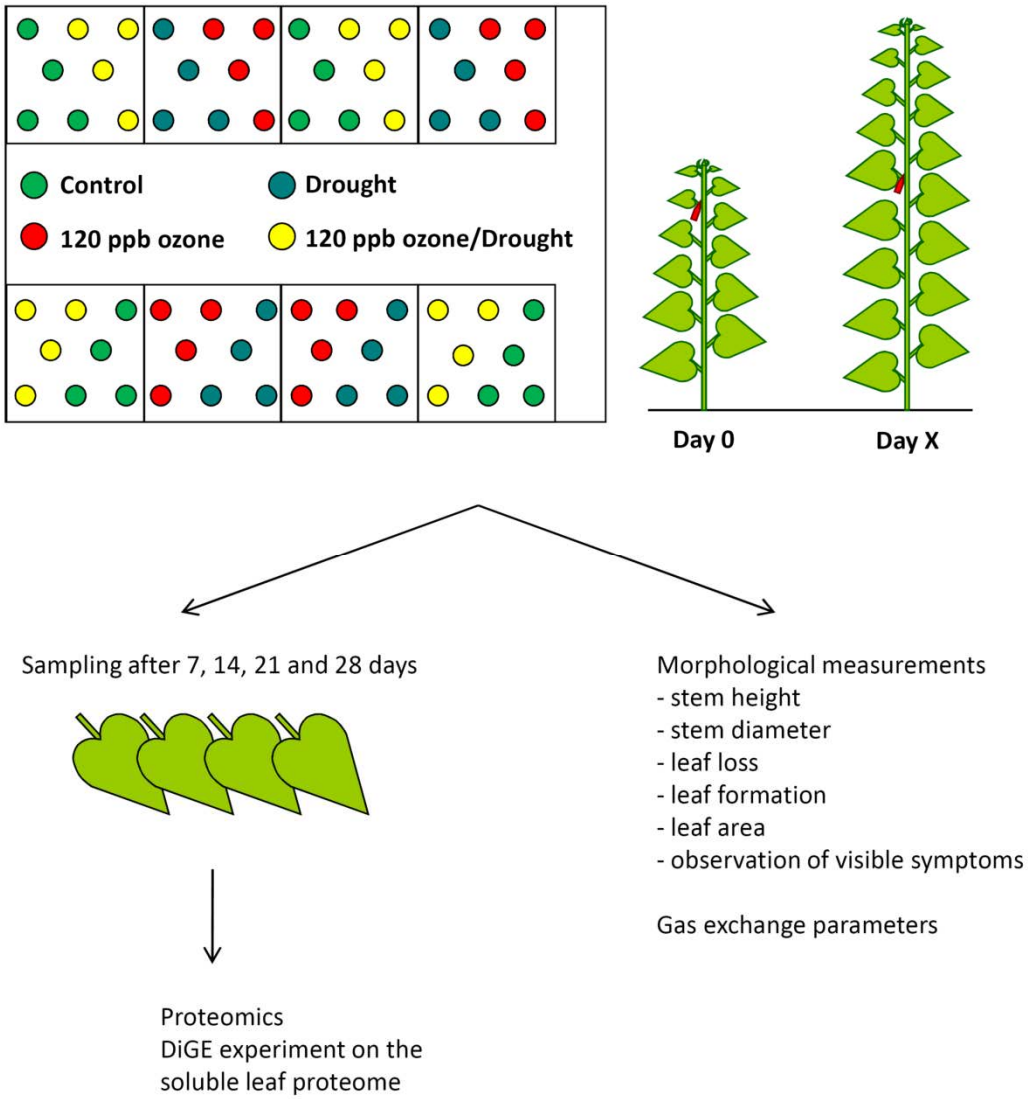

Figure 43: Experimental setup experiment 3

5.2. Material and methods

5.2.1. Plant material and ozone treatment

Poplar clones (*Populus tremula* L. x *P. alba* L. (*Populus* x *canescens* (Aiton) Smith) - clone INRA 717-1-B4) were multiplied *in vitro*, transferred to a mix of peat/perlite (Gramoflor SP1 Universel), transplanted into 5 L pots containing peat/perlite fertilized with 15 g of slow-release nutritive granules (Nutricote T-100, N/P/K/MgO 13/13/13/2, Fertil, Boulogne-Billancourt, France) after 2 weeks and grown at 75%/85% relative humidity (day/night) with a 14 h light period (Sun T Agro, Philips, Eindhoven, The Netherlands; intensity: 250–300 $\mu mol.m^{-2}.s^{-1}$) and 22°C/18°C ± 2°C (day/night) over a period of 5 weeks.

For the ozone treatment, plants were transferred into 8 fumigation chambers with 8 plants per chamber and acclimated for 3 weeks prior to the start of the treatment. Four randomly selected chambers were used for control treatment and the other 4 for ozone treatment. Control plants were grown in charcoal filtered air while treated plants were exposed to charcoal filtered air supplemented with 120 ppb of ozone for 13 h per day during the light period. In each chamber 4 plants were well-watered and 4 plants were submitted to drought. The water stress was created gradually by measuring the soil water content using a WET Sensor moisture meter (Delta-T Devices Ltd, Cambridge, UK) every day and adjusting all the pots to the highest measured value. Once 35% soil water content was reached, it was measured twice a day and continuously adjusted to 35%. Environmental conditions (light, temperature, relative humidity) were as described above. Leaf n° 4 (approximately 8 x 5 cm), counted from the last leaf emerged at the apex, was tagged at the beginning of the treatment on each plant. Those leaves were harvested after 7, 14, 21 and 28 days of exposure. Four biological replicates were made per condition per sampling date, each replicate corresponding to one chamber.

5.2.2. Morphological measurements

Stem growth (height and diameter) as well as the number of newly formed leaves was determined for each plant after 0, 7, 14, 21 and 28 days of exposure. Height measurement was based on the length of the stems from the collar to the apex and the diameter expansion was estimated via measurements of the stem 1.5 cm above the collar with a caliper. The number of abscised leaves and newly formed leaves was also recorded at the sampling days. Concomitantly, visible symptoms of ozone treatment (chlorosis and necrosis) were recorded.

The lobe length (petiole excluded) and width of the leaves of interest were measured on each sampling date between 0 and 21 days of treatment. Leaf area was calculated using a formula developed specifically for this poplar clone (Bagard et al. 2008).

5.2.3. Net CO_2 assimilation and stomatal conductance

Net CO_2 assimilation (A) and stomatal conductance (g) were measured three times a week with a hand-held Licor 6200 (LiCor, Inc. Lincoln, NE, USA). A leaf or part of a leaf was installed in the gas measurement chamber. The air flow was set to 500 µmol.s-^{1}. The measurements were taken over 30 sec kinetics. Atmospheric pressure was corrected for each day with the value given by the meteorological station at INRA Champenoux, France.

5.2.4. Protein extraction and labeling

Proteins were extracted from 1 leaf per chamber per sampling date, i.e. 4 leaves per treatment and per date, amounting to 4 biological replicates. Soluble protein extraction was carried out as described previously (Kieffer et al. 2009), with small modifications. Briefly, 300 mg of fresh leaf material were ground in liquid nitrogen and proteins were suspended in precipitation buffer (20% TCA and 0.1% w/v DTT in ice-cold acetone) and centrifuged. The pellet was washed three times with ice-cold acetone containing 0.1% w/v DTT. Precipitated protein pellets were dried. Dried samples were re-solubilized in labeling buffer (7 M urea, 2 M thiourea, 4% w/v CHAPS, 30 mM Tris) and the pH of the supernatant was adjusted to 8.5. The protein concentration was determined using the 2D Quant Kit (GE Healthcare, Little Chalfont, UK) according to the manufacturer's instructions. After extraction, proteins were used for a multiplexed analysis by fluorescence difference gel electrophoresis (DiGE) (Skynner et al. 2002).

Protein extracts and a pooled internal standard were labeled with CyDyes™ (GE Healthcare) prior to electrophoresis as previously described (Kieffer et al. 2009). Ninety micrograms of proteins (two samples of 30 µg each and 30 µg of internal standard) were loaded on each gel and separated by 2D electrophoresis.

5.2.5. Bidimensional electrophoresis.

The volume of each sample mix consisting of two samples and the internal standard was adjusted to 450 µL with labeling buffer. To this 2.7 µL of Destreak Reagent (GE Healthcare), 9 µL of IPG buffer 3-10 NL (GE Healthcare) and 5 µL of a saturated bromophenol blue solution were added. Sample loading on ReadyStrip IPG strips pH 3-10 NL, 24 cm (Biorad) was done overnight by passive rehydration. Isoelectric focusing (IEF) was carried out using an Ettan IPGphor Manifold (GE Healthcare) in an IPGphor IEF unit (GE Healthcare). The following protocol was used: 150 V for 4 h,

gradient to 500 V for 3 h, 500 V for 3 h, gradient to 1000 V for 3 hs, 1000 V for 3 hs, gradient to 10,000 V for 3 hs, 10,000 for 6 hs until approximately 83,000 Vhrs were reached at 20°C with a maximum current setting of 75 µA per strip. The second dimension was run on precast 12.5% polyacrylamide gels using the Ettan DALT 12 Buffer Kit according to the instructions of the manufacturer (The Gel Company, Tübingen, Germany). An Ettan DALT 12 Electrophoresis system (GE Healthcare) was used for the second dimension run (6 W for 2 h followed by 30 W for 14 h).

5.2.6. Image capture and analysis

The gel images of the different samples were acquired using a Typhoon Variable Mode Imager 9400 (GE Healthcare) at a resolution of 100 µm according to the instructions provided for each dye. Images were analyzed using the Decyder v7 software (GE Healthcare). Selected spots of interest (absolute abundance variation of at least 1.5-fold, ANOVA $p<0.01$) were located and a picking list was generated. Spots of interest were excised and digested as previously described (Bohler et al. 2007). MS and MS/MS spectra were acquired using an Applied Biosystems 4800 Proteomics Analyzer (Applied Biosystems, Sunnyvale, CA, USA), calibrated using the 4700 peptide mass calibration kit (Applied Biosystems). Proteins were identified by searching against the NCBI poplar protein databases (downloaded 2009.06.11; 99,629 sequences) and poplar EST (downloaded 2009.06.11, 419,944 sequences) using MASCOT (Matrix Science, www.matrixscience.com, London, UK). All searches were carried out allowing for a mass window of 150 ppm for the precursor mass and 0.75 Da for fragment ion masses. The search parameters allowed for carboxyamidomethylation of cysteine as fixed modification and oxidation of methionine and of tryptophan (single oxidation, double oxidation and kynurenin formation) and for pyrrolidone carboxylic acid (N-terminal glutamine and glutamic acid) as variable modifications. Homology identification was retained with a probability set at 95%.

5.2.7. Statistics

Statistical analysis of morphological and physiological parameters was done in MINITAB Statistical Software v.15.1.1.0. For stem length and diameter, leaf area, leaf loss and formation, 16 biological replicates were used per treatment and per day; for gas exchange measurements 4 biological measurements. The analysis was done using One-Way ANOVA and Tukey's family error rate for multiple comparisons.

Statistical analysis for proteomics was done with the Extended Data Analysis package of the Decyder software (GE Healthcare). Four biological replicates per sampling date were used, where each replicate represents one fumigation chamber. Normalization and standardization were done by

logarithmic transformation and standardization against the internal standard respectively, as described by the manufacturer. A Two-Way ANOVA was used for the differential protein abundance determination, using the treatment condition as factor 1, and the sampling time as factor 2. A p value<0.01 for condition 1 and an absolute abundance variation of at least 1.5-fold between control and treatment were considered significant. A principal component analysis was also done in EDA.

5.3. Results

5.3.1. Gas exchange

Stomatal conductance increased briefly between days 0 and 1 and then started decreasing for the remaining length of the experiment for all conditions (Figure 44A). Statistically a difference could only be observed at day 20; the combined ozone/drought treatment led to a lower conductance compared to ozone exposure. Although not statistically significant, a general trend is perceivable for the stomatal conductance. It was highest in ozone treated plants while it was lowest in the combined treatment. Control and drought-exposed plants had a very similar conductance situated in between the other two. Net CO_2 exchange (A) also increased during the first day of the experiment and then dropped slowly but irregularly until the end (Figure 44B). There is no statistically significant difference and no apparent trend can be observed.

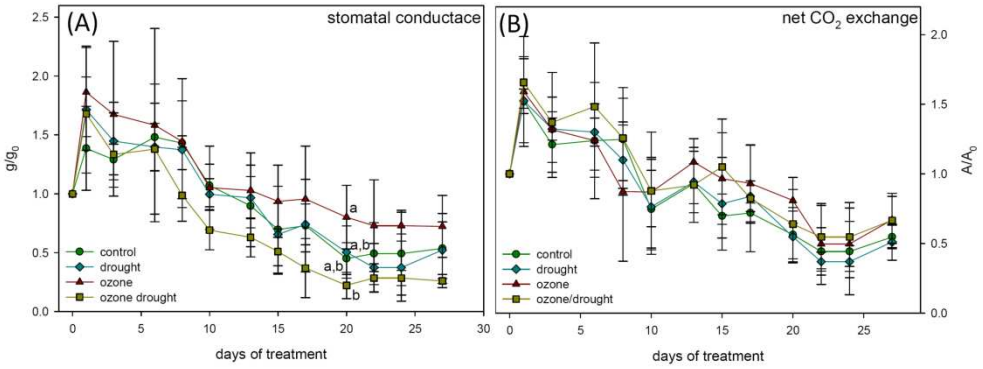

Figure 44: Gas exchange measurements (A) stomatal conductance and (B) net CO_2 exchange. Soil water content is represented as a gray line in the background. Statistical significance is expressed in letters for $p < 0.05$.

5.3.2. Morphological measurements

The general appearance of the plants at the end of the experiment strongly depended on the treatment. Control plants had deep green leaves with a glossy surface and showed little sign of leaf senescence (Figure 45A). Trees submitted to drought also had deep green leaves with a glossy surface, but the lower leaves were clearly senescing and the bottom leaves had been shed (Figure

45B). Ozone exposed trees showed chlorosed light green leaves and had lost the glossiness of the surface. Although the lower leaves were not apparently senescing, some more had been shed than in control plants (Figure 45C). The plants submitted to the combined ozone/drought treatment showed light green, chlorosed leaves similar to the ozone-treated trees, and a high number of leaves had been shed (Figure 45D).

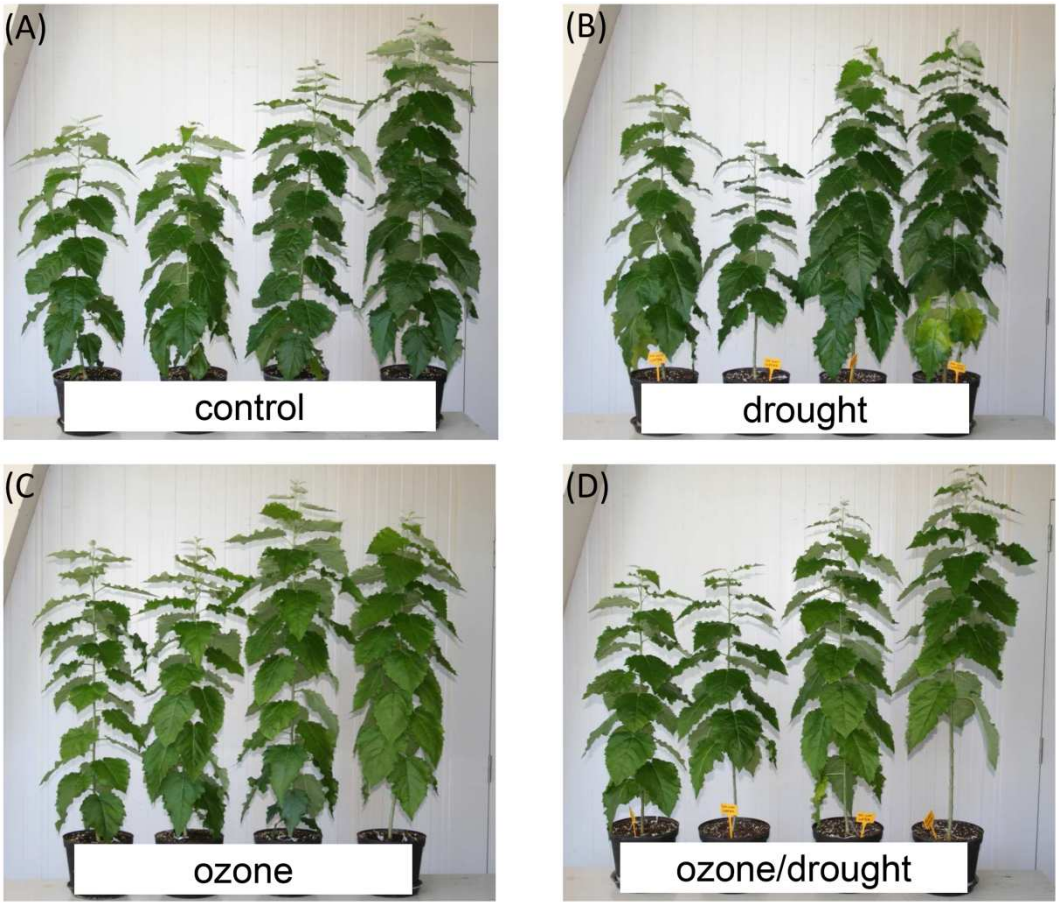

Figure 45: Representative plants at the end (day 28) of the experiment for the four treatment conditions (A) control (B) drought (C) ozone (D) ozone/drought combined.

Leaf area increased between days 0 and 14 for all conditions (Figure 46A). Significant differences between the treatments became apparent only after the leaves were fully grown. Leaves of ozone-treated plants had a significantly lower leaf area than drought treated plants. Control and ozone/drought leaves had an intermediate leaf area, although not significantly different from any of the other conditions. The number of shed leaves depended on the applied treatment (Figure 46B). The highest loss of leaves was observed for the combined ozone/drought treatment, while the control plants had the lowest number of abscised leaves. Single treatment ozone and drought conditions resulted in the shedding of a similar number of leaves, in between control and double

stressed plants. No significant difference between treatments could be observed for new leaf formation (Figure 46C). The general trend suggests that drought and ozone/drought plants produced slightly less new leaves.

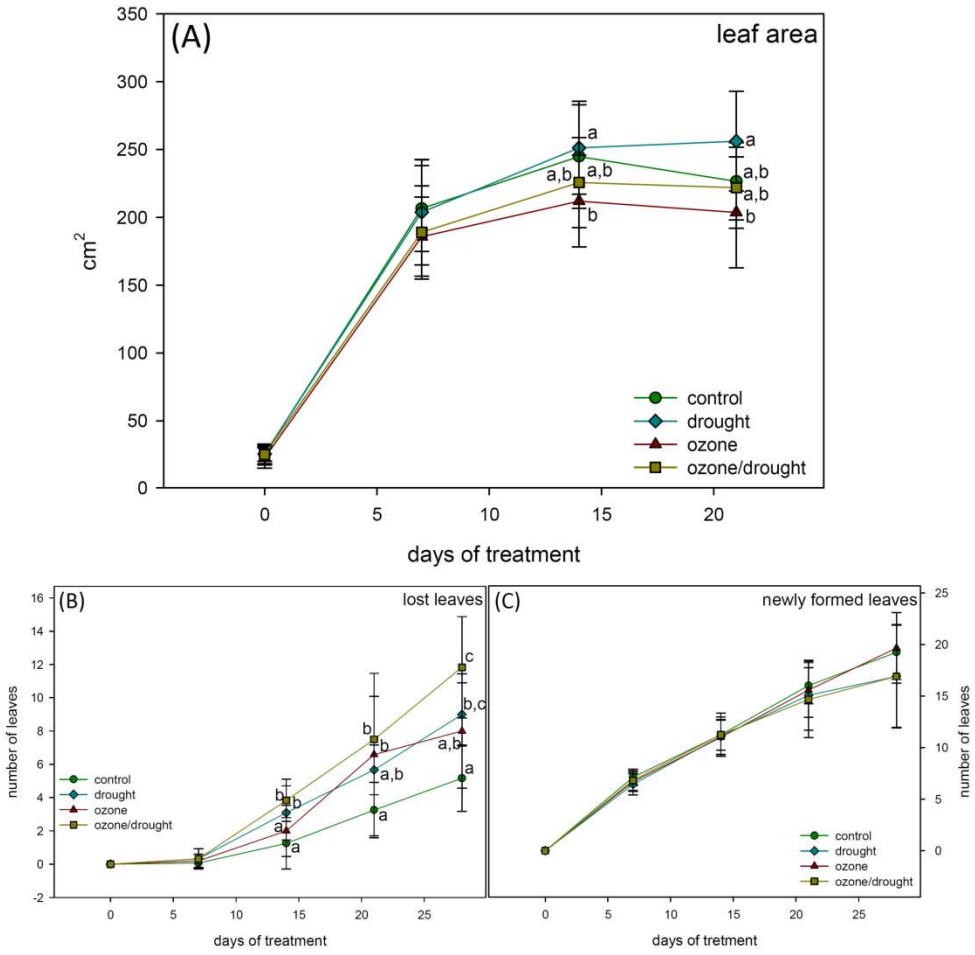

Figure 46: Parameters of leaf development (A) leaf area (B) leaf loss (C) formation of new leaves. Statistical significance is expressed in letters for $p < 0.05$.

No significant differences for height increment could be observed between treatments (Table 8). At the end of the treatment stem diameter increment was significantly lower in ozone, drought, and ozone/drought trees compared to controls (Table 8).

Table 8 : Morphological parameters. Stem height (cm) and diameter (mm) increment since day 0. Values ± standard deviation. Statistical significance is in bold and expressed by letters in brackets for $p < 0.05$.

		7	14	21	28
Height growth since day 0 (cm)	Control	12.78 ± 3.42	24.46 ± 5.22	35.71 ± 6.05	45.38 ± 7.58
	Drought	12.81 ± 3.72	25.04 ± 4.52	34.08 ± 6.89	40.42 ± 10.76
	Ozone	12.99 ± 1.56	24.49 ± 3.87	35.63 ± 6.61	44.31 ± 11.12
	Ozone/Drought	11.72 ± 1.96	24.54 ± 5.10	33.88 ± 8.81	39.63 ± 12.59
Diameter growth since day 0 (mm)	Control	1.66 ± 0.55	3.08 ± 0.66	3.65 ± 0.74	**5.08 ± 0.56 (a)**
	Drought	1.44 ± 0.65	2.79 ± 0.78	3.22 ± 0.73	**4.31 ± 0.94 (b)**
	Ozone	1.31 ± 0.53	2.43 ± 0.74	3.24 ± 0.53	**4.18 ± 0.64 (b)**
	Ozone/Drought	1.30 ± 0.44	2.51 ± 0.07	3.13 ± 0.06	**3.79 ± 0.59 (b)**

5.4. Proteomics

A final number of 237 proteins were differentially abundant in this experiment. Although the detailed analysis of these proteins is ongoing, descriptive statistics reveal first patterns in the effect of the different stress treatment on protein abundance. A PCA analysis (Figure 47A) and cluster analysis calculated in the EDA (Figure 47B) module in Decyder reveal a characteristic grouping of the experimental groups. Day 7 experimental groups cluster together regardless of the treatment conditions. Two other more heterogenic groups stand out from the analysis, one containing ozone 14, 21 and 28 and ozone/drought 28 form the third group, and the second one containing the remaining experimental groups.

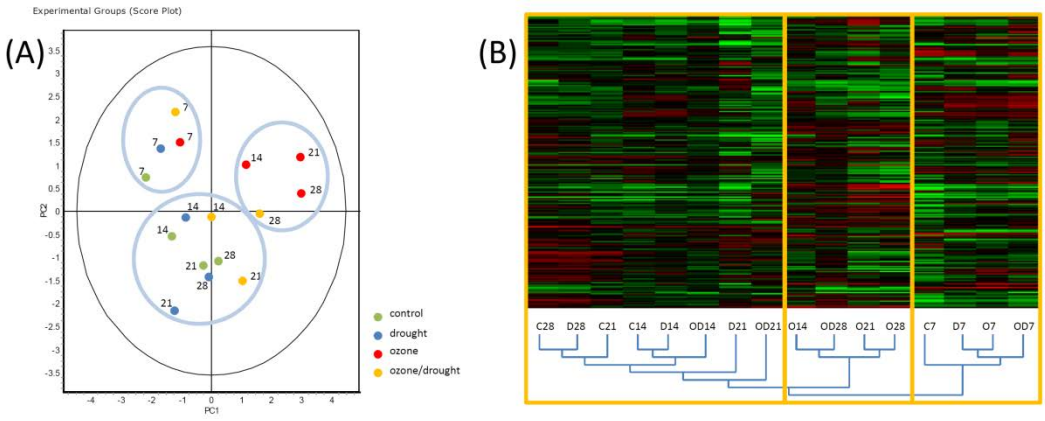

Figure 47: Descriptive statistics of the differentially abundant proteins. (A) PCA and (B) cluster analysis, both showing the distribution of the experimental groups towards each other. C, control; D, drought; O, ozone; CD, ozone/drought; 7, 14, 21, 28, days 7 to 28.

5.5. Discussion

From the data presented here it is clear that for the setup used in this study, drought does not have a significant protective effect against ozone-induced damage. Symptoms are clearly the strongest on plants submitted to the combined ozone/drought treatment, and for some parameters are even the sum of the symptoms observed on the plants exposed to single constraints (Figure 45). Although stomatal conductance is the highest in single ozone exposure and the lowest in the ozone/drought treatment, this stomatal closure is clearly insufficient to protect the plants against the applied ozone treatments. The steady level of 35% - 30% soil water content was reached around day 12 of the experiment, when the plants had already been exposed to 12 days of ozone (Figure 48). From Figure 44A it can be concluded that the decrease in stomatal conductance differentiates the combined treatment from the other conditions at day 8. Even though there is no statistical significance, the trend is clearly visible. At that time the soil water content decreased significantly and was between 45% and 35% for one week. It is clear that this marks the beginning of the response to the combined stress. Single ozone exposure shows first effects on stomatal conductance at day 15, when it starts to differ from the other treatments, showing that this single stress leads to a response later than the combined treatment, but in an opposite direction since it increases. Only for the single drought treatment no effect on stomatal conductance was recorded, probably relating to the fact that the specific clone used in this study is relatively drought sensitive. Although stomatal conductance varies slightly, no effect for net CO_2 exchange is observed for any treatment. A change in this factor could have been expected, especially since ozone exposure generally leads to a drop in CO_2 fixation but an increase in respiration and photorespiration. Leaf loss is an equally good indicator for the severity of the stress faced by the plants during the different treatments. Most leaves are lost by the combined treatment while the single stress treatments show a fairly similar rate of shedding. Growth in diameter during the experiment is reduced in all three stress treatments. Similar but attenuated trends can be observed as for the factors described above. The decrease is strongest for the combined stress and intermediate for the single treatments. It is clear that the three stress treatment conditions that were used afflict the observed factors in different ways. According to the parameters taken into consideration, it is clear that the combined stress is the most severe for the plants, showing that there is a synergetic effect of ozone and drought, while the single treatments are conceived as less stressful.

The descriptive statistics of the proteomic results (Figure 47) show that there is no effect yet by any treatment since the day 7 experimental groups cluster together. The grouping of day 14 to 28 ozone and day 20 ozone/drought show that after 28 days, the effects of ozone overpower the effects of

drought and that at least at that time point, there is no protective effect of drought. The third group contains control, drought and ozone/drought conditions. This shown that drought alone is relatively close to controls and does not have huge effects on the proteomic level. That fact that this group also contains the middle time points of the ozone/drought treatment shows that there could be a protective effect of drought on the proteomic level up to certain time.

Although growth parameters indicate that the combined ozone/drought treatment has the strongest effect on the plants, the preliminary proteomic results indicate that there could be a protective effect of drought in ozone treated leaves at the proteomic level up to 21 days of treatment. After 28 day this is not true anymore. The identification of the differentially abundant proteins could give an explanation for this behavior. Nevertheless, these results already show that there will be a considerable impact on plant production if episodes of high ozone concentrations and drought keep increasing in frequency and in duration and keep overlapping.

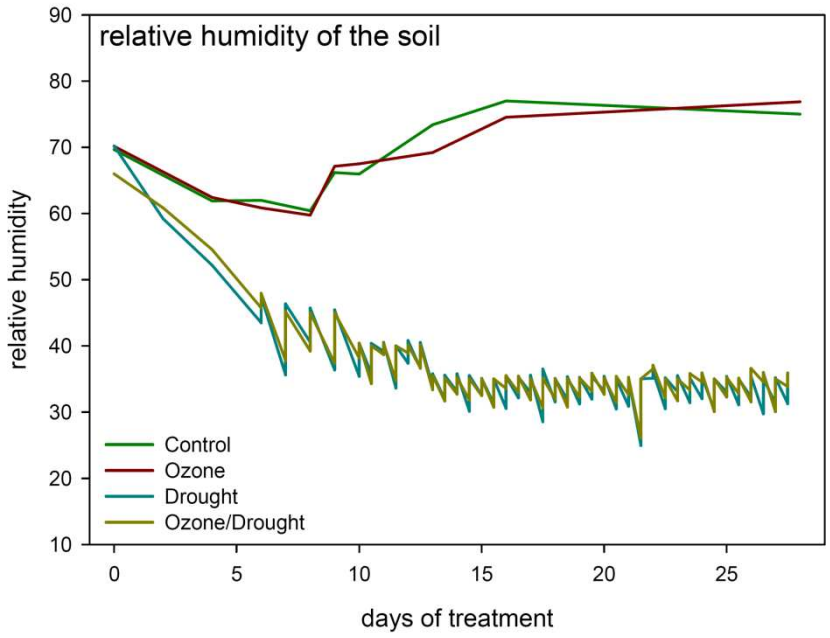

Figure 48: Progression of soil water content during the experiment.

Chapter 6

General Discussion

6.1. A tale of three experiments. Relation between the ozone dose and the impact on plants

The three experiments presented in Chapter 2 to Chapter 5 show similarities and differences. The differences in setup were detailed in the different chapters, but the similarities were only briefly mentioned. All three experiments used 120 ppb of ozone during 13 hours a day during the light period. If the cumulative exposure over a threshold of 40 ppb (AOT40) is used, this adds up to 80 ppb/h and a cumulative AOT40 of 1040 ppb per day. The AOT40 was developed as a tool for estimating potential damage to forest trees during ozone episodes (Fuhrer et al. 1997). The critical cumulated AOT40 level for forest trees was set to 10 ppm/h. AOT40 has largely been replaced by the effective ozone dose, taking into consideration stomatal parameters and detoxification capacity (see Chapter 1) (Dizengremel et al. 2009; Karlsson et al. 2004; Matyssek et al. 2004). Nevertheless, AOT40 remains a good tool to express ozone exposure levels after natural episodes or artificial enrichment treatments, when data of stomatal conductance and detoxification potential is not available.

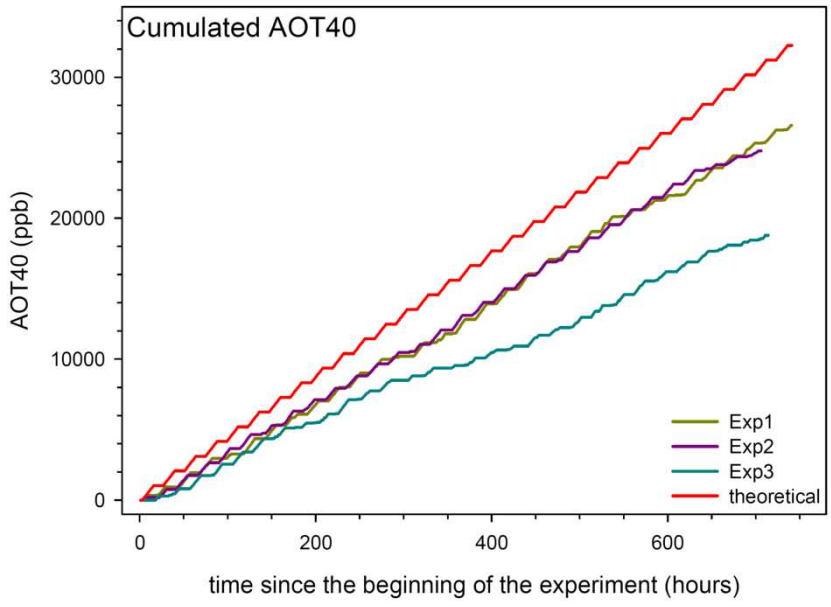

Figure 49: Cumulative AOT40 over the time course of the three experiments (Exp1, Chapter 2; Exp2, Chapter 3 and Chapter 4; Exp3, Chapter 5).

In Figure 49 the cumulative AOT40 over the time course of the three experiments are presented. The top line represents the theoretical AOT40, the two middle lines the measured AOT40 of experiment 1 (Chapter II) and experiment 2 (Chapter III and IV) and finally the lower line represents the AOT40 of experiment 3 (Chapter V). Although the theoretical AOT40 was never reached, the level of exposure was substantial in all three experiments since the critical level of 10 ppm was reached

approximately in the middle of the experiment for each experiment. Divergences mostly come from the mandatory stop in fumigation and ventilation during measurements and samplings. It was also taken care not to exceed 120 ppb, so that the actual ozone concentrations in the chambers were mostly between 110 and 120 ppb. Experiments 1 and 2 are highly similar, but experiment 3 is lower in AOT40, due to the soil water content measurements that had to be made twice a day, which increased the periods of non-fumigation. Indeed fumigation and ventilation had to be turned off in the chambers when measurements were taken due to technical and health reasons.

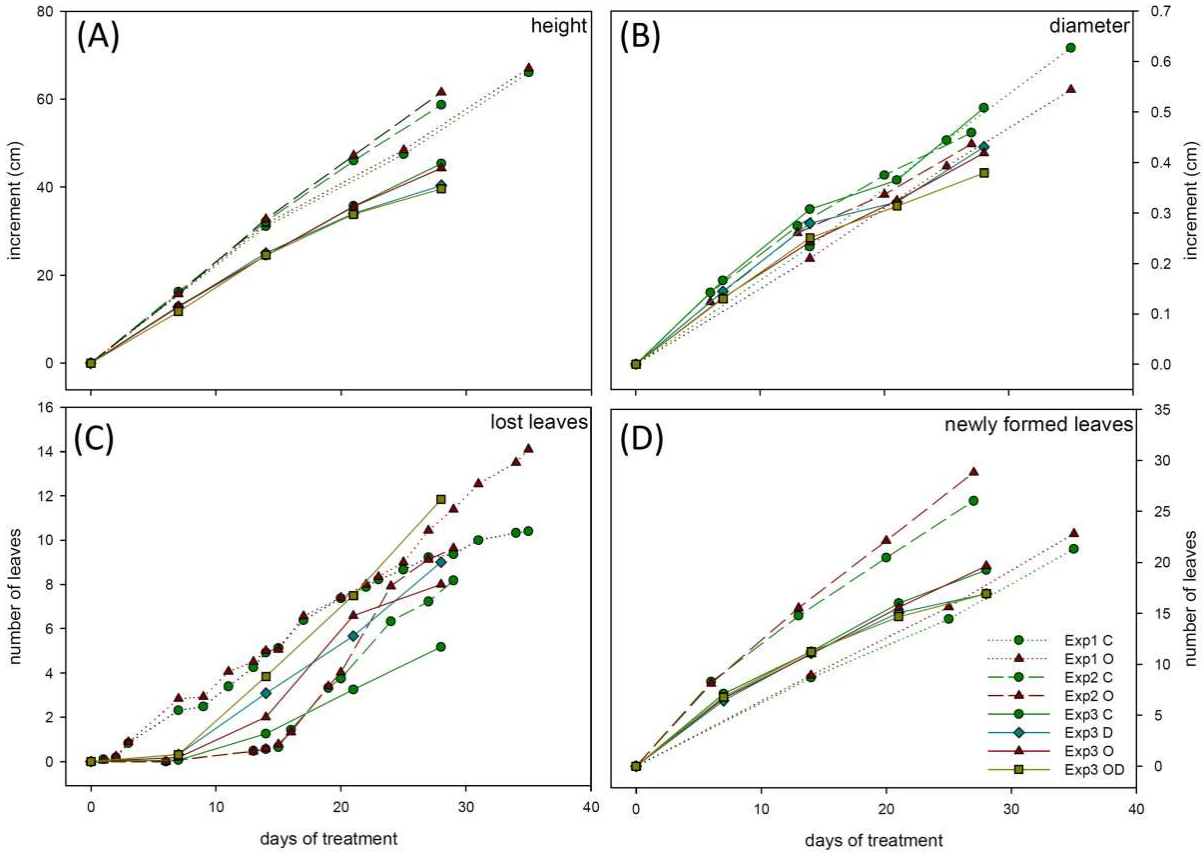

Figure 50: Growth parameters from the three experiments (Exp1, Chapter 2; Exp2, Chapter 3 and Chapter 4; Exp3, Chapter 5; C, control; O, ozone; D, drought; OD, ozone/drought, ,). (A) height increment since day 0; (B) diameter increment since day 0; (C) leaves lost since day 0; (D) newly formed leaves since day 0.

To estimate the similarity of plant response, the growth parameters of the three experiments were plotted side by side in Figure 50. It is clear that differences between the experiments are only minor. The similarities are most striking for diameter growth and height growth. Leaf loss and new leaf formation are slightly different from experiment to experiment, especially in the early parts of the

experiments for leaf loss. This is most probably due to slight differences in plant size at the beginning of the experiments.

According to these factors, the three experiments presented during this work are relatively similar to each other. A little caution should be taken in comparing the first two experiments with the third one, since the cumulated ozone exposure is a little lower, which means that the observed effects are probably lower than it was to be expected. However the three experiments still remain largely comparable among each other.

6.2. What came first, the chicken or the egg? The biochemical and photochemical parts of photosynthesis under ozone stress.

An interesting and recurring question in ozone research is whether the photochemical or the biochemical part of photosynthesis is impaired first during exposure. Most early studies discussing this specific point rely on measurements of RuBisCO activity and abundance and on chlorophyll fluorescence or leaf gas exchange data, and the existing hypothesis is that the biochemical part is affected first by the impairment of RuBisCO (Dizengremel 2001; Landry and Pell 1993; Pell et al. 1992). The problem with these studies is that they compare measurements at different levels (i.e. physiological and biochemical level) that can respond in different ways and rhythms. Independently of the studies constraint, gas exchange parameters can change very quickly in a stress situation, possibly before the underlying molecular processes are affected. They are highly plastic parameters that can change from plant to plant and even from leaf to leaf. Measurements of protein activity or quantity are relatively robust, but may not always reflect the physiological state of the plant, since the extraction of the protein can change its *in vitro* activity. Although these techniques are good estimates for the effects of ozone, it is not certain whether they can be compared directly.

The advantage of the work described in this manuscript is that it was possible to measure the abundance of proteins of the photochemical and biochemical part of photosynthesis in one single analysis that was repeated in the different setups. Although the protein abundance may not necessarily reflect the enzyme activity, the comparison is applied on the same level of measurement. Therefore the link between the two processes can be established directly. In experiment 1 (Chapter 2, soluble leaf proteome), the time points 3 and 21 days of treatment were of particular interest. After 3 days, several protein spots were significantly different in abundance, all containing RuBisCO activase, responsible for the activation of RuBisCO and previously shown to be influenced by ozone (Pelloux et al. 2001). At day 21, multiple proteins of both the biochemical and photochemical part of photosynthesis were observed to vary in abundance. Since RuBisCO activase is directly linked to

RuBisCO activity, its decrease in abundance can be considered a first step in the impairment of the Calvin cycle. The large gap between days 3 and 21 did not allow for a better resolution and it was impossible to determine what happens in-between in this experiment. For that reason, in experiment 2, the setup was changed to 7, 14, 21 and 28 days of treatment, increasing the resolution between 7 and 28 days. In the first part of that experiment (Chapter 4, soluble leaf proteome) one protein in one single copy significantly increased in abundance after 7 days of exposure (chloroplastic fructose bisphosphate aldolase) indicating insignificant changes in protein abundance after 7 days. At day 14, most of the Calvin cycle proteins varying during this experiment had already significantly decreased in abundance. Most electron transport chain proteins on the other hand became significantly different in abundance only at day 21 or even at day 28. The measurements of chlorophyll fluorescence and pigment contents, indicators of the condition of the chloroplast electron transport chain, showed significant variation starting at day 14, and increasing up to day 28. This is approximately the same pattern as the variation in protein abundance. It shows that a comparison of those factors, in the case of the setup presented here, is possible. However, it is difficult to compare the severity of the variation observed for different parameters, and it is impossible to say if for one of them the difference between ozone and control could already be stronger at a given point. Nevertheless, these results show that the biochemical part of photosynthesis is affected before the photochemical part.

The second part of experiment 2 (Chapter 3, chloroplast membrane proteome) shows a different picture. Significant variations in the abundance of electron transport chain protein were already observed after 7 days of treatment, and the abundance of most proteins was significantly different after 14 days, one sampling point earlier than before. The analyzed samples are identical between the two tests; however, in the second part only a sub-fraction was analyzed. The fractionation of a matrix (leaves) to a less complex one (chloroplast membranes) increases the sensitivity of the used technique. The fact that fewer proteins are present in the studied sample also means that they are present in a larger quantity, which makes the detection of differences between two conditions more sensitive and more reliable. It is therefore probable that a fractionation of chloroplast soluble proteins would also show an earlier variation.

Although the observations are different, the second part of experiment 2 in no way contradicts the results obtained for the soluble leaf proteome. There are strong indications that the biochemical part of photosynthesis is affected by ozone before the photochemical part, as already suggested in literature by the comparison of different techniques. Therefore a possibility exists that the perturbations of the photochemistry are a consequence of the changes in biochemistry.

6.3. The life and death of a poplar leaf.

In Chapter 4, leaf development was introduced as being studied in depth at its beginning and at its end, but poorly in between, although that is the period during which a leaf has the most importance for the plant. The fully expanded, non-senescent leaf has the highest photosynthetic activity and is the carbohydrate factory of the plant. In Chapter 4 it was confirmed that the proteins involved in carbon metabolism mostly remained stable in abundance and that proteins of the photosynthetic machinery even accumulated. The most interesting result of that part of the study may in fact be that not many changes in protein abundance occur during the adult life of a leaf. The metabolism is kept stable (as observed for protein abundance of several Calvin cycle proteins and Fv/Fm, 4.2. Bohler et al. Tree Physiology in press) in a highly efficient way by adapting to new situations like for example shading, but a perturbation can arise if too strong a constraint occurs, such as for instance a prolonged exposure to ozone. However even in that situation leaf processes remain relatively stable. The pattern of variation of proteins involved in photosynthesis and carbon metabolism during ozone exposure is astonishingly similar to the pattern in control leaves. Indeed the abundance of for instance electron transport proteins increases over time, even if it remains lower relative to controls. Some carbon metabolism enzymes are indeed lower in abundance in treated leaves, but there is no sudden drop; instead the decrease is gradual over time. On the contrary, some proteins not belonging to the primary metabolism do not follow the same pattern in control and treatment conditions, like proteins needed for protein folding or detoxification, proteins that are responsible for the protection of the primary leaf processes. This illustrates the flexibility, robustness and ability of a plant leaf to adapt. Weak constraints (e.g. shading) can be compensated so that the leaf processes can run efficiently, and strong constraints (e.g. chronic ozone exposure) are countered in the best possible way to uphold the functioning leaf for as long as possible.

In literature it is was very often discussed that ozone leads to an early onset of senescence because of the higher rate of leaf loss, but the molecular mechanisms behind this phenomenon remain unclear. As discussed in Chapter 4, senescence is a highly controlled and relatively slow process that starts long before the appearance of visible signs. Two observations of the ozone response in plants are similar to processes observed during senescence: the decrease in photosynthesis and associated reduction in chlorophyll content and a highly active catabolism. The signaling pathways induced by ozone (ethylene, salicylic acid, jasmonic acid) are also involved in the regulation of senescence. Our results described in Chapter 4, indicate that there was not yet a sign of senescence in the leaves after 28 days of growth in control conditions. Photosynthesis parameters and chlorophyll content were relatively stable and the abundance of photosynthetic enzymes was stable or increasing.

Similarly, there was no sign of an increase in catabolism. From the Supplemental Figures 1 and Supplemental Figures 2 it is obvious that even in ozone-treated leaves there is no sign of senescence after 28 days. There is a decrease in the abundance of photosystem proteins, but it is only a relative decrease compared to controls; the actual abundance of the proteins is still increasing even in treated leaves. Similarly, the chlorophyll content in treated leaves is lower compared to controls, but stable and not decreasing in time. In conclusion, there is clearly a response to ozone after 28 days of treatment, howerver there is no sign of senescence in the studied leaves. This indicates that the early response to ozone does not induce an accelerated senescence. It is therefore possible that the accelerated senescence observed during ozone treatment is due to the exhaustion of the leaves caused by a prolonged stress situation as it was previously described by Lichtenthaler (1996).

6.4. Remote control. Photosynthesis regulation and the effects of ozone

As previously described, photosynthesis is divided into two parts, the photochemical and the biochemical reactions, also called 'light reaction' and, erroneously, 'dark reaction'. The biochemical part of photosynthesis was called the 'dark reactions' because it does not need light to function *per se*, but it is still tightly regulated by light and does not function for a long time in the dark (Heldt and Heldt 2005). The regulation of the Calvin cycle is controlled by multiple factors and on the level of several enzymes. The key regulated enzymes in the Calvin cycle are the ones that catalyze irreversible reactions; these are RuBisCO, fructose-1,6-bisphosphatase, sedoheptulose-1,7-bisphosphatase and ribulose-5-phosphate kinase (Geiger and Servaites 1994; Harrison et al. 1997; Heldt and Heldt 2005; Quick and Neuhaus 1997; Stitt et al. 2010). Sedoheptulose-1,7-bisphosphatase is exclusive in the Calvin cycle and is, with RuBisCO, one of the rate limiting enzymes in the pathway and controls the flux of metabolites through the pathway (Quick and Neuhaus 1997).

RuBisCO itself is activated/inactivated by pH and Mg^{2+} concentration. In the dark, the pH of the chloroplast stoma is around 7, in the light it increases to 8, the ideal pH for the functioning of RuBisCO (Heldt and Heldt 2005; Quick and Neuhaus 1997). The enzyme also has to bind a molecule of CO_2 in a carbamylation reaction to be functional (this CO_2 molecule is not going to be used in the carboxylation reaction). Several carbohydrates, including ribulose bisphosphate can bind to the active site of RuBisCO thereby preventing the carbamylation of the enzyme and inactivating it. A very strong inhibitor is 2-carboxyarabinitol-1-phosphate (CA1P), which accumulates during the night and binds to the active site of RuBisCO. RuBisCO activase releases the bound carbohydrates upon consumption of ATP and frees the active site which allows for the carbamylation to take place (Heldt and Heldt 2005; Portis et al. 2008; Quick and Neuhaus 1997).

RuBisCO activase, fructose-1,6-bisphosphatase, sedoheptulose-1,7-bisphosphatase and ribulose-5-phosphate kinase are furthermore activated by reduction by thioredoxins, and are therefore tightly linked to the electron transport chain (Dunford et al. 1998; Heldt and Heldt 2005; Quick and Neuhaus 1997) (Figure 51). Thioredoxins are reduced by the use of ferredoxin which is itself reduced by PSI. Thioredoxins can activate the target Calvin cycle proteins only during the day, when the electron transport chain is active, which is the key to the diurnal regulation. Consequently RuBisCO can only be activated by carbamylation during the day, when RuBisCO activase can free the active site from bound carbohydrates.

A closer look at the proteins identified to be differentially abundant during ozone exposure shows that three of the four redox-regulated proteins were observed: RuBisCO, sedoheptulose-1,7-bisphosphatase and ribulose-5-phosphate kinase. Only plastid fructose-1,6-bisphosphatase was not observed, although the cytosolic isoform, the activation of which does not depend on redox regulation, was detected. Plastid fluctose-1,6-bisphosphate aldolase is redox-regulated but its inactivation does not limit the Calvin cycle until at least 40% of inactivation (for example by inserting an antisense cDNA construct) (Koßmann et al. 1994), contrary to for instance sedoheptulose-1,7-bisphosphatase for which a 40% reduction leads to considerable reductions in growth, and that allows for a very fine control (Harrison et al. 1997). It has been shown that ozone disturbs the redox state of the chloroplast and leads to the formation of ROS in the stroma (Pellinen et al. 1999; Schraudner et al. 1997). This increase in oxidation potential could affect the redox control of the enzymes and deactivate them (Figure 52 and Figure 53). In Chapter 2 and in Chapter 4 a reduced abundance in RuBisCO activase, which can be deactivated by oxidation, was observed; this can have a direct influence on the activation of RuBisCO. If RuBisCO activase is not present anymore to release the carbohydrates, RuBisCO remains inactive and its destruction, as it has been observed during ozone exposure, could follow (Dizengremel 2001; Eckardt and Pell 1994; Junqua et al. 2000). Ferredoxin-$NADP^+$-oxidoreductase (FNR) increasing in abundance in Chapter 2 and Chapter 3 could be a protective measure to keep the redox state of the chloroplast stable at the beginning of the treatment (Figure 52). After prolonged ozone exposure, it was observed that FNR and many electron transport chain proteins also decrease in abundance, which could be a consequence of ozone induced oxidative stress, but also of the accumulation of NADPH and ATP not used by the Calvin cycle (Figure 53).

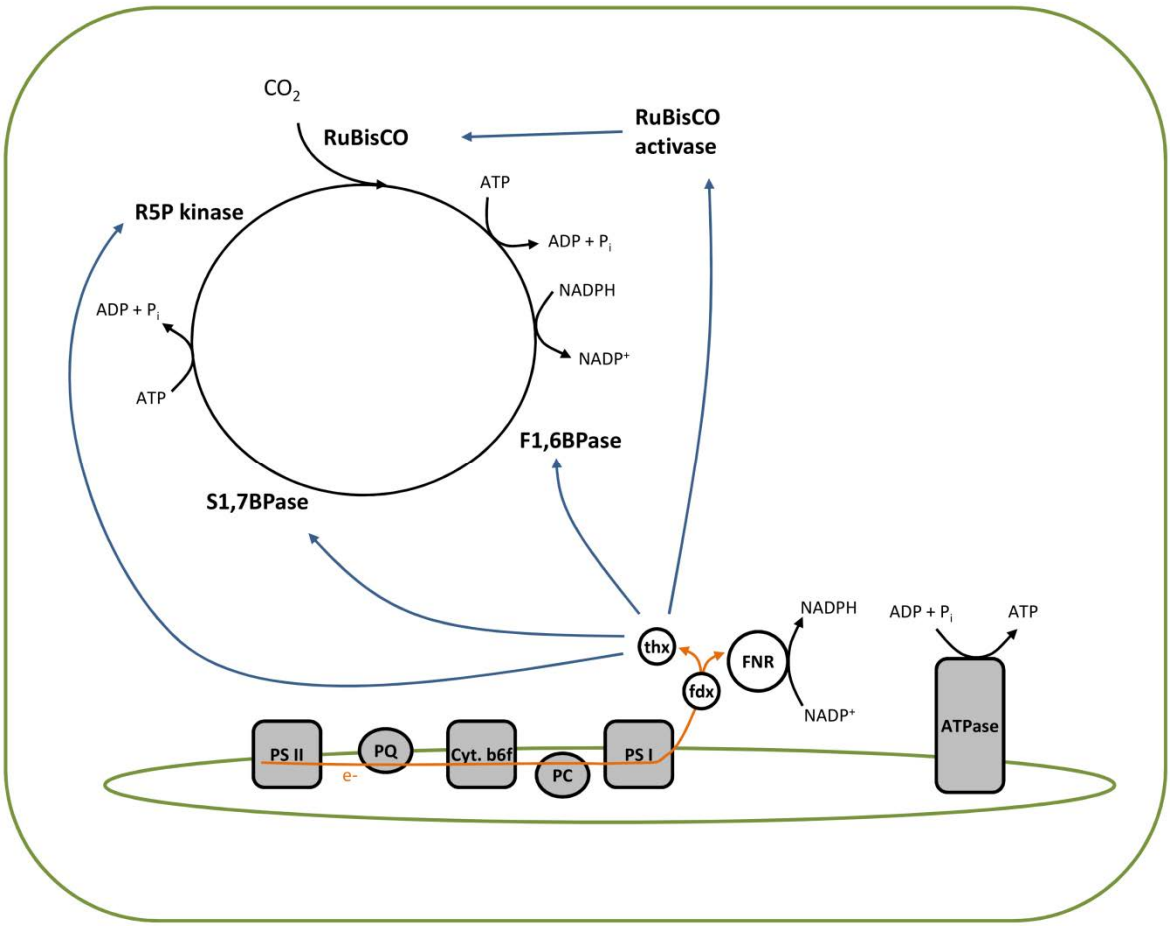

Figure 51: Regulation of the key Calvin cycle enzymes by reduction by thioredoxin in normal conditions. F1,6BPase, fructose-1,6-bisphosphatase; S1,7BPase, sedoheptulose-1,7-bisphosphatase; R5P kinase, ribulose-5-phosphate kinase; thx, thioredoxin; fdx, ferredoxin; FNR, ferredoxin-$NADP^+$-oxidoreductase; PC, plastocyanin; PQ, plastoquinone.

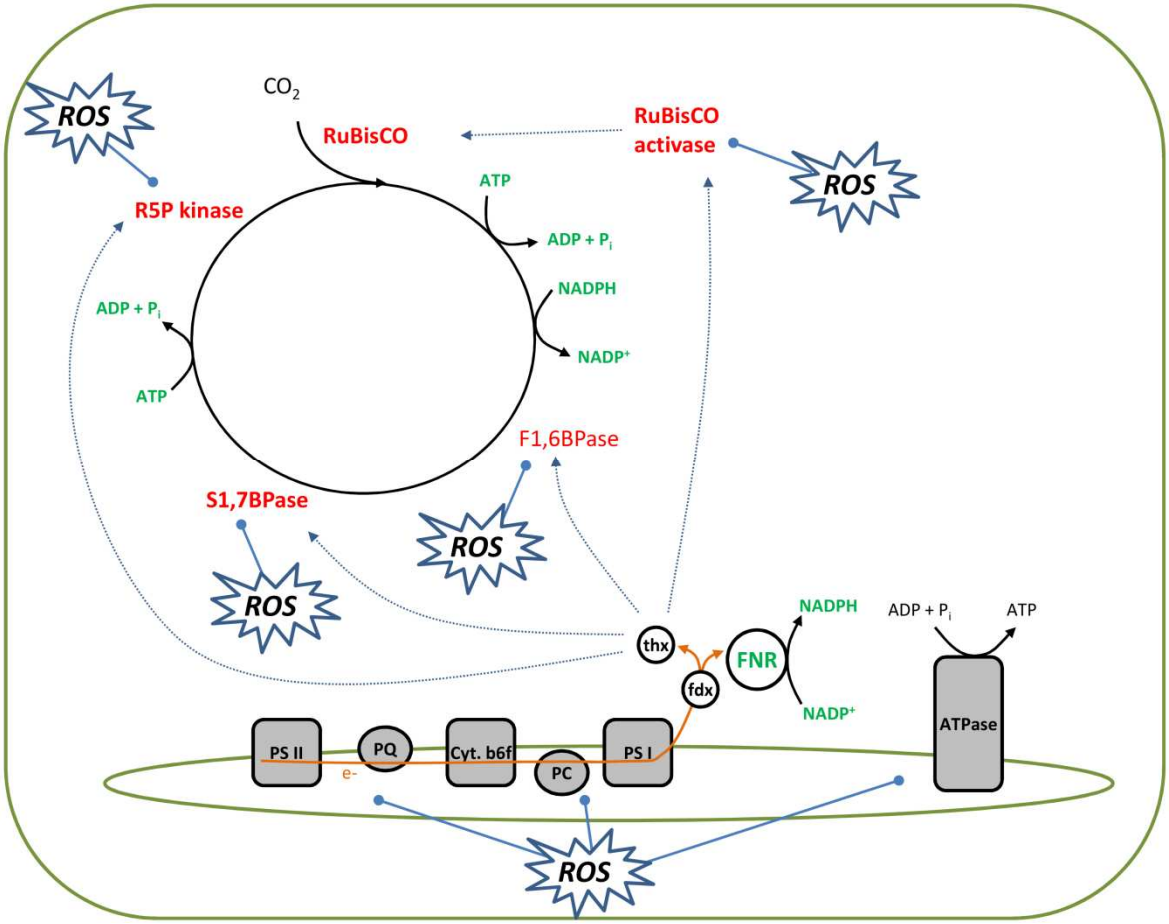

Figure 52: Regulation of the key Calvin cycle enzymes during early ozone treatment. ROS can disturb the regulation by thioredoxin and decrease the activity of key enzymes. ATP and NADPH can accumulate by the decrease in Calvin cycle activity but also by the observed increase in FNR abundance.

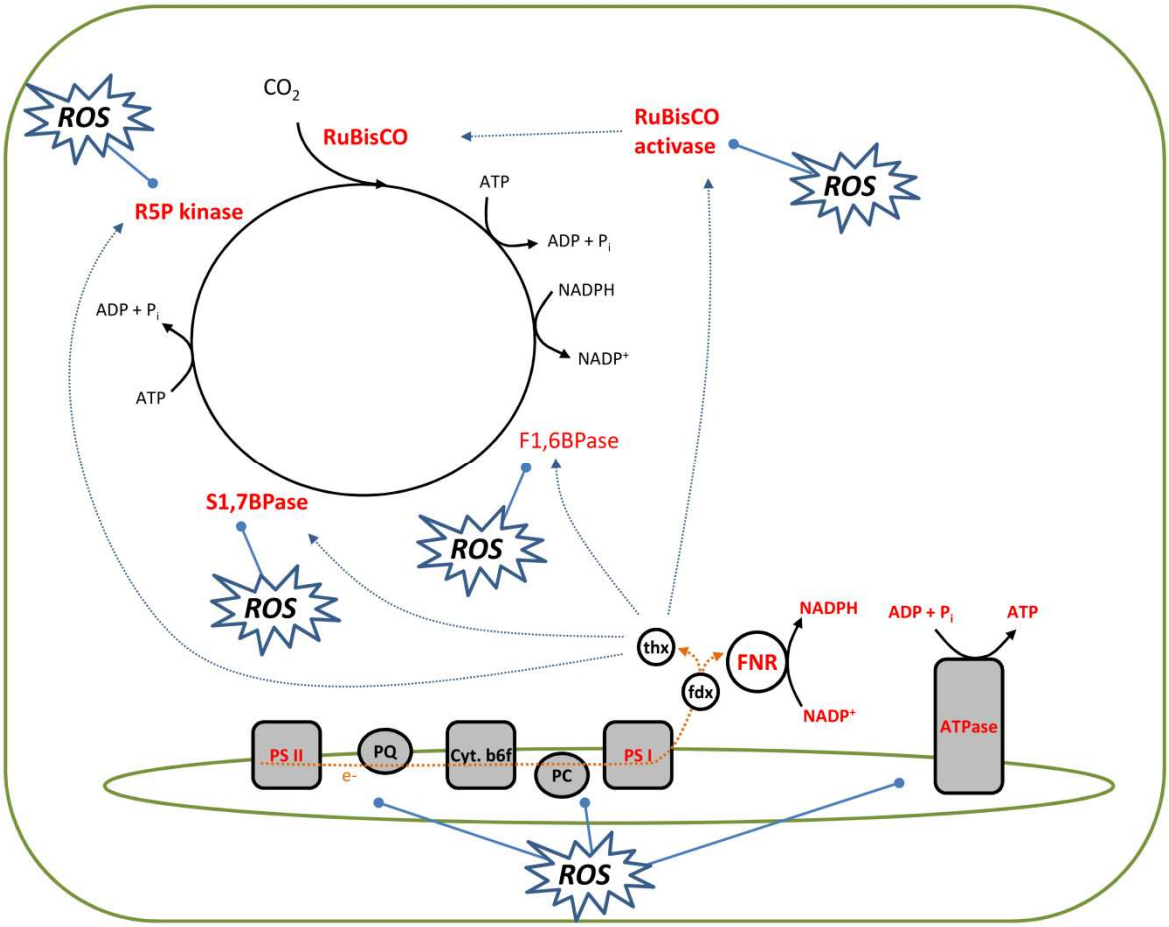

Figure 53: Regulation of the key Calvin enzymes during prolonged ozone treatment. Calvin cycle remains down-regulated and feedback between Calvin cycle and electron transport chain may lead to a general decrease in the photochemical part of photosynthesis.

6.5. In the eye of the observer: conclusion and perspectives

In the course of this work it was attempted to confirm results and established hypotheses by a global proteomic approach but also to find new clues about the effects of ozone on poplar and the response of the plant to the stress. It was shown that an important number of Calvin cycle enzymes decrease in abundance, amongst which three of the redox-regulated enzymes and RuBisCO activase. It is therefore hypothesized that the accumulation of ROS in the chloroplast and the loss of redox homeostasis interfere with the regulation of those enzymes and lead to their down-regulation and subsequent decrease in abundance. It was also shown that proteins of the electron transport chain decrease in abundance, but mostly at a later time than Calvin cycle proteins, confirming the hypothesis that the biochemical part of photosynthesis is affected by ozone before the photochemical part. Furthermore, there are some indications that there is an increase in carbon catabolism under ozone exposure, and that less triose phosphate is used to produce sucrose. It was also confirmed that ozone does induce a stress response, with the increased abundance of protective proteins such as HSPs or disulfide isomerase, but also of detoxification proteins like peroxidase.

As described earlier, plants have not co-evolved with dangerous concentrations of ozone. Therefore, the response to ozone is not a fully programmed response including receptors and specific response cascades, but rather a response to a series of signals that are mainly activated due to the consequences ozone-exposure has on the plant cell homeostasis, i.e. the accumulation of ROS leading to an oxidative stress. This non-recognition of the constraint *per se* that leads to a generalized response also leads to a cascade of effects that follow each other, such as the Calvin cycle responding to redox signaling, the electron transport chain responding to changes in the Calvin cycle and so forth.

It is discussed that the early response to ozone does not include the induction of an accelerated senescence, but that it is more probable that the accelerated senescence observed during the treatment is brought upon by the exhaustion of the leaves caused by a prolonged stress situation.

But not only data about ozone treated leaves was collected, also control plants were subjected to scrutiny. It was confirmed that young leaves construct the metabolic machinery during their growth, and that it is kept successfully stable in the mature leaf by adapting to new conditions if they are not too severe.

A detailed study of purified soluble chloroplast proteins could provide evidence for the hypothesis formulated here and is a logical follow-up of this work. Complemented by activity measurements

and Western blot analysis, this could confirm the hypothesis of the regulatory enzymes and confirm that they are the first impacted by ozone and lead to a down-regulation of the complete cycle.

Since this study focused entirely on leaves that were young at the beginning of the treatment and grew to mature leaves during the exposure, it could also be interesting to do a global study on leaves that were already mature at the beginning of the treatment and on leaves that were not yet initiated when the exposure was started. This could lead to new information about the differential impact of ozone on leaves of different ages. Similarly, the length of the studies could be prolonged until leaves are visibly senescent, to confirm that the accelerated senescence is in fact due to exhaustion.

On the level of leaf development in normal conditions and ozone treatment, it could be interesting to increase the resolution of the time line and make several samplings between days 0 and 14, when the leaf is in its growth phase, to even further observe the metabolic changes that take place during leaf development.

The work presented in this document allowed shedding a better light on many ongoing questions in ozone research on trees, and opened many paths for future studies that could confirm the answers proposed here.

Reference list

Agrawal, G.K., R. Rakwal, M. Yonekura, A. Kubo and H. Saji. 2002. Proteome analysis of differentially displayed proteins as a tool for investigating ozone stress in rice (*Oryza sativa* L.) seedlings. Proteomics. 2:947-959.

Akimoto, H. 2003. Global air quality and pollution. Science. 302:1716-1719.

Amir, R., Y. Hacham and G. Galili. 2002. Cystathionine gamma-synthase and threonine synthase operate in concert to regulate carbon flow towards methionine in plants. Trends Plant Sci. 7:153-156.

Anderson, J.M. and W.S. Chow. 2002. Structural and functional dynamics of plant photosystem II. Phil Trans R Soc Lond B. 357:1421-1430.

Anderson, P.D., B. Palmer, J.L.J. Houpis, M.K. Smith and J.C. Pushnik. 2003. Chloroplastic responses of ponderosa pine (*Pinus ponderosa*) seedlings to ozone exposure. Environ Int. 29:407-413.

Andersson, A., J. Keskitalo, A. Sjodin, R. Bhalerao, F. Sterky, K. Wissel, K. Tandre, H. Aspeborg, R. Moyle, Y. Ohmiya, A. Brunner, P. Gustafsson, J. Karlsson, J. Lundeberg, O. Nilsson, G. Sandberg, S. Strauss, B. Sundberg, M. Uhlen, S. Jansson and P. Nilsson. 2004. A transcriptional timetable of autumn senescence. Genome Biol. 5:R24.1-13.

Andre, C.M., M. Oufir, C. Guignard, L. Hoffmann, J.F. Hausman, D. Evers and Y. Larondelle. 2007. Antioxidant profiling of native Andean potato tubers (*Solanum tuberosum* L.) reveals cultivars with high levels of beta-carotene, alpha-tocopherol, chlorogenic acid, and petanin. J Agric Food Chem. 55:10839-10849.

Andreae, M.O. and P.J. Crutzen. 1997. Atmospheric aerosols: Biogeochemical sources and role in atmospheric chemistry. Science. 276:1052-1058.

Anyia, A.O. and H. Herzog. 2004. Water-use efficiency, leaf area and leaf gas exchange of cowpeas under mid-season drought. Eur J Agron. 20:327-339.

Archibald, J.M. 2009. The puzzle of plastid evolution. Curr Biol. 19:R81-R88.

Arie, M., K. Hikichi, K. Takahashi and M. Esaka. 2000. Characterization of a basic chitinase which is secreted by cultured pumpkin cells. Physiol Plant. 110:232-239.

Asada, K. 1999. The water-water cycle in chloroplasts: scavenging of active oxygens and dissipation of excess photons. Annu Rev Plant Physiol Plant Mol Biol. 50:601-639.

Ashmore, M., L. Emberson, P.E. Karlsson and H. Pleijel. 2004. New directions: A new generation of ozone critical levels for the protection of vegetation in Europe. Atmos Environ. 38:2213-2214.

Ashmore, M.R. 2005. Assessing the future global impacts of ozone on vegetation. Plant Cell Environ. 28:949-964.

Ashton, T.S. 1997. The industrial revolution 1760-1830. Oxford University Press, Oxford.

Atkin, O.K. and D. Macherel. 2009. The crucial role of plant mitochondria in orchestrating drought tolerance. Ann Bot. 103:581-597.

Babu, G.J., D. Wheeler, O. Alzate and M. Periasamy. 2004. Solubilization of membrane proteins for two dimensional gel electrophoresis: identification of sacroplasmic reticulum membrane proteins. Anal Biochem. 325:121-125.

Bacon, M.A., D.S. Thompson and W.J. Davies. 1997. Can cell wall peroxidase activity explain the leaf growth response of *Lolium temulentum* L. during drought? J Exp Bot. 48:2075-2085.

Bagard, M., D. Le Thiec, E. Delacote, M.P. Hasenfratz-Sauder, J. Banvoy, J. Gerard, P. Dizengremel and Y. Jolivet. 2008. Ozone-induced changes in photosynthesis and photorespiration of hybrid poplar in relation to the developmental stage of the leaves. Physiol Plant. 134:559-74.

Baggerman, G., E. Vierstraete, A. De Loof and L. Schoofs. 2005. Gel-based versus gel-free proteomics: A review. Comb Chem High Throughput Screen. 8:669-677.

Baginsky, S. and W. Gruissem. 2004. Chloroplast proteomics: potentials and challenges. J Exp Bot. 55:1213-1220.

Bahi, A. and G. Kahl. 1995. Air pollutant stress changes the steady-state transcript levels of three photosynthesis genes. Environ Pollut. 88:57-65.

Baier, M., A. Kandlbinder, D. Golldack and K.-J. Dietz. 2005. Oxidative stress and ozone: Perception, signalling and response. Plant Cell Environ. 28:1012-1020.

Baldasano, J., E. Valera and P. Jiménez. 2003. Air quality data from large cities. Sci Total Environ. 307:141-165.

Bassham, J.A., A.A. Benson and M. Calvin. 1950. The path of carbon in photosynthesis. J Biol Chem. 185:781-787.

Bauwe, H. 2010. Recent developments in photorespiration research. Biochem Soc Trans. 038:677-682.

Benkova, E., M. Michniewicz, M. Sauer, T. Teichmann, D. Seifertova, G. Jurgens and J. Friml. 2003. Local, efflux-dependent auxin gradients as a common module for plant organ formation. Cell. 115:591-602.

Berlett, B.S., R.L. Levine and E.R. Stadtman. 1996. Comparison of the effects of ozone on the modification of amino acid residues in glutamine synthase and bovine serum albumine. J Biol Chem. 271:4177-4182.

Bernard, S.M. and D.Z. Habash. 2009. The importance of cytosolic glutamine synthetase in nitrogen assimilation and recycling. New Phytol. 182:608-620.

Bernstein, L., P. Bosch, O. Canziani, Z. Chen, R. Christ, O. Davidson, W. Hare, S. Huq, D. Karoly and V. Kattsov. 2007. Climate change 2007: Synthesis report

Bino, R., R. Hall, O. Fiehn, J. Kopka, K. Saito, J. Draper, B. Nikolau, P. Mendes, U. Roessner-Tunali and M. Beale. 2004. Potential of metabolomics as a functional genomics tool. Trends Plant Sci. 9:418-425.

Black, V.J., C.R. Black, J.A. Roberts and C.A. Stewart. 2000. Impact of ozone on the reproductive development of plants. New Phytol. 147:421-447.

Blumenröther, M.C., M. Löw, R. Matyssek and W. Oßwald. 2007. Flux-based responses of sucrose and starch in leaves of adult beech trees (*Fagus sylvatica* L.) under free-air O_3 fumigation. Plant Biol. 9:207-214.

Bobbink, R. 1998. Impact of tropospheric ozone and airborne nitrogenous pollutants on natural and semi-natural ecosystems: a commentary. New Phytol. 139:161-168.

Bohler, S., M. Bagard, M. Oufir, S. Planchon, L. Hoffmann, Y. Jolivet, J.-F. Hausman, P. Dizengremel and J. Renaut. 2007. A DIGE analysis of developing poplar leaves subjected to ozone reveals major changes in carbon metabolism. Proteomics. 7:1584-1599.

Bortier, K., L. De Temmerman and R. Ceulemans. 2000. Effects of ozone exposure in open-top chambers on poplar (*Populus nigra*) and beech (*Fagus sylvatica*): A comparison. Environ Pollut. 109:509-516.

Bota, J., H. Medrano and J. Flexas. 2004. Is photosynthesis limited by decreased Rubisco activity and RuBP content under progressive water stress? New Phytol. 162:671-681.

Bovy, A., E. Schijlen and R. Hall. 2007. Metabolic engineering of flavonoids in tomato (*Solanum lycopersicum*): The potential for metabolomics. Metabolomics. 3:399-412.

Bradshaw, H., R. Ceulemans, J. Davis and R. Stettler. 2000. Emerging model systems in plant biology: Poplar (*Populus*) as a model forest tree. J Plant Growth Regul. 19:306-313.

Breemen, N.v., C.T. Driscoll and J. Mulder. 1984. Acidic deposition and internal proton sources in acidification of soils and waters. Nature. 307:599-604.

Brendley, B.W. and E.J. Pell. 1998. Ozone-induced changes in biosynthesis of Rubisco and associated compensation to stress in foliage of hybrid poplar. Tree Physiol. 18:81-90.

Brestic, M., G. Cornic, M.J. Freyer and N.R. Baker. 1995. Does photorespiration protect the photosynthetic apparatus in French bean leaves from photoinhibition during drought stress? Planta. 196:450-457.

Broadmeadow, M. 1998. Ozone and forest trees. New Phytol. 139:123-125.

Brugière, N., F. Dubois, C. Masclaux, R.S. Sangwan and B. Hirel. 2000. Immunolocalization of glutamine synthetase in senescing tobacco (*Nicotiana tabacum* L.) leaves suggests that ammonia assimilation is progressively shifted to the mesophyll cytosol. Planta. 211:519-527.

Brunner, A., V. Busov and S. Strauss. 2004. Poplar genome sequence: Functional genomics in an ecologically dominant plant species. Trends Plant Sci. 9:49-56.

Buchanan-Wollaston, V., T. Page, E. Harrison, E. Breeze, P.O. Lim, H.G. Nam, J.-F. Lin, S.-H. Wu, J. Swidzinski, K. Ishizaki and C.J. Leaver. 2005. Comparative transcriptome analysis reveals significant differences in gene expression and signalling pathways between developmental and dark/starvation-induced senescence in *Arabidopsis*. Plant J. 42:567-585.

Byrum, S., C.O. Montgomery, R.W. Nicholas and L.J. Suva. 2010. The promise of bone cancer proteomics. Ann N Y Acad Sci. 1192:222-229.

Cabané, M., J.-C. Pireaux, E. Léger, E. Weber, P. Dizengremel, B. Pollet and C. Lapierre. 2004. Condensed lignins are synthesized in poplar leaves exposed to ozone. Plant Physiol. 134:586-594.

Casano, L.M., J.M. Zapata, M. Martin and B. Sabater. 2000. Chlororespiration and poising of cyclic electron transport. J Biol Chem. 275:942-948.

Castagna, A., C. Nali, S. Ciompi, G. Lorenzini, G.F. Soldatini and A. Ranieri. 2001. Ozone exposure affects photosynthesis of pumpkin (*Cucurbita pepo*) plants. New Phytol. 152:223-229.

Castagna, A. and A. Ranieri. 2009. Detoxification and repair process of ozone injury: From O_3 uptake to gene expression adjustment. Environ Pollut. 157:1461-1469.

Cavalier-Smith, T. 2000. Membrane heredity and early chloroplast evolution. Trends Plant Sci. 5:174-182.

Chen, C., T. Frank and S. Long. 2009. Is a short, sharp shock equivalent to long-term punishment? Contrasting the spatial pattern of acute and chronic ozone damage to soybean leaves via chlorophyll fluorescence imaging. Plant Cell Environ. 32:327-335.

Chen, Z. and D.R. Gallie. 2005. Increasing tolerance to ozone by elevating foliar ascorbic acid confers greater protection against ozone than increasing avoidance. Plant Physiol. 138:1673-1689.

Cho, K., J. Shibato, G.K. Agrawal, Y.-H. Jung, A. Kubo, N.-S. Jwa, S. Tamogami, K. Satoh, S. Kikuchi, T. Higashi, S. Kimura, H. Saji, Y. Tanaka, H. Iwahashi, Y. Masuo and R. Rakwal. 2008. Integrated transcriptomics, proteomics, and metabolomics analyses to survey ozone response in the leaves of rice seedlings. J Proteome Res. 7:2980-2998.

Ciais, P., M. Reichstein, N. Viovy, A. Granier, J. Ogee, V. Allard, M. Aubinet, N. Buchmann, C. Bernhofer, A. Carrara, F. Chevallier, N. De Noblet, A.D. Friend, P. Friedlingstein, T. Grunwald, B. Heinesch, P. Keronen, A. Knohl, G. Krinner, D. Loustau, G. Manca, G. Matteucci, F. Miglietta, J.M. Ourcival, D. Papale, K. Pilegaard, S. Rambal, G. Seufert, J.F. Soussana, M.J. Sanz, E.D. Schulze, T. Vesala and R. Valentini. 2005. Europe-wide reduction in primary productivity caused by the heat and drought in 2003. Nature. 437:529-533.

Conklin, P. and C. Barth. 2004. Ascorbic acid, a familiar small molecule intertwined in the response of plants to ozone, pathogens, and the onset of senescence. Plant Cell Environ. 27:959-970.

Conklin, P.L. and R.L. Last. 1995. Differential accumulation of antioxidant mRNAs in *Arabidopsis thaliana* exposed to ozone. Plant Physiol. 109:203-212.

D'Haese, D., N. Noremans, W. De Coen and Y. Guisez. 2006. Identification of late O_3-responsive genes in *Arabidopsis thaliana* by cDNA microarray analysis. Physiol Plant. 128:70-79.

D'Haese, D., K. Vandermeiren, H. Asard and N. Horemans. 2005. Other factors than apoplastic ascorbate contribute to the differential ozone tolerance of two clones of *Trifolium repens* L. Plant Cell Environ. 28:623-632.

Davison, A. and J. Barnes. 1998. Effects of ozone on wild plants. New Phytol. 139:135-151.

Degl'Innocenti, E., L. Guidi and G.F. Soldatini. 2002. Effect of chronic O_3 fumigation on the activity of some Calvin cycle enzymes in two poplar clones. Photosynthetica. 40:121-126.

Derwent, R.G., M.E. Jenin, S.M. Saunders, M.J. Pilling, P.G. Simmonds, N.R. Passant, G.J. Dollard, P. Dumitrean and A. Kent. 2003. Photochemical ozone formation in north west Europe and its control. Atmos Environ. 37:1983-1991.

Deschamps, P., C. Colleoni, Y. Nakamura, E. Suzuki, J.-L. Putaux, A. Buleon, S. Haebel, G. Ritte, M. Steup, L.I. Falcon, D. Moreira, W. Loffelhardt, J.N. Raj, C. Plancke, C. d'Hulst, D. Dauvillee and

S. Ball. 2008. Metabolic symbiosis and the birth of the plant kingdom. Mol Biol Evol. 25:536-548.

Desikan, R., S.A.H. Mackerness, J.T. Hanock and S.J. Neil. 2001. Regulation of the *Arabidopsis* transcriptome by oxidative stress. Plant Physiol. 127:159-172.

Dettmer, K., P. Aronov and B. Hammock. 2007. Mass spectrometry-based metabolomics. Mass Spectrom Rev. 26:51-78.

Deusch, O., G. Landan, M. Roettger, N. Gruenheit, K.V. Kowallik, J.F. Allen, W. Martin and T. Dagan. 2008. Genes of cyanobacterial origin in plant nuclear genomes point to a heterocyst-forming plastid ancestor. Mol Biol Evol. 25:748-761.

Dhondt, S., P. Geoffroy, B.A. Stelmach, M. Legrand and T. Heitz. 2000. Soluble phospholipase A_2 activity is induced before oxylipin accumulation in tobacco mosaic virus-infected tobacco leaves and is contributed by patatin-like enzymes. Plant J. 23:431-440.

Di Baccio, D., A. Castagna, E. Paoletti, L. Sebastiani and A. Ranieri. 2008. Could the differences in O_3 sensitivity between two poplar clones be related to a difference in antioxidant defense and secondary metabolic response to O_3 influx? Tree Physiol. 28:1761-1772.

Diara, C., A. Castagna, B. Baldan, A.M. Sodi, T. Sahr, C. Langebartels, L. Sebastiani and A. Ranieri. 2005. Differences in the kinetics and scale of signalling molecule production modulate the ozone sensitivity of hybrid poplar clones: The roles of H_2O_2, ethylene and salicylic acid. New Phytol. 168:351-364.

Dickson, R.E. 1989. Carbon and nitrogen allocation in trees. Ann For Sci. 46:631s-647s.

Dillon, P.J., N.D. Yan, H.H. Harvey and D.W. Schindler. 1984. Acidic deposition: Effects on aquatic ecosystems. Crit Rev Environ Contr. 13:167-194.

Dizengremel, P. 2001. Effects of ozone on the carbon metabolism of forest trees. Plant Physiol Biochem. 39:729-742.

Dizengremel, P., D. Le Thiec, M. Bagard and Y. Jolivet. 2008. Ozone risk assessment for plants: central role of metabolism-dependent changes in reducing power. Environ Pollut. 156:11-15.

Dizengremel, P., D. Le Thiec, M.-P. Hasenfratz-Sauder, M.-N. Vaultier, M. Bagard and Y. Jolivet. 2009. Metabolic-dependent changes in plant cell redox power after ozone exposure. Plant Biol. 11:35-42.

Dizengremel, P. and M. Petrini. 1994. Effects of air pollutants on the pathways of carbohydrate breakdown. *In* Plant response to the gaseous environment: molecular, metabolic and physiological aspects Eds. R.G. Alscher and A.R. Wellburn. Chapman and Hall, London, pp 225-278.

Dizengremel, P., W. Sasekt, K.J. Brown and C.J. Richardson. 1994. Ozone-induced changes in primary carbon metabolism enzymes of Loblolly pine needles. J Plant Physiol. 144:300-306.

Doherty, M. and R. Beynon. 2006. Protein turnover on the scale of the proteome. Expert Rev Proteomics. 3:97-110.

Dunford, R.P., M.C. Durrant, M.A. Catley and T.A. Dyer. 1998. Location of the redox-active cysteines in chloroplast sedoheptulose-1,7-bisphosphatase indicates that its allosteric regulation is similar but not identical to that of fructose-1,6-bisphosphatase. Photosynth Res. 58:221-230.

Ebi, K.L. and G. McGregor. 2008. Climate change, tropospheric ozone and particulate matter, and health impacts. Environ Health Perspect. 116:1449-1455.

Eckardt, N.A. and E.J. Pell. 1994. O_3 -induced degradation on Rubisco protein and loss of Rubisco mRNA in relation to leaf age in *Solanum tuberosum* L. New Phytol. 127:741-748.

Eichacker, L.A., M. Helfrich, W. Rüdiger and B. Müller. 1996. Stabilization of chlorophyll a-binding apoproteins P700, CP47, CP43, D2, and D1 by chlorophyll a or Zn-pheophytin a*. J Biol Chem. 271:32174-32179.

Einig, W., U. Lauxmann, B. Hauch, R. Hampp, W. Landolt, S. Maurer and R. Matyssek. 1997. Ozone-induced accumulation of carbohydrates changes enzyme activities of carbohydrate metabolism in birch leaves. New Phytol.680.

El Khatib, R.T., E.P. Hamerlynck, F. Gallardo and E.G. Kirby. 2004. Transgenic poplar characterized by ectopic expression of a pine cytosolic glutamine synthetase gene exhibits enhanced tolerance to water stress. Tree Physiol. 24:729-736.

Eller, A.S.D. and J.P. Sparks. 2006. Predicting leaf-level fluxes of O_3 and NO_2: The relative roles of diffusion and biochemical processes. Plant Cell Environ. 29:1742-1750.

Eltayeb, A., N. Kawano, G. Badawi, H. Kaminaka, T. Sanekata, T. Shibahara, S. Inanaga and K. Tanaka. 2007. Overexpression of monodehydroascorbate reductase in transgenic tobacco confers enhanced tolerance to ozone, salt and polyethylene glycol stresses. Planta. 225:1255-1264.

Emberson, L.D., M.R. Ashmore, H.M. Cambridge, D. Simpson and J.P. Tuovinen. 2000. Modelling stomatal ozone flux across Europe. Environ Pollut. 109:403-413.

Eshed, Y., S.F. Baum, J.V. Perea and J.L. Bowman. 2001. Establishment of polarity in lateral organs of plants. Curr Biol. 11:1251-1260.

Fares, S., F. Loreto, E. Kleist and J. Wildt. 2008. Stomatal uptake and stomatal deposition of ozone in isoprene and monoterpene emitting plants. Plant Biol. 10:44-54.

Farley, A.R., A.J. Link, R.B. Richard and P.D. Murray. 2009. Identification and quantification of protein posttranslational modifications. *In* Methods in Enzymology. Academic Press, San Diego, pp 725-763.

Fearnside, P.M. 2000. Global warming and tropical land-use change: greenhouse gas emissions from biomass burning, decomposition and soils in forest conversion, shifting cultivation and secondary vegetation. Clim Change. 46:115-158.

Feng, Y., S. Komatsu, T. Furukawa, T. Koshiba and Y. Kohno. 2008. Proteome analysis of proteins responsive to ambient and elevated ozone in rice seedlings. Agric Ecosyst Environ. 125:255-265.

Finlayson-Pitts, B. and J. Pitts. 2000. Chemistry of the upper and lower atmosphere: theory, experiments, and applications. Academic Press, San Diego.

Finlayson-Pitts, B.J. and J.N. Pitts, Jr. 1997. Tropospheric air pollution: Ozone, airborne toxins, polycyclic aromatic hydrocarbons, and particles. Science. 276:1045-1052.

Fleming, A.J. 2005. The control of leaf development. New Phytol. 166:9-20.

Flexas, J., J. Bota, F. Loreto, G. Cornic and T.D. Sharkey. 2004. Diffusive and metabolic limitations to photosynthesis under drought and salinity in C3 plants. Plant Biol. 6:269-279.

Flexas, J. and H. Medrano. 2002. Drought-inhibition of photosynthesis in C3 plants: Stomatal and non-stomatal limitations revisited. Ann Bot. 89:183-189.

Fontaine, V., M. Cabané and P. Dizengremel. 2003. Regulation of phosphoenolpyruvate carboxylase in *Pinus halepensis* needles submitted to ozone and water stress. Physiol Plant. 117:445-452.

Fontaine, V., J. Pelloux, M. Podor, D. Afif, D. Gérant, P. Grieu and P. Dizengremel. 1999. Carbon fixation in *Pinus halepensis* submitted to ozone. Opposite response of ribulose-1,5-bisphosphate carboxylase:oxygenase and phosphoenolpyruvate carboxylase. Physiol Plant. 105:187-192.

Foyer, C.H. and G. Noctor. 2003. Redox sensing and signalling associated with reactive oxygen in chloroplasts, peroxisomes and mitochondria. Physiol Plant. 119:355-364.

Foyer, C.H. and G. Noctor. 2005. Redox homeostasis and antioxidant signaling: A metabolic interface between stress perception and physiological responses. Plant Cell. 17:1866-1875.

Fromme, P., P. Jordan and N. Krauß. 2001. Structure of photosystem I. Biochim Biophys Acta. 1507:5-31.

Fuhrer, J. 2009. Ozone risk for crops and pastures in present and future climates. Naturwissenschaften. 96:173-194.

Fuhrer, J., L. Skärby and M.R. Ashmore. 1997. Critical levels for ozone effects on vegetation in Europe. Environ Pollut. 97:91-106.

Fujiwara, T., K. Ito, T. Yamami and Y. Nakamura. 2004. Ribosome recycling factor disassembles the post-termination ribosomal complex independent of the ribosomal translocase activity of elongation factor G. Mol Microbiol. 53:517-528.

Fusco, A.C. and J.A. Logan. 2003. Analysis of 1970-1995 trends in tropospheric ozone at Northern Hemisphere midlatitudes with the GEOS-CHEM model. J. Geophys. Res. 108:ACH4.1-ACH4.25.

Gaspar, T., T. Franck, B. Bisbis, C. Kevers, L. Jouve, J. Hausman and J. Dommes. 2002. Concepts in plant stress physiology. Application to plant tissue cultures. Plant Growth Regul. 37:263-285.

Gaucher, C., N. Costanzo, D. Afif, Y. Mauffette, N. Chevrier and P. Dizengremel. 2003. The impact of elevated ozone and carbon dioxide on young *Acer saccharum* seedlings. Physiol Plant. 117:392-402.

Gaucher, C., N. Costanzo, P. Widden, J.P. Renaud, P. Dizengremel, Y. Mauffette and N. Chevrier. 2006. Response to an ozone gradient of growth and enzymes implicated in tolerance to oxidative stress in *Acer saccharum* (Marsh.) seedlings. Ann For Sci. 63:387-397.

Geiger, D.R. and J.C. Servaites. 1994. Diurnal regulation of photosynthetic carbon metabolism in C3 plants. Annu Rev Plant Physiol Plant Mol Biol. 45:235-256.

Gerosa, G., R. Marzuoli, F. Bussotti, M. Pancrazi and A. Ballarin-Denti. 2003. Ozone sensitivity of *Fagus sylvatica* and *Fraxinus excelsior* young trees in relation to leaf structure and foliar ozone uptake. Environ Pollut. 125:91-98.

Gevaert, K., P. Van Damme, B. Ghesquière, F. Impens, L. Martens, K. Helsens and J. Vandekerckhove. 2007. A la carte proteomics with an emphasis on gel-free techniques. Proteomics. 7:2698-2718.

Gevaert, K. and J. Vandekerckhove. 2000. Protein identification methods in proteomics. Electrophoresis. 21:1145-1154.

Giardi, M.T., A. Cona, B. Geiken, T. Kučera, J. Masojídek and A.K. Mattoo. 1996. Long-term drought stress induces structural and functional reorganization of photosystem II. Planta. 199:118-125.

Goode, D. and J. Buchhold. 1992. Effect of long term fumigation with ozone on the turnover of the D-1 reaction center polypeptide of photosystem II in spruce (*Picea abies*). Physiol Plant. 86:568-574.

Görg, A., C. Obermaier, G. Boguth, A. Harder, B. Scheibe, R. Wildgruber and W. Weiss. 2000. The current state of two-dimensional electrophoresis with immobilized pH gradients. Proteomics. 21:1037-1053.

Goulas, P.J., M. Schubert, T. Kieselbach, L.A. Kleczkowski, P. Gardeström, W. Schröder and V. Hurry. 2006. The chloroplast lumen and stromal proteomes of *Arabidopsis thaliana* show differential sensitivity to short- and long-term exposure to low temperature. Plant J. 47:720-734.

Grace, J. and R. Zhang. 2006. Predicting the effect of climate change on global plant productivity and the carbon cycle. *In* Plant growth and climate change Eds. J. Morison and M. Morecroft. Blachwell Publishing, Oxford, pp 187-207.

Grant, J.J., B.-W. Yun and G.J. Loake. 2000. Oxidative burst and cognate redox signalling reported by luciferase imaging: identification of a signal network that functions independently of ethylene, SA and Me-JA but is dependent on MAPKK activity. Plant J. 24:569-582.

Grbic, V. and A.B. Bleecker. 1995. Ethylene regulates the timing of leaf senescence in *Arabidopsis*. Plant J. 8:595-602.

Green, B.R. and D.G. Durnford. 1996. The chlorophyll-carotenoid proteins of oxygenic photosynthesis. Annu Rev Plant Physiol Plant Mol Biol. 47:685-714.

Grünhage, L., S.V. Krupa, A.H. Legge and H.J. Jäger. 2004. Ambient flux-based critical values of ozone for protecting vegetation: Differing spatial scales and uncertainties in risk assessment. Atmos Environ. 38:2433-2437.

Günthardt-Goerg, M.S., C.J. McQuattie, S. Maurer and B. Frey. 2000. Visible and microscopic injury in leaves of five deciduous tree species related to current critical ozone levels. Environ Pollut. 109:489-500.

Guidi, L., C. Nali, G. Lorenzini, F. Filippi and G.F. Soldatini. 2001. Effect of chronic ozone fumigation on the photosynthetic process of poplar clones showing different sensitivity. Environ Pollut. 113:245-254.

Guidi, L., C. Nali, G. Lorenzini and G.F. Soldatini. 1998. Photosynthetic response to ozone of two poplar clones showing different sensitivity. Chemosphere. 36:657-662.

Gupta, A.S., R.G. Alscher and D. McCune. 1991. Response of photosynthesis and cellular antioxidants to ozone in *Populus* leaves. Plant Physiol. 96:650-655.

Gupta, P., S. Duplessis, H. White, D.F. Karnosky, F. Martin and G.K. Podila. 2005. Gene expression patterns of trembling aspen trees following long-term exposure to interacting elevated CO_2 and tropospheric O_3. New Phytol. 167:129-142.

Guy, C., F. Kaplan, J. Kopka, J. Selbig and D. Hincha. 2008. Metabolomics of temperature stress. Physiol Plant. 132:220-235.

Haagen-Smit, A., E. Darley, M. Zaitlin, H. Hull and W. Noble. 1952. Investigation on injury to plants from air pollution in the Los Angeles area. Plant Physiol. 27:18-34.

Haberer, K., K. Herbinger, M. Alexou, M. Tausz and H. Rennenberg. 2007. Antioxidative defence of old growth beech (*Fagus sylvatica*) under double ambient O_3 concentrations in a free-air exposure system. Plant Biol. 9:215-226.

Haldrup, A., H. Naver and H.V. Scheller. 1999. The interaction between plastocyanin and photosystem I is inefficient in transgenic *Arabidopsis* plants lacking the PSI-N subunit of photosystem. Plant J. 17:689-698.

Hankamer, B., J. Barber and E.J. Boekema. 1997. Structure and membrane organization of photosystem II in green plants. Annu Rev Plant Physiol Plant Mol Biol. 48:641-671.

Harrison, E.P., N.M. Willingham, J.C. Lloyd and C.A. Raines. 1997. Reduced sedoheptulose-1,7-bisphosphatase levels in transgenic tobacco lead to decreased photosynthetic capacity and altered carbohydrate accumulation. Planta. 204:27-36.

Heath, R.L. 2008. Modification of the biochemical pathways of plants induced by ozone: what are the varied routes to change? Environ Pollut. 155:453-463.

Heilman, P.E., G. Ekuan and D.B. Fogle. 1994. First-order root development from cuttings of *Populus trichocarpa* x *P. deltoides* hybrids. Tree Physiol. 14:911-920.

Heinecke, J.W., W. Li, H.L. Daehnke, III and J.A. Goldstein. 1993. Dityrosine, a specific marker of oxidation, is synthesized by the myeloperoxidase-hydrogen peroxide system of human neutrophils and macrophages. J Biol Chem. 268:4069-4077.

Heldt, H.-W. and F. Heldt. 2005. The Calvin cycle catalyzes photosynthetic CO2 assimilation. *In* Plant Biochemistry (Third Edition). Academic Press, Burlington, pp 165-193.

Holtorf, H., M. Guitton and R. Reski. 2002. Plant functional genomics. Naturwissenschaften. 89:235-249.

Hopkins, M., C. Taylor, Z. Liu, F. Ma, L. McNamara, T.W. Wang and J.E. Thompson. 2007. Regulation and execution of molecular disassembly and catabolism during senescence. New Phytol. 175:201-214.

Hubbard, S.J. 2010. Computational approaches to peptide identification via tandem MS. *In* Methods in molecular biology Eds. S.J. Hubbard and A.R. Jones. Human Press, New York, p 23.

Hull, J. 1999. The second industrial revolution: The history of a concept. Storia Della Storiografia. 36:81-90.

Iglesias, D.J., n. Calatayud, E. Barreno, E. Primo-Millo and M. Talon. 2006. Responses of citrus plants to ozone: Leaf biochemistry, antioxidant mechanisms and lipid peroxidation. Plant Physiol Biochem. 44:125-131.

Inclán, R., R. Alonso, M. Pujadas, J. Terés and B.S. Gimeno. 1998. Ozone and drought stress: Interactive effects on gas exchange in Aleppo pine (*Pinus halepensis* Mill.). Chemosphere. 36:685-690.

Isebrands, J.G. and D.F. Karnosky. 2001. Environmental benefits of poplar culture. *In* Poplar Culture in North America Eds. D.I. Dickmann, J.G. Isebrands, J.E. Eckenwalder and J. Richardson, pp 207–218.

Ishida, A., A. Uemura, N. Koike, Y. Matsumoto and A.L. Hoe. 1999. Interactive effects of leaf age and self-shading on leaf structure, photosynthetic capacity and chlorophyll fluorescence in the rain forest tree, *Dryobalanops aromatica*. Tree Physiol. 19:741-747.

Jansson, S. and C.J. Douglas. 2007. Populus: A model system for plant biology. Annu Rev Plant Biol. 58:435-458.

Jehnes, S., G. Betz, G. Bahnweg, K. Haberer, H. Sandermann and H. Rennenberg. 2007. Tree internal signalling and defence reactions under ozone exposure in sun and shade leaves of European beech (*Fagus sylvatica* L.) trees. Plant Biol. 9:253-264.

Jonson, J., D. Simpson, H. Fagerli and S. Solberg. 2006. Can we explain the trends in European ozone levels? Atmos Chem Phys. 6:51-66.

Joo, J.H., S. Wang, J.G. Chen, A.M. Jones and N.V. Fedoroff. 2005. Different signaling and cell death roles of heterotrimeric G protein α and β subunits in the *Arabidopsis* oxidative stress response to ozone. Plant Cell. 17:957-970.

Junqua, M., J.-P. Biolley, S. Pie, M. Kanoun, R. Duran and P. Goulas. 2000. In vivo occurrence of carbonyl residues in *Phaseolus vulgaris* proteins as a direct consequence of a chronic ozone stress. Plant Physiol Biochem. 38:853-861.

Kangasjärvi, J., P. Jaspers and H. Kollist. 2005. Signalling and cell death in ozone-exposed plants. Plant Cell Environ. 28:1021-1036.

Kanofsky, J.R. and P. Sima. 1991. Singlet oxygen production from the reactions of ozone with biological molecules. J Biol Chem. 266:9039-9042.

Kanofsky, J.R. and P.D. Sima. 1995. Singlet oxygen generation from the reaction of ozone with plant leaves. J Biol Chem. 270:7850-7852.

Karl, T.R. and K.E. Trenberth. 2003. Modern global climate change. Science. 302:1719-1723.

Karlsson, P.E., J. Uddling, S. Braun, M. Broadmeadow, S. Elvira, B.S. Gimeco, D. Le Thiec, E. Oksanen, K. Vandermeiren, M. Wilkinson and L. Emberson. 2004. New critical levels for ozone effects on young trees based on AOT40 and simulated cumulative leaf uptake of ozone. Atmos Environ. 38:2283-2294.

Keech, O., E. Pesquet, A. Ahad, A. Askne, D. Nordvall, S. Vodnala, H. Tuominen, V. Hurry, P. Dizengremel and P. Gardeström. 2007. The different fates of mitochondria and chloroplasts during dark-induced senescence in *Arabidopsis* leaves. Plant Cell Environ. 30:1523-1534.

Keller, C. 2007. Global warming 2007. An update to global wanning: The balance of evidence and Its policy implications. ScientificWorldJournal. 7:381-399.

Keller, C.F. 2003. Global warming: The balance of evidence and its policy implications. A review of the current state-of-the-controversy. ScientificWorldJournal. 3:357-411.

Kennedy, R.A. and D. Johnson. 1981. Changes in photosynthetic characteristics during leaf development in apple. Photosynth Res. 2:213-223.

Kersten, B., G.K. Agrawal, P. Durek, J. Neigenfind, W. Schulze, D. Walther and R. Rakwal. 2009. Plant phosphoproteomics: An update. Proteomics. 9:964-988.

Keskitalo, J., G. Bergquist, P. Gardestrom and S. Jansson. 2005. A cellular timetable of autumn senescence. Plant Physiol. 139:1635-1648.

Kieffer, P., P. Schroder, J. Dommes, L. Hoffmann, J. Renaut and J.F. Hausman. 2009. Proteomic and enzymatic response of poplar to cadmium stress. J Proteomics. 72:379-396.

Kiehl, J. and K. Trenberth. 1997. Earth's annual global mean energy budget. Bull Amer Meteor Soc. 78:197-208

Kivimäenpää, M., A.M. Jönsson, I. Stjernquist, G. Selldén and S. Sutinen. 2004. The use of light and electron microscopy to assess the impact of ozone on Norway spruce needles. Environ Pollut. 127:441-453.

Kley, D., M. Kleinmann, H. Sanderman and S. Krupa. 1999. Photochemical oxidants: State of the science. Environ Pollut. 100:19-42.

Knight, K.L. and J.B. Mudd. 1984. The reaction of ozone with glyceraldehyde-3-phosphate. Arch Biochem Biophys. 229:259-269.

Koch, J.R., R.A. Creelman, S.M. Eshita, M. Seskar, J.E. Mullet and K.R. Davis. 2000. Ozone sensitivity in hybrid poplar correlates with insensitivity to both salicylic acid and jasmonic acid. The role of programmed cell death in lesion formation. Plant Physiol. 123:487-496.

Koch, J.R., A.J. Scherzer, S.M. Eshita and K.R. Davis. 1998. Ozone sensitivity in hybrid poplar is correlated with a lack of defense-gene activation. Plant Physiol. 118:1243-1252.

Koistinen, K.M., V.H. Hassinen, P.A.M. Gynther, S.J. Lehesranta, S.I. Keinänen, H.I. Kokko, E.J. Oksanen, A.I. Tervahaute, S. Auriola and S.O. Kärenlampi. 2002. Birch PR-10c is induced by factors causing oxidative stress but appears not to confer tolerance to these gents. New Phytol. 155:381-391.

Kolb, T.E. and R. Matyssek. 2001. Limitations and perspectives about scaling ozone impacts in trees. Environ Pollut. 115:373-393.

Kollist, H., H. Moldau, L. Mortensen, S.K. Rasmussen and L.B. Jorgensen. 2000. Ozone flux to plasmalemma in barley and wheat is controlled by stomata rather than by direct reaction of ozone with cell wall ascorbate. J Plant Physiol. 156:645-651.

Kontunen-Soppela, S., V. Ossipov, S. Ossipova and E. Oksanen. 2007. Shift in birch leaf metabolome and carbon allocation during long-term open-field ozone exposure. Glob Chang Biol. 13:1053-1067.

Korolainen, M.A., T.A. Nyman, T. Aittokallio and T. Pirttilä. 2010. An update on clinical proteomics in Alzheimer's research. J Neurochem. 112:1386-1414.

Koßmann, J., U. Sonnewald and L. Willmitzer. 1994. Reduction of the chloroplastic fructose-1,6-bisphosphatase in transgenic potato plants impairs photosynthesis and plant growth. Plant J. 6:637-650.

Kotiaho, T., M.N. Eberlin, P. Vainiotalo and R. Kostiainen. 2000. Electrospray mass and tandem mass spectrometry identification of ozone oxidation products of amino acids and small peptides. J Am Soc Mass Spectrom. 11:526-535.

Kreuzwieser, J. and A. Gessler. 2010. Global climate change and tree nutrition: Influence of water availability. Tree Physiol. 30:1221-1234.

Kruger, N. and R. Ratcliffe. 2007. Dynamic metabolic networks: Going with the flow. Phytochemistry. 68:2136-2138.

Kuroda, M., F. Sakiyama and K. Narita. 1975. Oxidation of tryptophan in lysozyme by ozone in aqueous solution. J Biochem. 78:641-651.

Kutík, J. 1998. The development of chloroplast structure during leaf ontogeny. Photosynthetica. 35:481-505.

Laisk, A., O. Kull and H. Moldau. 1989. Ozone concentration in leaf intercellular air spaces is close to zero. Plant Physiol. 90:1163-1167.

Lambert, J., M. Ethier, J. Smith and D. Figeys. 2005. Proteomics: From gel based to gel free. Anal Chem. 77:3771-3788.

Landolt, W., U. Bühlmann, P. Bleuler and J.B. Bucher. 2000. Ozone exposure-response relationships for biomass and root/shoot ratio of beech (*Fagus sylvatica*), ash (*Fraxinus excelsior*), Norway spruce (*Picea abies*) and Scots pine (*Pinus sylvestris*). Environ Pollut. 109:473-478.

Landolt, W., M.S. Günthardt-Goerg, I. Pfenninger, W. Einig, R. Hampp, S. Maurer and R. Matyssek. 1997. Effect of fertilization on ozone-induced changes in the metabolism of birch (*Betula pendula*) leaves. New Phytol. 137:389-397.

Landry, L.C. and E.J. Pell. 1993. Modification of Rubisco and altered proteolytic activity in O_3-stressed hybrid poplar (*Populus maximowizii* x *trichocarpa*). Plant Physiol. 101:1355-1362.

Langebartels, C., H. Wohlgemuth, S. Schieschan, S. Grün and H. Sandermann. 2002. Oxidative burst and cell death in ozone-exposed plants. Plant Physiol Biochem. 40:567-575.

Le Thiec, D. and S. Manninen. 2002. Ozone and water deficit reduced growth of Aleppo pine seedlings. Plant Physiol Biochem. 41:55-63.

Lee, S. and S.-C. Yun. 2006. The ozone stress transcriptome of pepper (*Capsicum annuum* L.). Mol Cells. 21:197-205.

Leitao, L., O. Bethenod and J.-P. Biolley. 2007a. The impact of ozone on juvenile maize (*Zea mays* L.) plant photosynthesis: effects on vegetative biomass, pigmentation, and carboxylases (PEPc and Rubisco). Plant Biol. 9:478-488.

Leitao, L., P. Dizengremel and J.-P. Biolley. 2008. Foliar CO_2 fixation in bean (*Phaseolus vulgaris* L.) submitted to elevated ozone: Distinct changes in Rubisco and PEPc activities in relation to pigment content. Ecotoxicol Environ Saf. 69:531-540.

Leitao, L., P. Goulas and J.-P. Biolley. 2007b. Time-course Rubisco oxidation in beans (*Phaseolus vulgaris* L.) subjected to a long-term ozone stress. Plant Sci. 165:613-620.

Leuschner, C., K. Backes, D. Hertel, F. Schipka, U. Schmitt, O. Terborg and M. Runge. 2001. Drought responses at leaf, stem and fine root levels of competitive *Fagus sylvatica* L. and *Quercus petraea* (Matt.) Liebl. trees in dry and wet years. For Ecol Manage. 149:33-46.

Li, P., S.A.P. Mane, A.A. Sioson, C. Vasquez Robinet, L.S. Heath, H.J. Bohnert and R. Grene. 2006. Effects of chronic ozone exposure on gene expression in *Arabidopsis thaliana* ecotypes and in *Thellungiella halophila*. Plant Cell Environ. 29:854-868.

Lichtenthaler, H.K. 1996. Vegetation stress: An introduction to the stress concept in plants. J Plant Physiol. 148:4-14.

Lighty, J., J. Veranth and A. Sarofim. 2000. Combustion aerosols: Factors governing their size and composition and implications to human health. Air Waste. 50:1565-1618.

Lopez, M.F. 2000. Better approaches to finding the needle in a haystack: Optimizing proteome analysis through automation. Electrophoresis. 21:1082-1093.

Lorenzini, G., L. Guidi, C. Nali and G.F. Soldatini. 1999. Quenching analysis in poplar clones exposed to ozone. Tree Physiol. 19:607-612.

Loreto, F., M. Centritto, C. Barta, C. Calfapietra, S. Fares and R. Monson. 2007. The relationship between isoprene emission rate and dark respiration rate in white poplar (*Populus alba* L.) leaves. Plant Cell Environ. 30:662-669.

Loreto, F. and S. Fares. 2007. Is ozone flux inside leaves only a damage indicator? Clues from volatile isoprenoid studies. Plant Physiol. 143:1096-1100.

Loreto, F., P. Pinelli, F. Manes and H. Kollist. 2004. Impact of ozone on monoterpene emissions and evidence for an isoprene-like antioxidant action of monoterpenes emitted by *Quercus ilex* leaves. Tree Physiol. 24:361-367.

Lottspeich, F. 2009. Introduction to Proteomics. *In* Proteomics: Methods and Protocols Eds. J. Reinders and A. Sickmann. Humana Press, New York, pp 3-10.

Löw, R., K.H. Hüberle, C.R. Warren and R. Matyssek. 2007. O_3 flux-related responsiveness of photosynthesis, respiration, and stomatal conductance of adult *Fagus sylvatica* to experimentally enhanced free-air O_3 exposure. Plant Biol. 9:197-206.

Ludwikow, A., P. Gallois and J. Sadowski. 2004. Ozone induced oxidative stress response in *Arabidopsis*: Transcription profiling by microarray approach. Cell Mol Biol Lett. 9:829-842.

Lütz, C., S. Anegg, D. Gerant, B. Alaoui-Soss,, J. Gérard and P. Dizengremel. 2000. Beech trees exposed to high CO_2 and to simulated summer ozone levels: Effects on photosynthesis, chloroplast components and leaf enzyme activity. Physiol Plant. 109:252-259.

Luwe, M.W.F., U. Takahama and U. Heber. 1993. Role of ascorbate in detoxifying ozone in the apoplast of spinach (*Spinacia oleracea* L.) leaves. Plant Physiol. 101:969-976.

Lux, D., S. Leonardi, J. Müller, A. Wiemken and W. Flückiger. 1997. Effects of ambient ozone concentrations on contents of non-structural carbohydrates in young *Picea abies* and *Fagus sylvatica*. New Phytol. 137:399-409.

Lyons, T., J.H. Ollerenshaw and J.D. Barnes. 1999. Impacts of ozone on *Plantago major*: Apoplastic and symplastic antioxidant status. New Phytol. 141:253-263.

Maayan, I., F. Shaya, K. Ratner, Y. Mani, S. Lavee, B. Avidan, Y. Shahak and O. Ostersetzer-Biran. 2008. Photosynthetic activity during olive (*Olea europaea*) leaf development correlates with plastid biogenesis and Rubisco levels. Physiol Plant. 134:547-558.

Macadam, J.W., R.E. Sharp and C.J. Nelson. 1992. Peroxidase activity in the leaf elongation zone of tall fescue: II. Spatial distribution of apoplastic peroxidase activity in genotypes differing in length of the elongation zone. Plant Physiol. 99:879-885.

Mahalingam, R., N. Jambunathan, S.K. Gunjan, E. Faustin, H. Weng and P. Ayoubi. 2006. Analysis of oxidative signalling induced by ozone in *Arabidopsis thaliana*. Plant Cell Environ. 29:1357-1371.

Mankovská, B., K.E. Percy and D.F. Kernosky. 2005. Impacts of greenhouse gases on epicuticular waxes of *Populus tremuloides* Michx.: Results from an open-air exposure and a natural O_3 gradient. Environ Pollut. 137:580-586.

Manzanares, D., K. Rodriguez-Capote, S. Liu, T. Haines, Y. Ramo, L. Zhao, A. Doherty-Kirby, G. Lajoie and F. Possmayer. 2007. Modification of tryptophan and methionine residues is implicated in the oxidative inactivation of surfactant protein B. Biochemistry. 46:5604-5615.

Marenco, A. 1994. Evidence of a long-term increase in tropospheric ozone from Pic du Midi data series: Consequences: Positive radiative forcing. J Geophys Res. 99:16617-16632.

Margulis, L. 1971. Symbiosis and evolution. Sci Am. 225:48-57.

Martyniuk, C.J. and N.D. Denslow. 2009. Towards functional genomics in fish using quantitative proteomics. Gen Comp Endocrinol. 164:135-141.

Maruta, T., A. Tanouchi, M. Tamoi, Y. Yabuta, K. Yoshimura, T. Ishikawa and S. Shigeoka. 2010. *Arabidopsis* chloroplastic ascorbate peroxidase isoenzymes play a dual role in photoprotection and gene regulation under photooxidative stress. Plant Cell Physiol. 51:190-200.

Matsuyama, T., T. Masanori, N. Nakajima, M. Aono, A. Kubo, S. Moriya, T. Ichihara, O. Suzuki and H. Saji. 2002. cDNA microarray assessment for ozone-stressed *Arabidopsis thaliana*. Environ Pollut. 117:191-194.

Matyssek, R., D.F. Karnosky, G. Wieser, K. Percy, E. Oksanen, T.E.E. Grams, M. Kubiske, D. Hanke and H. Pretzsch. 2010a. Advances in understanding ozone impact on forest trees: Messages from novel phytotron and free-air fumigation studies. Environ Pollut. 158:1990-2006.

Matyssek, R., D. Le Thiec, M. Löw, P. Dizengremel, A.J. Nunn and K.H. Häberle. 2006. Interactions between drought and O_3 stress in forest trees. Plant Biol. 8:11-17.

Matyssek, R., G. Wieser, R. Ceulemans, H. Rennenberg, H. Pretzsch, K. Haberer, M. Löw, A.J. Nunn, H. Werner, P. Wipfler, O.w. W, P. Nikolova, D.E. Hanke, H. Kraigher, M. Tausz, G. Bahnweg, M. Kitao, J. Dieler, H. Sandermann, K. Herbinger, T. Grebenc, M. Blumenröther, G. Deckmyn, T.E.E. Grams, C. Heerdt, M. Leuchner, P. Fabian and K.H. Häberle. 2010b. Enhanced ozone strongly reduces carbon sink strength of adult beech (*Fagus sylvatica*) - Resume from the free-air fumigation study at Kranzberg Forest. Environ Pollut. 158:2527-2532.

Matyssek, R., G. Wieser, A.J. Nunn, A.R. Kozovits, I.M. Reiter, C. Heerdt, J.B. Winkler, M. Baumgarten, K.H. Häberle, T.E.E. Grams, H. Werner, P. Fabian and W.M. Havranek. 2004. Comparison between AOT40 and ozone uptake in forest trees of different species, age and site conditions. Atmos Environ. 38:2271-2281.

Mazelis, M. and B. Vennesland. 1957. Carbon dioxide fixation into oxaloacetate in higher plants. Plant Physiol. 32:591-600.

McConnell, J.R., J. Emery, Y. Eshed, N. Bao, J. Bowman and M.K. Barton. 2001. Role of PHABULOSA and PHAVOLUTA in determining radial patterning in shoots. Nature. 411:709-713.

Melzer, E. and M.H. O'Leary. 1987. Anapleurotic CO_2 fixation by phosphoenolpyruvate carboxylase in C3 plants. Plant Physiol. 84:58-60.

Mereschkowsky, C. 1905. Über Natur und Ursprung der Chromatophoren im Pflanzenreiche. Biol Zentralbl. 25:539-604.

Mikkelsen, T. and H. Heide-Jørgensen. 1996. Acceleration of leaf senescence in *Fagus sylvatica* L. by low levels of tropospheric ozone demonstrated by leaf colour, chlorophyll fluorescence and chloroplast ultrastructure. Trees-Struct Funct. 10:145-156.

Miller, J.D., R.N. Arteca and E.J. Pell. 1999. Senescence-associated gene expression during ozone-induced leaf senescence in *Arabidopsis*. Plant Physiol. 120:1015-1023.

Mittler, R. 2002. Oxidative stress, antioxidants and stress tolerance. Trends Plant Sci. 7:405-410.

Mittler, R. 2006. Abiotic stress, the field environment and stress combination. Trends Plant Sci. 11:15-19.

Miyazaki, S., M. Fredricksen, K.C. Hollis, V. Poroyko, D. Shepley, D.W. Galbraith, S.P. Long and H.J. Bohnert. 2004. Transcript expression profiles of *Arabidopsis thaliana* grown under controlled conditions and open-air elevated concentrations of CO_2 and of O_3. Field Crops Res. 90:47-59.

Moeder, W., C. Barry, A. Tauriainen, C. Betz, J. Tuomainen, M. Utriainen, D. Grierson, H. Sandermann, C. Langebartels and J. Kangasjärvi. 2002. Ethylene synthesis regulated by biphasic induction of 1-aminocyclopropane-1-carboxylic acid synthase and 1-aminocyclopropane-1-carboxylic acid oxidase genes is required for hydrogen peroxide accumulation and cell death in ozone-exposed tomato. Plant Physiol. 130:1918-1926.

Molina, M.J. and F.S. Rowland. 1974. Stratospheric sink for chlorofluoromethanes: Chlorine atom-catalysed destruction of ozone. Nature. 249:810-812.

Monks, P.S. 2005. Gas-phase radical chemistry in the troposphere. Chem Soc Rev. 34:376-395.

Moraes, R.M., P. Bulbovas, C.M. Furlan, M. Domingos, S.T. Meirelles, W.B.C. Delitti and M.J. Sanz. 2006. Physiological responses of saplings of *Caesalpinia echinata* Lam., a Brazilian tree species, under ozone fumigation. Ecotoxicol Environ Saf. 63:306-312.

Mudd, J.B., R. Leavitt, A. Ongun and T.T. McManus. 1969. Reaction of ozone with amino acids and proteins. Atmos Environ. 3:669-682.

Musselman, R.C., A.S. Lefohn, W.J. Massman and R.L. Heath. 2006. A critical review and analysis of the use of exposure- and flux-based ozone indices for predicting vegetation effects. Atmos Environ. 40:1869-1888.

Nelson, N. and C.F. Yocum. 2006. Structure and function of photosystems I and II. Annu Rev Plant Biol. 57:521-565.

Neuhaus, H.E. and N. Schulte. 1996. Starch degradation in chloroplasts isolated from C3 or CAM (crassulacean acid metabolism)-induced *Mesembryanthemum crystallinum* L. Biochem J. 318:945-953.

Niyogi, K.K., O. Bjorkman and A.R. Grossman. 1997. The roles of specific xanthophylls in photoprotection. Proc Natl Acad Sci U S A. 94:14162-14167.

Noctor, G. 2006. Metabolic signalling in defence and stress: The central roles of soluble redox couples. Plant Cell Environ. 29:409-425.

Noctor, G., S. Veljovic-Jovanovic, S. Driscoll, L. Novitskaya and C.H. Foyer. 2002. Drought and oxidative load in the leaves of C_3 plants: A predominant role for photorespiration? Ann Bot. 89:841-850.

Nogués, I., S. Fares, E. Oksanen and F. Loreto. 2008. Ozone effects on the metabolism and the antioxidant system of poplar leaves at different stages of development. *In* Photosynthesis. Energy from the Sun Eds. J.F. Allen, E. Gantt, J. Golbeck and B. Osmond. Springer, Dordrecht, pp 1317-1322.

Ogaya, R., J. Peñuelas, J. Martínez-Vilalta and M. Mangirón. 2003. Effect of drought on diameter increment of *Quercus ilex*, *Phillyrea latifolia*, and *Arbutus unedo* in a holm oak forest of NE Spain. For Ecol Manage. 180:175-184.

Ögren, E. and G. Öquist. 1985. Effects of drought on photosynthesis, chlorophyll fluorescence and photoinhibition susceptibility in intact willow leaves. Planta. 166:380-388.

Ohta, H., T. Suzuki, M. Ueno, A. Okumura, S. Yoshihara, J.-R. Shen and I. Enami. 2003. Extrinsic proteins of photosystem II. Eur J Biochem. 270:4156-4163.

Oke, T.R. 1987. Boundary layer climates. Routledge, London.

Oksanen, E., E. Häikiö, J. Sober and D.F. Karnosky. 2004. Ozone-induced H_2O_2 accumulation in field-grown aspen and birch is linked to foliar ultrastructure and peroxisomal activity. New Phytol. 161:791-799.

Oksanen, E., J. Sober and D.F. Karnosky. 2001. Impacts of elevated CO_2 and/or O_3 on leaf ultrastructure of aspen (*Populus tremuloides*) and birch (*Betula papyrifera*) in the Aspen FACE experiment. Environ Pollut. 115:437-446.

Olbrich, M., G. Betz, E. Gerstner, C. Langebartels, H. Sanderman and D. Ernst. 2005. Transcriptomic analysis of ozone-responsive genes in leaves of Europeam beech (*Fagus sylvatica* L.). Plant Biol. 7:670-676.

Oltmans, S.J., A.S. Lefohn, J.M. Harris, I. Galbally, H.E. Scheel, G. Bodeker, E. Brunke, H. Claude, D. Tarasick, B.J. Johnson, P. Simmonds, D. Shadwick, K. Anlauf, K. Hayden, F. Schmidlin, T. Fujimoto, K. Akagi, C. Meyers, S. Nichol, J. Davies, A. Redondas and E. Cuevas. 2006. Long term changes in tropospheric ozone. Atmos Environ. 40:3156-3173.

Orzechowski, S., J. Socha-Hanc and A. Paszkowski. 1999. Alanine aminotransferase and glycine aminotransferase from maize (*Zea mays* L.) leaves. Acta Biochim Pol. 46:447-457.

Ossipov, V., S. Ossipova, V. Bykov, E. Oksanen, J. Koricheva and E. Haukioja. 2008. Application of metabolomics to genotype and phenotype discrimination of birch trees grown in a long-term open-field experiment. Metabolomics. 4:39-51.

Oufir, M., S. Legay, N. Nicot, K. Van Moer, L. Hoffmann, J. Renaut, J.-F. Hausman and D. Evers. 2008. Gene expression in potato during cold exposure: Changes in carbohydrate and polyamine metabolisms. Plant Sci. 175:839-852.

Overmyer, K., M. Brosché and J. Kangasjärvi. 2003. Reactive oxygen species and hormonal control of cell death. Trends Plant Sci. 8:335-342.

Overmyer, K., H. Tuominen, R. Kettunen, C. Betz, C. Langebartels and H. Sandermann. 2000. Ozone-sensitive *Arabidopsis* rcd1 mutant reveals opposite roles for ethylene and jasmonate signaling pathways in regulating superoxide-dependent cell death. Plant Cell. 12:1849-1862.

Pääkkönen, E., M.S. Günthardt-Goerg and T. Holopainen. 1998a. Response of leaf processes in sensitive birch (*Betula pedula* Roth) clone to ozone combined with drought. Ann Bot. 82:49-59.

Pääkkönen, E., S. Metsärinne, T. Holopainen and L. Kärenlampi. 1995. The ozone sensitivity of birch (*Betula pendula*) in relation to the developmental stage of leaves. New Phytol. 132:145-154.

Pääkkönen, E., S. Seppänen, T. Holopainen, H. Kokko, S. Kärenlampi, L. Kärenlampi and J. Kangasjärvi. 1998b. Induction of genes for the stress proteins PR-10 and PAL in relation to growth, visible injuries and stomatal conductance in birch (*Betula pendula*) clones exposed to ozone and/or drought. New Phytol. 138:295-305.

Pääkkonen, E., J. Vahala, T. Holopainen, R. Karjalainen and L. Karenlampi. 1996. Growth responses and related biochemical and ultrastructural changes of the photosynthetic apparatus in birch (*Betula pendula*) saplings exposed to low concentrations of ozone. Tree Physiol. 16:597-605.

Pääkkönen, E., J. Vahala, M. Pohjola, T. Holopainen and L. Kärenlampi. 1998c. Physiological, stomatal and ultrastructural ozone responses in birch (*Betula pendula* Roth.) are modified by water stress. Plant Cell Environ. 21:671-684.

Padu, E., H. Kollist, I. Tulva, E. Oksanen and H. Moldau. 2006. Components of apoplastic ascorbate use in *Betula pendula* leaves exposed to CO_2 and O_3 enrichment. New Phytol. 165:131-142.

Pandey, A. and M. Mann. 2000. Proteomics to study genes and genomes. Nature. 405:837-846.

Paoletti, E., N. Contran, P. Bernasconi, M.S. Günthardt-Goerg and P. Vollenweider. 2009. Structural and physiological responses to ozone in Manna ash (*Fraxinus ornus* L.) leaves of seedlings and mature trees under controlled and ambient conditions. Sci Total Environ. 407:1631-1643.

Parry, M., O. Canzaiani, J. Palutikof, P. Van der Linden and C. Hanson. 2007. Climate change 2007: Impacts, adaptation and vulnerability; Contribution of working group II to the fourth

assessment report of the intergovernmental panel on climate change. Intergovernmental Panel on Climate Change.

Parry, M.A.J., P.J. Andralojc, S. Khan, P.J. Lea and A.J. Keys. 2002. Rubisco activity: Effects of drought stress. Ann Bot. 89:833-839.

Pasqualini, S., G. Della Torre, F. Ferranti, L. Ederli, C. Piccioni, L. Reale and M. Antonielli. 2002. Salicylic acid modulates ozone-induced hypersensitive cell death in tobacco plants. Physiol Plant. 115:204-212.

Patton, W.F. 2002. Detection technologies in proteome analysis. J Chromatogr B Analyt Technol Biomed Life Sci. 771:3-31.

Pearson, M. and T.A. Mansfield. 1993. Interacting effects of ozone and water stress on the stomatal resistance of beech (*Fagus sylvatica* L.). New Phytol. 123:351-358.

Pell, E.J., N. Eckardt and A.J. Enyedi. 1992. Timing of ozone stress and resulting status of ribulose bisphosphate carboxylase/oxygenase and associated net photosynthesis. New Phytol. 120:397-405.

Pell, E.J., C.D. Schlagnhaufer and R.N. Arteca. 1997. Ozone induced oxidative stress: Mechanisms of action and reaction. Physiol Plant. 100:264-273.

Pell, E.J., J.P. Sinn, B.W. Brendley, L. Samuelson, C. Vinten-Johansen, M. Tien and J. Skillman. 1999. Differential response of four tree species to ozone-induced acceleration of foliar senescence. Plant Cell Environ. 22:779-790.

Pellinen, R., T. Palva and J. Kangasjärvi. 1999. Subcellular localization of ozone-induced hydrogen peroxide production in birch (*Betula pendula*) leaf cells. Plant J. 20:349-356.

Pelloux, J., Y. Jolivet, V. Fontaine, J. Banvoy and P. Dizengremel. 2001. Changes in Rubisco and Rubisco activase gene expression and polypeptide content in *Pinus halepensis* M. subjected to ozone and drought. Plant Cell Environ. 24:123-131.

Peltier, G. and L. Cournac. 2002. Chlororespiration. Annu Rev Plant Biol. 53:523-550.

Petrucco, S., A. Bolchi, C. Foroni, R. Percudani, G.L. Rossi and S. Ottonello. 1996. A maize gene encoding an NADPH binding enzyme highly homologous to isoflavone reducase is activated in response to sulfur starvation. Plant Cell. 8:69-80.

Peuke, A.D., C. Schraml, W. Hartung and H. Rennenberg. 2002. Identification of drought-sensitive beech ecotypes by physiological parameters. New Phytol. 154:373-387.

Plöchl, M., T. Lyons, J. Ollerenshaw and J. Barnes. 2000. Simulating ozone detoxification in the leaf apoplast through the direct reaction with ascorbate. Planta. 210:454-467.

Poon, F. and V.S. Mathura. 2009. Introduction to proteomics. *In* Bioinformatics: A Concept-Based Introduction Eds. V. Mathura and P. Kangueane. Springer, New York, pp 107-113.

Portis, A.R., Jr, C. Li, D. Wang and M.E. Salvucci. 2008. Regulation of Rubisco activase and its interaction with Rubisco. J Exp Bot. 59:1597-1604.

Pratt, J., J. Petty, I. Riba-Garcia, D. Robertson, S. Gaskell, S. Oliver and R. Beynon. 2002. Dynamics of protein turnover, a missing dimension in proteomics. Mol Cell Proteomics. 1:579-591.

Prozherina, N., V. Freiwald, M. Rousi and E. Oksanen. 2003. Interactive effect of springtime frost and elevated ozone on early growth, foliar injuries and leaf structure of birch (*Betula pendula*). New Phytol. 159:623-636.

Pryor, W.A., D.H. Giamalva and D.F. Church. 1984. Kinetics of ozonation. 2. Amino acids and model compounds in water and comparision to rates in nonpolar solvents. J Am Chem Soc. 106:7094-7100.

Pryor, W.A. and R.M. Uppu. 1993. A kinetic model for the competitive reactions of ozone with amino acid residues in proteins in reverse micelles. J Biol Chem. 268:3120-3126.

Quick, W.P. and H.E. Neuhaus. 1997. The regulation and control of photosynthetic carbon assimilation. *In* A molecular approach to primary metabolism in higher plants Eds. C.H. Foyer and W.P. Quick. Taylor & Francis Ltd, London, pp 41-62.

Quirino, B.F., E.S. Candido, P.F. Campos, O.L. Franco and R.H. Krüger. 2010. Proteomic approaches to study plant-pathogen interactions. Phytochemistry. 71:351-362.

Rajinikanth, M., S.A. Harding and C.J. Tsai. 2007. The glycine decarboxylase complex multienzyme family in *Populus*. J Exp Bot. 58:1761-1770.

Ranieri, A., G. D'Urso, C. Nali, G. Lorenzini and G.F. Soldatini. 1996. Ozone stimulates apoplastic antioxidant systems in pumpkin leaves. Physiol Plant. 97:381-387.

Ranieri, A., D. Giuntini, F. Ferraro, C. Nali, B. Baldan, G. Lorenzini and G.F. Soldatini. 2001. Chronic ozone fumigation induces alterations in thylakoid functionality and composition in two poplar clones. Plant Physiol Biochem. 39:999-1008.

Ranieri, A., R. Serini, A. Castagna, C. Nali, B. Baldan, G. Lorenzini and G.F. Soldatini. 2000. Differential sensitivity to ozone in two poplar clones. Analysis of thylakoid pigment-protein complexes. Physiol Plant. 110:181-188.

Rao, M.V. and K.R. Davis. 2001. The physiology of ozone induced cell death. Planta. 213:682-690.

Rao, M.V., J.R. Koch and K.R. Davis. 2000a. Ozone: A tool for probing programmed cell death in plants. Plant Mol Biol. 44:345-358.

Rao, M.V., H.-i. Lee, R.A. Creelman, J.E. Mullet and K.R. Davis. 2000b. Jasmonic acid signaling modulates ozone-induced hypersensitive cell death. Plant Cell. 12:1633-1646.

Rao, M.V., H.-i. Lee and K.R. Davis. 2002. Ozone-induced ethylene production is dependent on salicylic acid, and both salicylic acid and ethylene act in concert to regulate ozone-induced cell death. Plant J. 32:447-456.

Reich, P. 1987. Quantifying plant response to ozone: A unifying theory. Tree Physiol. 3:63-91.

Reich, P.B. 1983. Effects of low concentrations of O_3 on net photosynthesis, dark respiration, and chlorophyll contents in aging hybrid poplar leaves. Plant Physiol. 73:291-296.

Reichenauer, T., H.R. Bolhàr-Nordenkampf, U. Ehrlich, G. Soja, W.F. Postl and F. Halbwachs. 1997. The influence of ambient and elevated ozone concentrations on photosynthesis in *Populus nigra*. Plant Cell Environ. 20:1061-1069.

Reinbothe, C., A. Springer, I. Samol and S. Reinbothe. 2009. Plant oxylipins: Role of jasmonic acid during programmed cell death, defence and leaf senescence. FEBS J. 276:4666-4681.

Reinhardt, D., E.R. Pesce, P. Stieger, T. Mandel, K. Baltensperger, M. Bennett, J. Traas, J. Friml and C. Kuhlemeier. 2003. Regulation of phyllotaxis by polar auxin transport. Nature. 426:255-260.

Reisinger, V. and L.A. Eichacker. 2007. How to analyze protein complexes by 2D Blue Native SDS-PAGE. Proteomics. 10.1002/pmic.200700205

Renaut, J., S. Bohler, J.-F. Hausman, L. Hoffmann, K. Sergeant, N. Ahsan, Y. Jolivet and P. Dizengremel. 2009. The impact of atmospheric composition on plants: A case study of ozone and poplar. Mass Spectrom Rev. 28:495-516.

Renaut, J., J. Hausman and M. Wisniewski. 2006. Proteomics and low-temperature studies: Bridging the gap between gene expression and metabolism126:97-109.

Renaut, J., S. Lutts, L. Hoffmann and J.F. Hausman. 2004. Response of poplar to chilling temperatures: Proteomic and physiological aspects. Plant Biol. 6:81-90.

Rennenberg, H., F. Loreto, A. Polle, F. Brilli, S. Fares, R.S. Beniwal and A. Gessler. 2006. Physiological responses of forest trees to heat and drought. Plant Biol. 8:556-571.

Reumann, S. and A.P. Weber. 2006. Plant peroxisomes respire in the light: some gaps of the photorespiratory C2 cycle have become filled--Others remain. Biochim Biophys Acta. 1763:1496-1510.

Revelle, R. and H. Suess. 1957. Carbon dioxide exchange between atmosphere and ocean and the question of an increase of atmospheric CO_2 during the past decades. Tellus. 9:18-27.

Roose, J.L. and H.B. Pakrasi. 2008. The Psb27 protein facilitates manganese cluster assembly in photosystem II. J Biol Chem. 283:4044-4050.

Rose, J., S. Bashir, J. Giovannoni, M. Jahn and R. Saravanan. 2004. Tackling the plant proteome: Practical approaches, hurdles and experimental tools. Plant J. 39:715-733.

Saiga, S., C. Furumizu, R. Yokoyama, T. Kurata, S. Sato, T. Kato, S. Tabata, M. Suzuki and Y. Komeda. 2008. The *Arabidopsis* OBERON1 and OBERON2 genes encode plant homeodomain finger proteins and are required for apical meristem maintenance. Development. 135:1751-1759.

Samuel, M.A., G.P. Miles and B.E. Ellis. 2000. Ozone treatment rapidly activates MAP kinase signalling in plants. Plant J. 22:367-376.

Samuelson, L. and J.M. Kelly. 2001. Scaling ozone effects from seedlings to forest trees. New Phytol. 149:21-41.

Sandermann, H., Jr. 1996. Ozone and plant health. Annu Rev Phytopathol. 34:347-366.

Sandermann, H., Jr., D. Ernst, W. Heller and C. Langebartels. 1998. Ozone: An abiotic elicitor of plant defence reactions. Trends Plant Sci. 3:47-50.

Sanmartin, M., P.D. Drogoudi, T. Lyons, I. Pateraki, J. Barnes and A.K. Kanellis. 2003. Over-expression of ascorbate oxidase in the apoplast of transgenic tobacco results in altered ascorbate and glutathione redox states and increased sensitivity to ozone. Planta. 216:918-928.

Scheibe, R. 2004. Malate valves to balance cellular energy supply. Physiol Plant. 120:21-26.

Schenk, P.M., K. Kazan, I. Wilson, J.P. Anderson, T. Richmond, S.C. Somerville and J.M. Manners. 2000. Coordinated plant defense responses in *Arabidopsis* revealed by microarray analysis. Proc Natl Acad Sci U S A. 97:11655-11660.

Schoof, H., M. Lenhard, A. Haecker, K.F. Mayer, G. Jurgens and T. Laux. 2000. The stem cell population of *Arabidopsis* shoot meristems is maintained by a regulatory loop between the CLAVATA and WUSCHEL genes. Cell. 100:635-644.

Schraudner, M., D. Ernst, C. Langebartels and H. Sandermann, Jr. 1992. Biochemical plant responses to ozone Ill. Activation of the defense-related proteins fl-1,3-glucanase and chitinase in tobacco leaves. Plant Physiol. 99:1321-1328.

Schraudner, M., C. Langebartels and H. Sandermann. 1997. Changes in the biochemical status of plant cells induced by the environmental pollutant ozone. Physiol Plant. 100:274-280.

Schraudner, M., W. Moeder, C. Wiess, W. Van Camp, D. Inz,, C. Langebartels and H. Sandermann, Jr. 1998. Ozone-induced oxidative burst in the ozone biomonitor plant, tobacco Bel W3. Plant J. 16:235-245.

Schwender, J., J. Ohlrogge and Y. Shachar-Hill. 2004. Understanding flux in plant metabolic networks. Curr Opin Plant Biol. 7:309-317.

Sehmer, L., V. Fontaine, F. Antoni and P. Dizengremel. 1998. Effects of ozone and elevated atmospheric carbon dioxide on carbohydrate metabolism of spruce needles. Catabolic and detoxification pathways. Physiol Plant. 102:605-611.

Seki, M., T. Umezawa, K. Urano and K. Shinozaki. 2007. Regulatory metabolic networks in drought stress responses. Curr Opin Plant Biol. 10:296-302.

Sellmer, J.C., B.H. McCown and B.E. Haissig. 1989. Shoot culture dynamics of six *Populus* clones. Tree Physiol. 5:219-227.

Sétif, P. 2001. Ferredoxin and flavodoxin reduction by photosystem I. Biochim Biophys Acta. 1507:161-179.

Shao, H.-B., L.-Y. Chu, C.A. Jaleel and C.-X. Zhao. 2008a. Water-deficit stress-induced anatomical changes in higher plants. C R Biol. 331:215-225.

Shao, H.B., L.Y. Chu, M.A. Shao, C.A. Jaleel and H.M. Mi. 2008b. Higher plant antioxidants and redox signaling under environmental stresses. C R Biol. 331:433-441.

Sharma, Y.K. and K.R. Davis. 1994. Ozone-induced expression of stress-related genes in *Arabidopsis thaliana*. Plant Physiol. 105:1089-1096.

Sharp, R.E., V. Poroyko, L.G. Hejlek, W.G. Spollen, G.K. Springer, H.J. Bohnert and H.T. Nguyen. 2004. Root growth maintenance during water deficits: Physiology to functional genomics. J Exp Bot. 55:2343-2351.

Sherman, T.D., K.C. Vaughn and S.O. Duke. 1991. A limited survey of the phylogenetic distribution of polyphenol oxidase. Phytochemistry. 30:2499-2506.

Shortle, W.C. and E.A. Bondietti. 1992. Timing, magnitude, and impact of acidic deposition on sensitive forest sites. Water Air Soil Pollut. 61:253-267.

Shulaev, V., D. Cortes, G. Miller and R. Mittler. 2008. Metabolomics for plant stress response. Physiol Plant. 132:199-208.

Singh, A. and M. Agrawal. 2008. Acid rain and its ecological consequences. J Environ Biol. 29:15-24.

Skynner, H.A., T.W. Rosahl, M.R. Knowles, K. Salim, L. Reid, R. Cothilf, G. McAllister and P.C. Guest. 2002. Alterations of stress related proteins in genetically altered mice revealed by two-dimensional differential in-gel electrophoresis. Proteomics. 2:1018-1025.

Smith, A.M. and M. Stitt. 2007. Coordination of carbon supply and plant growth. Plant Cell Environ. 30:1126-1149.

Soldatini, G.F., G. Lorenzini, F. Filippi, C. Nali and L. Guidi. 1998. Photosynthesis of two poplar clones under long-term exposure to ozone. Physiol Plant. 104:707-712.

Soll, J. and E. Schleiff. 2004. Protein import into chloroplasts. Nat Rev Mol Cell Biol. 5:198-208.

Solomon, S., R.R. Garcia, F.S. Rowland and D.J. Wuebbles. 1986. On the depletion of Antarctic ozone. Nature. 321:755-758.

Song, Z., L. Chen and D. Xu. 2010. Bioinformatics methods for protein identification using peptide mass fingerprinting. *In* Methods in molecular biology Eds. S.J. Hubbard and A.R. Jones. Human Press, New York, pp 7-22.

Sponchiado, B.N., J.W. White, J.A. Castillo and P.G. Jones. 1989. Root growth of four common bean cultivars in relation to drought tolerance in environments with contrasting soil types. Exp Agr. 25:249-257.

Sterky, F., R. Bhalerao, P. Unneberg, B. Segerman, P. Nilsson, A. Brunner, L. Charbonnel-Campaa, J. Lindvall, K. Tandre and S. Strauss. 2004. A *Populus* EST resource for plant functional genomics. Proc Natl Acad Sci U S A. 101:13951-13956.

Stewart, D.H. and G.W. Brudvig. 1998. Cytochrome b559 of photosystem II. Biochim Biophys Acta. 1367:63-87.

Stitt, M., J. Lunn and B. Usadel. 2010. *Arabidopsis* and primary photosynthetic metabolism – More than the icing on the cake. Plant J. 61:1067-1091.

Streets, D.G., T.C. Bond, G.R. Carmichael, S.D. Fernandes, Q. Fu, D. He, Z. Klimont, S.M. Nelson, N.Y. Tsai, M.Q. Wang, J.H. Woo and K.F. Yarber. 2003. An inventory of gaseous and primary aerosol emissions in Asia in the year 2000. J Geophys Res. 108:30-1-30-23.

Strohm, M., M. Eiblmeier, C. Langebartels, L. Jouanin, A. Polle, H. Sandermann and H. Rennenberg. 1999. Response of transgenic poplar (*Populus tremula* x *P. alba*) overexpressing glutathion synthetase or glutathion reductase to acute ozone stress: Visible injury and leaf gas exchange. J Exp Bot. 50:365-374.

Sugiura, M. 1992. The chloroplast genome. Plant Mol Biol. 19:149-168.

Sumner, L., P. Mendes and R. Dixon. 2003. Plant metabolomics: Large-scale phytochemistry in the functional genomics era. Phytochemistry. 62:817-836.

Taiz, L. and E. Zeiger. 2002. Plant Physiology, Third Edition. Sinauer Associates, Sunderland.

Takahashi, S. and N. Murata. 2008. How do environmental stresses accelerate photoinhibition? Trends Plant Sci. 13:178-182.

Tamaoki, M., T. Matsuyama and N. Nakajima. 2004. A method for diagnosis of plant environmental stresses by gene expression profiling using cDNA macroarray. Environ Pollut. 131:137-145.

Tamaoki, M., N. Nakajima, A. Kubo, M. Aono, T. Matsuyama and H. Saji. 2003. Transcriptome analysis of O_3-exposed *Arabidopsis* reveals that multiple signal pathways act mutually antagonistically to induce gene expression. Plant Mol Biol. 53:443-456.

Tang, Y., B. Chevone and J. Hess. 1999. Ozone-responsive proteins in a tolerant and sensitive clone of white clover (*Trifolium repens*). Environ Pollut. 104:89-98.

Tausz, M., N.E. Grulke and G. Wieser. 2007. Defense and avoidance of ozone under global change. Environ Pollut. 147:525-531.

Tcherkez, G., G. Cornic, R. Bligny, E. Gout and J. Ghashghaie. 2005. *In vivo* respiratory metabolism of illuminated leaves. Plant Physiol. 138:1596-606.

Tezara, W., V.J. Mitchell, S.D. Driscoll and D.W. Lawlor. 1999. Water stress inhibits plant photosynthesis by decreasing coupling factor and ATP. Nature. 401:914-917.

Tkacz, B., B. Moody, J.V. Castillo and M.E. Fenn. 2008. Forest health conditions in North America. Environ Pollut. 155:409-425.

Torres, N.L., K. Cho, J. Shibato, M. Hirano, A. Kubo, Y. Masuo, H. Iwahashi, N.-S. Jwa, G.K. Agrawal and R. Rakwal. 2007. Gel-based proteomics reveals potential novel protein markers of ozone stress in leaves of cultivated bean and maize species of Panama. Electrophoresis. 28:4369-4381.

Tosti, N., S. Pasqualini, A. Borgogni, L. Ederli, E. Falistocco, S. Crispi and F. Paolocci. 2006. Gene expression profiles of O_3-treated *Arabidopsis* plants. Plant Cell Environ. 29:1686-1702.

Tuominen, H., K. Overmyer, M. Keinänen, H. Kollist and J. Kangasjärvi. 2004. Mutual antagonism of ethylene and jasmonic acid regulates ozone-induced spreading cell death in *Arabidopsis*. Plant J. 39:59-69.

Turcsányil, E., T. Lyons, M. Plöchl and J. Barnes. 2000. Does ascorbate in the mesophyll cell walls form the first line of defence against ozone? Testing the concept using broad bean (*Vicia faba* L.). J Exp Bot. 51:901-910.

Tuskan, G.A., S. Difazio, S. Jansson, J. Bohlmann, I. Grigoriev, U. Hellsten, N. Putnam, S. Ralph, S. Rombauts, A. Salamov, J. Schein, L. Sterck, A. Aerts, R.R. Bhalerao, R.P. Bhalerao, D. Blaudez, W. Boerjan, A. Brun, A. Brunner, V. Busov, M. Campbell, J. Carlson, M. Chalot, J. Chapman, G.L. Chen, D. Cooper, P.M. Coutinho, J. Couturier, S. Covert, Q. Cronk, R. Cunningham, J. Davis, S. Degroeve, A. Dejardin, C. Depamphilis, J. Detter, B. Dirks, I. Dubchak, S. Duplessis, J. Ehlting, B. Ellis, K. Gendler, D. Goodstein, M. Gribskov, J. Grimwood, A. Groover, L. Gunter, B. Hamberger, B. Heinze, Y. Helariutta, B. Henrissat, D. Holligan, R. Holt, W. Huang, N. Islam-Faridi, S. Jones, M. Jones-Rhoades, R. Jorgensen, C. Joshi, J. Kangasjarvi, J. Karlsson, C. Kelleher, R. Kirkpatrick, M. Kirst, A. Kohler, U. Kalluri, F. Larimer, J. Leebens-Mack, J.C. Leple, P. Locascio, Y. Lou, S. Lucas, F. Martin, B. Montanini, C. Napoli, D.R. Nelson, C. Nelson, K. Nieminen, O. Nilsson, V. Pereda, G. Peter, R. Philippe, G. Pilate, A. Poliakov, J. Razumovskaya, P. Richardson, C. Rinaldi, K. Ritland, P. Rouze, D. Ryaboy, J. Schmutz, J. Schrader, B. Segerman, H. Shin, A. Siddiqui, F. Sterky, A. Terry, C.J. Tsai, E. Uberbacher, P. Unneberg, et al. 2006. The genome of black cottonwood, *Populus trichocarpa* (Torr. & Gray). Science. 313:1596-1604.

UNECE. 2004. Present state of emission data EB.AIR/GE.1/2004/10, Geneva, Swizerland.

Uppu, R.M. and W.A. Pryor. 1994. The reactions of ozone with proteins and unsaturated fatty acids in reverse micelles. Chem Res Toxicol. 7:47-55.

Vahala, J., R. Ruonala, M. Keinanen, H. Tuominen and J. Kangasjarvi. 2003. Ethylene insensitivity modulates ozone-induced cell death in birch. Plant Physiol. 132:185-195.

van de Weert, M., F.M. Lagerwerf, J. Haverkamp and W. Heerma. 1998. Mass spectrometry analysis of oxidized tryptophan. J Mass Spectrom. 33:884-891.

van Hees, A. 1997. Growth and morphology of pedunculate oak (*Quercus robur* L) and beech (*Fagus sylvatica* L) seedlings in relation to shading and drought. Ann For Sci. 54:9-18.

van Hove, L.W.A., M.E. Bossen, F.A.M. de Bok and C.A.M. Hooijmaijers. 1999. The uptake of O_3 by poplar leaves: The impact of a long-term exposure to low O_3-concentrations. Atmos Environ. 33:907-917.

van Loon, L.C. 1997. Induced resistance in plants and the role of pathogenesis-related proteins. Eur J Plant Pathol. 103:753-765.

Verweij, H., K. Christiansen and J. van Steveninck. 1982. Ozone-induced formation of O,O'-dityrosine cross-links in proteins. Biochim Biophys Acta. 701:180-184.

Vesteg, M., R. Vacula and J. Krajčovič. 2009. On the origin of chloroplasts, import mechanisms of chloroplast-targeted proteins, and loss of photosynthetic ability — review. Folia Microbiol. 54:303-321.

Vestrengen, V., M. Adams and J. Goodwin. 2004. Inventory review 2004: Emission data reported to CLRTAP and under the NEC directive, EMEP/MSC-W status report 1/04. The Norvegian Meterological Institute, Oslo, Norway.

Viner, D., J. Morison and C. Wallace. 2006. Recent and future climate change and its implications for plant growth. *In* Plant growth and climate change Eds. J. Morison and M. Morecroft. Blachwell Publishing, Oxford, pp 1–16.

Wang, K.L.C., H. Li and J.R. Ecker. 2002. Ethylene biosynthesis and signaling networks. Trends Plant Sci. 14:S131-S151.

Weatherhead, E.C. and S.B. Andersen. 2006. The search for signs of recovery of the ozone layer. Nature. 441:39-45.

Weckwerth, W. 2003. Metabolomics in systems biology. Annu Rev Plant Biol. 54:669-689.

Wiese, C.B. and E.J. Pell. 1997. Influence of ozone on transgenic tobacco plants expressing reduced quantities of Rubisco. Plant Cell Environ. 20:1283-1291.

Wieser, G. and R. Matyssek. 2007. Linking ozone uptake and defense towards a mechanistic risk assessment for forest trees. New Phytol. 174:7-9.

Wilkins, M., C. Pasquali, R. Appel, K. Ou, O. Golaz, J. Sanchez, J. Yan, A. Gooley, G. Hughes and I. Humphery-Smith. 1996. From proteins to proteomes: Large scale protein identification by two-dimensional eectrophoresis and amino acid analysis. Nat Biotechnol. 14:61-65.

Wittig, I., H.-P. Braun and H. Sch„gger. 2006. Blue native PAGE1:418-428.

Wittig, V.E., E.A. Ainsworth and S.P. Long. 2007. To what extent do current and projected increases in surface ozone affect photosynthesis and stomatal conductance of trees? A meta-analytic review of the last 3 decades of experiments. Plant Cell Environ. 30:1150-1162.

Wittig, V.E., E.A. Ainsworth, S.L. Naidu, D.F. Karnosky and S.P. Long. 2009. Quantifying the impact of current and future tropospheric ozone on tree biomass, growth, physiology and biochemistry: A quantitative meta-analysis. Glob Chang Biol. 15:396-424.

Wittmann, C., R. Matyssek, H. Pfanz and M. Humar. 2007. Effects of ozone impact on the gas exchange and chlorophyll fluorescence of juvenile birch stems (*Betula pendula* Roth.). Environ Pollut. 150:258-266.

Wohlgemuth, H., K. Mittelstrass, S. Kschieschan, J. Bender, H.-J. Weigel, K. Overmyer, J. Kangasjärvi, H. Sandermann and C. Langebartels. 2002. Activation of an oxidative burst is a general feature of sensitive plants exposed to the air pollutant ozone. Plant Cell Environ. 25:717-726.

Yi, X., S. Hargett, L. Frankel and T. Bricker. 2008. The effects of simultaneous RNAi suppression of PsbO and PsbP protein expression in photosystem II of *Arabidopsis*. Photosynth Res. 98:439-448.

Yi, X., S.R. Hargett, L.K. Frankel and T.M. Bricker. 2006. The PsbQ protein is required in *Arabidopsis* for photosystem II assembly/stability and photoautotrophy under low light conditions. J Biol Chem. 281:26260-26267.

Yuan, H.-M., K.-L. Li, R.-J. Ni, W.-D. Guo, Z. Shen, C.-P. Yang, B.-C. Wang, G.-F. Liu, C.-H. Guo and J. Jiang. 2010. A systemic proteomic analysis of *Populus* chloroplast by using shotgun method. Mol Biol Rep. doi: 10.1007/s11033-010-9971-y

Yun, S.-C. and J. Laurence. 1999. The response of clones of *Populus tremuloides* differing in sensitivity to ozone in the field. New Phytol. 141:411-421.

Zhang, W., F. Li and L. Nie. 2010. Integrating multiple 'omics' analysis for microbial biology: Application and methodologies. Microbiology. 156:287-301.

Zheng, Y., H. Shimizu and J.D. Barnes. 2002. Limitations to CO_2 assimilation in ozone-exposed leaves of *Plantago major*. New Phytol. 155:67-78.

Additional material

A. Supplemental data

A1. Bohler et al., Proteomics 2007, 7:1584-1599, A DiGE analysis of developing poplar leaves subjected to ozone reveals major changes in carbon metabolism

Supplemental Figures 1: Abundance profiles for all discussed proteins are presented in charts. On the x axis are the days of treatment and on the y axis the standard abundance exported from the Decyder software. Multiple lines of the same color represent spots containing the same protein function. Green circles represent control and red triangles treatment conditions.

1.

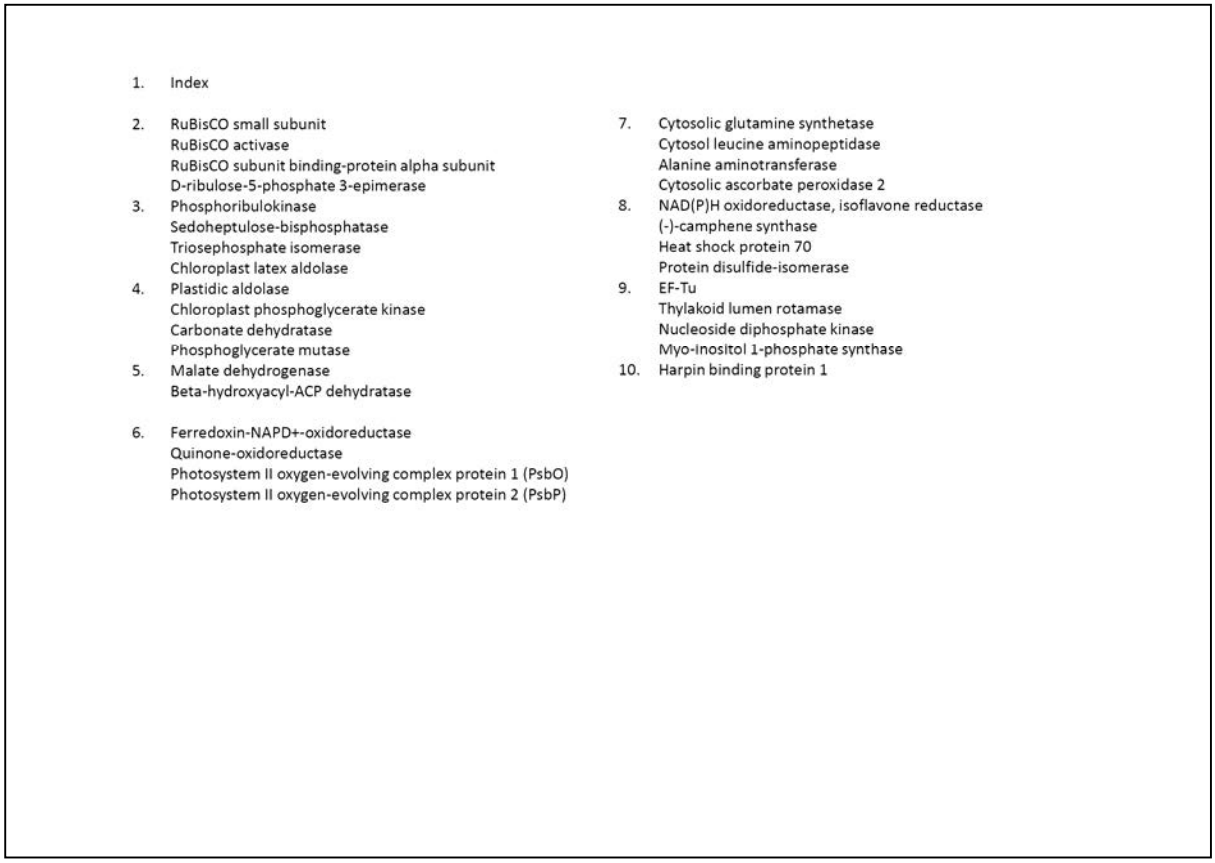

2.

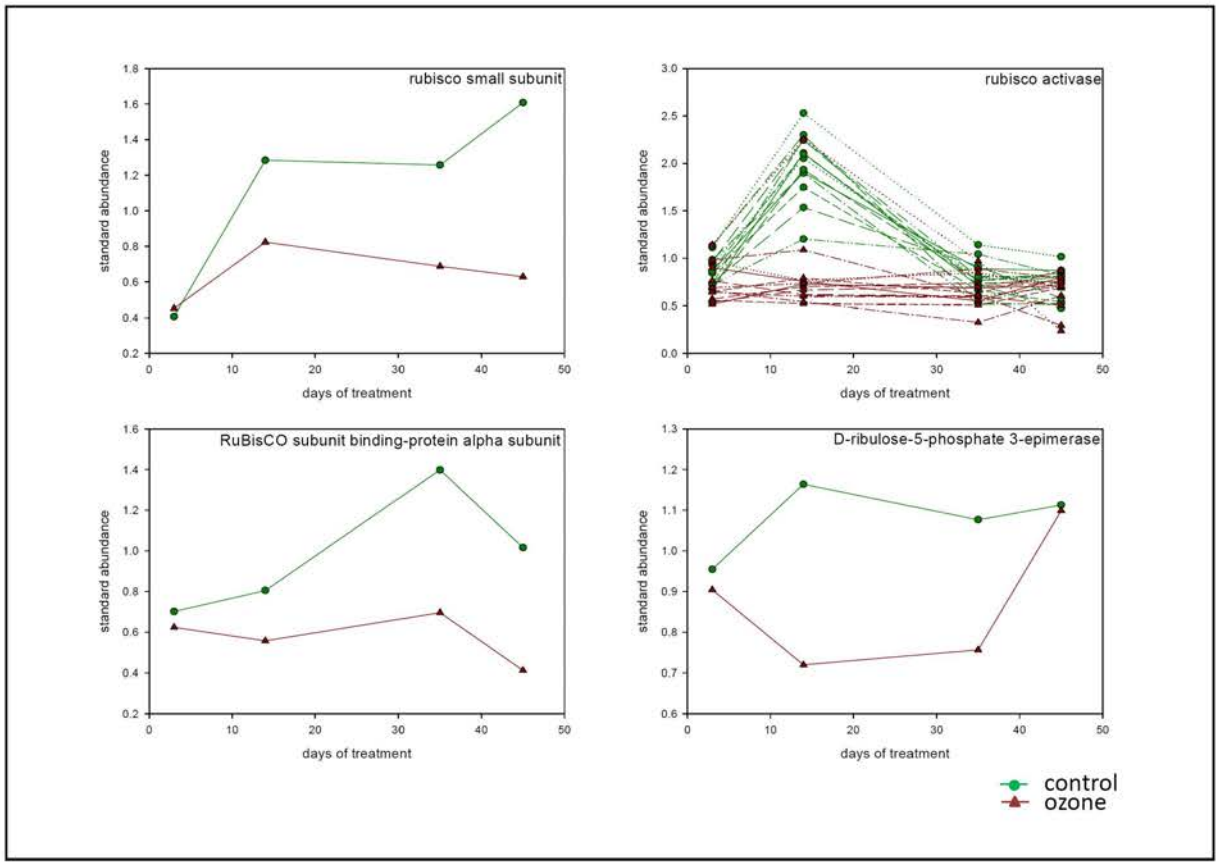
rubisco small subunit
rubisco activase
RuBisCO subunit binding-protein alpha subunit
D-ribulose-5-phosphate 3-epimerase
standard abundance
days of treatment
control
ozone

3.

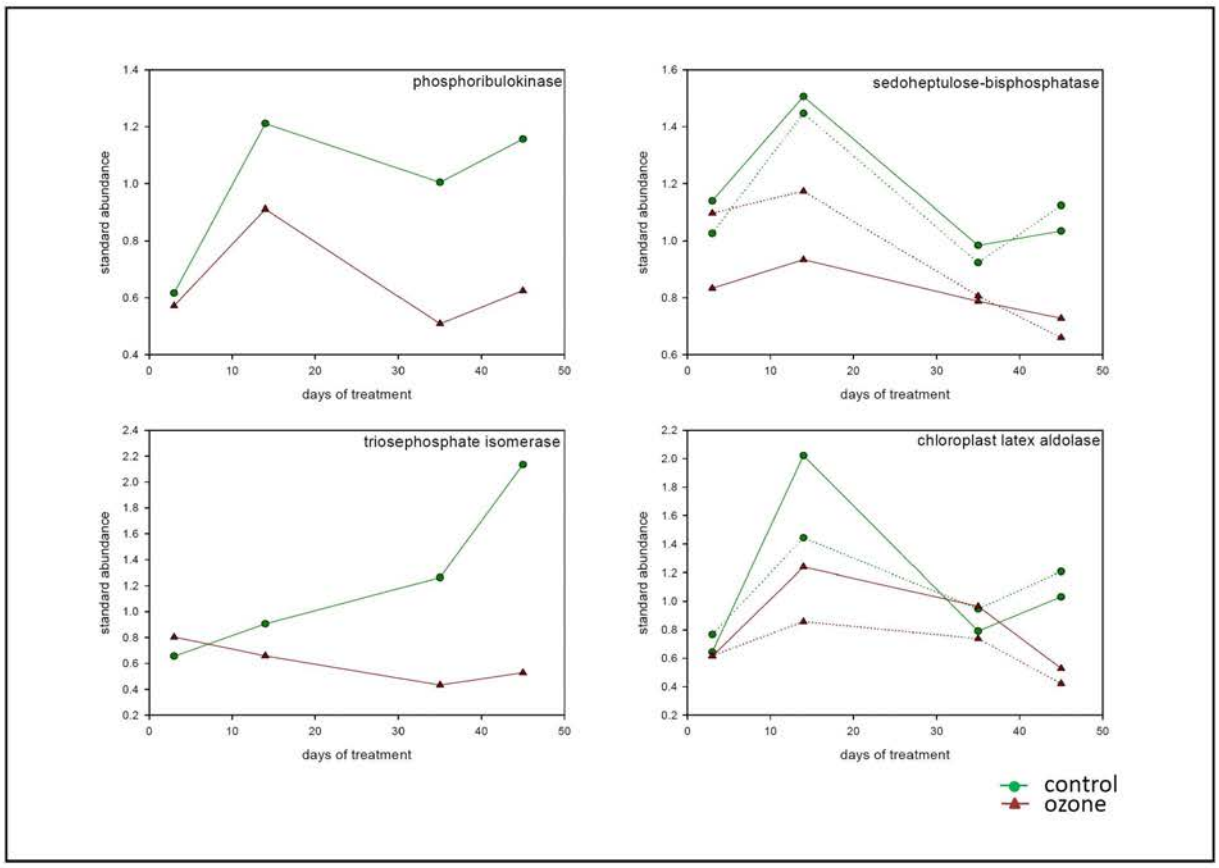
phosphoribulokinase
sedoheptulose-bisphosphatase
triosephosphate isomerase
chloroplast latex aldolase
standard abundance
days of treatment
control
ozone

4.

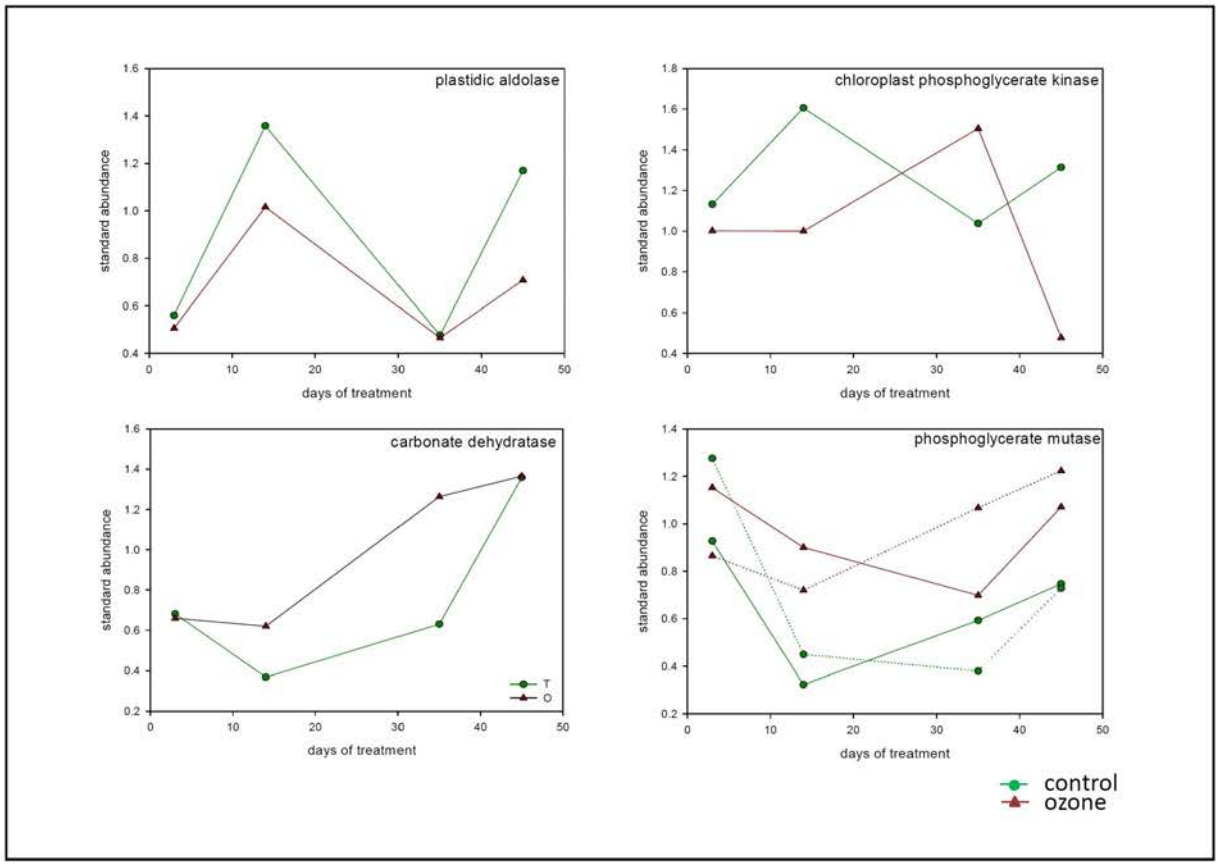
plastidic aldolase
chloroplast phosphoglycerate kinase
carbonate dehydratase
phosphoglycerate mutase
standard abundance
days of treatment
T
O
control
ozone

5.

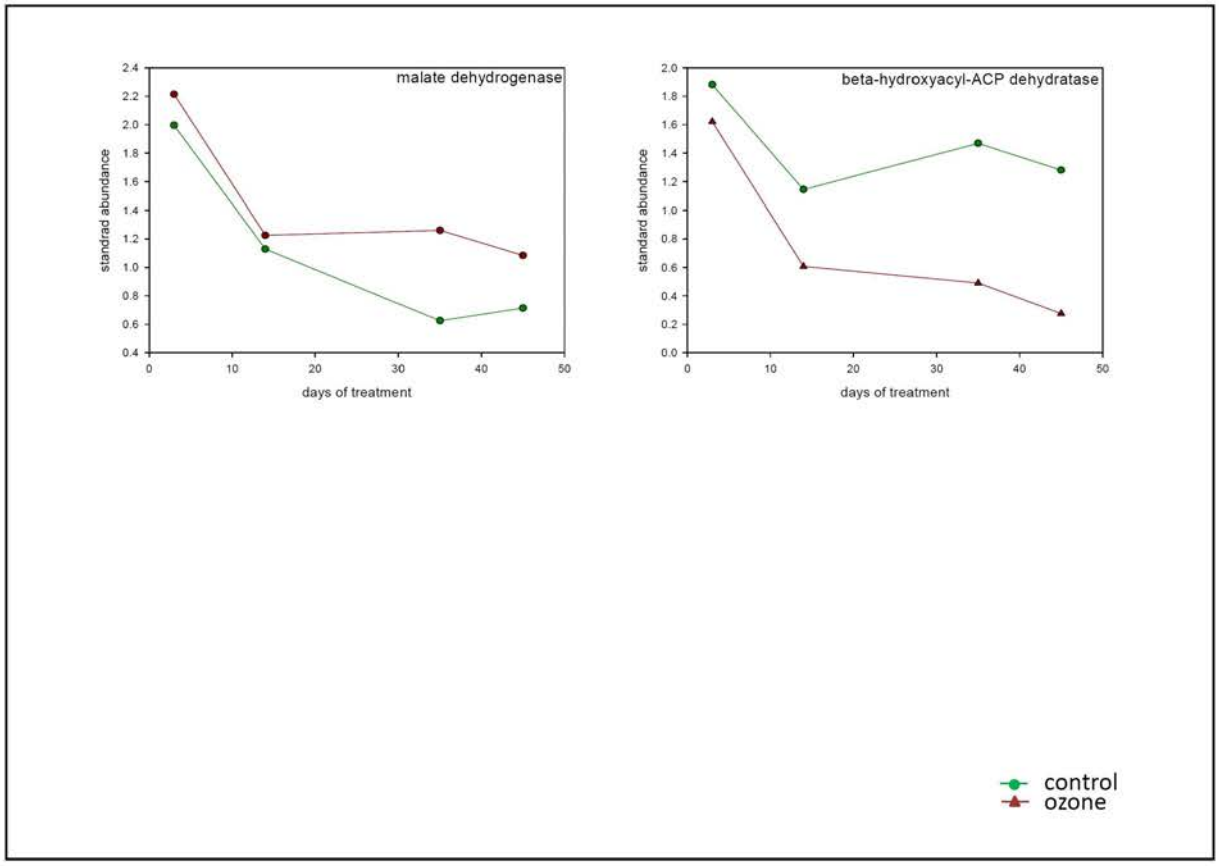
malate dehydrogenase
beta-hydroxyacyl-ACP dehydratase
standrad abundance
standard abundance
days of treatment
control
ozone

6.

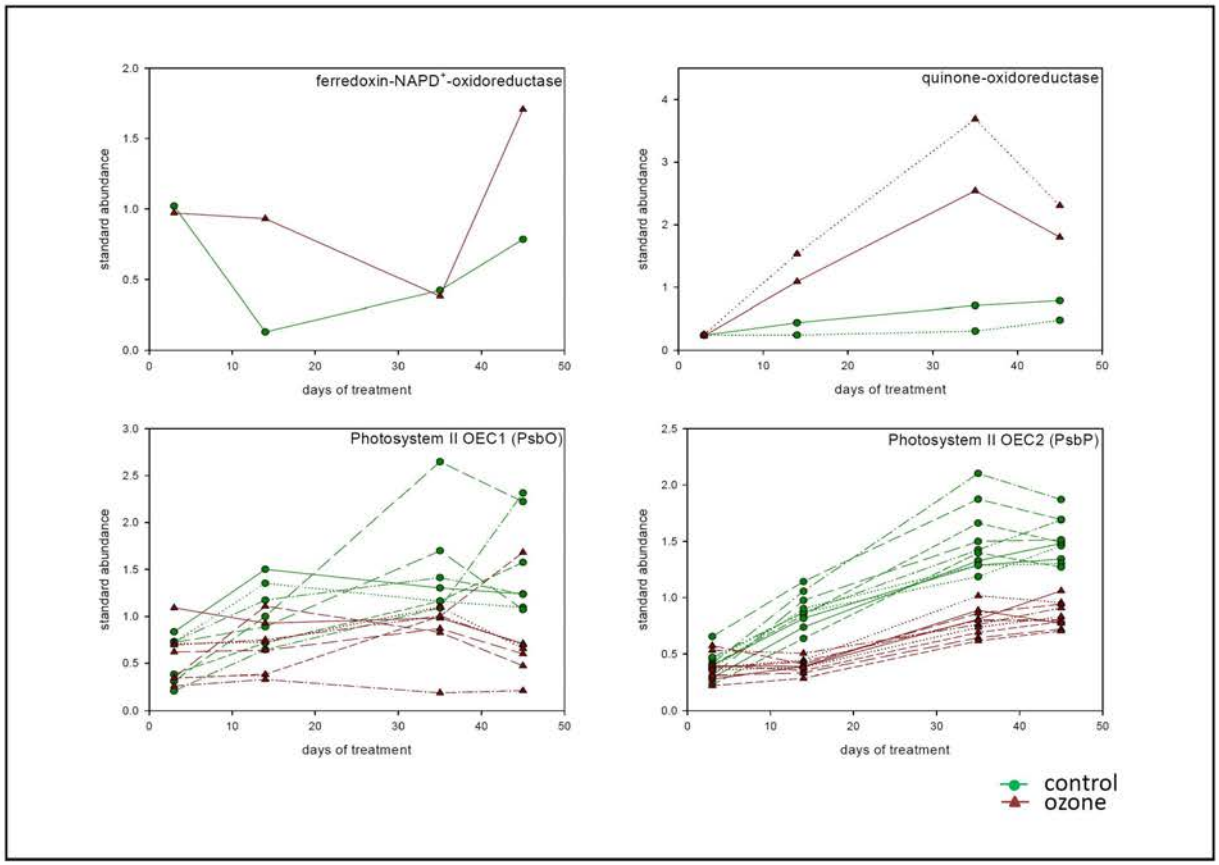
ferredoxin-NAPD+-oxidoreductase
quinone-oxidoreductase
Photosystem II OEC1 (PsbO)
Photosystem II OEC2 (PsbP)
standard abundance
days of treatment
control
ozone

7.

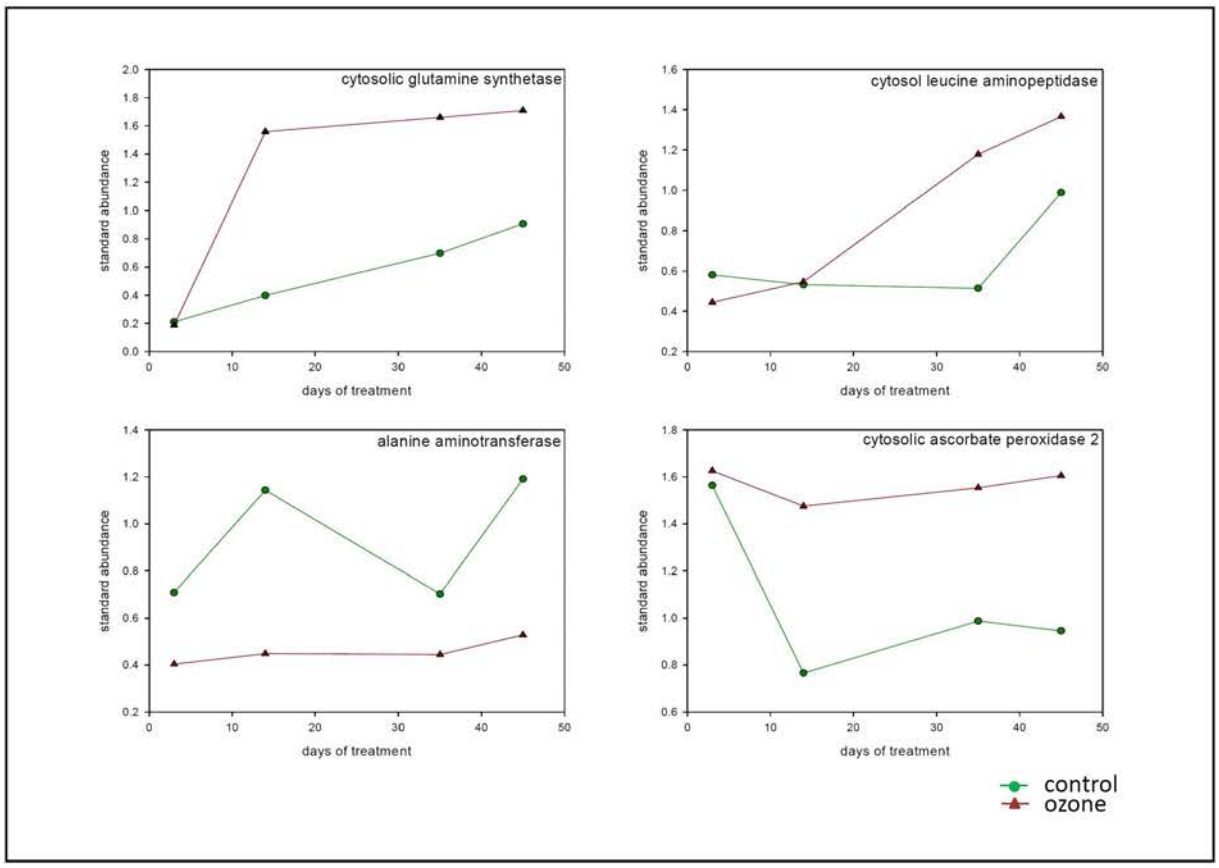
cytosolic glutamine synthetase
cytosol leucine aminopeptidase
alanine aminotransferase
cytosolic ascorbate peroxidase 2
standard abundance
days of treatment
control
ozone

8.

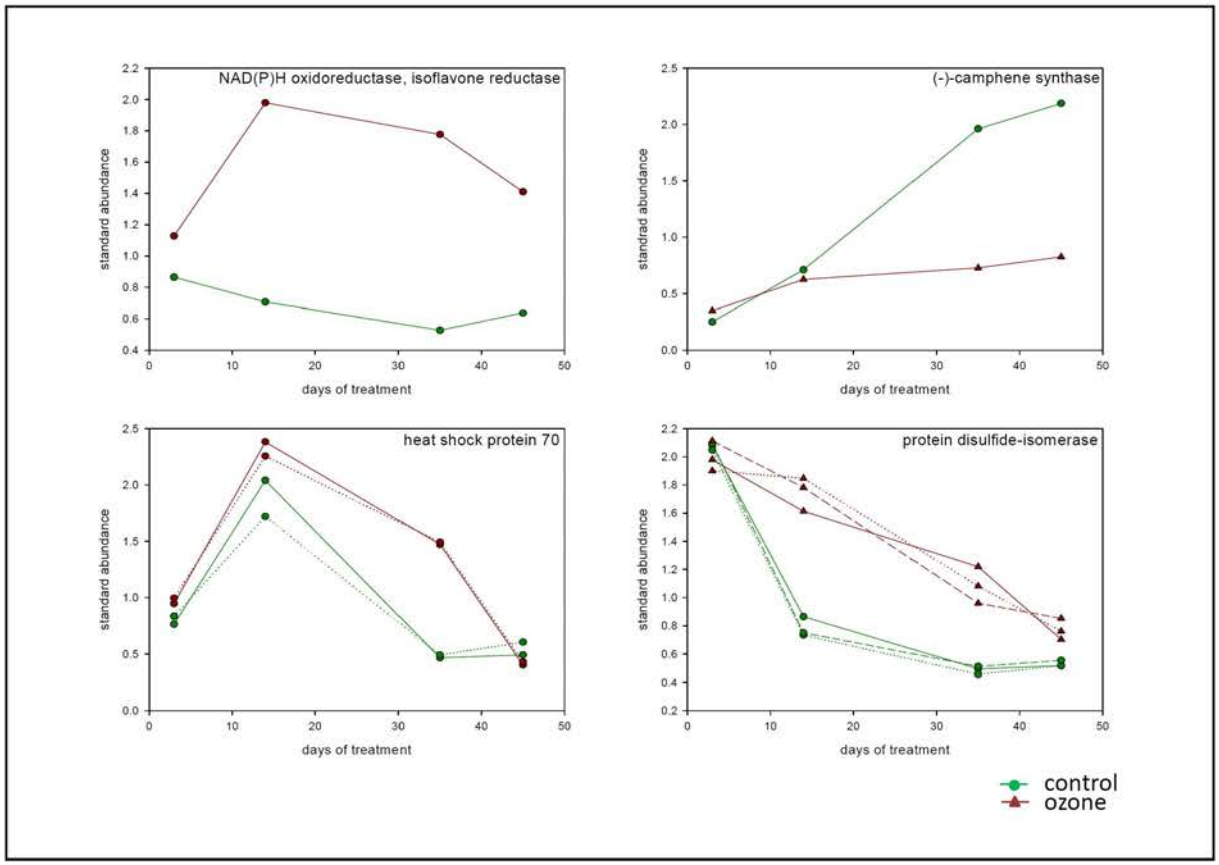
NAD(P)H oxidoreductase, isoflavone reductase
(-)-camphene synthase
heat shock protein 70
protein disulfide-isomerase
standard abundance
standrad abundance
days of treatment
control
ozone

9.

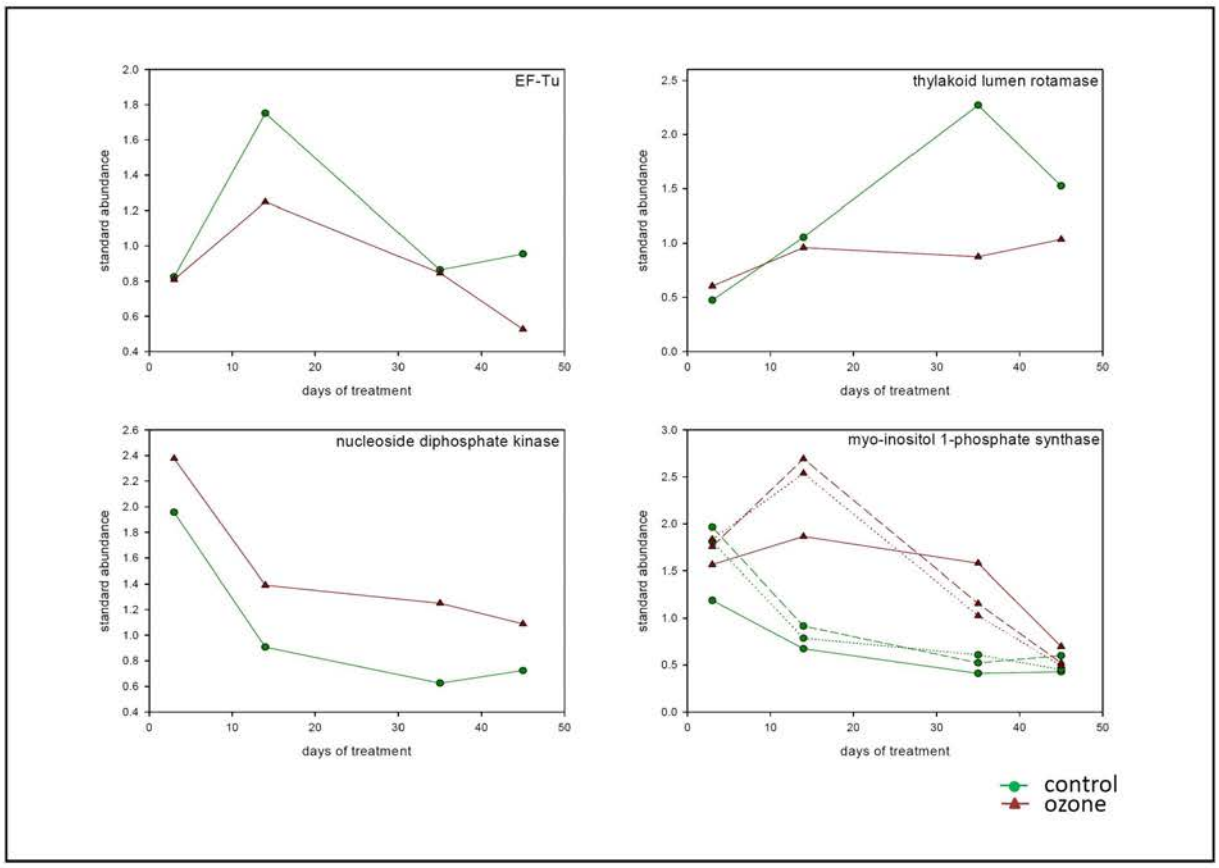
EF-Tu
thylakoid lumen rotamase
nucleoside diphosphate kinase
myo-inositol 1-phosphate synthase
standard abundance
days of treatment
control
ozone

10.

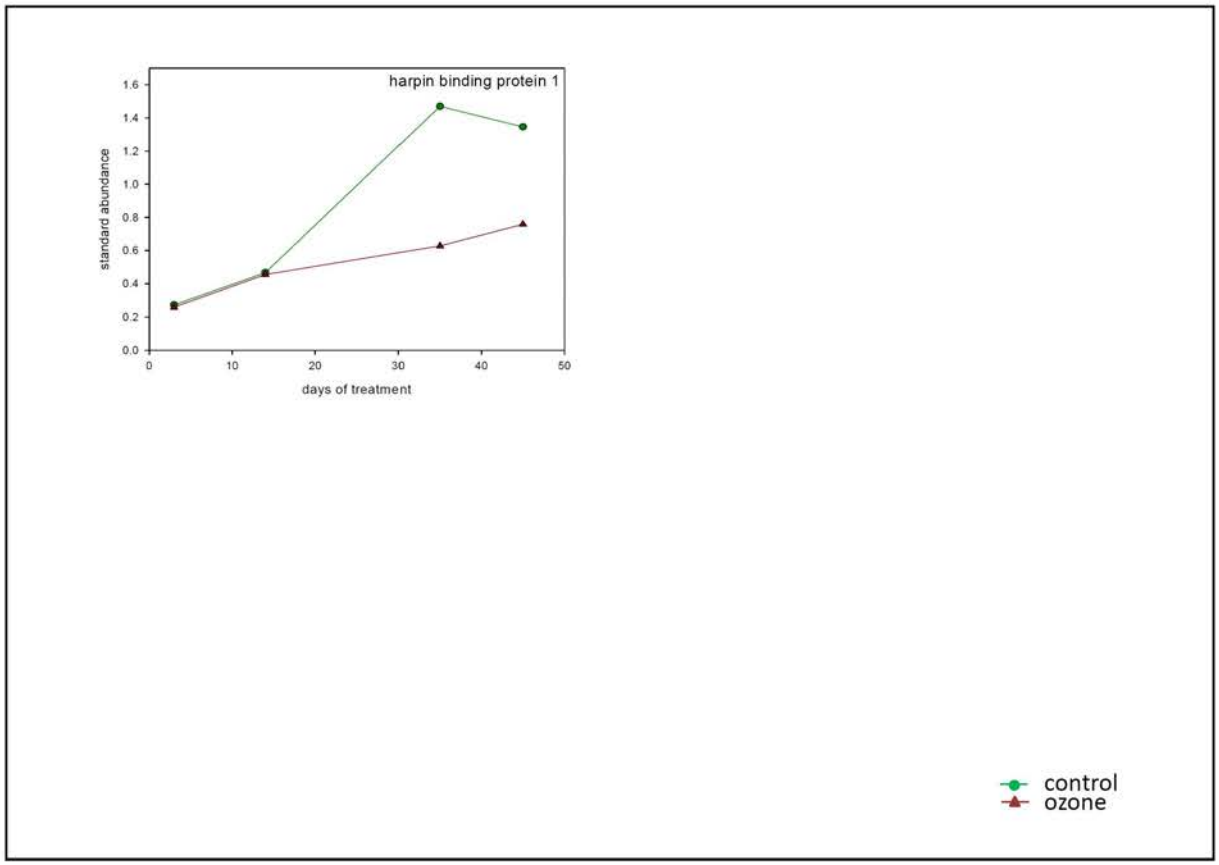
harpin binding protein 1
standard abundance
1.6
1.4
1.2
1.0
0.8
0.6
0.4
0.2
0.0
0
10
20
30
40
50
days of treatment
control
ozone

A2. Bohler et al. Journal of Proteomics submitted, A DiGE study on thylakoids isolated from poplar leaves reveals a negative impact of ozone exposure on membrane proteins

Supplemental Table 1: Full description of the statistical results obtained during the analysis of the effect of ozone treatment compared to control values at each time point. Average ratios are expressed and p-values of Two-Way ANOVA are represented with (i) ozone treatment (cond1); (ii) time course (cond2) and (iii) interaction between these 2 factors (interact). **Spot**: number of the spot on the Master gel; **NCBI**: accession returned by the search in database; **Blast**: the accession of the protein obtained after blasting the accession obtained in NCBI database if not providing a full name for the protein's function (e.g. 'predicted or hypothetical protein'); **Protein name**: Name of the protein as returned either by the search in the database or after blasting the accession obtained in the NCBI database.

Spot	NCBI	Blast	Protein name	Day 7 Av. Ratio	Day 14 Av. Ratio	Day 21 Av. Ratio	Day 28 Av. Ratio	2-ANOVA cond. 1	2-ANOVA cond. 2	2-ANOVA interact
1964	gi|190899066	GI:30013657	oxygen evolving complex 33 kDa photosystem II protein [Nicotiana	1.27	-2.24	-2.60	-2.71	2.24E-03	0.0253	0.402
1990		GI:30013657	tabacum] (PsbO)	-1.93	-1.02	-1.70	1.06	9.38E-03	2.48E-04	0.406
1991		GI:30013657		1.03	-1.83	-2.47	-1.97	1.61E-03	1.78E-03	0.421
1931		GI:30013657		1.10	-1.88	-2.50	-2.45	1.79E-03	3.64E-03	0.421
1946		GI:30013657		-1.20	-1.64	-2.25	-1.77	1.37E-03	3.15E-04	0.604
1898	gi|118489901	GI:30013657		1.52	-1.95	-2.55	-3.08	9.09E-03	0.0335	0.391
2251	gi|224062595	GI:255561128	Oxygen-evolving enhancer protein 2, chloroplast precursor, putative	1.19	-2.58	-4.65	-3.03	1.52E-03	0.0537	0.362
2309		GI:255561128	[Ricinus communis] (PsbP)	1.27	-3.67	-4.04	-1.93	1.03E-03	0.0101	0.34
2656	gi|224116338	GI:255555067	Oxygen-evolving enhancer protein 3, chloroplast precursor, putative	1.02	-2.35	-3.14	-2.18	1.34E-03	0.13	0.421
2671		GI:255555067	[Ricinus communis] (PsbQ)	-1.38	-1.61	-2.36	-1.84	1.12E-03	0.167	0.741
2674		GI:255555067		-2.10	-1.25	-2.46	-1.21	3.02E-03	0.123	0.783
2675		GI:255555067		-1.56	-2.53	-3.42	-1.78	**7.89E-04**	0.243	0.751
2683		GI:255555067		-1.89	-1.60	-2.22	-1.36	1.52E-03	0.126	0.796
2690		GI:255555067		-1.82	-1.85	-3.10	-1.40	**6.86E-04**	0.12	0.575
2692		GI:255555067		1.16	-3.49	-5.21	-3.11	1.15E-03	0.242	0.421
2696		GI:255555067		-1.18	-2.60	-3.96	-2.09	**7.96E-04**	0.238	0.532

2701		GI:255555067		-1.97	-1.74	-3.32	-1.55	7.89E-04	0.2	0.769
2735		GI:255555067		1.40	-2.20	-3.10	-1.77	1.01E-03	0.0983	0.34
2739		GI:255555067		1.10	-1.96	-2.93	-1.43	1.77E-03	0.137	0.34
2546	gi|224126283	GI:255563649	Oxygen-evolving enhancer protein 3-1, chloroplast precursor, putative [Ricinus communis] (PsbQ)	-1.36	-1.15	-1.61	-1.14	9.21E-03	0.146	0.79
2770	gi|224108990	GI:56744293	Putative oxygen evolving enhancer protein 3, identical [Solanum	-1.15	-1.33	-1.82	-1.64	7.89E-04	3.77E-03	0.57
2777		GI:56744293	demissum] (PsbQ)	1.04	-1.41	-1.73	-1.67	1.61E-03	2.91E-04	0.471
2782	gi|118489928	GI:255543290	Photosystem II 11 kDa protein precursor, putative [Ricinus communis]	-1.05	-1.49	-1.75	-1.90	2.18E-03	0.154	0.637
2852		GI:255543290	(Psb27)	1.09	-1.80	-2.39	-2.14	1.23E-03	0.127	0.406
2886		GI:255543290		-1.31	-1.23	-2.00	-1.64	2.12E-03	0.0663	0.75
2903		GI:255543290		-1.79	1.06	-1.72	-1.17	4.84E-03	0.121	0.391
3154	gi|31580909		PSII cytochrome b559 8kDa subunit [Nicotiana sylvestris] (PsbE)	-1.16	-1.48	-1.69	-1.24	1.61E-03	0.059	0.585
2211	gi|118489937	GI:224131950	light-harvesting complex I protein Lhca3 [Populus trichocarpa]	-1.00	-1.52	-1.87	-1.71	4.07E-03	0.0785	0.576
2232		GI:224131950		1.21	-1.81	-2.32	-2.23	1.76E-03	0.115	0.351
2236		GI:224131950		1.21	-1.73	-1.72	-2.06	2.54E-03	0.0385	0.351
2996	gi|118489284	GI:255571379	Photosystem I reaction center subunit N, chloroplast precursor, putative	-1.34	-1.16	-1.51	-1.39	6.83E-03	0.0542	0.807
3037		GI:255571379	[Ricinus communis] (PsaN)	-1.02	-1.40	-1.86	-1.68	5.83E-03	0.118	0.659
2573	gi|118484742	GI:26986114	putative photosystem I reaction centre subunit IV [Populus x canadensis]	-1.26	-1.55	-2.18	-1.40	7.89E-04	0.0414	0.575
2579		GI:26986114	(PsaE)	1.07	-1.63	-1.73	-1.53	4.81E-03	0.083	0.575
2584		GI:26986114		-1.21	-1.58	-2.05	-1.36	1.14E-03	0.0935	0.655
2588		GI:26986114		-1.62	-1.04	-1.38	-1.09	9.99E-03	0.0176	0.57
2589		GI:26986114		-1.08	-1.56	-1.74	-1.63	1.12E-03	0.105	0.604
2595		GI:26986114		-1.18	-1.16	-1.48	-1.30	4.81E-03	2.67E-07	0.79
2608		GI:26986114		-1.77	-1.13	-1.71	-1.06	5.89E-03	0.157	0.634
2609		GI:26986114		-1.53	-1.28	-1.70	-1.05	3.96E-03	0.146	0.75
2615		GI:26986114		-1.88	-1.11	-1.99	-1.04	4.81E-03	0.0794	0.499
1729	gi|118489189	GI:6899972	chloroplast ferredoxin-NADP+ oxidoreductase precursor [Capsicum	-1.24	-1.27	-1.77	-1.34	5.72E-03	8.17E-03	0.794
1733		GI:6899972	annuum]	-1.02	-1.59	-2.18	-1.54	2.57E-03	3.18E-03	0.576
1734		GI:6899972		1.23	-1.85	-1.92	-2.02	8.95E-03	0.026	0.522
1739		GI:6899972		-1.08	-1.45	-2.13	-1.77	3.98E-03	1.01E-03	0.682
1746		GI:6899972		1.22	-2.13	-2.80	-1.85	1.76E-03	3.18E-03	0.391
1765		GI:6899972		1.50	-2.43	-2.92	-2.35	1.97E-03	2.30E-03	0.34
1773		GI:6899972		1.50	-2.29	-2.15	-2.01	5.89E-03	5.75E-04	0.409
1778		GI:6899972		1.65	-2.77	-3.32	-2.86	1.61E-03	1.08E-03	0.34
1760	gi|224074257	GI:6899972		1.94	-3.29	-4.38	-2.81	1.61E-03	0.0112	0.34
1747	gi|147791392	GI:222841756	predicted protein [Populus trichocarpa] homologous to chloroplast	1.75	-2.55	-2.66	-1.76	4.07E-03	0.0102	0.34
			ferredoxin-NADP+ oxidoreductase precursor [Capsicum annuum]							
1008	gi|110227086		ATP synthase beta subunit [Populus alba]	1.30	-2.17	-3.17	-2.90	7.89E-04	0.0349	0.34
1028				1.05	-1.78	-2.67	-2.33	7.89E-04	0.0579	0.351
1048	gi|22094585		ATPase beta subunit [Populus tomentosa]	-1.16	-1.44	-2.29	-1.89	8.33E-04	0.083	0.532
1068				-1.39	-1.15	-1.98	-1.50	1.61E-03	0.118	0.65
1017	gi|134093182		ATP synthase CF1 alpha subunit [Populus trichocarpa]	-1.17	-1.24	-1.42	-1.57	9.38E-03	0.038	0.79
1049				1.28	-1.78	-2.42	-2.32	1.52E-03	2.74E-03	0.34

1076				1.36	-2.07	-2.89	-2.70	1.03E-03	0.038	0.34
1086				1.08	-1.67	-2.39	-2.08	1.03E-03	0.0663	0.362
1095				-1.21	-1.32	-2.07	-1.64	1.03E-03	0.101	0.576
1117				-1.55	-1.01	-1.73	-1.32	3.97E-03	0.119	0.575
2707	gi|110227085		ATP synthase CF1 epsilon subunit [Populus alba]	-1.04	-1.53	-1.96	-1.87	**7.89E-04**	0.179	0.391
2710				1.00	-1.55	-2.45	-1.66	1.61E-03	2.34E-03	0.492
2746				1.09	-1.55	-1.73	-1.51	4.40E-03	0.209	0.471
2758				-1.15	-1.30	-1.95	-1.52	1.59E-03	0.0157	0.575
2755	gi|224141905	GI:15236722	ATP synthase family [Arabidopsis thaliana].	1.06	-1.54	-2.37	-1.77	1.76E-03	0.0766	0.471
1575	gi|118489494	GI:255554879	ATP synthase gamma chain 2, chloroplast, putative [Ricinus communis]	-1.19	-1.40	-1.87	-1.34	2.46E-03	0.067	0.743
1589		GI:255554879		-1.47	-1.24	-1.87	-1.43	1.79E-03	0.171	0.794
1591		GI:255554879		-1.17	-1.53	-2.33	-1.68	1.03E-03	0.2	0.604
1600		GI:255554879		-1.25	-1.65	-2.66	-1.75	**7.89E-04**	0.0552	0.634
1601		GI:255554879		-1.04	-1.64	-1.74	-1.94	1.59E-03	0.251	0.57
1610		GI:255554879		1.14	-1.64	-1.91	-1.81	5.95E-03	0.0178	0.675
1612		GI:255554879		1.03	-1.95	-2.69	-2.15	**7.89E-04**	0.0198	0.421
1613		GI:255554879		1.51	-2.19	-2.79	-2.48	2.54E-03	0.031	0.391
1618		GI:255554879		1.31	-2.31	-3.15	-2.54	**8.52E-04**	0.0102	0.34
1628		GI:255554879		1.02	-1.77	-2.54	-2.13	**7.89E-04**	0.141	0.406
1629		GI:255554879		-1.05	-1.84	-2.66	-2.07	**7.89E-04**	0.026	0.454
1632		GI:255554879		1.21	-2.23	-2.83	-2.20	1.59E-03	0.125	0.463
1638		GI:255554879		1.24	-2.22	-3.02	-2.52	**1.00E-03**	0.0328	0.351
1605	gi|114643		ATP synthase gamma chain, chloroplastic	1.15	-1.77	-1.42	-1.73	8.16E-03	0.0878	0.52
1606	gi|114640			1.19	-1.37	-1.71	-1.58	4.07E-03	0.0135	0.351
2729	gi|224087120	GI:255572525	Thylakoid lumenal 16.5 kDa protein, chloroplast precursor, putative [Ricinus communis]	1.23	-1.85	-2.24	-2.17	1.59E-03	4.21E-03	0.34
1521	gi|195634659	GI:195634659	fructose-bisphosphate aldolase [Zea mays]	1.22	-1.71	-1.86	-1.90	7.59E-03	0.218	0.575
1525	gi|224121620	GI:1773330	glycolate oxidase [Mesembryanthemum crystallinum]	-1.10	-2.13	-3.23	-1.76	**8.22E-04**	2.70E-04	0.406
1532		GI:1773330		-1.34	-1.46	-2.08	-1.31	1.23E-03	3.56E-05	0.682
1533		GI:1773330		-1.25	-1.79	-2.37	-1.69	**7.96E-04**	5.67E-05	0.644
1534		GI:1773330		1.02	-2.27	-3.19	-2.21	**7.89E-04**	3.84E-04	0.362
1537		GI:1773330		-1.40	-1.61	-2.32	-1.30	1.06E-03	6.49E-05	0.615
2059	gi|224082097	GI:255545804	L-ascorbate peroxidase, putative [Ricinus communis]	-1.19	-2.59	-2.76	-2.35	**8.60E-05**	0.113	0.34
2040		GI:255545804		-1.28	-1.32	-1.53	-1.88	2.90E-03	0.115	0.769
2052		GI:255545804		-1.02	-3.05	-4.47	-3.05	**8.60E-05**	0.0403	0.34
1026	gi|224097398		precursor of transferase serine hydroxymethyltransferase 2 [Populus trichocarpa]	1.09	-1.69	-2.42	-1.84	3.83E-03	2.69E-05	0.522
2501	gi|255547634	GI:255547634	peptidyl-prolyl cis-trans isomerase, putative [Ricinus communis]	1.20	-1.76	-1.82	-1.72	4.11E-03	0.0224	0.469
1506	gi|224094418	GI:224094418	predicted protein [Populus trichocarpa] homologous to patatin-like protein 3	1.39	1.51	1.39	-1.09	8.87E-03	0.0197	0.567
1520		GI:224094418	[Nicotiana tabacum]	2.16	2.00	2.18	1.07	2.32E-03	0.21	0.656
1922	gi|118489963	GI:77744911	chloroplast lipocalin [Ipomoea nil]	1.01	-1.48	-1.88	-2.12	1.41E-03	0.0711	0.436
2642	gi|224081186		predicted protein [Populus trichocarpa]	-1.14	-1.54	-1.85	-1.29	3.27E-03	0.0138	0.723

A3. Bohler et al. Tree Physiology in press, Differential impact of chronic ozone exposure on expanding and fully expanded poplar leaves

Supplemental Table 2: Full description of the statistical results obtained during (i) the analysis to the effect of ozone treatment compared to control values at each time point AND (ii) the ageing of the leaves upon control conditions compared towards the value at day 0. Average ratios are expressed and p-value of 2-ways ANOVA are represented for the ozone experiment with (i) ozone treatment (cond1); (ii) time course (cond2) and (iii) interaction between these 2 factors (interact), while only the p-value of One-way ANOVA is represented for the comparison of the different time points in the development of the leaf under control conditions.

					Ozone								Ageing				
					0	7	14	21	28				7	14	21	28	
master number	Protein name	NCBI/EST gi	NCBI blast	subcellular location	Av. Ratio					2-ANOVA cond1	2-ANOVA cond2	2 ANOVA interact	Av. Ratio				1-ANOVA
	Carbon metabolism																
2170	carbonic anhydrase.	gi|1354515	GI:1354515	chl	1.13	-1.01	-1.64	-1.67	-2.70	4.53E-05	1.67E-01	1.52E-03	1.24	1.83	1.62	2.11	4.35E-03
665	rubisco subunit binding-protein beta subunit, rubb, putative [Ricinus communis].	gi|224073124	GI:223537354	chl	1.41	-1.03	1.06	1.89	1.67	1.87E-02	8.36E-12	4.62E-01	-5.93	-5.86	-7.83	-8.28	5.31E-06
667	putative rubisco subunit binding-protein alpha subunit [Trifolium pratense].	gi|224104681	GI:84468456	chl	-1.09	1.08	-1.06	1.16	1.12	7.03E-01	3.45E-06	7.94E-01	1.58	-1.07	-1.14	-1.48	1.04E-03
773	ribulose-1,5-bisphosphate carboxylase/oxygenase large subunit [Populus alba]	gi|17136019	GI:1102708	chl	1.19	-1.15	-1.39	-1.46	-2.18	9.96E-04	3.66E-03	2.10E-02	-1.23	1.04	-1.13	-1.12	3.31E-01
821	ribulose-1,5-bisphosphate carboxylase/oxygenase large subunit [Populus alba]	gi|17136019	GI:1102708	chl	1.16	-1.21	-1.26	-1.11	1.30	5.54E-01	1.18E-06	7.58E-01	6.38	4.53	6.61	3.57	7.95E-05
824	ribulose-1,5-bisphosphate carboxylase/oxygenase large subunit [Populus alba]	gi|17136019	GI:1102708	chl	1.22	-1.16	-1.26	-1.26	-1.15	1.65E-01	7.53E-03	5.67E-01	2.49	1.75	2.54	1.67	1.71E-03
828	ribulose-1,5-bisphosphate carboxylase/oxygenase large subunit [Populus alba]	gi|17136019	GI:1102708	chl	1.19	-1.18	-2.09	-1.73	-2.22	3.12E-04	8.06E-03	3.24E-02	1.34	1.26	1.28	-1.03	4.03E-01
829	ribulose-1,5-bisphosphate carboxylase/oxygenase large subunit [Populus alba]	gi|17136019	GI:1102708	chl	1.15	-1.21	-1.51	-1.07	1.13	4.24E-01	3.04E-10	5.67E-01	11.25	8.73	9.62	6.48	2.87E-06
831	ribulose-1,5-bisphosphate carboxylase/oxygenase large subunit [Populus alba]	gi|17136019	GI:1102708	chl	1.45	-1.22	-1.37	-1.53	-1.69	4.88E-02	3.33E-03	2.71E-01	2.60	1.89	2.43	1.54	6.21E-03
832	ribulose-1,5-bisphosphate carboxylase/oxygenase large subunit [Populus alba]	gi|17136019	GI:1102708	chl	1.32	-1.35	-1.35	-1.54	-1.89	8.57E-03	5.29E-03	1.71E-01	1.99	1.48	1.71	1.15	1.55E-02
833	ribulose-1,5-bisphosphate carboxylase/oxygenase large subunit [Populus alba]	gi|17136019	GI:1102708	chl	1.06	-1.23	-1.39	-2.20	-1.72	5.37E-04	7.22E-04	1.04E-01	-1.04	-1.22	1.20	-1.56	6.08E-02
835	ribulose-1,5-bisphosphate carboxylase/oxygenase large subunit [Populus alba]	gi|17136019	GI:1102708	chl	1.06	-1.20	-1.40	-1.22	-1.05	1.73E-01	4.48E-13	7.96E-01	10.08	7.71	8.75	6.09	3.14E-07
836	ribulose-1,5-bisphosphate carboxylase/oxygenase large subunit [Populus alba]	gi|17136019	GI:1102708	chl	1.10	-1.11	-1.61	-1.51	-1.97	9.97E-03	3.72E-03	4.39E-01	1.58	1.20	1.66	1.06	1.03E-01
838	ribulose-1,5-bisphosphate carboxylase/oxygenase large subunit [Populus alba]	gi|17136019	GI:1102708	chl	-1.02	-1.16	-1.57	-1.42	-1.57	6.19E-04	1.31E-10	2.44E-01	3.76	3.50	3.45	2.77	9.44E-07
842	ribulose-1,5-bisphosphate carboxylase/oxygenase large subunit [Populus alba]	gi|17136019	GI:1102708	chl	1.09	-1.12	-1.57	-1.57	-2.00	2.44E-04	2.35E-03	2.61E-02	1.63	1.80	1.57	1.30	6.86E-03
844	ribulose-1,5-bisphosphate carboxylase/oxygenase large subunit [Populus alba]	gi|17136019	GI:1102708	chl	1.41	-1.24	-1.47	-2.16	-3.32	1.72E-04	2.68E-07	7.11E-04	-1.20	-1.33	1.02	-1.71	1.17E-01
846	ribulose-1,5-bisphosphate carboxylase/oxygenase large subunit [Populus alba]	gi|17136019	GI:1102708	chl	1.24	-1.06	-1.83	-1.79	-2.56	2.06E-05	1.08E-07	5.09E-04	-1.62	-1.24	-1.42	-1.64	2.81E-02
847	ribulose-1,5-bisphosphate carboxylase/oxygenase large subunit [Populus alba]	gi|17136019	GI:1102708	chl	1.54	-1.19	-1.31	-2.33	-2.68	4.08E-03	3.22E-04	7.51E-03	1.14	-1.03	1.73	-1.20	2.59E-01
825	ribulose-1,5-bisphosphate carboxylase/oxygenase large subunit [Populus alba]	gi|343104	GI:1102708	chl	1.21	-1.23	-1.32	-1.11	1.27	4.90E-01	1.95E-08	6.27E-01	10.58	7.46	10.17	5.77	4.76E-06
1047	Ribulose bisphosphate carboxylase/oxygenase activase 1, chloroplast precursor, putative [Ricinus communis]	gi|224109480	GI:223536483	chl	1.10	-1.14	-2.58	-1.92	-1.86	4.41E-06	1.87E-13	2.29E-03	1.02	-1.17	-2.35	-3.46	6.33E-06
1051	Ribulose bisphosphate carboxylase/oxygenase activase 1, chloroplast precursor, putative [Ricinus communis]	gi|224109480	GI:223536483	chl	1.09	-1.19	-2.19	-1.77	-1.83	4.31E-06	0.00E+00	3.70E-03	-1.96	-2.22	-4.33	-6.62	1.34E-07
1052	Ribulose bisphosphate carboxylase/oxygenase activase 1, chloroplast precursor, putative [Ricinus communis]	gi|224109480	GI:223536483	chl	1.11	-1.16	-2.09	-1.61	-1.77	2.68E-03	5.43E-12	1.14E-01	-2.53	-2.23	-5.38	-4.68	9.47E-05
1102	Ribulose bisphosphate carboxylase/oxygenase activase 1, chloroplast precursor, putative [Ricinus communis]	gi|224109480	GI:223536483	chl	1.20	-1.16	-2.49	-1.70	-1.10	3.04E-03	3.90E-13	1.53E-02	-1.96	-2.11	-3.87	-6.38	1.17E-06
1208	Ribulose bisphosphate carboxylase/oxygenase activase 1, chloroplast precursor, putative [Ricinus communis]	gi|224109480	GI:223536483	chl	1.32	-1.24	-1.30	-1.02	1.38	6.82E-01	1.77E-03	9.05E-01	3.87	3.11	2.52	1.40	2.93E-04
1211	Ribulose bisphosphate carboxylase/oxygenase activase 1, chloroplast precursor, putative [Ricinus communis]	gi|224109480	GI:223536483	chl	1.02	-1.24	-1.72	-1.34	-1.16	3.63E-02	1.60E-07	5.39E-01	5.51	4.02	2.68	1.36	6.08E-06
1238	Ribulose bisphosphate carboxylase/oxygenase activase 1, chloroplast precursor, putative [Ricinus communis]	gi|224109480	GI:223536483	chl	1.12	-1.12	-2.14	-2.12	-2.02	3.17E-07	2.33E-15	3.31E-04	-1.80	-1.88	-2.95	-3.56	1.13E-06
1212	Ribulose bisphosphate carboxylase/oxygenase activase 1, chloroplast precursor, putative [Ricinus communis]	gi|118486739	GI:223536483	chl	-1.07	-1.26	-1.71	-1.51	-1.28	8.13E-04	1.09E-10	4.03E-01	3.48	2.35	1.65	-1.06	3.94E-06
1217	Ribulose bisphosphate carboxylase/oxygenase activase 1, chloroplast precursor, putative [Ricinus communis]	gi|118486739	GI:223536483	chl	-1.08	-1.32	-2.34	-1.75	-1.39	2.05E-05	5.20E-10	4.98E-02	2.73	2.06	1.25	-1.58	4.50E-06
1226	Ribulose bisphosphate carboxylase/oxygenase activase 1, chloroplast precursor, putative [Ricinus communis]	gi|118489408	GI:223536483	chl	-1.02	-1.23	-2.06	-1.66	-1.64	1.36E-06	3.58E-11	3.09E-03	1.68	1.42	-1.33	-2.07	3.52E-06
1232	Ribulose bisphosphate carboxylase/oxygenase activase 1, chloroplast precursor, putative [Ricinus communis]	gi|118489105	GI:223536483	chl	-1.03	-1.20	-2.39	-1.88	-1.64	3.74E-08	6.00E-15	6.98E-04	1.16	-1.00	-1.83	-2.83	1.03E-07
1069	ribulose-1,5-bisphosphate carboxylase/oxygenase activase 2 [Gossypium hirsutum]	gi|224109480	GI:12620883	chl	1.03	-1.16	-1.85	-1.94	-1.62	1.38E-07	3.07E-12	7.38E-04	1.67	1.25	-1.05	-1.51	5.85E-06
1233	ribulose-1,5-bisphosphate carboxylase/oxygenase activase 2 [Gossypium hirsutum]	gi|224109480	GI:12620883	chl	1.05	-1.18	-2.30	-1.92	-1.93	1.54E-08	0.00E+00	2.08E-04	-1.47	-1.66	-2.87	-3.84	1.94E-07
448	transketolase 1 [Capsicum annuum].	gi|224063766	GI:3559814	chl	1.10	-1.21	-1.35	-1.57	-1.53	5.86E-03	4.38E-09	3.30E-01	4.47	2.97	3.46	2.98	5.03E-06
451	transketolase 1 [Capsicum annuum].	gi|224063766	GI:3559814	chl	1.03	-1.20	-1.43	-1.68	-1.98	2.97E-05	1.76E-08	3.80E-02	3.12	2.25	2.54	2.24	5.94E-06
447	transketolase, putative [Ricinus communis].	gi|224063766	GI:223548870	chl	1.19	-1.19	1.16	-1.24	-1.14	6.09E-01	1.29E-07	3.72E-01	3.37	2.02	2.75	2.19	7.72E-05
453	transketolase 1 [Capsicum annuum].	gi|227467170	GI:3559814	chl	1.06	-1.19	-1.36	-1.80	-2.07	4.83E-05	6.89E-04	1.28E-02	1.71	1.30	1.38	1.28	3.05E-02
454	transketolase 1 [Capsicum annuum].	gi|227467170	GI:3559814	chl	1.20	-1.24	-1.38	-1.88	-1.95	4.67E-04	6.02E-03	2.11E-02	1.26	-1.03	1.02	1.05	4.92E-01
456	transketolase 1 [Capsicum annuum].	gi|224127366	GI:3559814	cyt	1.23	-1.29	-1.46	-1.92	-2.28	2.20E-05	6.24E-03	2.35E-03	1.83	1.41	1.58	1.48	8.34E-03
457	transketolase 1 [Capsicum annuum].	gi|224127366	GI:3559814	cyt	1.15	-1.14	-1.50	-1.91	-2.47	3.41E-05	3.70E-02	2.07E-03	1.52	1.38	1.44	1.49	8.23E-02
461	transketolase 1 [Capsicum annuum].	gi|224127366	GI:3559814	cyt	1.26	-1.14	-1.32	-2.12	-2.52	2.11E-04	7.10E-05	1.71E-03	-1.15	-1.22	-1.15	-1.24	8.61E-01
1363	glyceraldehyde 3-phosphate dehydrogenase, putative [Ricinus communis]	gi|24072834	GI:255543455	chl	1.24	-1.15	1.10	-1.05	-1.19	9.01E-01	5.25E-04	5.76E-01	2.19	2.10	2.59	2.64	9.67E-03
1369	glyceraldehyde 3-phosphate dehydrogenase, putative [Ricinus communis]	gi|118488847	GI:223547801	chl	-1.05	1.04	1.12	1.13	1.22	1.62E-01	1.58E-11	7.73E-01	2.56	2.22	2.47	2.40	1.66E-05
1392	glyceraldehyde 3-phosphate dehydrogenase, putative [Ricinus communis]	gi|118488847	GI:223547801	chl	-1.08	1.10	1.14	1.30	1.27	8.88E-02	1.15E-10	5.06E-01	2.59	2.29	2.49	2.69	8.75E-05
1391	glyceraldehyde 3-phosphate dehydrogenase, putative [Ricinus communis]	gi|224119602	GI:223550350	cyt	-1.11	1.11	1.27	1.34	1.32	4.87E-03	9.99E-16	1.07E-01	3.26	3.01	3.19	3.11	6.58E-07
1408	glyceraldehyde 3-phosphate dehydrogenase, putative [Ricinus communis]	gi|224119602	GI:223550350	cyt	-1.01	1.07	1.13	1.13	1.07	2.01E-01	1.88E-08	6.93E-01	1.60	1.64	1.59	1.85	2.47E-05
1440	glyceraldehyde 3-phosphate dehydrogenase, putative [Ricinus communis]	gi|224119602	GI:223550350	cyt	-1.00	1.10	1.15	1.05	-1.34	7.14E-01	2.18E-09	2.92E-01	-3.47	-2.64	-3.25	-2.20	1.03E-06
869	RecName: Full=NADP-dependent glyceraldehyde-3-phosphate dehydrogenase; AltName: Full=Non-phosphory	gi|75206970		cyt	-1.08	-1.04	-1.08	-1.46	-1.36	2.31E-03	8.38E-10	2.23E-01	2.10	1.98	2.03	1.46	1.97E-05
1213	phosphoglycerate kinase, putative [Ricinus communis].	gi|224109060	GI:223547261	chl	1.18	-1.01	-1.91	-1.72	-1.65	3.87E-06	2.31E-07	1.11E-04	-1.15	1.04	-1.34	-1.20	6.37E-02
1214	phosphoglycerate kinase, putative [Ricinus communis].	gi|224109060	GI:223547261	chl	1.01	1.06	-1.70	-1.26	-1.63	1.24E-03	4.01E-02	1.97E-02	-1.14	1.12	-1.22	1.23	8.53E-02
1221	phosphoglycerate kinase, putative [Ricinus communis].	gi|224109060	GI:223547261	chl	1.14	1.03	-1.90	-1.37	-1.43	4.97E-03	7.96E-04	2.69E-02	1.16	1.13	-1.16	-1.13	1.90E-01
1222	phosphoglycerate kinase, putative [Ricinus communis].	gi|224109060	GI:223547261	chl	1.19	1.01	-2.00	-2.10	-1.60	7.14E-05	5.09E-06	1.41E-03	1.30	1.23	-1.10	-1.15	7.56E-03
1234	phosphoglycerate kinase, putative [Ricinus communis].	gi|224109060	GI:223547261	chl	1.10	1.09	-1.36	-1.62	-2.79	4.18E-04	2.69E-06	5.69E-04	-1.98	-1.36	-1.70	-1.32	6.09E-03
1230	phosphoglycerate kinase, putative [Ricinus communis].	gi|224101335	GI:223547261	cyt	1.24	1.11	-1.60	-1.53	-2.04	1.48E-04	7.74E-02	1.05E-04	-1.21	1.19	1.03	1.26	1.62E-02
1242	phosphoglycerate kinase, putative [Ricinus communis].	gi|118489457	GI:223547261	chl	1.11	-1.02	-1.77	-1.90	-2.69	2.55E-06	1.04E-01	2.49E-04	1.19	1.38	1.20	1.46	8.99E-02
2114	triosephosphate isomerase, putative [Ricinus communis].	gi|118481011	GI:223527042	cyt	1.09	-1.02	-1.02	-1.31	-1.16	2.19E-01	1.17E-04	4.68E-01	-1.17	1.08	1.42	1.72	5.88E-04
2111	triosephosphate isomerase, putative [Ricinus communis].	gi|224098421	GI:223527042	cyt	-1.09	1.01	-1.65	-1.38	-1.99	1.06E-04	6.81E-04	2.92E-02	-1.52	-1.12	-1.50	-1.07	4.13E-02
2140	triosephosphate isomerase, putative [Ricinus communis].	gi|118481564	GI:223527042	cyt	1.01	-1.04	-1.58	-1.53	-2.28	2.48E-05	1.32E-09	2.17E-03	-1.79	-1.55	-2.29	-1.73	2.46E-04

2144	triose phosphate isomerase cytosolic isoform-like [Solanum tuberosum].	gi|224112769	GI:77745458	cyt	-1.03	-1.22	-1.32	-1.11	-1.61	1.12E-03	2.03E-07	1.79E-01	-2.05	-1.16	-1.45	-1.00	8.72E-04
1426	fructose 1,6-bisphosphatase [Brassica rapa subsp. pekinensis].	gi|224082438	GI:73811203	cyt	-1.05	-1.01	-1.07	-1.37	-1.67	2.56E-03	4.45E-01	4.33E-02	1.07	1.04	1.11	1.44	1.24E-01
1294	fructose-bisphosphate aldolase, putative [Ricinus communis].	gi|118489355	GI:223528861	chl	1.18	1.70	-1.44	-1.07	-1.35	2.41E-01	2.36E-06	3.21E-01	-5.55	-1.97	-2.32	-2.55	7.25E-03
1351	fructose-bisphosphate aldolase, putative [Ricinus communis].	gi|73870782	GI:223528861	chl	1.03	1.02	1.49	1.19	1.10	1.57E-01	1.78E-08	7.66E-01	-2.32	-2.45	-3.16	-2.95	6.52E-06
1323	fructose-bisphosphate aldolase-like [Solanum tuberosum].	gi|118489199	GI:78191410	cyt	-1.06	1.23	-1.31	-1.36	1.12	2.74E-01	5.75E-07	7.90E-01	-4.71	-3.23	-3.86	-4.00	3.71E-04
1373	fructose-bisphosphate aldolase [Glycine max].	gi|14490650	GI:40457267	cyt	1.20	-1.01	-1.76	-1.32	-2.24	6.25E-03	2.10E-03	2.37E-02	-1.30	1.25	-1.34	-1.16	1.35E-01
1304	sedoheptulose-1,7-bisphosphatase, chloroplast, putative [Ricinus communis].	gi|224098511	GI:223530064	chl	1.08	-1.09	-1.70	-1.18	1.27	2.59E-01	4.98E-09	1.90E-01	4.13	3.85	3.18	2.20	5.02E-06
1309	sedoheptulose-1,7-bisphosphatase, chloroplast, putative [Ricinus communis].	gi|224098511	GI:223530064	chl	1.14	-1.09	-1.37	-1.16	1.04	2.18E-01	5.47E-06	1.65E-01	2.08	2.01	1.83	1.35	2.33E-04
1316	sedoheptulose-1,7-bisphosphatase, chloroplast, putative [Ricinus communis].	gi|224098511	GI:223530064	chl	1.15	1.01	-1.19	-1.06	1.07	9.61E-01	1.68E-07	1.10E-01	-1.20	-1.06	-1.33	-1.54	1.03E-03
1315	sedoheptulose-1,7-bisphosphatase, chloroplast, putative [Ricinus communis].	gi|3854546	GI:255579134	chl	1.07	-1.08	-1.26	-1.18	1.04	1.03E-01	6.29E-10	1.65E-01	2.15	2.16	1.88	1.61	4.51E-07
637	NADP-dependent malic protein [Ricinus communis].	gi|224142207	GI:8118507	cyt	1.14	-1.09	1.54	1.64	1.21	3.75E-03	2.84E-09	7.96E-02	-2.39	-1.89	-1.58	-1.04	1.65E-05
647	NADP-dependent malic protein [Ricinus communis].	gi|224142207	GI:8118507	cyt	-1.18	1.19	1.21	1.41	-1.23	5.02E-01	0.00E+00	6.81E-02	1.44	4.10	4.20	8.22	7.95E-11
643	NADP-dependent malic protein [Ricinus communis].	gi|20469	GI:8118507	cyt	1.02	1.17	1.41	1.51	1.03	2.80E-02	6.99E-15	3.83E-01	1.33	2.61	3.52	5.97	1.93E-07
635	malic enzyme [Populus trichocarpa].	gi|20469	GI:20469	cyt	1.03	-1.07	1.22	1.89	1.52	3.09E-03	8.74E-10	3.97E-02	-2.32	-1.32	-1.51	1.16	5.84E-04
651	malic enzyme.	gi|23987329	GI:228412	cyt	-1.38	-1.13	1.44	1.36	-1.59	6.33E-01	3.68E-07	8.55E-02	-1.31	1.21	1.33	2.83	3.93E-04
1466	NAD-dependent malate dehydrogenase [Prunus persica].	gi|224102193	GI:15982948	cyt	-1.05	-1.00	-1.32	-1.35	-1.44	9.74E-04	3.59E-12	1.32E-01	-2.44	-2.05	-2.48	-2.15	2.40E-06
1601	malate dehydrogenase, putative [Ricinus communis].	gi|224061310	GI:223536453	mit	-1.08	-1.03	1.18	1.04	1.07	5.55E-01	4.02E-10	8.16E-01	-1.86	-2.93	-2.45	-2.56	3.65E-05
1563	malate dehydrogenase, putative [Ricinus communis].	gi|224061310	GI:223536453	mit	-1.23	-1.15	-1.73	-1.34	-1.64	2.10E-04	7.69E-05	3.96E-01	-2.07	-1.19	-1.47	-1.31	1.84E-02
1510	malate dehydrogenase, putative [Ricinus communis].	gi|224114557	GI:223536453	mit	-1.02	1.04	1.06	-1.03	-1.33	3.40E-01	9.94E-13	3.74E-01	-3.38	-3.19	-3.56	-2.80	2.27E-06
1395	glycolate oxidase	gi|228403		per	1.18	-1.06	-1.09	-1.73	-1.96	1.11E-03	9.43E-02	1.65E-03	1.16	1.03	1.19	1.25	2.95E-01
1561	enoyl-ACP reductase [Malus x domestica].	gi|224053010	GI:82569446	n.a.	-1.00	-1.01	-1.06	-1.06	-1.14	4.89E-01	1.63E-12	9.47E-01	-2.90	-3.51	-4.11	-3.66	4.32E-06
1494	Quinone oxidoreductase-like protein [Arabidopsis thaliana].	gi|224140597	GI:21553644	cyt	1.18	1.00	-1.40	-1.58	-1.83	2.52E-04	2.81E-14	1.27E-03	-2.11	-1.84	-2.54	-2.79	3.58E-06
1474	Quinone oxidoreductase-like protein [Arabidopsis thaliana].	gi|224140597	GI:21553644	cyt	-1.26	-1.01	-1.03	1.06	1.09	6.39E-01	5.36E-13	3.27E-01	2.45	1.87	1.72	1.69	1.84E-05
799	mitochondrial lipoamide dehydrogenase [Populus tremuloides]	gi|50061579	GI:134142802	mit	1.06	-1.02	1.11	-1.23	-1.28	2.23E-01	5.10E-10	1.52E-01	2.36	1.95	2.24	1.92	6.22E-06
800	dihydrolipoamide dehydrogenase [Novosphingobium aromaticivorans DSM	gi|68052018	GI:87199200	mit	-1.05	-1.02	1.06	-1.32	-1.50	1.58E-02	8.18E-11	6.00E-02	2.32	2.24	2.52	2.31	1.27E-06
807	dihydrolipoamide dehydrogenase [Novosphingobium aromaticivorans DSM	gi|134142802	GI:87199200	mit	-1.02	1.03	-1.03	-1.45	-1.75	4.30E-03	2.99E-02	1.39E-02	1.04	1.02	1.17	1.03	8.74E-01
1482	lactoylglutathione lyase, putative [Ricinus communis].	gi|224078584	GI:223542315	cyt	-1.05	1.11	-1.10	-1.31	-1.89	2.08E-02	2.77E-04	2.05E-02	-1.15	-1.00	1.07	2.08	1.61E-03
785	ATP synthase beta subunit [Populus alba].	gi|110227086	GI:110227086	chl	1.19	-1.01	-1.28	-1.23	-1.62	6.59E-02	5.26E-04	1.98E-01	1.96	1.79	2.10	2.36	2.79E-04
2423	LHCA1 [Arabidopsis thaliana].	gi|145332845		chl	1.16	-1.03	-1.36	-1.78	-1.63	6.20E-04	2.17E-05	7.16E-03	1.81	1.97	2.36	2.40	2.02E-05
2419	light-harvesting complex I protein Lhca1 [Populus trichocarpa].	gi|118489209	GI:224109746	chl	1.04	-1.03	-1.76	-2.23	-2.18	1.59E-07	1.94E-11	1.45E-04	2.62	3.31	3.97	4.65	3.26E-08
2244	light-harvesting complex I protein Lhca3 [Populus trichocarpa].	gi|118489937	GI:224131950	chl	-1.18	1.06	-1.19	1.05	1.15	8.76E-01	0.00E+00	5.78E-01	6.59	7.60	9.86	9.26	4.26E-08
2286	light-harvesting complex I protein Lhca3 [Populus trichocarpa].	gi|118489937	GI:224131950	chl	-1.09	1.15	-1.15	-1.27	-1.80	2.70E-04	1.11E-16	2.71E-04	1.69	2.53	3.18	4.57	2.46E-10
2292	light-harvesting complex I protein Lhca3 [Populus trichocarpa].	gi|118489937	GI:224131950	chl	-1.13	1.11	-1.35	-1.34	-1.96	2.82E-07	6.38E-12	2.30E-05	-1.04	1.61	1.78	2.70	3.17E-10
2104	light-harvesting complex II protein Lhcb1 [Populus trichocarpa].	gi|118489863	GI:224083006	chl	1.03	1.31	-1.23	-1.31	-1.30	2.18E-01	4.54E-14	3.41E-02	1.62	2.81	3.34	4.86	3.41E-07
2132	light-harvesting complex II protein Lhcb1 [Populus trichocarpa].	gi|118489863	GI:224083006	chl	1.02	1.15	1.06	-1.30	-1.95	9.99E-02	5.14E-05	5.14E-02	1.15	1.22	2.12	2.85	3.20E-04
1833	oxygen evolving enhancer protein 1 precursor [Bruguiera gymnorhiza]	gi|118489276	GI:119952178	chl	1.00	1.08	-1.63	-1.42	-1.30	9.33E-03	1.12E-03	2.06E-01	-1.91	-1.20	-1.32	-1.01	1.32E-04
1805	oxygen evolving enhancer protein 1 precursor [Bruguiera gymnorhiza]	gi|118489276	GI:119952178	chl	-1.04	1.04	-1.33	-1.02	1.16	6.13E-01	9.89E-12	5.62E-01	2.98	3.70	4.58	3.82	2.01E-06
1818	oxygen evolving enhancer protein 1 precursor [Bruguiera gymnorhiza]	gi|118489276	GI:119952178	chl	-1.16	1.03	-1.40	-1.05	-1.06	5.85E-02	0.00E+00	3.31E-01	3.69	5.16	5.08	5.27	2.65E-09
1824	oxygen evolving enhancer protein 1 precursor [Bruguiera gymnorhiza]	gi|118489276	GI:119952178	chl	-1.09	1.02	-1.49	-1.11	-1.25	1.31E-02	5.92E-10	3.38E-01	1.60	2.60	2.26	2.80	2.10E-06
1885	Oxygen-evolving enhancer protein 1, chloroplast precursor, putative [Ricinus communis]	gi|190899066	GI:223538464	chl	-1.01	1.03	-1.47	-1.29	-1.77	9.14E-04	1.39E-04	4.17E-02	-1.80	-1.22	-1.43	-1.10	1.88E-03
1807	Oxygen-evolving enhancer protein 1, chloroplast precursor, putative [Ricinus communis]	gi|190899066	GI:223538464	chl	-1.08	1.04	-1.28	-1.00	1.05	5.03E-01	1.44E-11	7.43E-01	3.12	3.97	4.29	3.91	1.17E-06
1876	Oxygen-evolving enhancer protein 1, chloroplast precursor, putative [Ricinus communis]	gi|190899066	GI:223538464	chl	1.09	1.01	-1.29	1.06	1.18	8.78E-01	1.01E-13	3.50E-01	3.78	4.49	5.01	4.15	2.58E-07
1883	Oxygen-evolving enhancer protein 1, chloroplast precursor, putative [Ricinus communis]	gi|190899066	GI:223538464	chl	-1.10	1.01	-1.45	-1.18	1.07	1.70E-01	1.14E-11	2.13E-01	2.98	3.83	3.92	3.19	1.14E-05
1884	Oxygen-evolving enhancer protein 1, chloroplast precursor, putative [Ricinus communis]	gi|190899066	GI:223538464	chl	-1.11	1.02	-1.42	-1.07	-1.24	1.36E-02	1.42E-09	3.75E-01	1.60	2.36	2.03	2.38	4.11E-06
2327	Oxygen-evolving enhancer protein 2, chloroplast precursor, putative [Ricinus communis]	gi|224085421	GI:223539254	chl	1.02	1.09	-1.44	-1.31	-1.68	8.46E-04	1.99E-09	1.55E-02	1.50	2.45	2.60	3.08	4.36E-08
2278	Oxygen-evolving enhancer protein 2, chloroplast precursor, putative [Ricinus communis]	gi|224062595	GI:223539254	chl	1.07	1.03	-1.44	-1.26	-1.74	1.11E-03	4.64E-03	1.39E-02	1.02	1.52	1.51	1.89	1.29E-04
2935	chloroplast oxygen-evolving enhancer protein [Manihot esculenta].	gi|224078826	GI:56122682	chl	-1.15	1.32	-1.85	-1.71	-1.76	6.82E-04	2.79E-14	6.57E-03	1.39	5.57	6.76	7.80	3.30E-08
2714	Photosystem I reaction center subunit II, chloroplast precursor, putative [Ricinus communis].	gi|224099787	GI:223543860	chl	1.09	1.10	-1.24	-1.07	-1.13	3.71E-01	4.92E-14	2.51E-01	1.72	2.83	3.09	3.53	1.15E-07
2717	Photosystem I reaction center subunit II, chloroplast precursor, putative [Ricinus communis].	gi|118489639	GI:223543860	chl	-1.14	1.09	-1.17	-1.16	1.02	6.22E-01	5.48E-11	9.33E-01	2.74	3.92	5.16	5.32	3.56E-05
2729	Photosystem I reaction center subunit II, chloroplast precursor, putative [Ricinus communis].	gi|224099787	GI:223543860	chl	-1.11	1.08	-1.10	-1.01	1.18	8.95E-01	0.00E+00	7.95E-01	3.89	5.89	8.05	8.02	2.03E-08
2732	chloroplast photosystem I protein [Populus tremula].	gi|192764683	GI:192764631	chl	-1.02	1.22	1.10	1.10	1.70	1.36E-01	1.30E-12	5.14E-01	2.95	3.87	6.19	4.91	2.94E-07
2932	PSI reaction center subunit III [Citrus sinensis].	gi|118484742	GI:157678952	chl	-1.07	1.16	-1.35	-1.20	-1.46	4.70E-02	3.14E-10	2.20E-01	1.41	2.80	2.64	3.39	3.07E-05
1675	ferredoxin-NADP oxidoreductase	gi|170111		chl	1.05	1.07	-1.21	-1.66	-1.92	4.54E-03	6.00E-08	3.02E-02	3.22	2.48	3.10	2.91	1.20E-05
1699	chloroplast ferredoxin-NADP+ oxidoreductase precursor [Capsicum annuum]	gi|118489189	GI:6899972	chl	1.09	1.14	-1.40	-1.98	-2.76	4.07E-04	1.09E-02	1.06E-03	1.54	1.52	1.60	1.71	4.62E-02
1693	chloroplast ferredoxin-NADP+ oxidoreductase precursor [Capsicum annuum]	gi|52536292	GI:6899972	chl	-1.03	1.04	-1.47	-1.64	-1.97	6.03E-04	8.99E-10	4.76E-02	3.49	3.52	3.46	3.42	1.62E-06
1714	chloroplast ferredoxin-NADP+ oxidoreductase precursor [Capsicum annuum]	gi|118489189	GI:6899972	chl	1.21	1.12	-1.31	-1.34	-2.06	4.35E-02	1.02E-10	6.55E-02	-1.78	-2.06	-3.26	-3.52	5.65E-05
1666	chloroplast ferredoxin-NADP+ oxidoreductase precursor [Capsicum annuum]	gi|52536292	GI:6899972	chl	1.06	-1.08	-1.18	-1.41	-1.42	8.81E-02	4.96E-08	6.20E-01	4.27	3.07	3.81	3.34	2.00E-04
680	polyphenol oxidase [Populus trichocarpa].	gi|224116966	GI:224117444	chl	1.20	-1.25	2.26	3.57	1.98	1.44E-05	8.83E-06	1.76E-03	2.17	1.48	1.51	2.02	1.67E-02
683	polyphenol oxidase [Populus trichocarpa].	gi|224116966	GI:224117444	chl	1.00	-1.17	2.57	3.09	1.95	3.76E-05	1.18E-06	2.03E-03	2.12	1.46	1.82	2.00	5.21E-02
685	polyphenol oxidase [Populus trichocarpa].	gi|224116966	GI:224117444	chl	1.05	1.22	1.35	3.52	1.91	9.08E-05	1.74E-04	1.01E-02	-1.38	1.18	-1.03	1.17	1.71E-01
	Protein metabolism																
1327	glutamine synthetase [Gossypium raimondii].	gi|224079530	GI:159138927	cyt	-1.12	1.03	2.13	1.42	1.60	1.83E-03	8.83E-11	2.94E-02	1.33	1.94	2.54	2.71	2.02E-04
1332	glutamine synthetase [Gossypium raimondii].	gi|224079530	GI:159138927	cyt	1.01	1.11	1.98	1.23	1.07	8.50E-03	1.25E-11	6.11E-02	1.78	2.50	2.85	3.25	1.79E-05
1311	glutamine synthetase [Gossypium raimondii].	gi|224079530	GI:159138927	cyt	-1.07	1.08	1.49	1.54	1.25	5.92E-04	2.39E-10	3.04E-02	-1.58	1.14	1.23	1.33	6.60E-04
425	vitamin-b12 independent methionine synthase, 5-methyltetrahydropteroyltriglutamate-homocysteine [Populus trichocarpa]	gi|224131686	GI:224131686	cyt	1.01	-1.06	-1.12	-1.88	-1.63	7.44E-03	1.05E-05	1.16E-01	-1.76	-1.73	-2.01	-1.65	2.97E-03
429	vitamin-b12 independent methionine synthase, 5-methyltetrahydropteroyltriglutamate-homocysteine [Populus trichocarpa]	gi|224131686	GI:224131686	cyt	1.07	-1.00	-1.01	-1.33	-1.97	4.32E-02	5.01E-09	8.42E-02	-3.28	-2.24	-3.53	-2.61	9.01E-06
430	vitamin-b12 independent methionine synthase, 5-methyltetrahydropteroyltriglutamate-homocysteine [Populus trichocarpa]	gi|224131686	GI:224131686	cyt	1.13	-1.07	1.09	-3.89	-2.98	1.94E-02	1.06E-08	5.20E-03	-2.54	-2.09	-2.77	-2.66	2.58E-04
984	s-adenosylmethionine synthetase 4 [Populus trichocarpa].	gi|224130888	GI:224130888	cyt	-1.15	-1.03	1.27	1.27	1.31	1.69E-01	5.72E-05	3.80E-01	-1.10	-1.64	-1.87	-2.06	1.74E-04
993	s-adenosylmethionine synthetase 4 [Populus trichocarpa].	gi|224130888	GI:224130888	cyt	-1.07	-1.00	1.31	-1.05	1.16	9.54E-01	5.48E-09	9.10E-01	-2.38	-2.53	-3.55	-5.46	4.68E-07
1002	s-adenosylmethionine synthetase 4 [Populus trichocarpa].	gi|224130888	GI:224130888	cyt	-1.03	-1.00	1.10	-1.31	-1.28	2.83E-01	5.64E-08	6.61E-01	-2.15	-2.47	-2.91	-4.95	2.24E-05
1005	alanine aminotransferase 2 [Glycine max].	gi|224110900	GI:158122137	per	1.14	-1.02	-1.17	-1.61	-1.96	7.55E-03	4.57E-12	2.95E-02	-2.79	-2.25	-2.83	-3.48	3.71E-05
971	alanine aminotransferase 2 [Glycine max].	gi|224110900	GI:158122137	per	-1.37	-1.02	-1.10	-1.65	-1.29	7.66E-03	2.64E-03	4.24E-01	1.17	1.11	1.00	-1.20	3.90E-01
982	alanine aminotransferase 2 [Glycine max].	gi|224110900	GI:158122137	per	1.06	-1.11	-1.27	-1.82	-2.03	4.91E-04	9.66E-10	2.97E-02	-1.41	-1.35	-1.80	-2.32	2.28E-03
1630	serine carboxypeptidase (carboxypeptidase D), putative [Musa acuminata].	gi|224096538	GI:102139937	per	1.07	1.13	2.14	2.19	2.10	7.00E-07	3.56E-03	1.21E-02	-1.23	-1.23	-1.10	-1.02	7.20E-01
418	glycyl-tRNA synthetase / glycine--tRNA ligase [Arabidopsis thaliana].	gi|222845136	GI:18397278	cyt	-1.19	1.05	1.19	1.19	1.04	5.15E-01	1.05E-12	3.15E-01	4.23	2.72	2.61	3.02	2.77E-07
941	mitochondrial serine hydroxymethyltransferase [Populus tremuloides].	gi|224087339	GI:134142067	mit	1.06	-1.02	-1.24	-1.54	-1.36	1.31E-02	3.01E-07	1.30E-01	-1.39	-1.13	-1.38	-2.28	3.13E-03
	Protein folding																
364	heat shock protein [Arabidopsis thaliana].	gi|224111838	GI:1906830	chl	1.17	1.05	1.18	1.18	-1.17	2.85E-01	1.94E-11	8.17E-01	-2.24	-2.75	-4.01	-4.61	8.64E-05
467	chloroplast HSP70 [Cucumis sativus].	gi|224120086	GI:124245039	chl	-1.04	-1.03	1.06	-1.07	1.20	8.41E-01	1.19E-05	7.87E-01	1.92	1.17	1.28	-1.08	1.72E-03
468	chloroplast HSP70 [Cucumis sativus].	gi|224120086	GI:124245039	chl	1.14	1.06	-1.33	-1.22	-1.22	1.64E-01	6.03E-14	2.68E-01	-2.74	-2.76	-3.80	-3.34	2.37E-06
283	heat shock protein 90 [Oryza sativa].	gi|224085900	GI:18855040	cyto	1.11	1.38	2.19	1.87	1.69	9.39E-06	2.68E-04	8.37E-02	1.33	1.42	1.23	1.10	2.28E-01
472	heat shock protein 70 [Cucumis sativus].	gi|224072248	GI:6911549	cyto	-1.11	1.12	1.61	1.74	1.50	1.91E-03	5.19E-03	4.37E-02	1.37	1.06	-1.28	-1.12	2.67E-02
475	heat shock protein 70 [Cucumis sativus].	gi|224072248	GI:6911549	cyto	1.07	1.11	1.60	1.53	1.85	5.90E-04	1.50E-03	1.97E-01	1.69	1.25	1.20	1.10	4.58E-02

476	heat shock protein 70 [Cucumis sativus].	gi|224072248	GI:6911549	cyto	1.06	1.15	1.79	1.31	-1.03	1.68E-01	4.37E-07	4.37E-01	-2.59	-2.99	-3.94	-3.10	2.86E-05
479	heat shock protein 70 [Cucumis sativus].	gi|224072248	GI:6911549	cyto	1.11	1.09	1.34	1.19	-1.14	8.58E-01	4.10E-07	7.93E-01	-3.83	-4.16	-5.49	-3.48	4.13E-05
500	heat shock protein, putative [Ricinus communis].	gi|224100971	GI:223527999	cyto	1.18	1.08	1.08	-1.21	-1.73	3.79E-01	4.94E-12	2.24E-01	-4.99	-5.22	-8.29	-5.38	2.79E-06
504	heat shock protein, putative [Ricinus communis].	gi|224113495	GI:223527999	cyto	-1.10	1.06	1.19	1.47	1.04	2.63E-01	8.03E-03	2.78E-01	1.07	-1.26	-1.80	-1.25	5.75E-04
505	heat shock protein, putative [Ricinus communis].	gi|224113495	GI:223527999	cyto	1.05	1.12	1.32	1.12	-1.43	8.42E-01	1.13E-11	1.88E-01	-2.56	-3.32	-5.26	-2.86	3.29E-07
503	heat shock protein, putative [Ricinus communis].	gi|224113495	GI:223527999	cyto	-1.05	1.05	1.40	1.61	1.44	7.05E-05	2.16E-08	1.09E-02	1.90	1.31	1.03	1.27	3.42E-05
508	heat shock protein, putative [Ricinus communis].	gi|224113495	GI:223527999	cyto	-1.00	1.06	1.63	1.52	1.75	3.60E-07	5.69E-07	1.54E-03	1.69	1.05	1.14	1.13	5.28E-04
654	protein disulfide isomerase, putative [Ricinus communis].	gi|118489117	GI:223546830	cyto	-1.13	-1.01	1.74	1.85	1.82	1.04E-04	2.02E-09	1.21E-03	2.47	1.77	1.58	1.46	2.26E-04
655	protein disulfide isomerase, putative [Ricinus communis].	gi|118489117	GI:223546830	cyto	1.03	1.09	1.63	1.36	1.71	5.54E-04	1.72E-07	1.51E-01	-1.80	-2.13	-2.67	-2.41	4.05E-07
2690	isomerase peptidyl-prolyl cis-trans isomerase [Populus trichocarpa].	gi|224072532	GI:224057792	chl	1.01	-1.01	-1.25	-1.21	-1.54	1.38E-02	4.99E-10	2.00E-01	-2.11	-2.10	-2.45	-2.09	9.38E-05
1450	Protein grpE, putative [Ricinus communis].	gi|224126029	GI:223529469	chl	1.18	1.11	1.24	1.22	1.28	2.28E-03	5.22E-08	9.39E-01	-1.47	-1.84	-2.02	-1.85	1.52E-04
	Detoxification																
1204	monodehydroascorbate reductase [Vitis vinifera].	gi|224069008	GI:146432261	cyt	1.28	-1.03	-1.34	-1.41	-1.69	4.94E-02	7.92E-06	9.65E-02	-2.25	-1.66	-1.52	-1.65	1.96E-03
2053	cytosolic ascorbate peroxidase [Vitis vinifera].	gi|224104631	GI:161778778	cyt	1.01	1.10	1.06	1.17	1.23	3.12E-02	3.04E-12	5.92E-01	2.12	1.86	1.92	1.86	4.39E-08
2063	cytosolic ascorbate peroxidase [Vitis vinifera].	gi|224104631	GI:161778778	cyt	-1.18	1.13	1.10	1.13	-1.16	8.61E-01	4.08E-04	6.03E-02	-1.32	-1.37	-1.63	-1.26	3.59E-03
2074	cytosolic ascorbate peroxidase [Vitis vinifera].	gi|224104631	GI:161778778	cyt	-1.14	1.12	-1.03	-1.26	-1.32	7.23E-02	7.51E-10	2.85E-01	-2.23	-2.17	-2.53	-2.03	2.03E-05
2276	glutathione-s-transferase theta, gst, putative [Ricinus communis].	gi|224065727	GI:223551315	cyt	-1.01	-1.01	-1.94	-2.00	-2.17	3.55E-06	8.31E-03	2.66E-03	1.52	1.97	1.68	2.20	2.51E-03
2281	glutathione-s-transferase theta, gst, putative [Ricinus communis].	gi|224065727	GI:223551315	cyt	-1.00	1.02	-1.35	-1.34	-1.77	5.54E-04	1.08E-01	1.69E-02	-1.23	1.13	1.19	1.37	1.46E-02
2306	glutathione-s-transferase theta, gst, putative [Ricinus communis].	gi|224065727	GI:223551315	cyt	-1.06	1.13	-1.85	-2.11	-2.80	1.95E-07	3.96E-07	2.50E-05	-1.50	-1.06	-1.52	-1.13	8.70E-02
2613	glutathione peroxidase [Populus trichocarpa].	gi|118489959	GI:224089376	n.a.	-1.22	-1.02	-1.33	-1.07	-1.26	6.07E-02	9.29E-11	7.67E-01	2.74	3.56	3.80	4.54	1.48E-06
873	RecName: Full=Catalase isozyme 2			per	-1.06	-1.05	-1.33	-1.68	-1.79	2.98E-04	8.27E-07	7.39E-02	2.35	2.09	2.14	1.55	1.15E-03
876	catalase [Populus trichocarpa].	gi|118489349	GI:224065685	per	-1.01	-1.05	-1.30	-1.56	-1.53	4.73E-04	6.15E-08	5.48E-02	2.00	2.23	1.90	1.35	8.83E-05
880	catalase [Populus trichocarpa].	gi|118489349	GI:224065685	per	-1.04	-1.02	-1.36	-1.95	-2.13	2.58E-07	7.69E-08	1.57E-04	1.44	1.50	1.50	1.06	1.47E-02
883	catalase [Populus trichocarpa].	gi|118489349	GI:224065685	per	-1.04	-1.02	-1.40	-1.94	-2.42	2.41E-07	2.70E-09	1.07E-04	-1.18	-1.01	-1.10	-1.51	3.88E-02
886	catalase [Populus trichocarpa].	gi|118489349	GI:224065685	per	1.15	-1.03	-1.40	-2.18	-2.40	6.85E-07	3.40E-11	1.29E-05	-1.14	-1.14	-1.18	-1.72	3.65E-03
885	peroxidase [Nicotiana tabacum].	gi|224082496	GI:14031049	cyt	-1.07	1.02	1.66	2.12	2.61	1.59E-03	1.02E-01	1.11E-01	-1.79	-1.65	-2.17	-1.92	2.14E-01
891	peroxidase [Nicotiana tabacum].	gi|224082496	GI:14031049	cyt	-1.03	1.10	2.07	2.19	2.60	1.34E-05	2.09E-04	6.78E-03	-1.21	1.12	1.07	1.01	4.92E-01
1340	peroxidase [Nicotiana tabacum].	gi|57894628	GI:14031049	cyt	1.01	1.19	-1.23	-1.51	-1.35	3.22E-02	2.49E-06	6.02E-02	1.82	2.11	2.16	1.71	4.48E-04
1270	peroxidase [Nicotiana tabacum].	gi|24104432	GI:14031049	cyt	1.08	1.12	-1.35	1.42	1.45	4.40E-01	1.37E-03	4.28E-01	-1.73	-1.61	-2.21	-1.44	9.61E-04
1279	peroxidase [Nicotiana tabacum].	gi|224082494	GI:14031049	cyt	-1.22	1.24	2.22	1.78	2.49	2.81E-05	1.84E-03	4.34E-03	-1.45	-1.13	-1.09	-1.10	4.65E-01
1283	peroxidase [Nicotiana tabacum].	gi|224082494	GI:14031049	cyt	1.01	1.31	2.33	1.79	2.61	3.96E-04	5.94E-03	1.41E-01	-1.46	1.06	1.08	1.06	1.41E-01
	Pathogenesis related																
1980	class I chitinase, putative [Ricinus communis].	gi|224080749	GI:223534957	cyt	-1.24	1.19	2.22	1.78	3.56	3.80E-04	1.40E-07	6.10E-03	-1.13	1.53	2.08	1.81	1.82E-02
1963	class I chitinase, putative [Ricinus communis].	gi|224080749	GI:223534957	cyt	-1.03	1.34	3.62	2.92	3.69	1.34E-09	3.29E-14	9.71E-05	1.30	1.89	3.02	3.26	1.40E-05
1971	class IV chitinase [Pyrus pyrifolia].	gi|118487728	GI:222139394	cyt	-1.22	1.11	1.59	1.92	1.82	9.65E-03	1.90E-04	1.23E-01	-2.35	-1.19	-1.38	-1.37	2.89E-02
2094	Acidic endochitinase SE2 precursor, putative [Ricinus communis].	gi|224116850	GI:223547519	cyt	-1.26	1.43	3.67	2.67	3.84	8.04E-07	2.05E-06	2.59E-03	-1.20	1.06	1.42	1.25	1.64E-01
2098	Acidic endochitinase SE2 precursor, putative [Ricinus communis].	gi|224116850	GI:223547519	cyt	-1.02	1.16	2.33	1.24	2.13	5.83E-04	8.14E-03	2.39E-02	-1.49	-1.41	-1.37	-1.11	3.27E-02
1685	beta-1,3 glucanase [Populus x canescens].	gi|24065540	GI:6960214	cyt	-1.22	1.10	1.56	2.04	3.71	1.32E-03	8.18E-03	1.06E-02	-1.07	1.24	1.21	-1.12	5.19E-01
1694	beta-1,3 glucanase [Populus x canescens].	gi|23999435	GI:6960214	cyt	-1.24	1.12	1.71	1.65	2.48	2.18E-03	1.52E-02	3.09E-02	-1.48	-1.12	-1.01	-1.28	3.72E-01
1688	beta-1,3-glucanase [Hevea brasiliensis].	gi|118489363	GI:32765543	cyt	-1.15	-1.07	1.85	1.53	3.74	1.55E-04	3.32E-08	3.87E-04	1.94	1.81	2.52	1.60	4.08E-03
1692	beta-1,3-glucanase [Hevea brasiliensis].	gi|118489363	GI:32765543	cyt	-1.04	1.18	2.92	3.44	4.08	2.66E-07	1.57E-06	5.09E-04	-1.11	1.18	1.45	1.29	3.94E-01
2335	kunitz trypsin inhibitor TI3 [Populus alba].	gi|78643954	GI:78643954	cyt	-1.20	1.21	2.44	2.19	3.51	1.75E-03	2.48E-03	9.93E-02	-2.24	-1.29	-1.10	1.02	1.57E-01
	Protein synthesis																
1529	60S acidic ribosomal protein P0 [Zea mays]	gi|162460698		cyt	-1.10	1.00	1.14	1.12	1.35	2.21E-01	1.61E-06	3.85E-01	1.64	1.12	-1.29	-1.17	5.73E-04
1542	60S acidic ribosomal protein P0, putative [Ricinus communis].	gi|224109342	GI:223533772	cyt	-1.04	1.05	-1.01	-1.09	-1.54	1.84E-01	4.77E-12	2.49E-01	-2.43	-2.55	-3.92	-2.60	1.98E-05
1579	60S acidic ribosomal protein P0, putative [Ricinus communis].	gi|224101117	GI:223533772	cyt	1.01	1.06	1.10	1.01	-1.17	8.63E-01	4.68E-11	7.01E-01	-2.09	-2.43	-3.18	-2.96	8.64E-07
1702	ribonucleoprotein, chloroplast, putative [Ricinus communis]	gi|38581022	GI:223547067	chl	1.14	1.10	-1.91	-1.94	-2.25	1.55E-04	1.36E-10	3.79E-03	-1.58	-1.78	-2.42	-2.85	1.39E-06
2251	ribosome recycling factor, putative [Ricinus communis].	gi|24057024	GI:255559434	n.a.	-1.02	1.17	-1.59	-1.84	-2.40	2.19E-06	8.16E-02	5.28E-05	-1.08	1.45	1.19	1.71	1.86E-03
1154	chloroplast translational elongation factor Tu [Pelargonium graveolens].	gi|224074859	GI:12830555	chl	1.14	-1.04	-1.54	-1.70	-1.74	2.44E-05	2.23E-11	1.35E-03	-1.11	-1.45	-1.62	-1.75	7.09E-04
1155	chloroplast translational elongation factor Tu [Pelargonium graveolens].	gi|224053971	GI:12830555	cyt	1.15	-1.09	-1.41	-1.71	-2.14	1.50E-06	1.41E-14	6.56E-05	-1.34	-1.97	-1.90	-2.14	6.30E-06
2757	eukaryotic translation initiation factor 5A isoform I [Hevea brasiliensis].	gi|118489891	GI:33325117	cyt	-1.12	1.19	-1.43	-1.49	-1.70	5.81E-04	3.19E-03	1.30E-02	-1.73	-1.20	-1.36	-1.11	2.63E-03
375	translation elongation factor G, putative [Ricinus communis].	gi|224074699	GI:223549480	chl	1.02	-1.11	-1.35	-1.23	-2.06	2.40E-03	1.30E-05	8.69E-02	2.12	1.28	1.32	2.27	2.16E-03
	Miscellaneous																
2421	Auxin-binding protein ABP19a precursor, putative [Ricinus communis].	gi|118487720	GI:223539406	chl	1.15	-1.10	-1.80	-2.32	-2.69	6.32E-06	2.22E-16	1.25E-03	8.57	10.17	12.72	15.05	6.23E-09
2434	Auxin-binding protein ABP19a precursor, putative [Ricinus communis].	gi|52398886	GI:223539406	chl	1.27	1.03	-1.90	-2.30	-3.05	1.25E-06	3.24E-04	9.55E-06	1.74	2.47	2.30	3.51	2.14E-05
2439	Auxin-binding protein ABP19a precursor, putative [Ricinus communis].	gi|224058663	GI:223539406	vac	1.19	1.01	-1.58	-1.96	-2.42	1.32E-05	1.88E-11	1.50E-04	2.90	4.12	3.99	5.81	2.41E-07
560	vacuolar H+-ATPase catalytic subunit [Gossypium hirsutum].	gi|224109966	GI:3169287	vac	-1.14	-1.06	1.11	1.11	1.17	4.52E-01	2.43E-12	4.26E-01	2.86	2.26	2.30	2.33	2.33E-05
561	vacuolar H+-ATPase catalytic subunit [Gossypium hirsutum].	gi|224097420	GI:3169287	chl	1.05	-1.07	-1.07	-1.22	-1.47	5.10E-02	2.69E-06	2.40E-01	-1.41	-1.62	-1.85	-1.29	6.98E-03
595	poly(A)-binding protein [Cucumis sativus].	gi|224060514	GI:7528270	chl	-1.37	-1.06	1.18	1.43	1.39	5.96E-02	3.78E-05	1.69E-03	-1.03	-1.46	-1.91	-1.77	6.29E-05
607	poly(A)-binding protein [Cucumis sativus].	gi|224060514	GI:7528270	n.a.	-1.10	-1.01	1.36	1.53	1.45	3.68E-03	2.54E-06	6.86E-02	-1.63	-1.81	-2.52	-2.36	1.91E-04
1506	NAD dependent epimerase/dehydratase, putative [Ricinus communis].	gi|52535872	GI:255542956	n.a.	-1.17	-1.03	1.03	-1.47	-1.38	2.17E-02	7.78E-10	3.76E-01	3.12	2.07	2.73	2.24	1.78E-05
1519	NAD dependent epimerase/dehydratase, putative [Ricinus communis].	gi|14489029	GI:255542956	n.a.	-1.03	-1.02	-1.48	-1.96	-1.55	1.51E-03	2.43E-07	7.49E-02	2.80	2.26	2.39	2.11	1.54E-03
1523	NAD dependent epimerase/dehydratase, putative [Ricinus communis].	gi|118489564	GI:223548502	n.a.	1.02	1.00	-1.26	-1.57	-1.53	1.84E-03	4.02E-10	4.31E-02	2.89	2.47	2.51	2.25	1.96E-05
1531	NAD dependent epimerase/dehydratase, putative [Ricinus communis].	gi|118489564	GI:223548502	n.a.	1.08	1.09	-1.52	-1.86	-1.94	4.20E-05	3.85E-07	7.76E-04	2.07	1.83	1.70	1.69	2.06E-03
1553	NAD dependent epimerase/dehydratase, putative [Ricinus communis].	gi|118489564	GI:223548502	n.a.	1.09	-1.00	-1.61	-2.14	-2.43	6.05E-07	2.20E-04	3.36E-05	1.05	1.07	1.08	1.09	9.67E-01
1554	NAD dependent epimerase/dehydratase, putative [Ricinus communis].	gi|118489564	GI:223548502	n.a.	1.13	1.11	-1.60	-2.16	-2.85	7.69E-06	1.72E-06	3.94E-05	-1.09	-1.06	-1.24	-1.10	8.26E-01
1556	NAD dependent epimerase/dehydratase, putative [Ricinus communis].	gi|118489564	GI:223548502	n.a.	-1.02	1.08	-1.56	-2.05	-2.22	2.63E-06	1.18E-05	2.94E-04	1.74	1.67	1.53	1.60	5.86E-03
1958	NAD-dependent epimerase/dehydratase [Zea mays].	gi|224090705	GI:226499246	cyt	-1.03	1.18	-1.46	-1.32	-1.62	3.80E-03	1.49E-10	1.29E-02	-2.09	-1.76	-2.57	-1.75	2.37E-04
725	lysosomal alpha-mannosidase, putative [Ricinus communis].	gi|224065294	GI:223547850	cyt	1.06	-1.02	1.02	1.47	1.23	5.03E-02	1.42E-06	2.30E-01	-1.97	-1.83	-2.00	-1.60	5.71E-04
1433	coproporphyrinogen III oxidase, putative [Ricinus communis].	gi|224116070	GI:223542241	cyt	1.02	1.03	-1.61	-1.32	-1.16	6.08E-03	2.71E-02	9.47E-02	1.21	1.66	1.13	1.28	4.16E-03
1631	phenylcoumaran benzylic ether reductase 3 [Populus trichocarpa].	gi|224105373	GI:224105373	n.a.	-1.15	1.18	1.60	2.01	1.34	4.81E-04	2.32E-03	2.64E-02	-1.46	-1.09	-1.40	1.03	1.07E-01
2136	oxidoreductase NAD-binding domain-containing protein [Arabidopsis thaliana].	gi|224111562	GI:18394201	cyt	1.01	1.03	-1.07	-1.35	-1.41	4.55E-02	1.17E-06	2.00E-01	-1.76	-1.75	-1.65	-1.61	2.46E-03
1153	actin 9 [Populus trichocarpa].	gi|224116600	GI:224116600	cyt	1.02	-1.01	-1.33	-1.44	-1.64	1.94E-04	2.32E-13	1.51E-02	-2.08	-2.18	-2.48	-2.23	1.19E-06
2938	glycine-rich RNA-binding protein [Euphorbia esula].	gi|224077836	GI:2674201	cyt	1.00	1.30	-1.65	1.17	1.32	5.28E-01	3.26E-06	1.48E-02	-1.79	-1.23	-2.30	-2.18	1.14E-03
1101	ankyrin-repeat protein HBP1 [Nicotiana tabacum].	gi|224132484	GI:13310811	n.a.	1.07	-1.03	-1.19	-1.17	-1.16	6.33E-02	1.07E-09	5.25E-01	-1.35	-1.62	-1.79	-1.83	1.05E-05
1173	Chain A, Crystal Structure Of Ll-Diaminopimelate Aminotransferase From Arabidopsis Thaliana Complexed With L-Malate Ion.	gi|118483001	GI:152149569	n.a.	-1.02	-1.05	-1.20	-1.50	-1.80	2.07E-04	1.83E-04	3.60E-02	1.44	1.57	1.79	2.23	3.14E-04
2122	Stem 28 kDa glycoprotein precursor, putative [Ricinus communis]	gi|118487771	GI:223544854	n.a.	-1.10	1.18	-1.13	1.02	-1.13	6.01E-01	1.21E-11	5.87E-01	1.03	2.45	1.94	2.55	2.18E-06
2314	DNA-binding protein p24 [Solanum tuberosum].	gi|23996237	GI:9651810	chl	1.08	1.01	1.13	-1.07	-1.09	8.95E-01	6.36E-08	6.80E-01	-1.36	-1.80	-1.84	-1.58	5.09E-04
1167	predicted protein [Populus trichocarpa]	gi|224145977	GI:224145977	chl	1.07	-1.17	-1.45	-1.27	-1.84	4.75E-03	9.82E-02	2.06E-01	1.54	1.56	1.51	1.44	6.59E-02
1378	predicted protein [Populus trichocarpa] (low homology)	gi|161916531	GI:224061357	cyt	-1.10	-1.07	-1.32	-1.04	-1.25	1.45E-02	2.30E-05	6.59E-01	1.69	1.54	1.33	1.60	2.64E-04
1568	predicted protein [Populus trichocarpa] (low homology)	gi|46842263	GI:224061357	cyt	-1.12	-1.01	1.10	1.83	1.31	9.32E-03	3.10E-05	4.89E-03	1.74	1.35	1.02	1.40	4.26E-03
2437	predicted protein [Populus trichocarpa] (no significant homology found	gi|224078196		cyt	-1.17	-1.04	1.43	1.28	1.58	5.13E-03	3.53E-05	9.20E-03	-1.08	-1.01	1.22	1.08	2.90E-01

Supplemental Figures 2: abundance profiles for all discussed proteins are presented in charts similar to Figure 39. On the x axis are the days of treatment and on the y axis the standard abundance exported from the Decyder software. Multiple lines of the same color represent spots containing the same protein function. Green circles represent control and red triangles treatment conditions.

1.

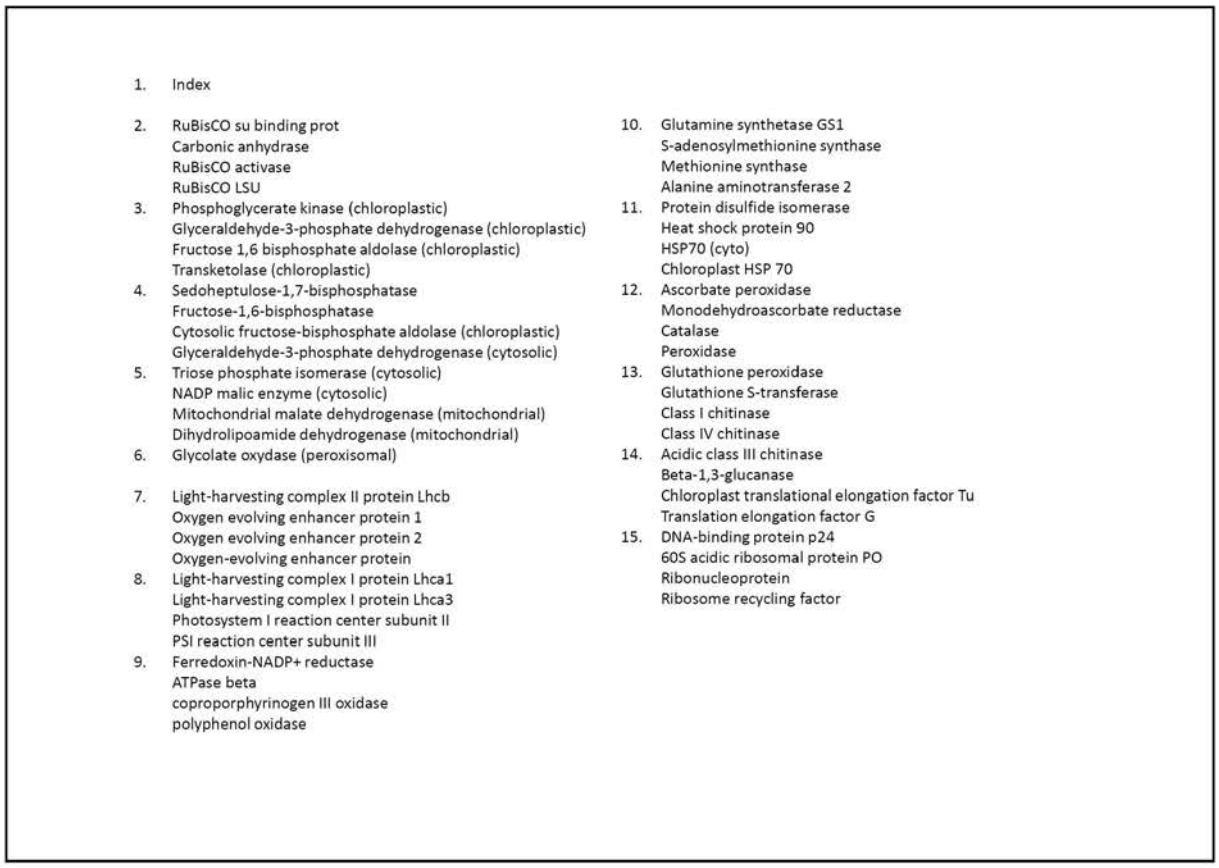

2.

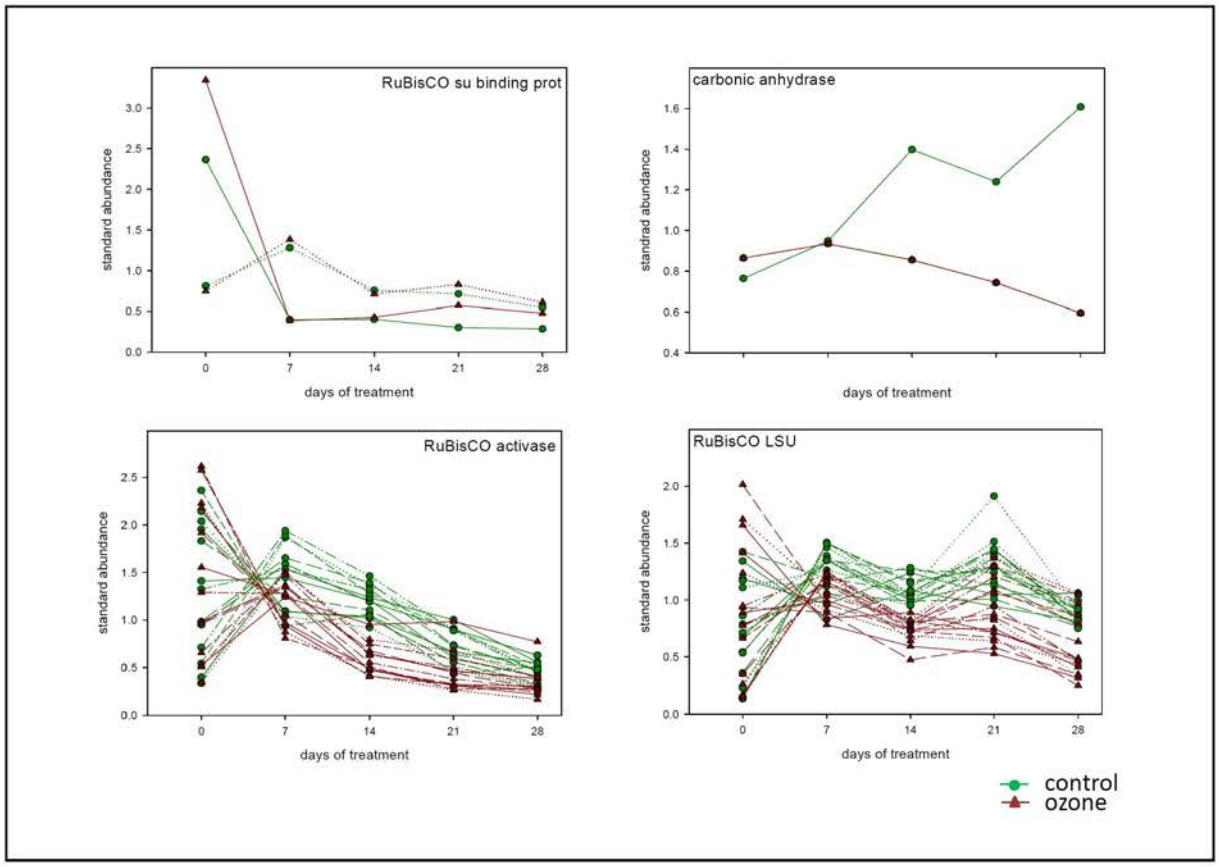
RuBisCO su binding prot
carbonic anhydrase
RuBisCO activase
RuBisCO LSU
standard abundance
standrad abundance
days of treatment
control
ozone

3.

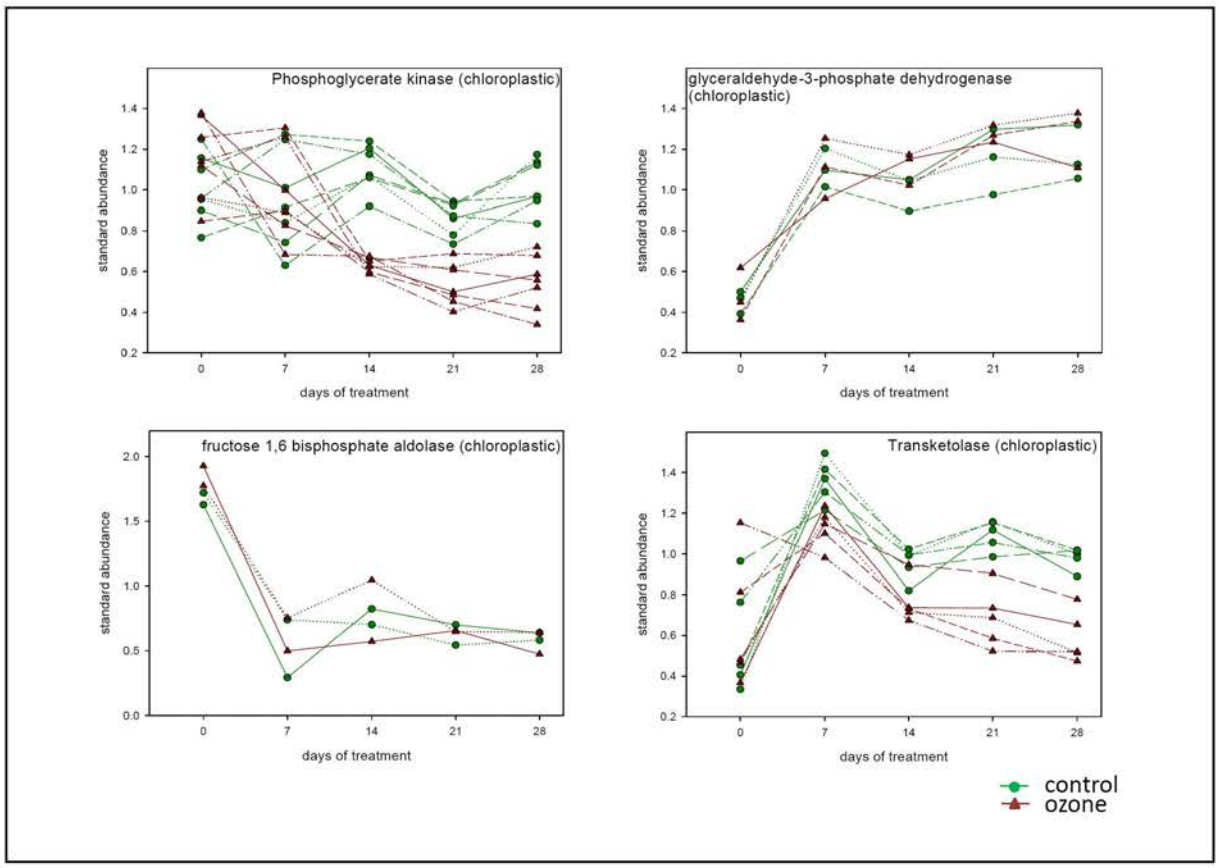
Phosphoglycerate kinase (chloroplastic)
glyceraldehyde-3-phosphate dehydrogenase (chloroplastic)
fructose 1,6 bisphosphate aldolase (chloroplastic)
Transketolase (chloroplastic)
standard abundance
days of treatment
control
ozone

4.

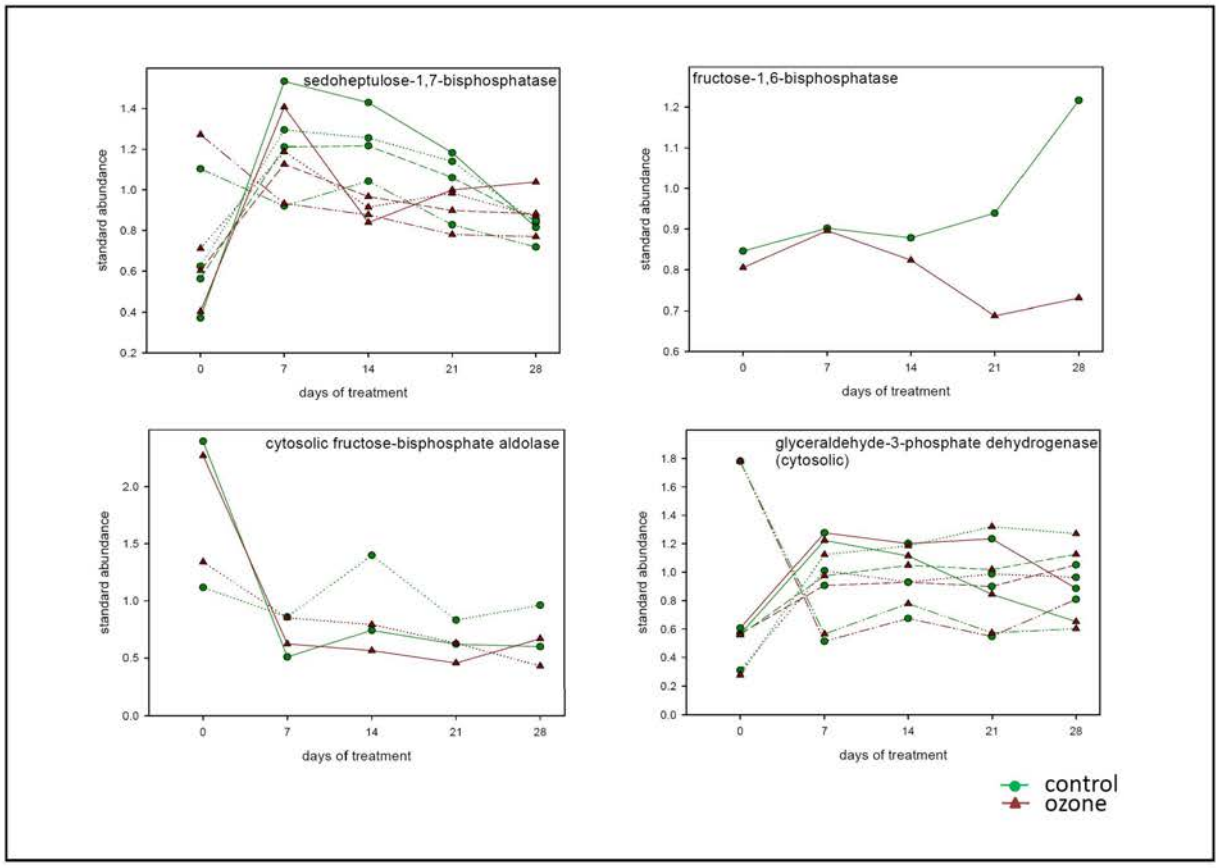
sedoheptulose-1,7-bisphosphatase
fructose-1,6-bisphosphatase
cytosolic fructose-bisphosphate aldolase
glyceraldehyde-3-phosphate dehydrogenase (cytosolic)
standard abundance
days of treatment
control
ozone

5.

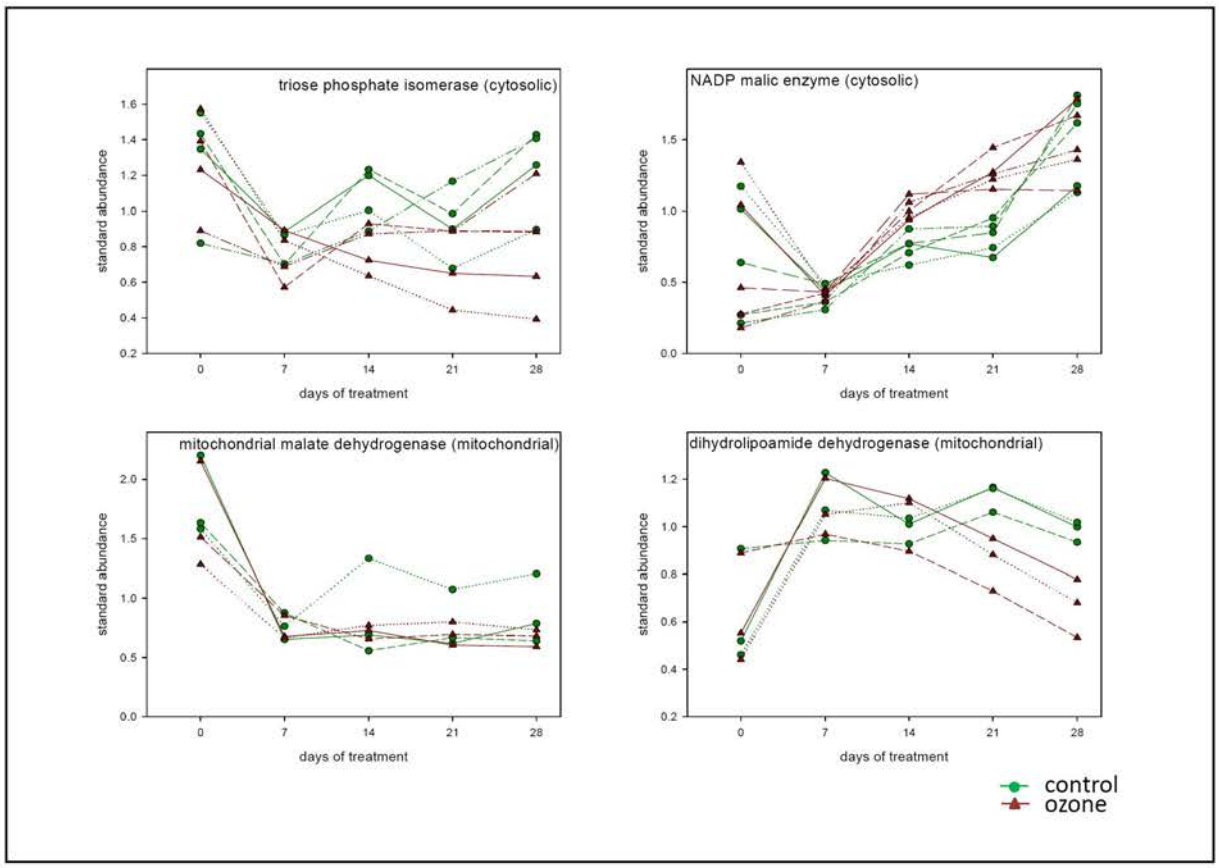
triose phosphate isomerase (cytosolic)
NADP malic enzyme (cytosolic)
mitochondrial malate dehydrogenase (mitochondrial)
dihydrolipoamide dehydrogenase (mitochondrial)
standard abundance
days of treatment
control
ozone

6.

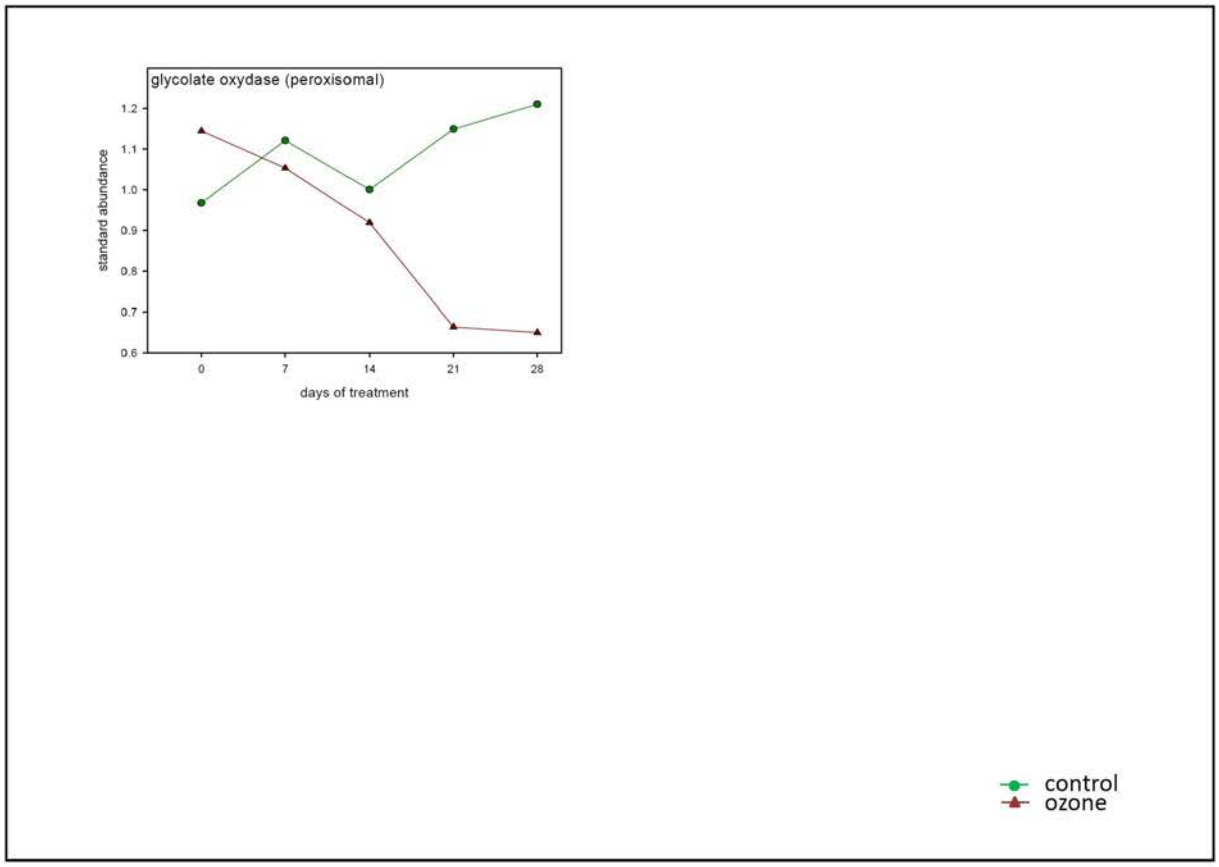
glycolate oxydase (peroxisomal)
standard abundance
days of treatment
control
ozone

7.

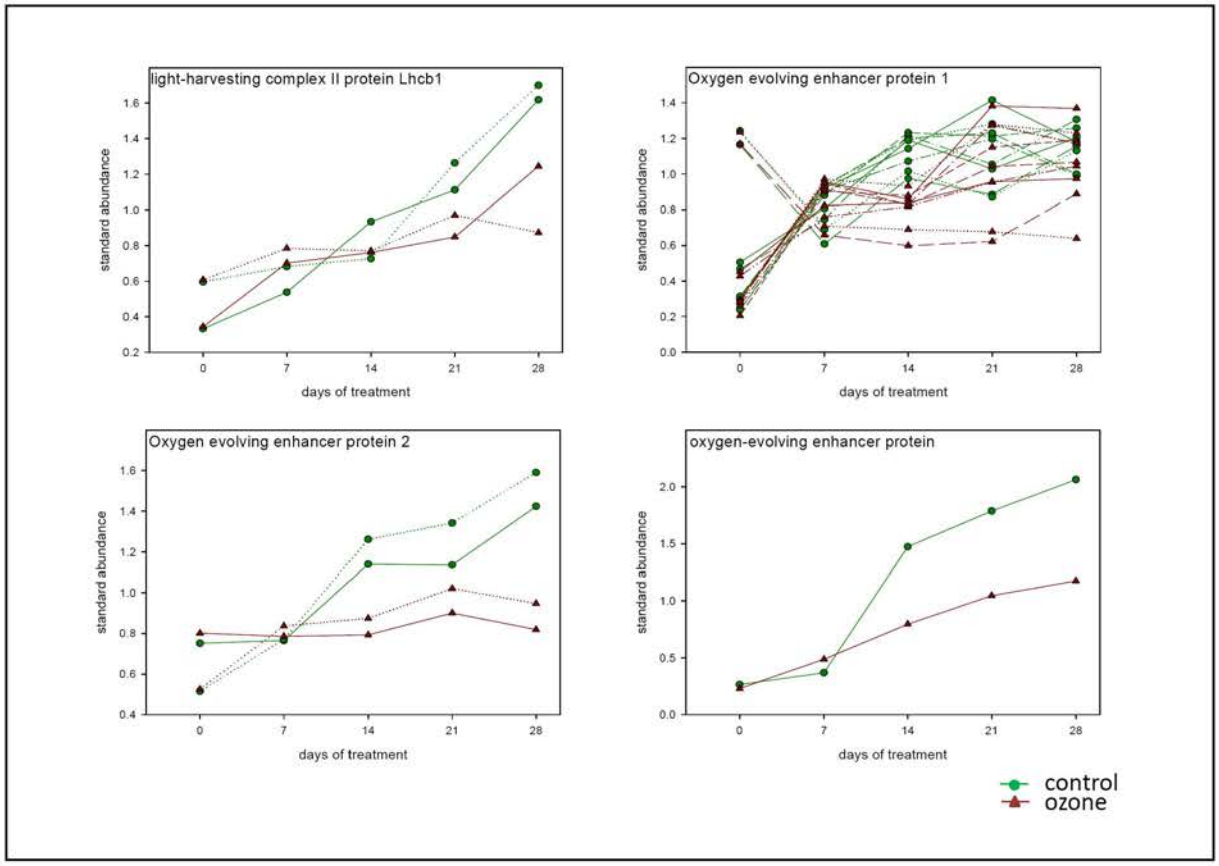
light-harvesting complex II protein Lhcb1
Oxygen evolving enhancer protein 1
Oxygen evolving enhancer protein 2
oxygen-evolving enhancer protein
standard abundance
days of treatment
control
ozone

8.

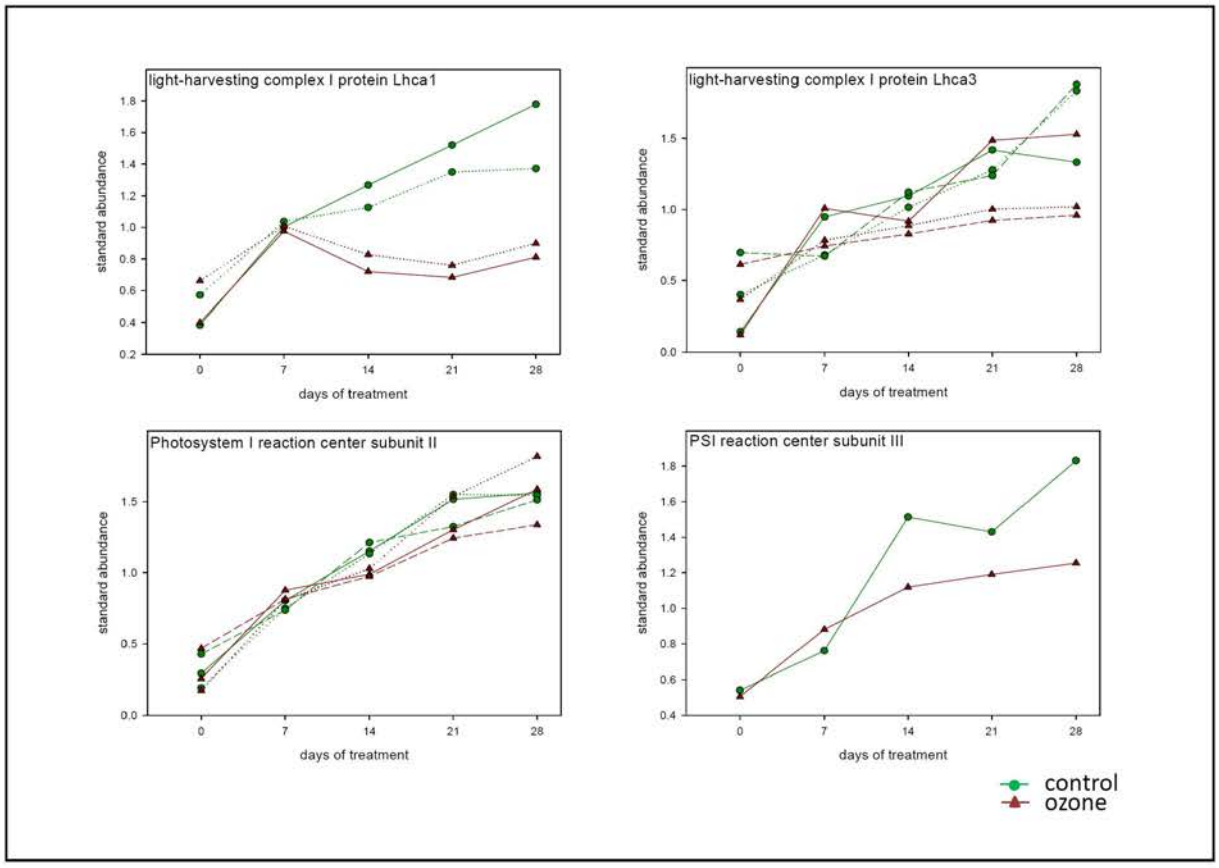
light-harvesting complex I protein Lhca1
light-harvesting complex I protein Lhca3
Photosystem I reaction center subunit II
PSI reaction center subunit III
standard abundance
days of treatment
control
ozone

9.

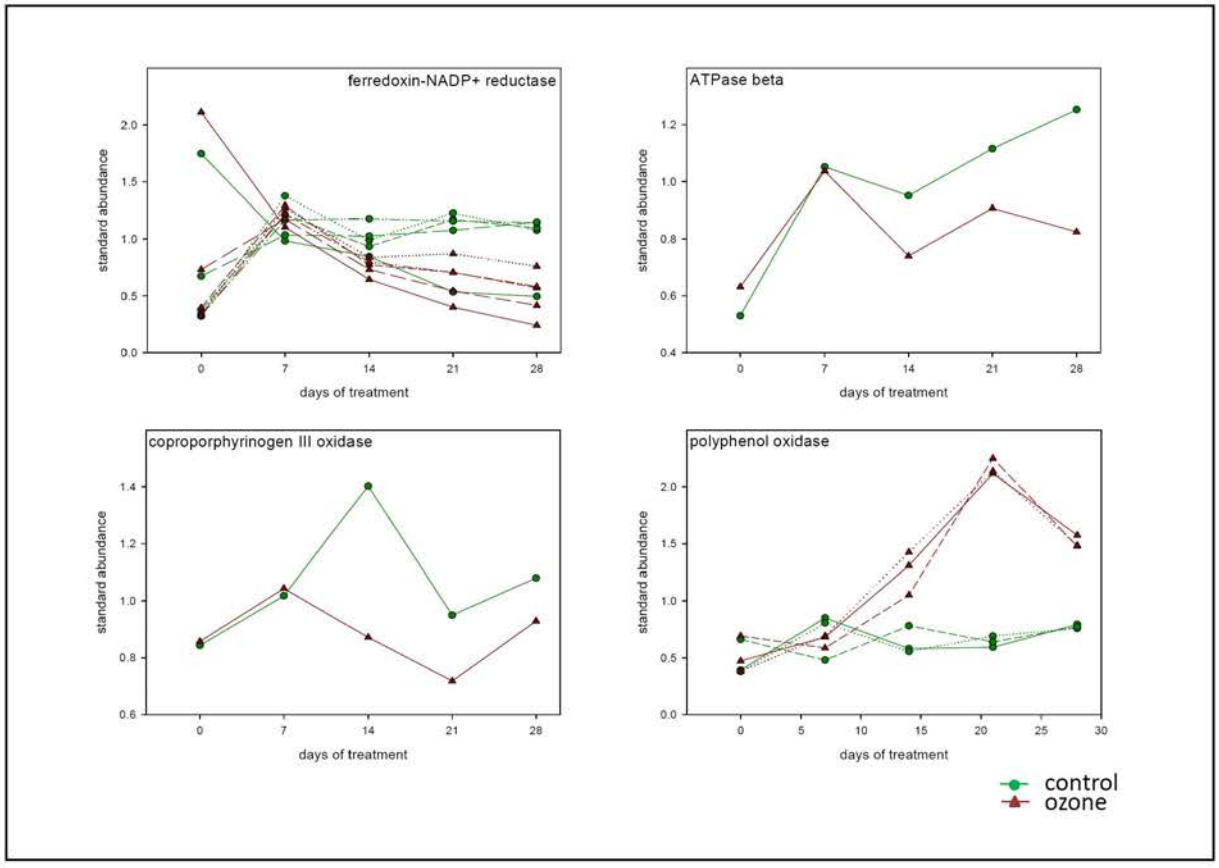
ferredoxin-NADP+ reductase
ATPase beta
coproporphyrinogen III oxidase
polyphenol oxidase
standard abundance
days of treatment
control
ozone

10.

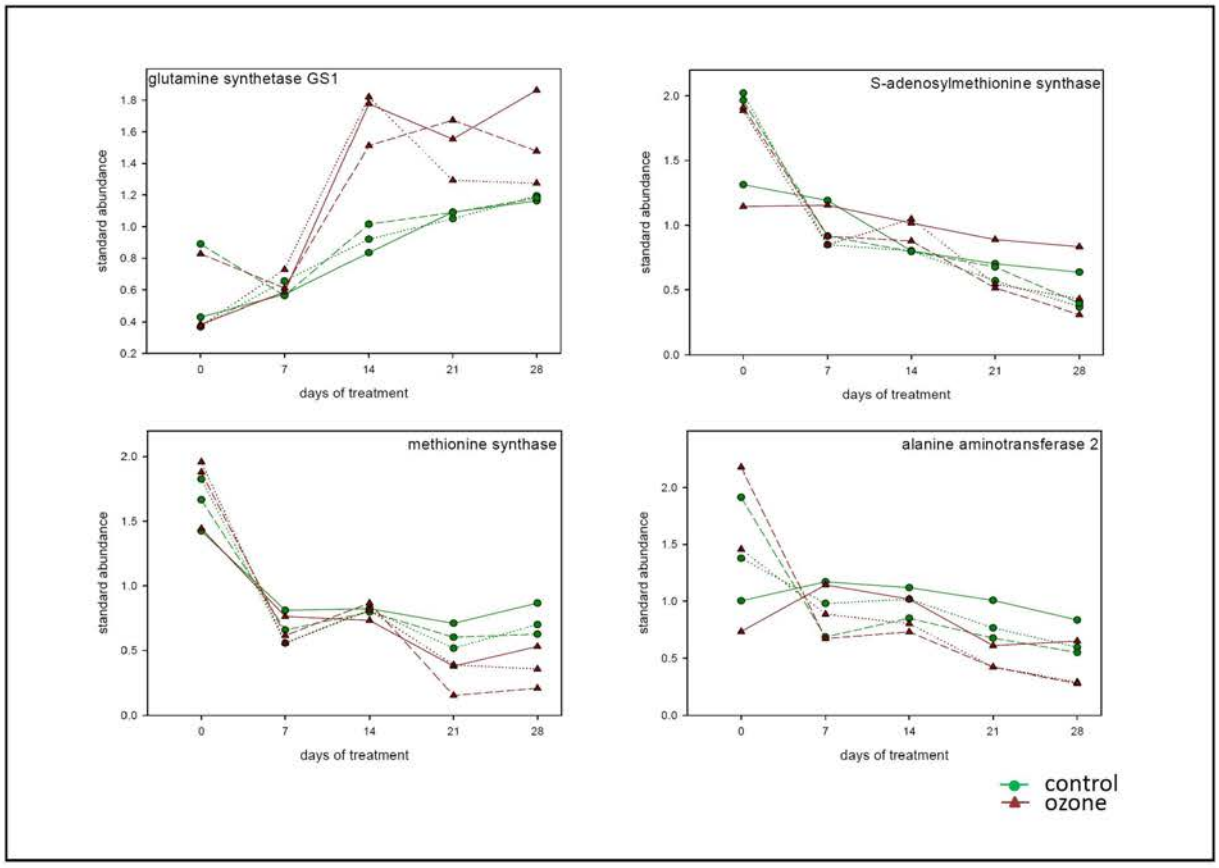
glutamine synthetase GS1
S-adenosylmethionine synthase
methionine synthase
alanine aminotransferase 2
standard abundance
days of treatment
control
ozone

11.

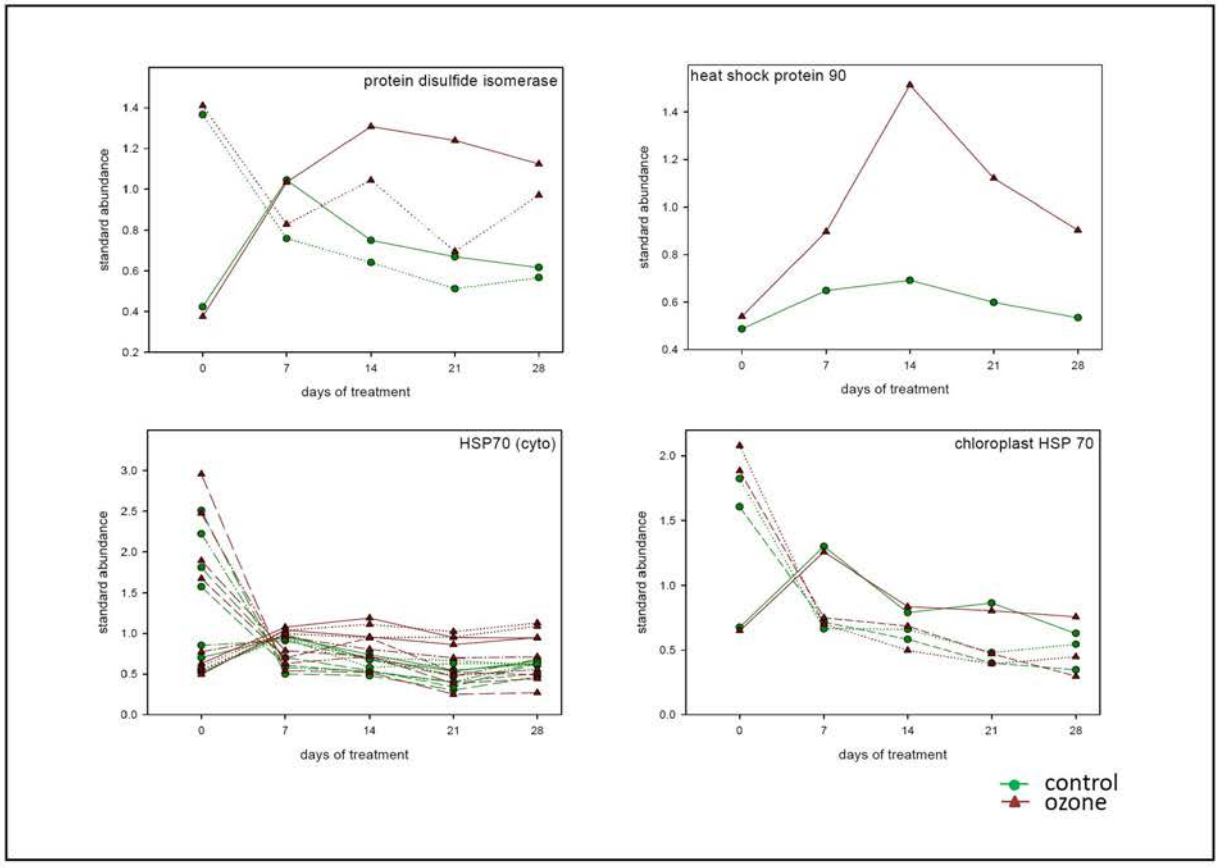
protein disulfide isomerase
heat shock protein 90
HSP70 (cyto)
chloroplast HSP 70
standard abundance
days of treatment
control
ozone

12.

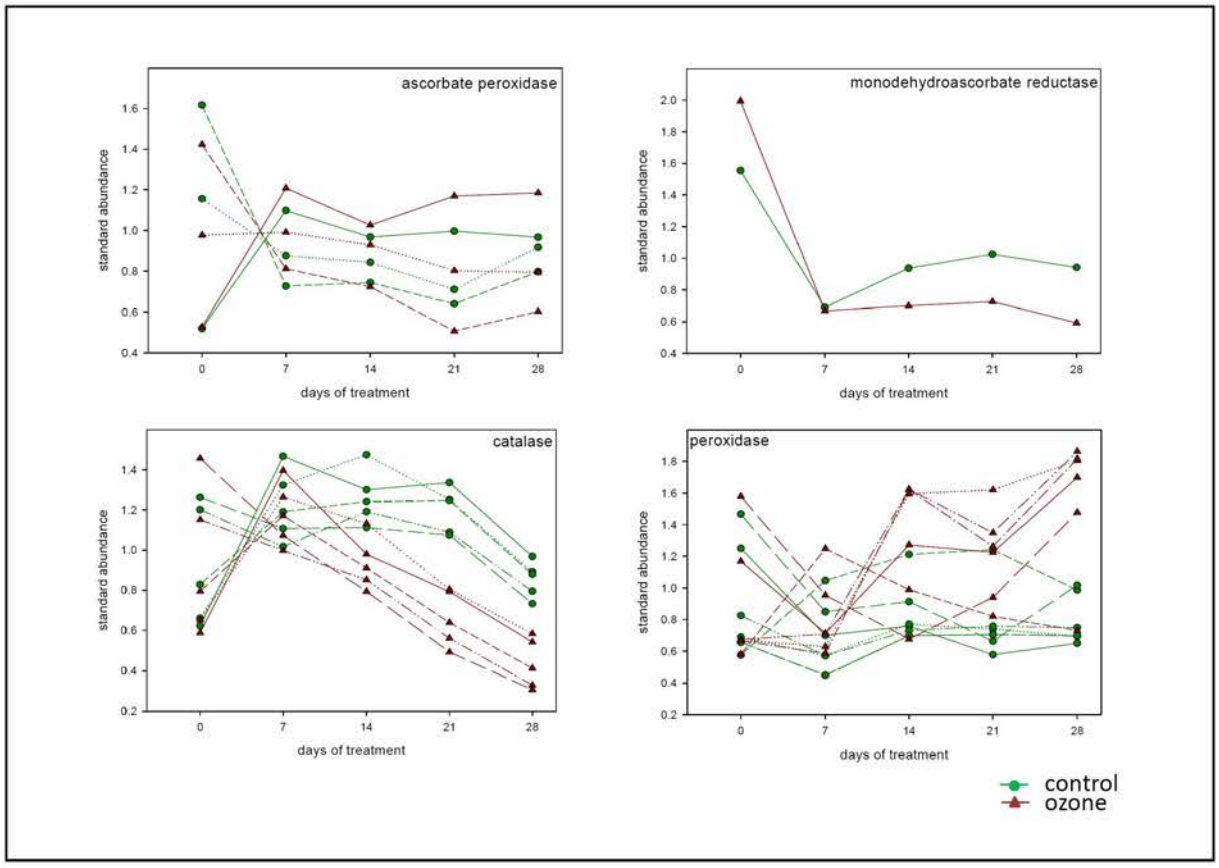
ascorbate peroxidase
monodehydroascorbate reductase
catalase
peroxidase
standard abundance
days of treatment
control
ozone

13.

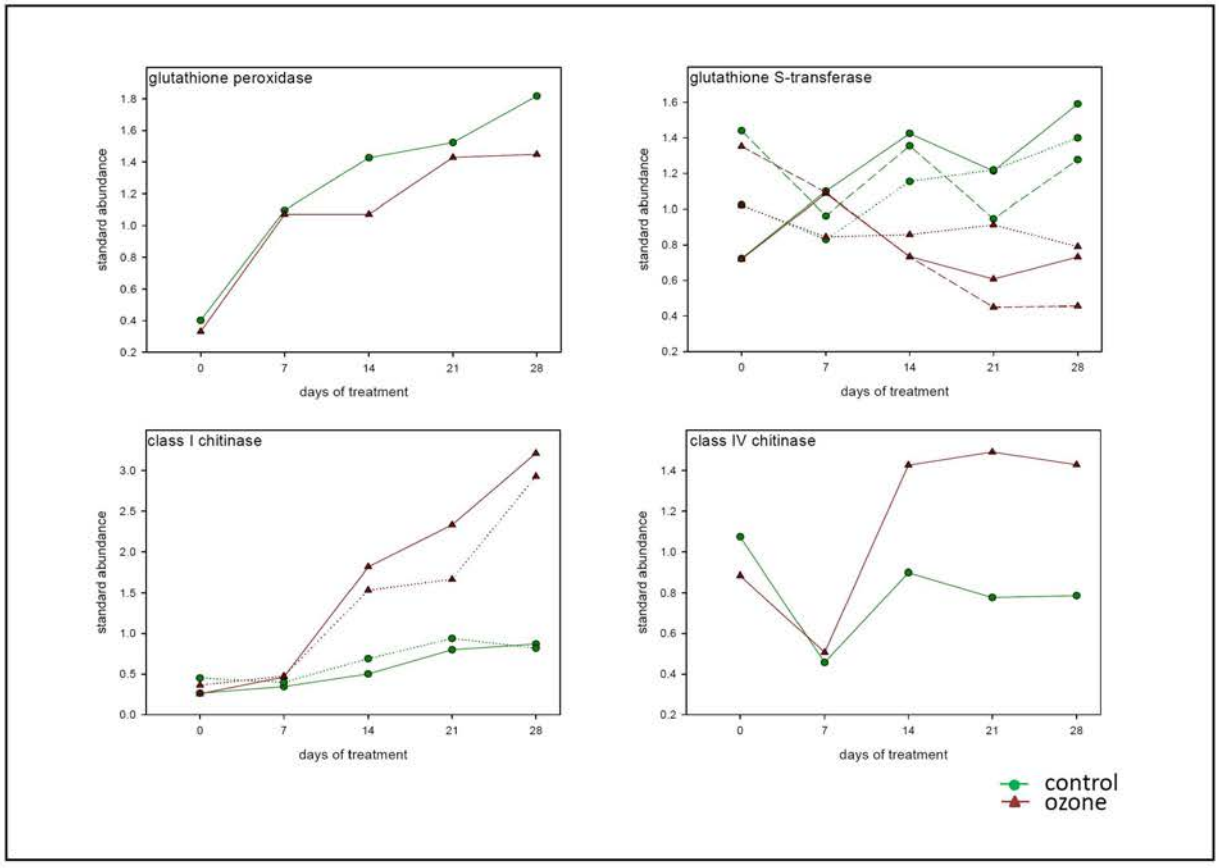
glutathione peroxidase
glutathione S-transferase
class I chitinase
class IV chitinase
standard abundance
days of treatment
control
ozone

14.

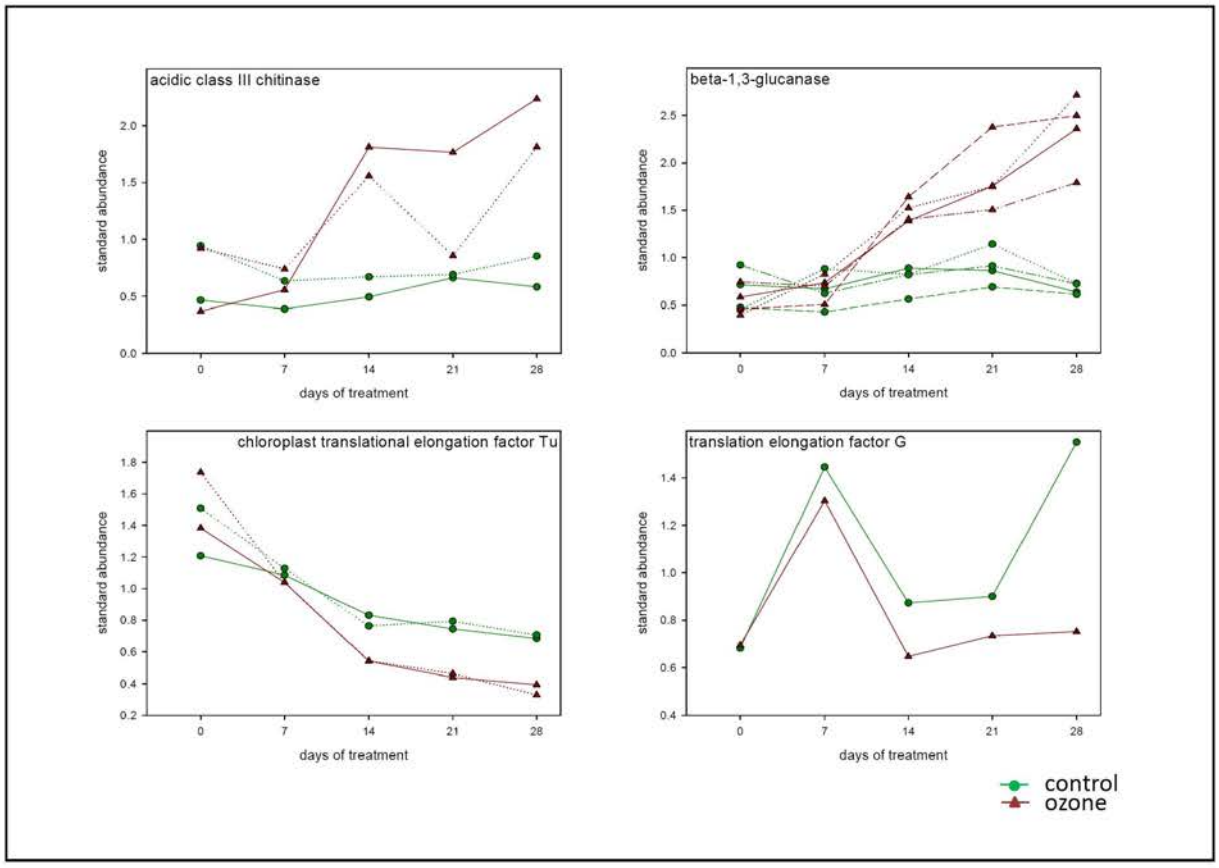
acidic class III chitinase
beta-1,3-glucanase
chloroplast translational elongation factor Tu
translation elongation factor G
standard abundance
days of treatment
control
ozone

15.

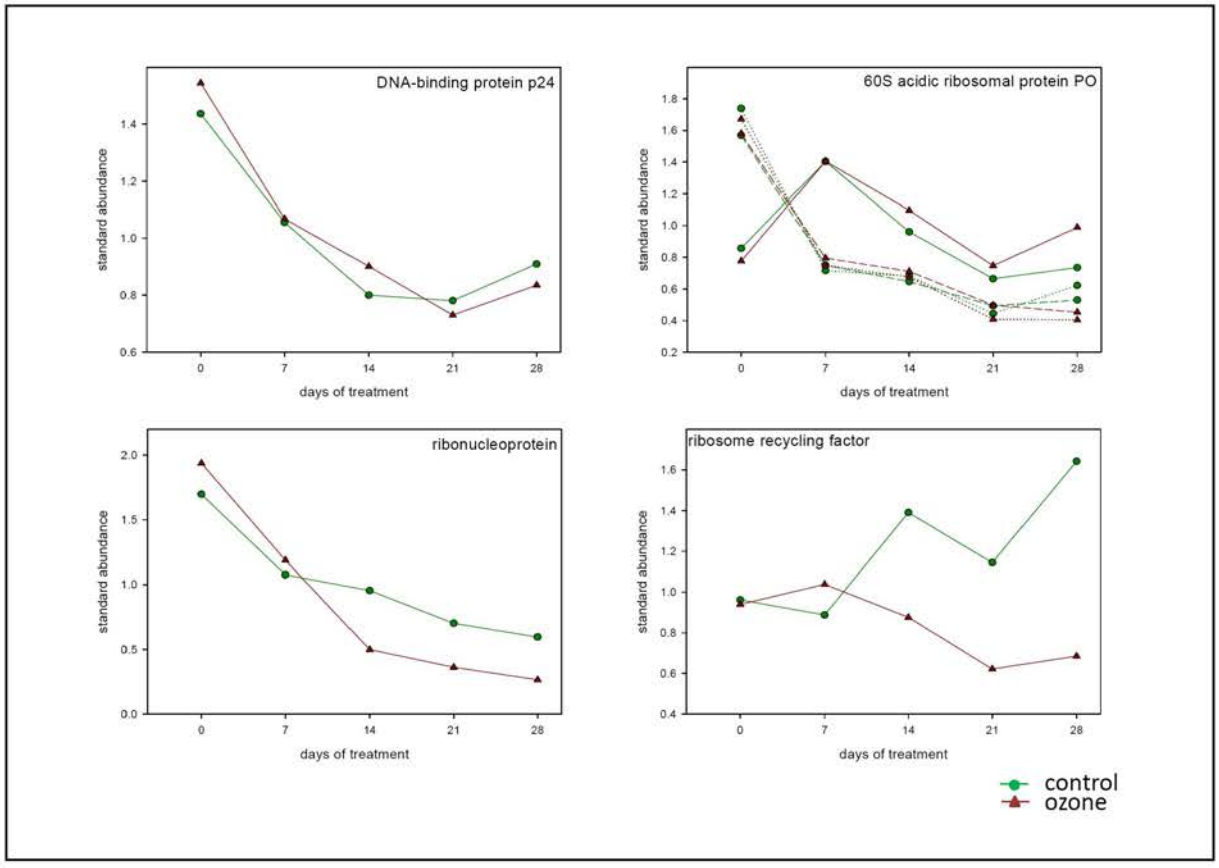
DNA-binding protein p24
60S acidic ribosomal protein PO
ribonucleoprotein
ribosome recycling factor
standard abundance
days of treatment
control
ozone

The End

Abstract français

Depuis les révolutions industrielles des années 1700 et 1800, et pendant l'industrialisation des siècles les suivant, une accumulation de composés polluants a eu lieu dans l'atmosphère, principalement due à la combustion de matières fossiles comme le charbon et le pétrole. Outre les polluants directement émis comme les oxydes de souffre et d'azote, des polluants secondaires comme l'ozone se sont accumulés. Aujourd'hui, l'ozone est le troisième gaz responsable du réchauffement climatique, mais est également dangereux pour la santé humaine et responsable de dommages sur la végétation. Depuis les années cinquante, les effets de l'ozone sur les plantes et les réponses de ces dernières ont été étudiés de façon ciblée. Aujourd'hui, avec l'apparition de techniques permettant l'étude globale du transcriptome ou du protéome, il est possible d'aborder le problème d'une façon non biaisée, permettant des études plus complètes du stress.

Dans le cadre de ce travail, une étude protéomique des effets de l'ozone sur les processus foliaires du peuplier a été proposée. Cette technique, complétée par des approches biochimiques, physiologiques, et des observations morphologiques, a permis de confirmer certains résultats d'études ciblées, mais également d'émettre des nouvelles hypothèses sur les mécanismes d'action de l'ozone sur le métabolisme du peuplier. En parallèle, l'étude du stress a aussi permis d'éclaircir les changements du métabolisme lors de la croissance de feuilles en conditions de stress et en conditions normales. Dans les pages de ce document, les procédures, résultats et conclusions de ce travail seront présentés en détail.

English abstract

After the industrial revolution of the 1700s and 1800s, and the subsequent industrialization, many pollutants have accumulated in the atmosphere, mainly due to the use of coal and fossil fuels. Besides the primary pollutants such as nitrogen oxides and sulfur oxides, secondary oxides such as ozone started to accumulate. Nowadays, ozone is the third gas involved in global climate change, but is also a major health risk for humans, and induces considerable damage to vegetation. Starting in the 50s, ozone research was based on targeted studies. Nowadays, with the advent of global techniques such as transcriptomics and proteomics, new results can be produced in an unbiased way.

In the thesis presented here, a proteomic study of the effects of ozone on poplar leaf processes was carried out. With the help of this technique, complemented with biochemical and physiological approaches and with morphological observations, it was possible to confirm previous results, but also to elaborate new hypotheses concerning the effects of ozone on poplar leaf metabolism. In parallel, studying the stress also allowed to clarify some of the changes that occur in metabolism during leaf development, under stress conditions and under control conditions. In this document, the procedures, results and conclusions obtained during this study are presented in detail.